THE UNIVERSITY OF CHICAGO

COMMUNITY-LEVEL BIOTIC RESPONSE TO INCREASING CLIMATE VARIABILITY DURING THE LAST 150 YEARS: STEADY AND WARMING CONDITIONS ON THE CONTINENTAL SHELF OF THE PACIFIC ARCTIC

A DISSERTATION SUBMITTED TO
THE FACULTY OF THE DIVISION OF THE PHYSICAL SCIENCES
IN CANDIDACY FOR THE DEGREE OF
DOCTOR OF PHILOSOPHY

DEPARTMENT OF GEOPHYSICAL SCIENCES

BY

CAITLIN ANA MEADOWS

CHICAGO, ILLINOIS

DECEMBER 2020

"Gentlemen", I said, "I've studied the maps

And if what I'm thinking is right

There's another new world at the top of the world

For whoever can break through the ice"...

After that it got colder the world got quiet

It was never quite day or quite night

And the sea turned the color of sky turned the color

Of sea turned the color of ice

'Til at last all around us was fastness

One vast glassy desert of arsenic white...

The crew gathered closer at first for the comfort

But each morning would bring a new set

Of the tracks in the snow leading over the edge

Of the world 'til I was the only one left...

- Josh Ritter, Another New World, 2010

TABLE OF CONTENTS

LIST OF FIGURES

LIST OF TABLES

ACKNOWLEDGMENTS

I would like to thank: the American Chemical Society, Petroleum Research Fund (PRF) for funding this research; Mid-American Paleontology Society (MAPS) Outstanding Student Research Award, the Geological Society of America, John T. Dillon Alaska Research Award, Smithsonian Institution Short-Term Visitor Fellowship, Conchologist of America Student Research Grants, University of Chicago Gurley Fund for funding this research. The NOAA, NSF, and other funding sources used to acquire the specimen housed in museums and data archived online.

The Office of shared Research Facilities at the University of Chicago for access to the SEM and other instruments; Jordon Bright and Darrell Kaufman at the Quaternary Geology Lab at Northern Arizona University for AAR dating and helpful advising. All of the curators, support, and hosts at the museums' collections used in these analyses, with special thanks to Prof. Peter Roopnarine, Elizabeth Kools, and Christina Piotrowski at the California Academy of Sciences, Prof. Andres Lopez and Angela Gastaldi at the University of Alaska Museum of the North, Prof. Ellen Strong, Dr. Bill Mosher, Amanda Robinson, and Karen Reed at the Smithsonian Institution Invertebrate Zoology, and Prof. Stanislav Denisenko at the Russian Academy of Sciences Invertebrate Zoology, for access to collections, hosting, and helpful advising. The crew and scientists onboard all research cruises presented here, with special thanks to those onboard the USCGC Healy (WAG-B) 1702, 1801, and 1901.

Adam Tomasovych, and Matthew Kosnik for advising about age dating, and applying analytical methods they developed to this dataset; Quan Hua, Jessica Cross for helpful conversations about this project. The statistics consulting team – Team Bivalve – for developing the Poisson model and other helpful conversations, including Jess Kunke, Huanlin Zhou, Benjamin Harris, Margarita Orlova, Timothy Morrison, Weilin Chen with faculty advisors, Mei Wang and Peter McCullagh.

Jacqueline Grebmeier, Lee Cooper, Christina Goethel and the crews of Arctic research cruises for collecting dead shell assemblage, supplying live collected individuals for analysis, supplying "modern survey data" for analyses, and providing advising and helpful conversation about the Pacific

Arctic System. My advisor Susan Kidwell for feedback on this manuscript and the supportive advising needed to complete this project; and, my remaining committee members Michael Foote, Cathy Pfister, and David Jablonski for invaluable advising.

ABSTRACT

Ecosystem monitoring since 1980 has established that the boundary between the Arctic and the Subarctic on the Bering continental shelf, maintained by ice-influenced bottom water, shifted northward between 1998 and 2001. However, this benthic data are only collected through observation consistently since the 1980's; while additional long term data are available through dead shell assemblages and natural history collections (NHCs) since 1865. By extracting and integrating insights from these diverse and scattered sources, I have been able to reconstruct a 150-year history of benthic community change in the northern Bering and Chukchi Seas to answer the following questions: (1) Do dead-shell assemblages capture the shifting Subarctic-Arctic boundary in the Pacific Arctic ecosystem?, (2) How long can biogenic carbon persist on the Pacific Arctic continental shelf? (3) WHow long does biogenic carbon persist on the Pacific Arctic continental shelf? (3) What is history of bivalve family geographic distributions in the N Bering and Chukchi Seas over the last 150 years?

Arctic Death Assemblages. Time-averaged molluscan death assemblages sampled from tropical to temperate open continental shelves commonly disagree in species composition with local living communities that have changed in response to anthropogenic eutrophication and other locally intense human stresses, providing a means of recognizing shifted baselines. In contrast, the ability of live-dead discordance to resolve the spatially heterogeneous effects of human-induced climate change has not been tested in high-latitudes, where cold waters are antagonistic to carbonate shell preservation. In habitats where either Subarctic or Arctic conditions have persisted, bivalve death assemblages agree closely with counterpart living communities in taxon and guild composition and are not subject to significant post-mortem bias. Significant live-dead discordance occurs only in areas with documented changes in community composition over the last several decades; there, dead assemblages are mixtures of shells from pre- and post-transition communities. This spatial pattern is robust to both numerical abundance- and biomass-based measures of community composition. In fact, biomass is especially powerful in revealing fine, station-level discordance that is strongly

tied to known sites within habitats where new carbon deposition levels, grain size, or benthos have occurred since 1980. Live-dead discordance can thus reliably differentiate between stable and rapidly changing habitats in cold, high-latitude settings, relevant to evaluating climate change, and biomass-based currencies of community composition are as robust as numerical abundance data, and in fact improve spatial resolution.

Persistence of Biogenic Aragonite. The Bering and Chukchi continental shelves have high macrobenthic biomass, producing fully bioturbated seabeds with abundant dead shell assemblages. Given high rates of bioturbation and undersaturated overlying water, we expect high postmortem loss rates and thus younger median shell ages and lower sequestration rates than in tropical and temperate shelves. Overall, shells were young: all specimens of *Nuculana* were < 1600 years old with a median age of 50 years, and all *Macoma* shells were < 850 years old with a median age of about 30 years. These maximum shell ages are an order of magnitude lower than encountered at lower latitudes, while median shell ages are similar to those at lower latitudes. The lowest median shell ages and highest rates of shell loss are in the northern Bering Sea and the southeastern Chukchi Sea, which are consistent with centers of high benthic oxygen demand, and high seafloor biomass. High biologic productivity increases the input of shells to the seafloor, but also increases their rate of loss, for a net result of very short windows of time-averaging per dead-shell assemblage. These results indicate that shell preservation is more strongly correlated with biological activity in the seabed than with the temperature and chemistry of overlying water, which is contrary to usual assumptions.

Historic Benthic Ecology. Semi-quantitative periodic benthic surveys began in 1845 and are archived in NHCs. The past geographic distributions of these bivalves can then be modeled with occurrence data to identify the southern or northern edges ("frontiers") of past populations; NHCs from the 1970s onward that overlap with the era of quantitative benthic survey data are used to evaluate the reliability of the older, pre-1970s collections. Using historic occurrence data for seven families from NHCs, bivalve communities underwent a significant reorganization in the interval

between 1940 and 1960. This reorganization included (1) the expansion of Nuculanidae populations southward into the Bering Sea, and (2) the expansion of Cardiidae populations throughout the region from the Bering-Sea occurrences where they had previously (1900-1940) been concentrated. Frontier positions based on NHCs do not differ significantly from those based on quantitative biomonitoring during the window of 1970-2000 when both data types are available. Historic observations on bivalve family distributions inferred from 150 years of NHCs thus indicate that the ecologic baseline inferred from the first quantitative surveys in the 1970s was at that point only a recently completed (1960s) reorganization of the benthic community; this reorganization, recognized using NHC data, had started in the 1940s, coinciding with the initial, 20th-century onset of seasonal sea ice retreat. A collections-based historic perspective on benthic populations in the Arctic over the past 150 years thus reveals that the close coupling of biological and physical changes through multiple climate shifts.

CHAPTER 1

HIGH-LATITUDE BENTHIC BIVALVE BIOMASS AND RECENT CLIMATE CHANGE: TESTING THE POWER OF LIVE-DEAD DISCORDANCE IN THE PACIFIC ARCTIC

1.1 Abstract

Time-averaged molluscan death assemblages sampled from tropical to temperate open continental shelves commonly disagree in species composition with local living communities only in areas that have changed in response to anthropogenic eutrophication and other locally intense human stresses, providing a means of recognizing shifted baselines. In contrast, the ability of live-dead discordance to resolve the spatially heterogeneous effects of human-induced climate change has not been tested in high-latitudes, where climate change entails substantial changes in nutrient cycling with consequences for benthic biomass and where cold waters are antagonistic to carbonate shell preservation. North Pacific Arctic and Subarctic seabeds offer ideal conditions for testing the resolving power of molluscan live-dead discordance, using well-documented ecologic changes in nutrient cycling and benthic biomass in response to reduced sea ice. Ecosystem monitoring since 1980 has established that the boundary between the Arctic and the Subarctic on the Bering Sea continental shelf, maintained by ice-influenced bottom water, shifted northward between 1998 and 2001. The benthic community in the transitioned area now experiences new pelagic predators, more variable quantity and quality of deposited food, and altered sediment grain size, and macrofaunal dominance has shifted from diverse communities of specialized suspension or deposit feeders to facultative deposit feeding guilds. We find that in habitats where either Subarctic or Arctic conditions have persisted, bivalve death assemblages agree closely with counterpart living communities in taxon and guild composition and are not subject to significant post-mortem bias. Significant live-dead discordance occurs only in areas with documented changes in carbon delivery, sediment grain size, and community composition over the last several decades; there, death assemblages are mixtures of shells

from pre- and post-transition communities, as confirmed by monitoring data. This spatial pattern is robust to both numerical abundance- and biomass-based measures of community composition. In fact, biomass is especially powerful in revealing fine, station-level discordance that is strongly tied to known sites within habitats where new carbon deposition levels, grain size, or benthos have occurred since 1980. Live-dead discordance can thus reliably differentiate between stable and rapidly changing habitats in cold, high-latitude settings, relevant to evaluating climate change, and biomass-based currencies of community composition are as robust as numerical abundance data, and in fact, improve spatial resolution.

1.2 Introduction

Extensive field studies by geologists in temperate and tropical latitudes demonstrate that a time-averaged accumulation of empty mollusc shells on the seafloor — a "death assemblage"— sums input from communities over many decades, and thus has potential to register ecological changes over much longer periods than typically encompassed by biomonitoring and other observational data, which rarely start before the 1970s [for review see 164, 161]. Moreover, meta-analysis finds that significant live-dead discordance in molluscan species composition is associated only with recent human-driven change in the benthic community, not natural variability [160], confirmed by focused tests [e.g. 37, 95, 105, 109, 288]. Comparing the numerical abundances and diversity of species and functional groups in death assemblages with counterpart information from living assemblages in the same habitat thus allows an investigator to detect whether today's community is shifted from earlier states, and the longer the duration of time-averaged shell accumulation, the longer the ecological memory of the death assemblage.

The fidelity of death assemblages to living communities has, however, never been tested under the aggressive postmortem conditions of high-latitudes, where overlying water can be under-saturated with respect to calcium carbonate, at least seasonally [147], and the ability of live-dead comparison to detect human-induced climate change has never been tested at any latitude, with

the exception of [245] that recently tested this change using several commercial mollusc species. Live-dead comparisons have also focused almost exclusively on species' presence-absence and numerical abundance data, rather than their biomass. Rare tests of biomass have been promising, showing that it can resolve past dominance [245, 287].

Here, we use bivalve death assemblages from North Pacific and Arctic shelves to advance live-dead analysis and paleoecological re- construction in these and other critical, high-latitude settings. In the few other Arctic assemblage studies, researchers have tested for unique taphonomic damage and whether enough material is preserved to yield meaningful results [115]. North Pacific Arctic waters pose a clear preservational challenge to biogenic carbonate. The low concentration of carbonate, the low temperature, and the intense activity of both microbial and macrobenthic communities can amplify processes leading to shell deterioration and loss [24, 202, 223, 224]. Notwithstanding these challenges, including low diversity even where shells are well-preserved, fully buried Arctic fossil assemblages can record significant paleoecologic changes such as deglaciation of the high Arctic Archipelago [9, 38, 115]. In light of this promise, Arctic live-dead discordance deserves quantitative testing in modern seabeds to assess its ability to detect changes in the environment caused by humans and secular warming.

The amount of time represented by Arctic death assemblages is still largely unknown, but the previously mentioned preservational challenges suggest a short window of time averaging. The high density of biologic activity on the northern Bering and Chukchi shelves would contribute to postmortem shell loss, despite the continual addition of new skeletal debris to the death assemblage [52, 124], particularly as the productivity of these marine shelves has the capacity to mix and irrigate to core-depths $\geq$ 18 cm despite moderately high sedimentation rates (median 0.12 cm/yr; [52]). The median postmortem age of a shell in an Arctic death assemblage is thus likely much younger than in counterpart temperate-shelf death assemblages, where median ages are 50-100 years (e.g. southern California Bight; [305]). Despite projected high rates of shell loss, a small subset of shells are likely to survive from previous millennia, much as they do elsewhere (e.g.

maximum shell age ≈ 8000 years in the southern North Sea [99] and ≈ 10,000 years on the southern California middle shelf [305]; for review, see [161]). For now, we expect each hotspot to reflect a similar window of time- averaging, with median ages < 100 years and a centennial rather than millennial total duration; geologic age-dating is in progress.

Extensive observations in the North Pacific Arctic, conducted by a multi-institutional consortium across ?10 degrees of latitude, have established a known gradient of biotic reaction to climate change over recent decades, making it an ideal setting for testing the fidelity of high-latitude death assemblages and, in particular, the power of live-dead discordance to detect ecological change. The DBO was established to monitor the response of ocean chemistry, circulation, seabed conditions (organic and nutrient flux, sediment grain size), and biological communities to climate change, particularly sea-ice retreat, focusing on several "hotspots" of persistently high macrobenthic biomass [43, 215]. These and other observations have established a strong coupling between physical oceanography, primary productivity, and the living infaunal community [119, 132, 130, 120]. Regional response to the retreat of sea ice during the last 20 years has manifested as a "softening" and northward movement of the Arctic-Subarctic boundary, which was initially defined by extensive seasonal sea-ice cover and a very cold (< -1 °C) bottom water layer south of St. Lawrence Island [133].

The "Subarctic" Bering Sea ecosystem is characterized by seasonal ice cover in the middle-to-northern regions, variable primary production, and a high level of pelagic and demersal fish production and co- incident pelagic predator levels. The Northern Bering Sea is a transition region between Subarctic-Arctic conditions, with the Northern Bering Sea supporting smaller bivalves of the F. Nuculidae (deposit feeder) and F. Tellinidae (facultative deposit feeder) [119, 293] compared to larger bivalves (F. Tellinidae, F. Cardiidae, F. Astartidae) in the more Arctic Chukchi Sea to the north. In the Northern Bering Sea, the diving spectacled eider *Somatera fuscgeri* consume the smaller Nuculanidae and Tellinidae bivalves whereas walrus *Odobenus rosmarus divergens* feed on larger Tellinidae and Cardiidae bivalves in the same region [50, 119, 128]. In response

to recent warming seawater conditions, the Subarctic ecosystem in the northern Bering Sea has expanded northward into the ”Arctic” southern Chukchi Sea, creating a gradient of Subarctic to Arctic conditions through the Bering Strait to interface with the ”Arctic proper” which has more extensive ice cover with later retreat, colder and more nutrient-rich water, and higher primary productivity carbon export to the sediments, all that support rich benthic faunal populations and benthivore predators [119].

Environmental conditions and faunal composition have changed to different degrees in each hotspot across the Pacific Arctic region, often with change focused on single stations within each hotspot rather than pervasively throughout a hotspot [112, 111]. In general, the Northern Bering Sea (DBO1) hotspot has been relatively productive, but shows changes in composition as well as declining biomass at some stations, with increasing but persistent Subarctic influence [125]. For example, the Spectacled Eider and their preferred bivalve prey (F. Nuculanidae) have been declining in the Northern Bering Sea with the increase in the smaller, less preferred small bivalve (F. Nuculidae) [50, 123]. In contrast, the northern DBO2 hotspot in the Chirikov Basin just south of Bering Strait and the DBO3 hotspot in the SE Chukchi Sea have each undergone varying levels of community transition from more Arctic to Subarctic conditions as sea ice retreats earlier coincident with warming seawater seasonally. The newly variable productivity and biomass in DBO2, DBO3, and even the NE Chukchi Sea DBO4 region are associated with increased current flow through the Bering Strait, increasing variability of carbon deposition in the Chukchi Sea over the last 10-20 years, and more northern movement of gray whales and other subarctic marine mammals [29, 119, 128, 121, 272].

This well-established framework of spatial and temporal variation in benthic communities suggests that (1) live-dead agreement in community composition and structure should be highest in the relatively stable hotspots (DBO1 and DBO3) and poorest — overall but particularly at a station-level — in the transitioned hotspots (DBO2 and DBO4). (2) Observed live-dead discordance should match known changes in community dominants (i.e. death assemblages should contain a

mixture of dominants of past and present community states). (3) Given the potential for postmortem bias in species' preservation under aggressive high-latitude waters, live-dead agreement will not necessarily be 'perfect' even in hotspots or stations known to have experienced little ecological change; these sites will provide a benchmark for analytically correcting death-assemblage data from other sites for taphonomic bias. The availability of biomass data from variable DBO regions also permits (4) a novel taphonomic test of this ecological currency, moving beyond presence-absence and numerical abundance data and expanding live-dead analysis to ecosystem science.

Using DBO death assemblages, this study aims to answer the following questions:

1. In cold water with potentially low rates of preservation, do death assemblages reliably reflect spatial patterns in the raw abundance and composition of living assemblages?

2. Is biomass more sensitive than numerical abundance in using death assemblages to detect spatial and temporal variation in benthic communities?

3. Can live-dead discordance detect known ecological shifts related to climate change?

1.3 Methods

1.3.1 Bivalve living and death assemblages

Living and death assemblages were acquired from benthic samples collected by the Arctic Research Group (ARG; Chesapeake Biological Laboratory/UMCES) during a summer 2014 cruise of the Canadian Coast Guard Ship Sir Wilfrid Laurier (SWL14). Sampling stations were distributed among four areas of known high benthic biomass (DBO hotspots; Figure 1.1): five stations from DBO1 and ten from DBO3, which are areas with productive benthic communities that have been regionally stable over the past decade, but punctuated by intense station level changes; and four stations from DBO2 and six stations from DBO4, where the benthic community is less productive and more heterogeneous, and environmental conditions have changed significantly [29, 119, 122].

At each station 1.1, two to five vanVeen grabs (0.1 m^2) were used to collect sediment and infauna, with the sample sieved through a 1 mm screen with seawater and then preserved in 10% seawater-buffered formalin. The species composition of death and fossil assemblages can, like living assemblages, be sensitive to sieve size, but processing using a 1 mm sieve has been standard for the ARG monitoring effort, as it is for many agency surveys. A study by Pirtle-Levy (2006) [242], at many of these benthic shelf hotspot sites found that, on average, 97% of the station macrofaunal biomass was caught on the 1 mm screen, compared to 3% remaining on the 0.5 mm screen, with more variable abundance levels on the combined screen size due to meiofauna and juvenile macrofauna. The collections on the 1 mm screen allow investigators to focus on adult individuals as opposed to juveniles and larvae, whose living abundance is more sensitive to the timing of a survey and whose dead shells are especially prone to post-mortem destruction [157, 158, 172]. In the Bering and Chukchi Seas, small-bodied taxa (1-2 mm) such as Thyaisridae and Thraciidae are present both alive and dead, but comprise a very small proportion of bivalve biomass (see 1.4). Thus, for the analyses here focused on biomass and only one cruise's worth of data, the 1 mm sieve size was deemed sufficient to capture the composition of living and death bivalve assemblages.

The sampled living assemblage was sorted and identified to the family and species level by the ARG, and then archived in 50% propanol [127]. The remaining shell-rich residue from the sorting process was dried and identified at the University of Chicago. An empty bivalve shell or shell fragment was considered an individual if it was adult (body size >1 mm) and retained ≥50% of the hinge line, as is standard in live-dead analysis [164]. Each dead bivalve was identified to the lowest taxonomic level possible using print resources shared between the UMCES ARG and UChicago [46, 102] and using two digital voucher collections (one created by the first author during visits to the ARG, and the other created by ARG collaborators to coordinate invertebrate researchers on the DBOs; [156]). With these resources, bivalve families and most species could be confidently identified using shell morphology. Each family represents a single guild, and thus family-level

identification suffices to differentiate living communities among DBO hotspots, and even poorly preserved shells can be confidently identified to the family level.

For both living and death assemblages, bivalve abundances were reported as individuals per m^2 of seafloor and reflect pooling of all samples (replicates) collected at a given station in 2014. Assignment of bivalve taxa to guilds is based on both life habit (infaunal, epifaunal, nestling) and trophic group, following [300]: chemosymbiont-bearing, obligate deposit feeding, and facultative deposit-feeding infauna; suspension-feeding infauna, epifauna, and nestlers; and commensal. Predatory bivalves (e.g. cuspidariids) are not represented in the fauna.

Bivalve biomass (gC) was measured for living assemblages by the ARG using family level conversion factors developed by [293, 118] that converted total wet mass to grams of organic (soft-tissue) carbon. To acquire comparable information on the biomass (B) of death assemblages, we used the conversion developed by [207]:

$$B = \frac{\alpha}{\beta} * \frac{x}{\gamma} \tag{1.1}$$

Where α is a conversion from total wet mass to organic carbon mass, β is a conversion from shell mass to total wet mass, x is the measured fossil mass, and γ is an estimate of the percent of the original shell preserved as the fossil, which also serves as an estimate of post mortem damage. For bivalve shells showing evidence of intense postmortem dissolution (chalkiness) or other shell loss, we estimated biomass using a conventional method based on linear dimensions (e.g. [35]). Only bivalve shells that were sufficiently intact to be counted as individuals were used in the calculation of biomass. Both living and dead biomass are reported as g organic Carbon per m^2.

1.3.2 Live-Dead Comparison

Death Assemblage Fidelity

The fidelity of death assemblages to living assemblages is assessed two ways: (1) comparing the amount of bivalve material preserved per station (Figure 1.2), using both counts of individuals and biomass; this tests for the resolution of spatial patterns in secondary productivity on the seabed (Figure 1.2); and (2) comparing the proportional biomass of guilds within each biomass hotspot (Figure 1.3), a means of testing for differential preservation that might bias paleoecological inference.

Live-Dead Discordance

Live-dead discordance focuses on two measures of pairwise, live-dead similarity: (1) in taxon rank abundances, expressed as a correlation (Spearman's ρ), and (2) in taxonomic similarity, that is presence-absence corrected for disparate sample sizes (Jaccard-Chao Index), following the widely used approach of [164]. Rank-abundance correlation compares lists ordered by taxon abundance in the live and dead collections. A positive ρ indicates that taxa that dominate the living assemblage are also highly ranked in the death assemblages and that taxa that are rare in one assemblage are also rare (or absent) in the other; a ρ of 1 requires that taxa are ranked identically in both assemblages. The Jaccard-Chao (JC) index of taxonomic similarity expresses the proportion of taxa shared by two assemblages, using information on the numbers of singletons and doubletons to correct for 'unseen taxa' in the smaller sample [41]. A JC index of 1 indicates that the live and the dead taxa lists are identical, that is all species are shared. Here, both JC and ρ are calculated using bivalve families. The results are displayed on a cross-plot of JC versus ρ, where stations falling in the upper-right quadrat have the least live-dead discordance (high proportion of shared species, with those species having similar relative abundances both alive and dead). This method has previously only been used with numerical abundance data, and originally only at the habitat level, i.e. after

data from multiple stations had been pooled [160]. Here, both numerical abundance and biomass data are used, and discordance is evaluated at the station level.

Canonical correspondence analysis (CCA)

Canonical correspondence analysis (CCA) was designed to identify environmental gradients within community data, based on the theory that species sort themselves among sites based on their realized niche and physiological optimum [33, 299, 298]. With this theory as backing, CCA computes the χ^2 distances using the relative abundances of taxa among sites and taxa, to then find the relationships between environmental variables and the realized niches of the taxa sampled within the community at the sites (Figure 1.1 in [299]). This approach was chosen over nonparametric multidimensional scaling (NMDS) and detrended correspondence analysis (DCA) because CCA allows both a comparison of the environment and the community and the calculation of a statistical correlation between the matrices in the constructed space [33]. The CCA space was constructed using family-level data on bivalve biomass, producing a live (circle) and a dead (squares) data point for each station. A multivariate method, like CCA, is a necessary addition to live-dead comparison as the low diversity and uneven community structures in the DBO regions are likely to result in small changes in JC and ρ, limiting the sensitivity of the traditional live-dead cross plots (described in section 1.3.2).

Environmental data have been collected annually across the Bering and Chukchi Seas since 2010 as part of several multi-national efforts including the DBO [43]; longer time series from 1970 are available for many sites as part of the Pacific Marine Arctic Regional Synthesis (PacMARS; [121]). Here, in CCA, we consider the environmental parameters most important to benthic life and mediated by sea-ice cover and water circulation in the benthic zone: sediment grain size, specifically the weight-% of mud (<0.062mm, ≥5 phi); total organic carbon (TOC); total organic nitrogen (TON); and the carbon to nitrogen ratio (C:N), all based on surface sediment (top 1 cm of van Veen grab). However, because death assemblages sum bivalve communities over multiple

years rather than a single year, we focus on change in environmental variables rather than single-season observations. To do this, for each station, the linear trend in a variable over the length of the measured time series (variable/yr) was found using the sediment variables gathered in the PacMARS between 1970 and 2012 [122], SWL cruises in 2013-2014 [122], subsequent SWL cruises in 2013 and 2014 [126, 127] and the Chukchi Sea Environmental Studies Program (CSESP) from 2007 to 2014 [30, 320]. Environmental change is displayed as arrows in the direction of the greatest positive trend in that variable. All spaces were constructed with the cca() function in the R vegan package [228].

1.4 Results

1.4.1 Comparison of bivalve abundances

In numerical abundance, dead-shell assemblages contain on average 3.2 individuals per live individual sampled, with per-station dead:live ratios ranging from 0.6 to 6.2. Death assemblages also contain more bivalve biomass except for one station, with an average of 18 grams of organic-C biomass (extrapolated from preserved shell mass; [207]) for every gram in the counterpart sample of the living assemblage (Figure 1.2). Larger average body sizes are also found in the death assemblages than in living assemblages, as suggested by the representative photographs in Figure 1.3. Death assemblage sample sizes from standard benthic grabs are thus sufficiently large to support confident analysis, containing three times more individuals and much more biomass than the standard minimum of 1 g/m2 generally required for living biomass.

1.4.2 Comparison of Bivalve Guilds

With few exceptions, all seven guilds were found both dead and alive: in each DBO hotspot, the high functional diversity (6 or 7 guilds) observed in living assemblages is maintained in death assemblages (Figure 1.3). Epifaunal suspension feeding bivalves were the only exception,

occurring alive-only in one area (DBO2) and dead-only in another (DBO3), but occurring in such small numbers (singleton specimens) that intolerance of benthic conditions rather than sampling is the likely explanation. They occur in substantial numbers both alive and dead in the other two hotspots (Figure 1.3).

Guilds also represent similar proportions of biomass in death and living assemblages in all hotspots (r^2 ranging from 0.775 to 0.9464; Figure 1.3), even though the dominant guild varies among areas: obligate deposit feeders in DBO1, facultative deposit feeders in DBO1 and DBO3, and infaunal suspension feeders in DBO4 (Figure 1.3). Chemosymbiotic taxa (Lucinidae and Thyasiridae) constitute a greater proportion of living than dead biomass in all four areas. This bias against dead chemosymbiotic taxa is likely due to their relatively small sizes (1-5 mm valve height): most dead shells and living individuals of other species are larger-bodied, suggesting that preservation under these cold-water conditions selects against small individuals and thus small-bodies species. No other consistent live-dead difference emerges among bivalve guilds.

1.4.3 Comparison of Bivalve Taxonomic Composition

Using both numbers of individuals and biomass as currencies of abundance, death assemblages closely resemble counterpart living assemblages, with stations falling mostly within the upper right (high live-dead agreement) quadrant of the cross-plots of taxonomic similarity and rank-correlation in Figure 1.4. A high proportion of families are shared between living and death assemblages at each station, and families that dominate (or are rare in) one assemblage tend also to dominate (or are rare in) the other. Differences do appear between hotspots and among stations within hotspots (Figure 1.4). Regional trends among DBOs are most apparent in numerical abundance (Figure 1.4A), the standard currency for live-dead comparison. Regionally, stations in DBO1 and DBO3, which are both highly productive and relatively stable [119], all exhibit very high live-dead agreement and plot closely to one another in the upper right corner (Figure 1.4A). In contrast, stations in DBO2 and DBO4, which are more spatially heterogeneous [119], exhibit lower live-dead agreement and

greater between-station differences (Figure 1.4A).

Live-dead agreement is also very high for biomass data, except for five stations (Figure 1.4B). These five stations – SLIP3 from DBO1, UTBS4 from DBO2, SEC3 from DBO3, and DBO4.4 and DBO4.2 – are all being monitored for either biotic or environmental change because they are among the stations positioned in transition zones between water masses [51, 118, 122, 293]. The proportional biomass of guilds at the station level also shows large discordances (Figure 1.5). In general, facultative deposit feeders (Tellinidae) are more abundant in living than in counterpart death assemblages, which tend to contain a greater diversity of guilds.

1.4.4 Variation in bivalves with the environment

Canonical Correspondence Analysis (CCA) indicates that live-dead differences in family composition are associated significantly with large net changes in environmental parameters (Figure 1.6; p-value = 0.027). This association preserves known changes in the most highly variable and heterogeneous DBO regions. For example, the DBO2 and DBO4 hotspots (gold and blue icons in Figure 1.6) comprise benthic communities known to have changed significantly in past decades, and the environment there has become muddier and more carbon-rich, in general. The stations in the DBO2 and DBO4 hotspots exhibiting large distances between living and death assemblages are aligned with stations experiencing increasing mud and TOC (Figure 1.6) [119, 124, 122]. In addition, the five stations exhibiting high live-dead discordance in Figure 1.4 maintain large separations between living and death assemblages in this CCA space (icons with black outlines, Figure 1.6). The relationship between changes in the environment and live-dead discordance can be seen most clearly within DBO1, which is regionally stable but has recently undergone large station level shifts (red icons in Figure 1.6). In DBO1, death assemblages fall in the lower left quadrant of CCA space, associated with the obligate deposit-feeder Nuculanidae, relatively high nutrients, and coarser grain size. In contrast, living assemblages of DBO1 are in the upper right quadrant, associated with the facultative deposit-feeder Tellinidae, which are common alive in all

four hotspots, and with fewer nutrients and finer grain sizes. Assemblages from other DBO hotspots show a similar but less strong live-dead separation, generally with a more trophically diverse death assemblage and a living assemblage dominated by a single family common throughout the region (usually Tellinidae). These environmental gradients do not align precisely with a change in a single environmental variable, but instead align weakly with a change in both sediment TOC and TON content and with grain size composition (Figure 1.6).

1.5 Discussion

1.5.1 Ecologic Fidelity of high-latitude Death Assemblages

Despite cold waters that present challenging conditions for shell preservation, expected to lead to low ecological fidelity, we found strong positive and statistically robust relationships between living and death assemblages in hotspots known to have relatively stable environmental conditions and community compositions. Live-dead discordance was encountered only in hotspots known to have transitioned in recent decades, and that discordance was of the type predicted by known changes in the benthic community. Both results indicate that these high-latitude death assemblages are useful ecological records of local conditions over at least decadal scales. Live-Dead discordance was not focused in one hotspot or habitat. Each of the five stations exhibiting live-dead discordance in biomass — SLIP3 (DBO1), UTBS4 (DBO2), SEC3 (DBO3), DBO4.2 and DBO4.4 — has different dominant water masses and grain sizes, and each station represents a known ecologic shift in the benthic community (see section 4.2). Taphonomically, death assemblages from these five stations range from high (>500 individuals; SLIP3 and SEC3, DBO 4.2) to low (100-50 individuals; UTBS4, DBO4.4) abundance and biomass. Overall, the DBO housed relatively small numbers of dead shells — a dead:live ratio of ≈3, compared with a global median of 8 for tropical and temperate settings (Kidwell, 2013) — is consistent with a high rate of post-mortem shell loss and a short window of time-averaging. However, the range of sample sizes and habitats in both

well-agreed and poorly-agreed stations argues against a consistent preservational bias, as does the spatial matching of discordance to observed temporal changes mentioned above. Live-dead discordance thus most likely reflects ecologic change in hotspots rather than preservational bias. Thus, although Arctic death assemblages are less abundant and less diverse than their temperate and tropical counterpart [305], the dense secondary productivity of the Alaskan shelf still supplies sufficient material to assess ecologic change using death assemblages, especially with biomass as an added paleoecologic currency (Figure 1.2). The largest-bodied taxa include Tellinidae (maximum valve height >45 mm), Cardiidae (60 mm), and Astartidae (a few >34 mm). However, other smaller-bodied taxa are regularly collected near their maximum recorded size (e.g. Nuculanidae >15 mm; pers. comm. David Jablonski 2017). All taxa are represented by a broad range of individual sizes, from the minimum of 1-2 mm to the larger sizes listed previously. Small and large body sizes are found throughout the region with no apparent bias based on the hotspot. Areas with coarser grain sizes (muddy sand in select stations in DBO4 and DBO2) contained more shell fragments and fewer small dead individuals, but these stations still contained suitable sample sizes (>30 individuals) and the grain size had no clear correlation with high or low live-dead agreement. Fossil assemblages of all ages commonly contain few specimens of ontogenetically young individuals, regardless of adult body size and despite the high mortality expected among young individuals, suggesting that shell loss is not a simple function of shell size (Kidwell, 2013). In death assemblages from our study area, few specimens are smaller than 5 mm in length, regardless of species, and maximum shell sizes are larger than are observed in counterpart living assemblages. Larger bodied individuals are also more abundant in death than living assemblages in the study area, which may arise from three possibilities, not mutually exclusive. First, large shells might be preserved more readily than small shells, which is both expected and observed for fossil assemblages in general [53, 59, 162, 308]. Second, finding larger body sizes in past generations is consistent with anecdotal evidence that bivalves in the region have been getting smaller since the 1970s [92, 112, 218, 293]. Third, van Veen grab gear is less effective in sampling larger bodied and thus deeper burrowing living

individuals, making them appear to be proportionally more abundant dead than alive [246]. To test for such an artefact, we re-ran our JC and ρ analyses omitting large dead shells (>30 mm Height and >0.42 g valve mass) and found that overall live-dead agreement decreased slightly but remained high in both abundance and biomass and the 5 stations with lower biomass live-dead agreement maintained their discordance (stations identified in section 3.3). A secular reduction in adult body size might have several drivers, including increased mortality from pre-mortem dissolution and bioerosion heightened by ocean acidification [112] or a decrease in body size due to increasing bottom water temperature [197, 218]. For example, stations within DBO3 and DBO4 are known to have bottom waters that are undersaturated in aragonite today [112, 201, 239]. Ocean acidification in this region is progressing more rapidly and over a more extended period than is increasing bottom water temperature, which has remained relatively stable until recently [286, 321]. In late 2018, after the SWL14 survey, bottom water temperatures increased above 0°C in DBO1 for the first time (bottom water anomalies $\approx$ +2°C; [125, 286]). Whether this new temperature anomaly in DBO continues into 2019 and onwards is uncertain, and whether it will start affecting bivalve physiology on the Bering Sea Shelf, as well as allowing more demersal and pelagic predators access to the seafloor communities requires further study [111, 125, 128, 286]. As stated in [224], Arctic shells must persist through (1) bioerosion and dissolution while still alive, (2) bioerosion and microbial maceration after death, (3) abrasion, disarticulation, and fragmentation that increase reactive surface area, and (4) postmortem dissolution occurring at or just below the sediment-water interface [11, 103], although antagonistic porewaters are possible at any latitude (e.g. [13]). These stages of shell loss can leave different signatures as a function of shell microstructure and life habit [224]. However, in general, one expects preferential loss of shells with high-organic microstructures, shells constructed of crystallites having a high surface area to volume ratios, and small-bodied or very thin-shelled individuals [110]. Despite these limits, the ”taphonomically vulnerable” families of Mytilidae, Nuculidae, and Nuculanidae with reactive microstructure are all abundant in death assemblages and their rank abundances similar to that in living assemblages.

Members of Tellinidae, characterized by especially thin aragonitic shells, exhibit the same pattern (Figure 1.3). The similar proportional abundances of these ”vulnerable” taxa in both living and death assemblages in areas of little ecological change suggests the persistence of their populations over the duration of time-averaging, counterbalancing preservational biases that should favor other groups with relatively thick shells. Preservational conditions are arguably extremely difficult for all shell types, but families do differ strongly in preservation potential. Preservational caveats related to shell type and body size are thus essential to consider when interpreting Arctic death assemblages. However, in this system, they do not appear to be a barrier to confident paleoecological inference at the habitat level: every life habit represented in the living assemblage in a DBO is also found in the death assemblage there (Figure 1.3). Exceptionally, chemosymbiotic bivalves (Lucinidae, Thraciidae) were proportionally more abundant alive than dead, even if they remained a small part of the overall bivalve assemblage biomass (Figs. 3, 4). While evidence suggests that freshwater inputs, anoxic muds, and increasing temperatures allow chemosymbiotic bivalves to increase in number in Arctic ecosystems [138], the sample sizes examined here were too small to identify such a pattern. Future work will be aimed to examine the living and death bivalve assemblages for more small size fraction bias in Arctic death assemblages and possible recent changes in chemosymbiotic bivalve abundance within the DBOs. 'Live-live' comparisons among stations in the DBO4 hotspot, using the same metrics as used for live-dead comparisons, reveal more spatial heterogeneity than do live-dead comparisons (using biomass data, an average live-live Jaccard-Chao of 0.78 and average Spearman ρ of 0.54, compared to an average live-dead JC of 0.83 and ρ of 0.58). This spatial heterogeneity is confirmed by current benthic monitoring [30, 29, 125, 121]. Live-live discordance is only slightly larger than live-dead discordance, however, still falling in the upper-right, well-agreed corner of Figure 1.4. The low diversity and uneven community structures in the Arctic thus have little effect on taxonomic composition and rank abundance measures, and these measures should be paired with multivariate analysis to increase sensitivity. Multivariate analysis of proportional biomass data also reveals greater dispersion among living assemblages than death

assemblages in DBO4, but it is again very slight (Figure 1.6). Therefore, death assemblages are capturing the spatial heterogeneity in this region despite being time-averaged recorders of ecology, indicating that the time averaging window may be short due to the preservational caveats listed in this section. This study was somewhat challenged by small sample sizes, especially of the living assemblages. Typically, DBO benthic surveys are conducted over an entire summer, revisiting stations on as many as three cruises per season, and trends are compiled over multiple years of such summer sampling (e.g. [124]). Here, however, we acquired death assemblages from only a single cruise in order not to overwhelm the shipboard protocol, and thus we considered only the living assemblage from those same samples, as is standard in live-dead analysis. Despite using considerably smaller total numbers of individuals than is typical in live-dead studies, and only a fraction of the information ordinarily available to biologists on these living bivalve communities, significant patterns emerged.

1.5.2 Power of live-dead discordance to detect benthic response to climate change

Given preservational concerns and small samples, the results presented here probably represent a conservative estimate of the ability of live-dead discordance to detect changes in the benthic ecosystem in the last 10-20 years. These results are thus very encouraging for using death assemblages and live-dead comparison in other high-latitude and cold-water settings. Death assemblages from additional years and seasons would likely yield similar results, as most bivalve taxa in this region have long lives and experience multiple seasons. Although live-dead discordance does not identify all stations that are being monitored for ecological changes, the five stations exhibiting relatively high live-dead discordance (Figure 1.4B) are representative of three types of benthic transitions being recognized in DBO regions via biomonitoring:

1. A shift from a more diverse bivalve community toward dominance by Tellinidae. This change is exemplified by live-dead discordance at SLIP3 (DBO1) and SEC3 (DBO3) but occurs at

stations in each DBO region (Figure 1.4B; Figure 1.6). The Tellinidae shift is related to an increase in either sediment TOC to the benthos or decrease in sediment grain size, which have been mediated by sea-ice retreat altering bottom-water circulation in the Northern Bering and Chukchi Seas [112, 119, 183, 321]. The Tellinidae shift seems to be associated with a shift in hydrography and not necessarily the direction of that change. For example, within DBO1, a recent increase in Tellinidae is correlated with an increase in surface sediment TOC and a decrease in grain size, largely owing to the likely slowing of the Anadyr stream or variable seasonal current flow in the region. The community is so altered at these stations that it is now most similar to samples taken much farther north in DBO3, which has also seen a rise in Tellinidae biomass since 2004 [112, 119, 129, 281]. As freshwater inputs and temperature continue to increase across the shelf, this new dominance of Tellinidae is likely to be accompanied by an increase in the abundance of chemosymbiotic bivalves (Lucinidae and Thraciidae), such as already seen in estuaries and bays in the Arctic [138]. This shift towards Tellinidae, which are proportionally more abundant alive than dead, is unlikely to arise from taphonomic bias because the stations undergoing this transition contain abundant and diverse death assemblages (>500 individuals and >7 families). These death assemblages contain many other families with low preservation potential (e.g. Nuculanidae at SLIP3, Cardiidae at SEC3). In addition, Tellinidae maintain high ranks (1st or 2nd in DBO3) in the proportional biomass in death assemblages (Figure 1.5); but the discordance here results from Tellinidae of live assemblages unevenly dominating the community resulting in a much less diverse living assemblage (e.g. 54% Tellinidae in Dead SEC3 to 99% in Live SEC3; Figure 1.5).

2. A shift in dominance among groups within the same trophic guild, exemplified by live-dead discordance throughout DBO2 and especially at UTBS4. Monitoring data show that DBO2 once hosted abundant amphipods in a gray whale feeding ground, but amphipod dominance has waned since the 2000s and been replaced by polychaetes and, in some cases, facultative

deposit-feeding and suspension-feeding bivalves (Grebmeier, 2012). This change was not accompanied by large shifts in functional diversity among bivalves (see Figure 1.5). However, associated with this decline in amphipods, the dominant bivalve families have shifted within a functional group. For example, a slight difference in dominance from Yoldiidae in death assemblages to Nuculidae in live assemblages within the obligate deposit feeding functional group. Similarly, within the suspension feeding functional group, the family Cardiidae was found only in death assemblages at UTBS4 and the family Astartidae was found only in living assemblages at UTBS4 resulting in little discernible difference between live and dead proportional biomass of infaunal suspension feeding at that station (Figure 1.5) but live-dead discordance in the family composition (Figure 1.4). This shift in dominance is unlikely to be the result of taphonomic bias as taxa shift in dominance within a feeding guild, and do not follow expected bias for shell preservation (i.e. thinner/organic-rich mereologies are not always found more in death assemblages). Particularly in the examples provided from UTBS4, families with thinner shells (Yoldiidae and Cardiidae) are found in death assemblages in higher proportional abundance than more robust shells (Nuculidae and Astartidae).

3. A decline in the abundance of "Alaskan taxa" such as the infaunal suspension-feeding Astartidae, obligate deposit-feeder Yoldiidae, and epifaunal suspension-feeder Mytilidae (all more abundant dead than alive) is responsible for live-dead discordance at DBO4.2 and DBO4.4. At these two stations, the reduced proportional biomass of these taxa is compensated for by slightly higher abundances of Cardiidae, Nuculidae, and Tellinindae. The population decline observed in the 2000s of these once-dominant Alaskan taxa may be due to a combination of a recent increase in organic carbon and a more prolonged decline in aragonite saturation of bottom waters, beginning in 1975-1985 [58, 112, 239]. DBO 4.2 and 4.4 experienced possible ocean acidification conditions in summer 2017, (post-dating our 2014 live-dead data), with evidence of shell dissolution on living bivalves collected in 2017 (e.g. chalky mineral where periostracum absent, personal observation). In the past, ocean acidification in the Chukchi

Sea was associated with discrete upwelling events, but now corrosive, low aragonite saturation waters form and persist on the shelf for the majority of the year [58]. This prolonged exposure has the potential to alter the bivalve community through failed settlement and other early mortality of select taxa, particularly at the interface between the Alaskan Coastal water and rapidly moving shelf waters, such as those at DBO4. Bivalves collected in 2014 and 2015 were examined and subjected to ocean acidification (OA) experiments to determine the effect of these new chemical conditions in DBO3 and DBO4 [112]. The "Alaskan taxa" known to be in decline here, however, proved to be relatively resilient to OA conditions in the lab, whereas open shelf associated taxa such as Cardiidae, Nuculidae, and Tellinidae that increase in proportional abundance alive were more sensitive. In other DBO regions with less extensive OA, Tellinidae and at fewer stations Cardiidae and Nuculidae have continued to dominate the living community, contrasting with DBO4, where these taxa have shifted into top ranks, but the bivalve community structure has remained relatively even. Loss of the "Alaskan taxa" in DBO4 may be related to a combination of oceanic parameters and because of the region's heterogeneity, examining live-dead agreement in 2015 could show if the Alaskan taxa regained their dominance after longer exposure to ocean acidification [29, 112]. This shift away from "Alaskan taxa" is unlikely to be the result of taphonomic bias because both "Alaskan taxa" and the open shelf associated bivalves (Cardiidae, Nuculidae, and Tellinidae) are present in high abundances in living and death assemblages (e.g. typically >75 dead individuals per station) but in varying proportions in no clear relationship to their size or shell mineralogy (e.g. Alaskan: Mytilidae with calcite and high-organic nacre found in death assemblages and not live at DBO4.2).

Each of these ecologic shifts inferred from live-dead discordance is a documented ecologic change from macrobenthic time series started in the 1980s. Live-dead discordance is thus able to detect regional and local changes in the benthic bivalve community related to sea ice retreat in the last 10 years.

1.5.3 Biomass as a paleoecologic currency

Live-dead comparison based on biomass data can reveal spatially finer, station-level discordances than can numerical abundance data alone and is moreover linked more directly to changes in the hydrographic variables. Previous live-dead studies performed with biomass found similar spatial benefits and, because shelled molluscs are so much larger-bodied than numerically dominant polychaetes, allow the paleoecologist to work with a greater proportion of the total community [207, 247, 287]. Live-dead analysis has previously been performed almost exclusively using numerical abundance data [164]. Here, however, we wanted to bring paleoecological insights to the recent history of organic carbon biomass, linking to the 40-year record of benthic ecosystem monitoring of the Pacific Arctic [118, 119, 121, 293]. This long time-series of observations is rare in ecology and has established connections between physical processes, such as sea-ice loss, and primary and secondary productivity through pelagic-benthic coupling [50, 130, 132]. To take full advantage of our finding of robust live-dead agreement in Arctic waters, further work is needed to establish the amount of time represented in these time-averaged death assemblages and, in particular, the geologic age-range of specimens from species that are more abundant dead than alive. Such temporal calibration of changes within the last century can be accomplished by individually dating shells, as used to such ends elsewhere [171, 303]; using radiocarbon-calibrated amino-acid racemization, decadal (<50 year) resolution of shell ages should be possible. Despite these caveats, biomass-based live-dead analysis shows the ability of death assemblages to capture both regional shifts in dominance (Figure 1.5) and station-level community reactions to changes in the physical environment (Figure 1.6).

1.6 Conclusions

Bivalve death assemblages from a single cruise (SWL14) demonstrate that an immense amount of ecologic information is often discarded at the end of processing benthic samples for living animals. The fidelity of dead skeletal debris was tested here by comparing live-dead discordance to known

changes in the Pacific Arctic ecosystem. Here we use stations as a test of the spatial resolution of death assemblages and find that, regardless of ecologic currency, all stations show live-dead agreement of the expected kind — good where conditions have been stable, and poorer where they have transitioned — showing that stations represent a reasonable scale of spatial resolution for death assemblages on this productive shelf. The opportunity to use biomass and the station spatial scale allowed access to the large amount of data gathered by the DBO and other similar missions at these stations in the last 40 years. This view of the past can be used to test the strength of ecosystem linkages today, such as those emerging within the northern Bering Sea between community composition and sediment organic carbon content [183]. Death assemblages constitute a valuable and new kind of historical data that can add temporal depth to existing directly-observed Arctic time series, providing information on the community that lived in a station sometime before the time of benthic sampling. This study sought to test the reliability of high-latitude death assemblages in general, the power of biomass in particular as a new currency in live-dead analysis, and the ability of live-dead analysis to capture known shifts in ecology related to climate change. We found positive results on all three fronts: death assemblages are reliable averages of past community structure, differentiating areas that have changed from those that have been stable and with station-level resolution, especially using biomass data; live-dead discordance was not detected at every station that has undergone an ecological shift, but never exists where conditions have been stable, making live-dead discordance a conservative guide, as found in other, lower-latitude settings [160]. Regional and station-level variation in shell abundance is almost certainly a function of the net effects of locally high benthic production and the composition of bottom- and pore-water, a rich topic for future analysis. Quantifying the ages of shells in these death assemblages (work in progress) will determine the full scale of time-averaging of the assemblage and thus its historical reach, the better to determine the timing of changes in species' ranges and population sizes and to understand the dynamics of post-mortem shell loss. This promising test of the ecological fidelity of high-latitude death assemblages, despite taphonomic challenges, indicates that they should be more

fully exploited in high-latitude settings, expanding into areas without long records of biophysical monitoring, to gain information about previously unknown Arctic ecologic baselines.

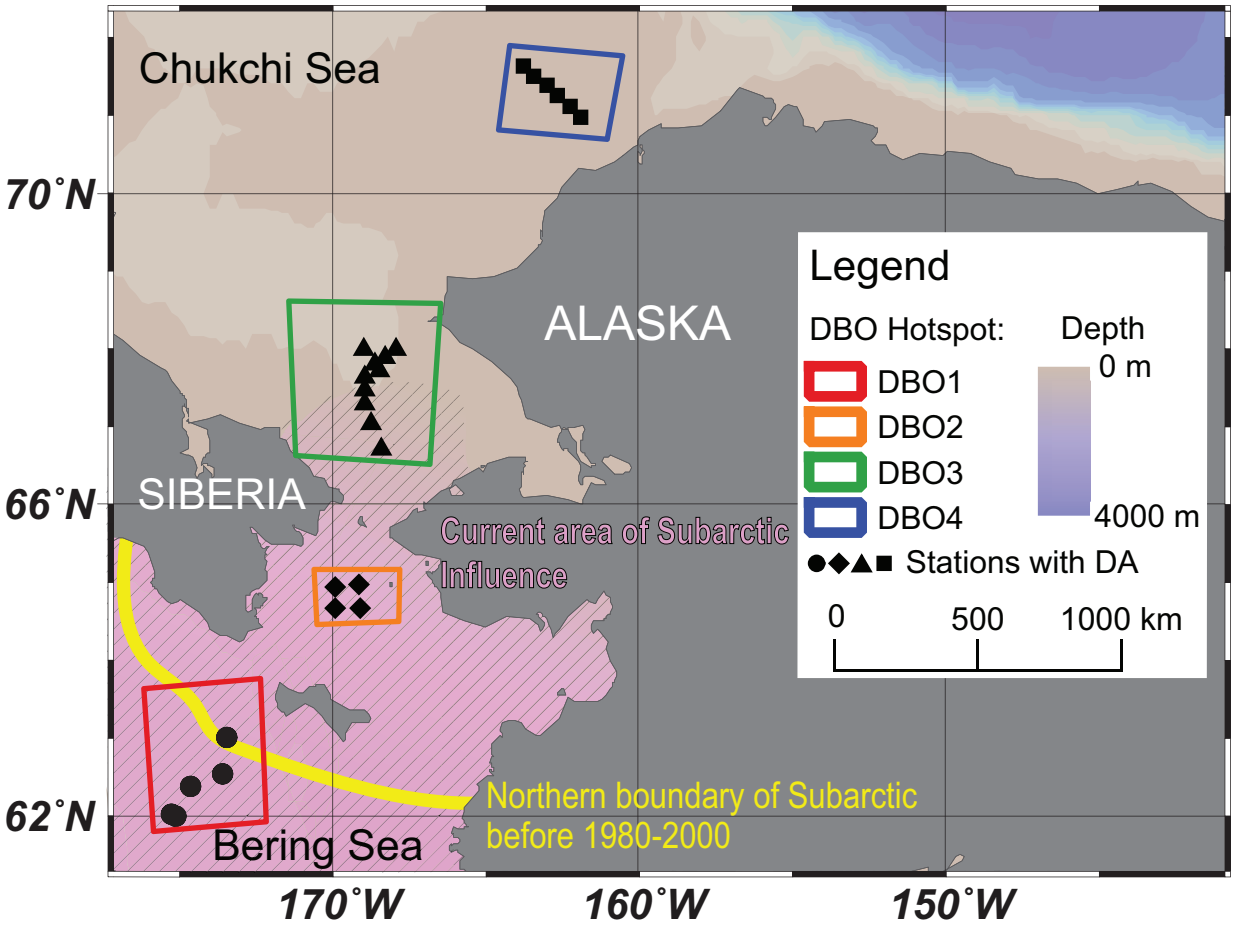

Figure 1.1: Map of the Distributed Biological Observatory (DBO) stations: Stations (black dots) sampled for bivalve live and dead assemblages during the summer 2014 CCGS Sir Wilfrid Laurier cruise. Analyses focus on data from four DBO 'hotspots' of high benthic biomass: the persistently subarctic northern Bering Sea (DBO1=red box, circle stations), the persistently Arctic Chukchi Sea (DBO 4=blue box, square stations), and areas in the Bering Strait and southern Chukchi Sea that began to transition from Arctic to subarctic conditions within the last 10 years (DBO2=orange box diamond stations, DBO3=green box, triangle stations). All DBOs in water depths 35-81 m

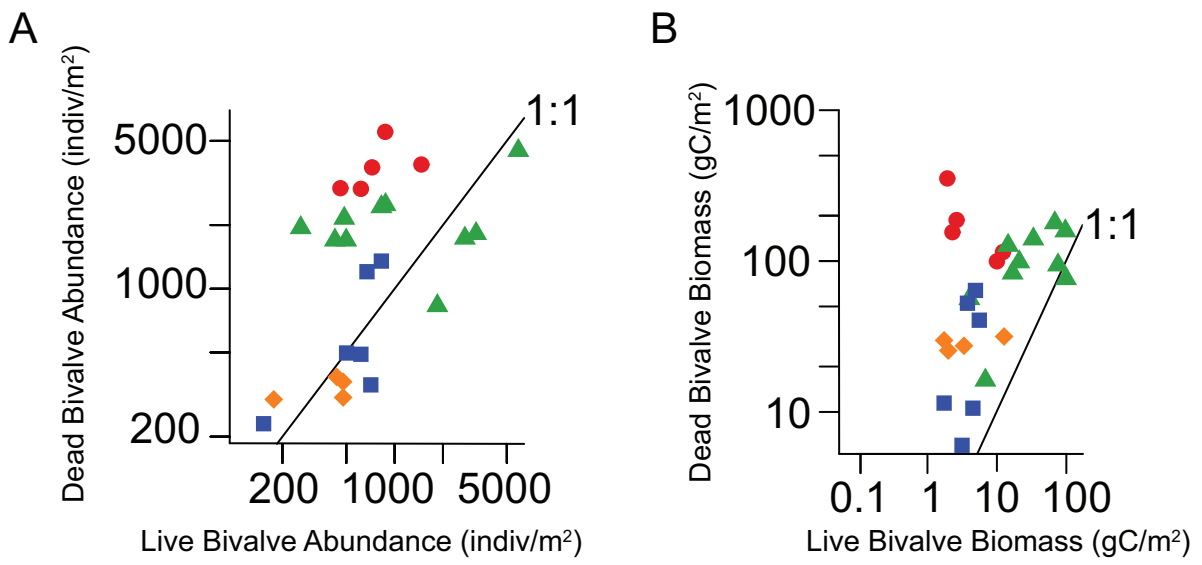

Figure 1.2: Station biomass and abundance comparison. Comparison of live and dead bivalve biomass (density, gC/m2) by station. Stations are color-coded according to the biomass hotspots as in Figure 1.1 (DBO1=red circles; DBO2=orange diamonds; DBO3=green triangles, DBO4=blue squares). Although the time-averaged dead biomass is almost always greater than the standing live biomass at a station (above the black line representing unity), commonly by several orders of magnitude, the ranking of hotspots by live density is preserved.

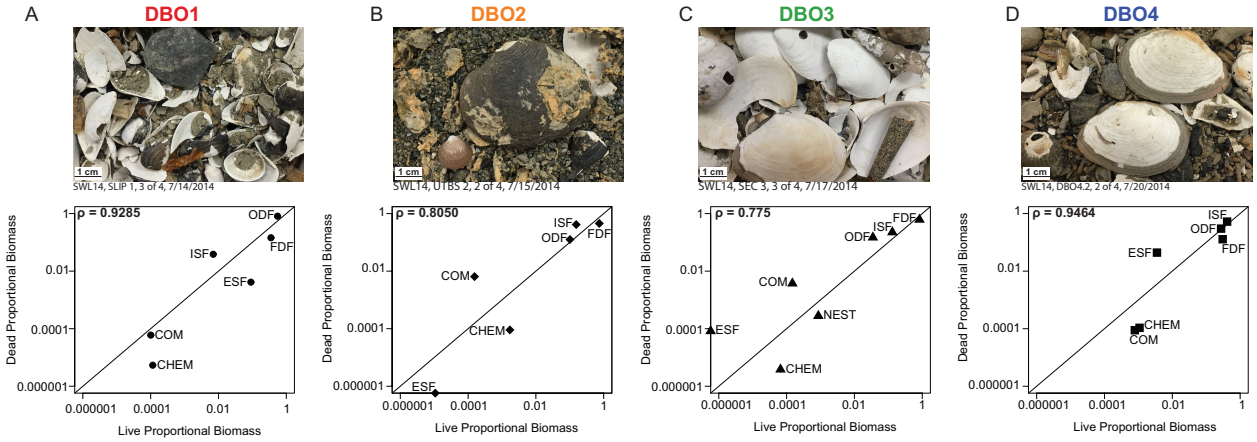

Figure 1.3: Hotspot Bivalve Guild Comparison. Representative death assemblages (top row) and bivariate plots of the proportional biomasses of bivalve guilds in live and dead assemblages by DBO hotspot. Data points appearing on axes indicate the guild occurred live-only or dead-only because 0 cannot be displayed on a logarithmic scale. The black line denotes 1:1. ρ on each plot denotes the agreement between live and dead functional groups at the hotspot spatial-level. Feeding guilds abbreviated as follows; ODF=obligate deposit feeder, FDF=facultative deposit feeder, ISF=infaunal suspension feeder, ESF=epifaunal suspension feeder, COM=commensal, CHEM=chemosymbiotic, and NEST=nestling.

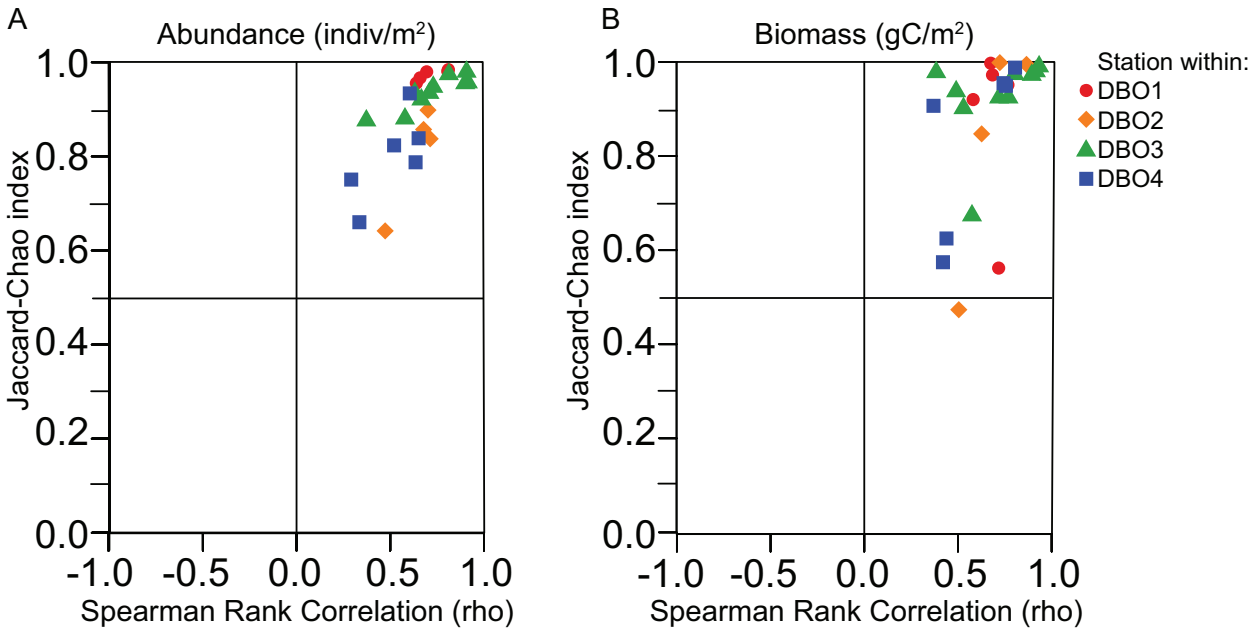

Figure 1.4: Live-Dead Agreement. Comparing the live and dead taxonomic composition (shared taxa; Jaccard-Chao index) and relative abundance (rank correlation; Spearman rho), where taxa are ranked using (A) numerical abundance (number of individuals/m^2; left diagram) or (B) biomass (gC/m^2; right diagram). Each dot represents live-dead agreement at a single station, color-coded by DBO hotspot (DBO1=red circles; DBO2=orange diamonds; DBO3=green triangles, DBO4=blue squares), and is based on family-level data (22 total families). Stations with very low sample sizes (< 10 dead individuals) omitted; stations with identical live and dead assemblages would fall at the upper right corner of the cross-plot. (A) Stations exhibiting the highest live-dead agreement are from the highest-biomass portions of DBO1 and DBO3.

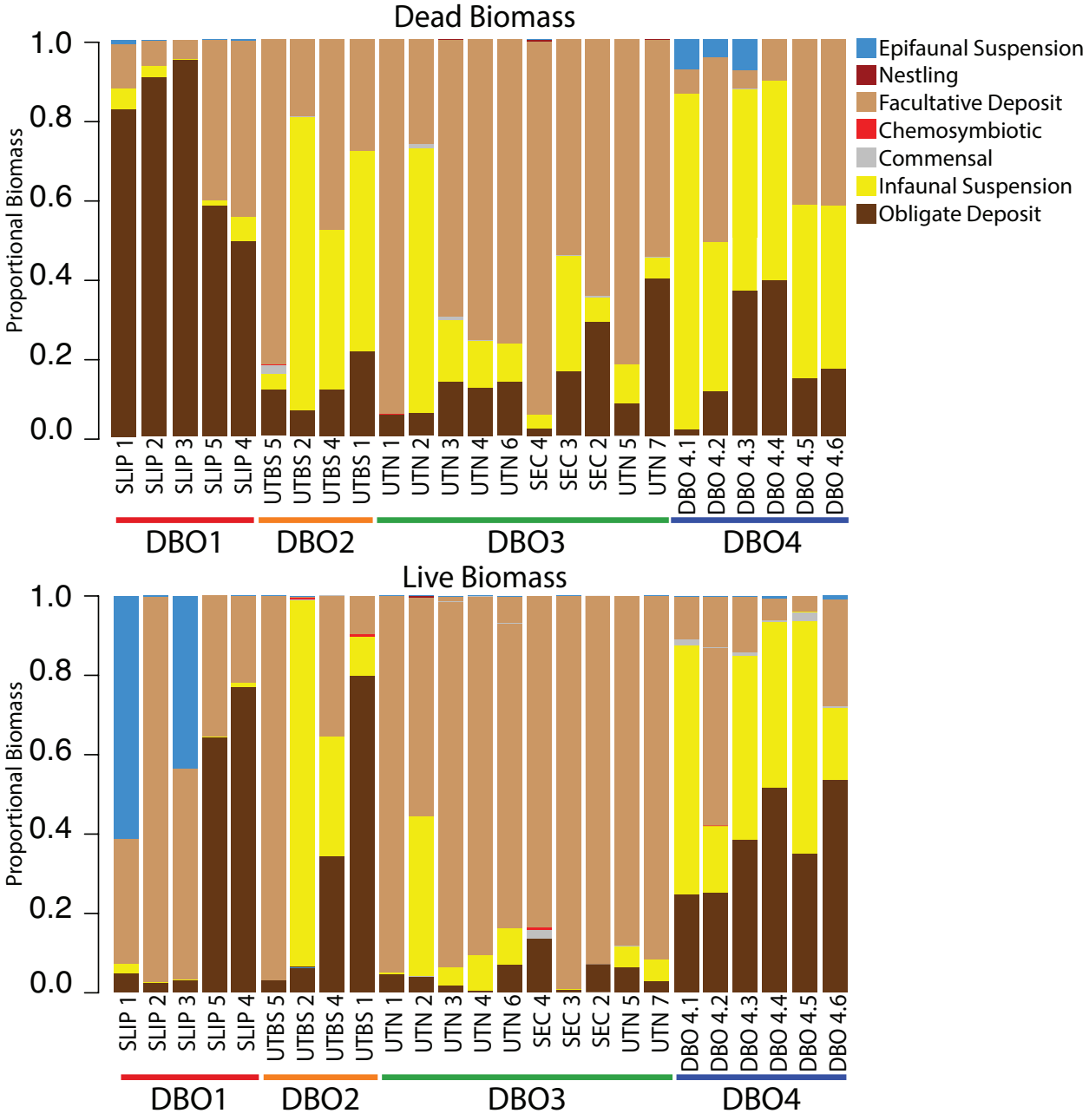

Figure 1.5: Biomass of bivalve guilds by DBO Station. Dead (top) and live assemblages (bottom) by station and by guild in proportional biomass. By guild, obligate deposit feeders are much more abundant dead than live in the DBO 1 and 3 stations, in DBO3 and at specific stations throughout the region. Facultative deposit feeders are most dominant in the 2014 live.

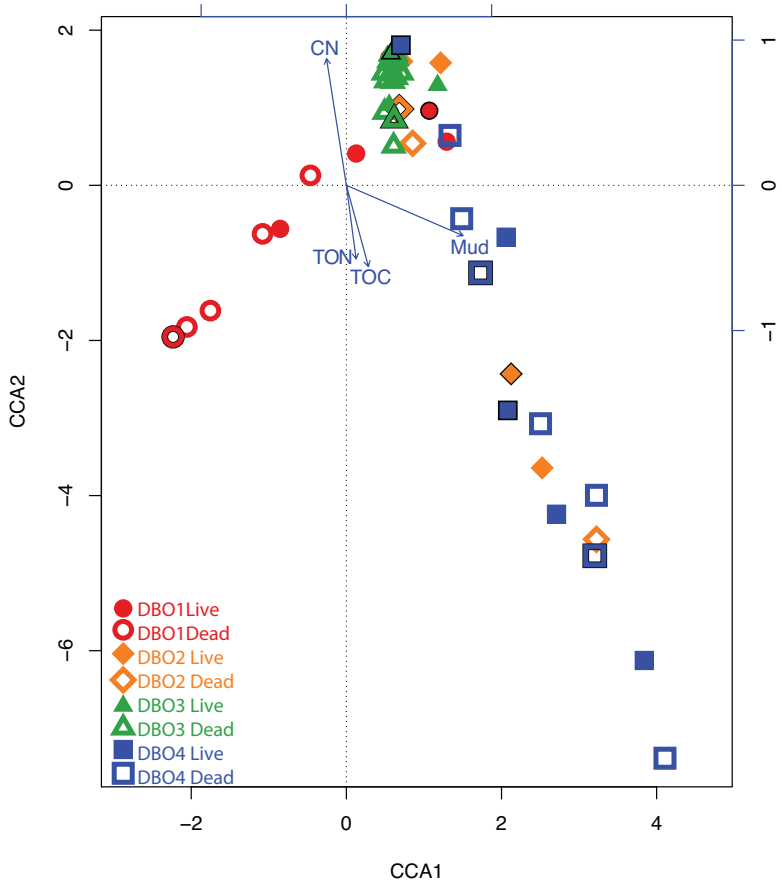

Figure 1.6: Canonical correspondence analysis of Live and Dead assemblages. CCA based on family biomass. Each point represents a live (closed shape) or dead (open shape) assemblage from a single station, which are color-coded by DBO hotspot (DBO1=red circles; DBO2=orange diamonds; DBO3=green triangles, DBO4=blue squares). The five points outlined in black fell outside the main group in Figure 1.4B (DBO 4.4 (blue), DBO 4.2 (blue), SEC 3 (green), UTBS 4 (orange), and SLIP 3 (Red)). Blue arrows denote the direction of increase in the annual value of an environmental variable: (C/N=carbon:nitrogen, TON=total organic nitrogen, TOC=total organic carbon, weight-percent mud) over the duration of in situ observations. The arrangement of these stations with these environmental variables is slightly significant according to Anova test (p-value=0.027)

CHAPTER 2

POREWATER VERSUS OVERLYING WATER CHEMISTRY: THE DOMINANT CAUSES OF BIOGENIC ARAGONITE LOSS IN PACIFIC ARCTIC

2.1 Abstract

The Alaskan continental shelf is characterized by high macrobenthic biomass, producing fully bioturbated seabeds with abundant dead shell assemblages, but the scale of time-averaging of such aragonitic remains in such high-latitude, cold-water settings is unknown. From overlying waters (OW) undersaturated with respect to aragonite, especially when combined with bioturbation and sediment irrigation, we expect higher postmortem loss rates and thus younger median shell ages than in tropical and temperate shelves, where median shell ages are typically 50-100 years and maximum ages are 10-20 ka. AMS-calibrated, amino acid racemization was used to date 213 shells from two aragonitic bivalve genera (*Macoma* and *Nuculana*) collected from the top 10 cm of 50-100m deep seabeds at three sites on the Alaskan shelf, each characterized by a different combination of benthic activity and OW aragonite saturation. We find that all shell remains of *Nuculana* were <1600 years old with a median age of 50 years, and all *Macoma* shells were <850 years with a median age <50 years. All assemblages experience fast initial loss rates, with decadal half-lives similar to those in warmer seabeds, but much slower net sequestration rates: a long tail of old shells does not develop, thus shortening the time-averaging window for paleobiologic inference. For most assemblages, rates of carbonate loss are best modeled by a one-phase loss model rather than the two-phase models used in lower latitudes. The highest loss rates are in the northern Bering Sea and southeastern Chukchi Sea, which are both well-documented centers of high organic flux to the seabed and high benthic oxygen demand, implying high aerobic decomposition and porewater acidification. Such conditions exacerbate shell loss, even though the strongest seasonal aragonite undersaturation of overlying waters is found elsewhere. These results quantify, for the first time

on geological (^{14}C) time-scales, (1) high aragonite loss rates in Arctic seabeds, (2) that loss arises from low sequestration, and (3) within this generally aggressive setting, loss rates are highest where benthic activity is highest, rather than where overlying water is most undersaturated, contrary to usual suppositions. Given their short window of time-averaging, Arctic dead-shell assemblages provide a high-resolution source of information for ecological analysis, largely reflecting the last 100 years of ecological history.

2.2 Introduction

Marine continental shelf facies dominate the fossil record, and so understanding the dynamics of aragonite loss and preservation in such settings is fundamental to paleontological interpretation [305, 283, 110, 44]. While accumulating in seafloor sediment, individual aragonitic shells have a characteristic residence period within the sediment surface mixed layer (SML) where they are subject to porewater conditions and reworking before being sequestered and permanently buried, thereby entering the fossil record (about 0 to 10-20 cm depending on the seabed) [305, 10, 304]. For example, in the top10 cm of the seabed of warm-temperate and tropical shelves, a majority of shells are lost rapidly, but those that survive the first several centuries – only 0.1-1% of all shells produced – can then persist for millennia [305, 164]. Thus, processes of shell loss within the sediment mixed layer play a large role in determining the content of the fossil record.

However, there have been no estimates of time-averaging or preservation in cold polar ecosystems, where a confluence of conditions that should be antagonistic to the long-term preservation of biogenic aragonite. Cold waters pose a well-appreciated preservational barrier for biogenic carbonate because of the sensitivity of the aragonite saturation state to temperature, creating a strong latitudinal gradient in carbonate dissolution (Figure 2.1). In this work we took advantage of the development of a Distributed Biological Observatory (DBO), which was established to monitor biophysical responses of several "hotspots" of persistently high benthic biomass to climate change and with sea ice retreat in particular [202]. These and other observations over the last xx

years have established a strong coupling between physical and chemical oceanography, primary productivity, and the benthic infaunal community [58, 123, 130, 132]. Three of these biological hotspots – in the northern Bering Sea (DBO1), Southeast Chukchi Seas (DBO3), and Northeast Chukchi Sea (DBO4) – are arrayed along a gradient of organic flux to the seabed, fed by slowing currents that allow particulate organic matter to settle to the seabed [58, 119, 55] (Figure 2.2). This organic flux feeds dense populations of benthic macrofauna, which in turn create bioturbated and thus well-aerated sediments; $C0_2$ produced from benthic respiration are thought to contribute, to seasonally strong acidification of bottom waters in both the Bering and Chukchi Sea (Table 2.1) [58, 105, 84, 202], and so strong aragonite undersaturation of sedimentary porewaters is likely. We thus expect (1) higher rates of aragonite loss in Arctic seabeds than in lower-latitude shelves related to the colder water conditions, but further expect (2) a gradient within the Arctic linked to variation in organic flux and conditions in the seabed itself, which could promote aragonite shell loss both from chemical dissolution (attack of mineral crystallites by metabolic pCO2 and redox cycling) and from microbial maceration (attack of shell organic matrix, which liberates crystallites from the microstructure) [110, 134, 216, 13, 14].

Dead-shell assemblages sieved from Arctic seafloors of the North Pacific offer an ideal opportunity to evaluate the relative contributions of bottom water aragonite saturation, and biologically altered porewaters, to the postmortem loss of biogenic carbonate. Long-term research and annual monitoring of physical, chemical, and biological conditions over the last 50 years have established that Pacific Winter Water is seasonally undersaturated with respect to aragonite in the northern Bering and Chukchi Seas (Table 2.1) [58, 202, 201]. From south to north, the saturation state of aragonite (Ω_{arag}) in this overlying water decreases, and becomes more prolonged (longer season) and more spatially extensive (larger proportion of shelf bottom waters affected). Each hotspot thus represents a different projected combination of aragonite saturation state in the overlying water and biologic activity within the seabed (Table 2.1). If the undersaturation of overlying waters are the primary cause of biogenic aragonite loss, then we would expect to see the youngest shell ages and

highest rates of loss in the Northeast Chukchi Sea, which is the region with the lowest average aragonite saturation state (Table 2.1) [203, 200, 201, 202, 241, 323, 57, 58]. If, alternatively, biologically-mediated porewater undersaturation (i.e., organic flux to the seabed from primary productivity, benthic respiration, and bioturbation) is the dominant cause of shell loss, then the youngest median shell ages and highest rates of loss should occur in the Southeast Chukchi Sea and the northern Bering Sea [125].

Here we use radiocarbon-calibrated amino-acid racemization (AAR) age-dating [154, 213] of two genera of aragonitic bivalves from this array of benthic hotspots (Figure 2.2) to (1) determine the scale of time- averaging of molluscan aragonite in the sediment surface mixed layers of high latitudes, testing for a first-order latitudinal gradient in the temporal resolution of paleobiological information, (2) quantify rates of aragonitic shell loss and sequestration in the Arctic for the first time, estimated by modeling shell age-frequency distributions (AFDs), and (3) map how shell loss varies spatially as a function of overlying water and biological activity. AAR dating allows for more accurate age estimates than radiocarbon dating alone, and matches the methods used in lower-latitude continental shelf death assemblage studies [164].

2.3 Methods

2.3.1 Study Area

We analyzed empty shells collected from eight stations within three DBO hotspots (Table 2.2) that encompass a gradient in conditions expected to be antagonistic to the preservation of aragonitic shells, namely: DBO1 - the northern Bering Sea, specifically the location of a winter polynya (open water area within sea ice) that forms persistently south of St. Lawrence Island; DBO3 - Southeast Chukchi Sea, just north of the Bering Strait; and DBO4 - the Northeast Chukchi Sea, off the coast of Wainwright, Alaska (Figure 2.2, Table 2.2). DBO1 is characterized by an intermediate level of biological activity with bottom waters that experience moderate seasonal

undersaturation of aragonite; DBO3 is characterized by high biological activity with mild seasonal undersaturation of aragonite; and DBO4 is characterized by low biological activity with strong seasonal undersaturation (Table 2.1).

2.3.2 Sample Selection

All bivalve shells were collected in 2014 and 2015 as part of sampling effort in the DBO program, during cruises of the Canadian Coast Guard Cutter (CCGC) Sir Wilfred Laurier to the Bering and Chukchi Seas [127, 215]. Bivalves were collected from three DBO hotspots located in the DBO1, DBO3, and DBO4 (Figure 2.2, Table 2.2). All bivalves were collected from silt-dominated sediments (phi modal grain size 5, 90% mud) between 40-75 m water depth, using 0.1 m^2 van Veen grabs and a 1 mm mesh screen. In total, 213 bivalve shells were selected for amino acid racemization (AAR) analysis (98 *Macoma* and 104 *Nuculana*). Shells were photographed, measured for height and width dimensions, and scored for postmortem damage using a 10x light microscope. A subset of bivalves was also examined using a scanning electron microscope (SEM) without coating (Zeiss Merlin SEM).

2.3.3 Amino Acid Racemization (AAR) Age Dating of Shells

Amino acid racemization is the change in the relative frequencies of left- ("L") and right-handed ("D") amino acid isomers during protein diagenesis, with the ratio equilibrating at 0.5 [213, 12, 154]. This D:L ratio can be used to estimate a relative age of a specimen post-mortem, with higher values indicating older post-mortem ages. Post-mortem calendar ages can be inferred by pairing the D:L values with an independent age estimate, such as from radiocarbon analysis using a calibration function [12].

Enantiomeric ratios of D- and L-aspartic acid and glutamic acid were determined for shells at the Amino Acid Geochronology Lab at Northern Arizona University. As part of AAR analysis, the shells of specimens collected alive inn 2014-2019 from the Bering and Chukchi Seas were

also measured to establish D:L ratios at the time of death, as an aid to calibrating AAR ages of dead-collected shells (Table 2.4). Aspartic is a “fast” racemizing acid and glutamic is a “slow” racemizing acid, and thus the combination of rates gives good temporal resolution for both younger and older shells.

Accelerated mass spectrometer (AMS) carbon dating of a subset of the dead-collected specimens was used to calibrate the D:L ratios of aspartic and glutamic acids (Table 2.5). Because so many shells were very young – the initial calibration indicated that many were “post-bomb” (<1950 CE) – a full calibration of the AAR data required that we create a post-bomb radiocarbon curve for the region. This was accomplished by AMS-dating a series of live-collected bivalve individuals collected between 1957 to 2019, using specimens archived in the Invertebrate Zoology collections at the University of Alaska Fairbanks (Museum of the North) and in the collections of Prof. Grebmeier at UMCES (Table 2.3). Radiocarbon analysis was conducted by staff at the University of California Irvine’s Keck Carbon Cycle Accelerator Mass Spectrometer facility. All AMS carbon ages were modeled with the OxCal software using the Marine13 curve with a local reservoir offset of $\Delta R = 436 \pm 135$ years [257, 205, 251]. The local "post-bomb" 14C curve created from these specimen is in Table 2.3.

Because so few specimen returned ages older than 1950 CE, most shells are best described as having three possible ages: (1) an age before 1950 that could be modeled using the Marine 13 curve alone; (2) an age that spanned 1950 as modeled using both the Marine 13 curve and our local post-bomb curve; and (3) an age younger than 1950 that was modeled using only the post-bomb curve. The three age estimates resulted in a total uncertainty of 60 years in the age estimate of each specimen. To reflect this uncertainty, we use three alternative age-calibrations for the AAR data (Table 2.5):

1. Old Calibration: age of shell AAR data modeled using only the Marine 13 curve with $\Delta R = 436(135)$;

2. Middle Calibration: modeled using both the Marine 13 curve with $\Delta R = 436(135)$ and

the local Post-Bomb curve, including specimen HA0277 collected alive in 1957 from Point Barrow; ranges include the lowest estimates from the Marine 13 curve, because distributions were truncated at 1950 CE; and

3. Young Calibration: modeled using both the Marine 13 curve with ΔR = 436(135) and the local Post-Bomb curve but excluding specimen HA0277.

All calibrated ages are median ages reported as years before 2020 CE. The age ranges are reported as intervals because the range boundaries were determined by the 95% confidence intervals of distributions in OxCal software, allowing for truncated distributions.

The AAR values of live-collected specimens detects any racemization of amino acids during the life of an animal: D:L ratios need not be zero at the time of death. All dead shell ages are reported after correction for this value. The reliability of individual AAR datapoints was assessed following the standards detailed by [170] for outliers. This procedure eliminated 11 samples (shells), for a final sample size of 202 shells with AMS-calibrated AAR age estimates (Table 2.2).

For each radiocarbon calibration, the relationship between DL values and radiocarbon age was tested against four models, using the methods described in [12].

1. Apparent Parabolic Kinetics (APK):

$$t = a_{APK}(R_t - R_0)^{b_{APK}} \tag{2.1}$$

2. Simple Power-Law Kinetics (SPK):

$$t = a_{SPK}(R_t^{b_{SPK}} - R_0^{b_{SPK}}) \tag{2.2}$$

3. Constrained Power-Law Kinetics (CPK):

$$t = a_{CPK}([\frac{1 + R_t}{1 - R_t}]^{b_{CPK}} - [\frac{1 + R_0}{1 - R_0}]^{b_{CPK}}) \tag{2.3}$$

4. Time-Dependent Reaction Kinetics (TDK):

$$t = a_{TDK}(arctanh[\frac{R_t - R_0}{1 - R_t R_0}]^b_{TDK} \approx a_{TDK} R_t^{1/(1-\alpha)} \tag{2.4}$$

$$a_{TDK} \equiv (\frac{1-\alpha}{k_0})^{1/1-\alpha} \tag{2.5}$$

For equations 1-5, t represents the estimated age, a is the inverse rate parameter for each model and b is estimated from the data with values greater than 0, and R is the DL ratio of the target amino acid, R_0 is the initial racemization (either 0 or estimated from the data), and R_t represents the DL ratio of the sample when measured. The uncertainty associated with each model was also compared to lognormal, and gamma statistical distributions [12]. We combined all samples of one genus, regardless of collection location for model fitting.

Each of the three age calibrations (Table 2.4) was modeled using aspartic and glutamic acids and the approach described by [12]. This method uses a Bayesian model fitting procedure to compare the data to the models listed above, estimating the mean age and uncertainty of the specimen using lognormal, and gamma distributions. Models were also tested using R_0 = 0 or R_0 estimated from the data, denoted by 0 or 1 at the end of the model name (e.g., SPK1; Table 2.6) The resulting models are a weighted combination of the best fitting models derived from this process, described in Table 2.6. The weights of each model were determined by Bayesian Information Criteria (BIC) statistics. An AAR calibration model was created from all models within 1 BIC of the best model. Since the BIC cut-off value is chosen by the investigator, several ΔBIC limits were tested. The ΔBIC limit was increased when the models within 1 BIC did not include calibration functions for both aspartic and glutamic acids (Table 2.6). If needed, the new BIC value was chosen to match previously published work (e.g., ΔBIC limit = 4 in [12] or ΔBIC limit = 6 in [105]), or to include at least one model for each amino acid (e.g., Old Calibration *Nuculana* ΔBIC limit = 8).

For many runs the overall non-parametric correlation between age and DL ratio was low (r-squared < 0.2, and p-value > 0.1; $*$ in Table 2.6). Models were forced to run regardless of this

correlation, as the correlation ages only spanned about 200 years and 0.1 units of the DL ratios. Correlations were strongest for the Middle calibration, which also represents the most reliable age dates. In total, nine shell age models were created to estimate the AAR ages of shells.

2.3.4 Shell-Age Frequency Distributions

Age-frequency distributions (AFDs) using calendar years were produced for each genus in each of the three DBO collection areas. Bins within the AFDs were all set at 200 years, which approximates the 150-year uncertainty in the AAR ages. This bin size also reflects the generally low racemization rates (slowed by low temperature) and by using a single calibration for the entire study area, rather than having separate post-bomb radiocarbon curves for the Bering and Chukchi Seas. Here we show smaller bins than 200 years to examine the differences between AAR calibration models, and the radiocarbon calibrations on the ages of shells. All ages are reported relative to 2020 CE.

2.3.5 Models of Shell Loss

Loss rates were estimated using both the one-phase and two-phase models of shell loss developed elsewhere [305]. Shell loss denotes the sum of all processes that destroy a shell (disintegration) or otherwise remove it from the sediment surface mixed layer (SML) of the seabed (e.g., permanent burial, [305]. In the one-phase model, shell loss from the sediment SML is modeled with one (exponential) loss rate, denoted as λ, which applies to a shell regardless of its postmortem age; therefore, λ represents both disintegration and burial out of the sediment SML. In the two-phase model, the sediment SML is divided into two phases: the initial phase, when shells reside in the surface, most taphonomically active zone (TAZ), characterized by a high loss rate (λ_1), and a second phase, when shells occupy a sequestration zone (SZ), characterized by a much lower loss rate (λ_2). τ describes the movement of shells from the TAZ to the SZ, i.e. the time required to attain sequestration, and can be interpreted as the net sequestration rate. In both models, shell loss from lateral transport away from a site and from permanent burial are both assumed to be

small; therefore, for the most part, both of the loss rates (λ) represent the actual disintegration of shells by some process (e.g., dissolution, maceration, and/or fragmentation into a taxonomically unidentifiable state) [305].

Shell AFDs were analyzed using both the one-phase and two-phase models to determine fit. Owing to the challenges of very young shells and high age-uncertainty related to the bomb-effect on radiocarbon, the AFD data were also tested against a 'truncated' form of the models. The truncated model offsets the "start" of the model by the age of the youngest shell.. That is instead of modeling loss rates from zero years postmortem, loss rates are estimated from the age of the youngest shell until the oldest shell measured [305]. The preferred shell loss models were determined by the lowest AICc values for each calibration model.

2.4 Results

2.4.1 Shell-Age Frequency Distributions

The Old, Middle, and Young AMS calibrations resulted in similar age estimates for each bivalve data set ((Figure 2.3, and Figure 2.4). For *Macoma*, the Young calibration resulted in the youngest median shell ages (27 to 30 years), with a very narrow interquartile range (IQR = 4-7 years; Figure 2.3, Table 2.7). The Middle age calibration resulted in slightly older median ages (36-42 years) and a similar IQR (6-19 years; Figure 2.3, Table 2.7). The Old calibration resulted in the oldest median shell ages (63 to 128 years), and a broad IQR (18-65 years; Figure 2.3, Table 2.7). Changing the ΔBIC limit (1 to 4) resulted in less than a 5-year change in the ages of *Macoma* shells. Regardless of calibration, mean and median postmortem shell ages for *Macoma* were consistently less than 150 years, and the oldest dated shell was 819 years (from DBO1, using the Young calibration; Table 2.7).

The Old, Middle, and Young AMS calibrations affect *Nuculana* ages similarly (Figure 2.4). However, all estimates are slightly older, with the oldest dated shell at 1513 years (DBO4 - Middle

Calibration) (Figure 2.4; Table 2.7). The Young Calibration resulted in the youngest median shell ages for *Nuculana* (51-54 years), with narrow IQRs (10-20 years). The Old Calibration resulted in slightly older median shell ages (76-88 years) and broader IQRs (35-65 years), followed by the Middle Calibration (99-118 years, IQRs 25-51; Table 2.7). Changing the ΔBIC limit of the model created a larger effect on the *Nuculana* shell ages than on the *Macoma* shell ages, particularly in the Young Calibration, where the ΔBIC limit set at 2 resulted in a 400-year increase in the total age range, while IQRs increased from 10 to 20 years. In all calibrations, mean and median *Nuculana* shell ages are less than 200 years (Figure 2.4; Table 2.7).

The scale of time-averaging varies slightly among the three sites. For *Macoma* shells, DBO3, which is characterized by the highest oxygen demand and presumably the most undersaturated porewaters, exhibits the least time-averaging of all three hotspots, regardless of the metric of time- averaging (median, IQR, maximum, total range) and the calibration used (Figure 2.3, Table 2.7). DBO4, the region expected to have the most undersaturated overlying water, exhibits the greatest time-averaging (excepting using the Young calibration, where DBO4 exhibits intermediate time-averaging). For *Nuculana* shells, the pattern is less consistent. DBO3 exhibits the least time-averaging using two models (the Middle calibration and the Young calibration version ΔBIC 1), and DBO4 exhibits the least time-averaging using the other two models (Old calibration, Young calibration version ΔBIC2, Figure 2.4, Table 2.7).

2.4.2 Shell-Loss Rates

All age calibrations, genera, and regions favored the truncated one-phase models, that is, where the rates of shell loss are best modeled using the youngest observed shell age rather than zero. The absence of extremely young shells in the most recent phase of production is an artifact of AAR and AMS dating uncertainties (Table 2.8). For *Macoma*, all but the Young Calibration was most consistent with the truncated one-phase model. *Macoma* at DBO3 showed the highest rates of shell loss for all age calibrations, yielding the shortest half-life of 15-30 years (Figure 2.5A). For all of

the supported one-phase models of *Macoma* (closed circles in Figure 2.5A), the lowest rates of loss are found in DBO4. For *Nuculana*, all but the Young DBO1 and Middle DBO4 were most consistent with the truncated one-phase model. Overall, *Nuculana* loss rates and half-lives are on the order of 10 – 35 years and exhibit less variation among DBO regions, except when using the Middle calibration (Figure 2.5B, Table 2.8). The middle calibration for *Nuculana* ranks regions in the same order as the *Macoma* shells (highest loss rates at DBO3 and lowest rates at DBO4).

For all truncated two-phase models the loss rates in the first phase (λ_1, within the TAZ) are equal to those estimated by the truncated one-phase model for both *Nuculana* and *Macoma* (Figure 2.5, Figure 2.6). Half-lives for the first-phase are between 10-110 years for both *Macoma* and *Nuculana*. For *Macoma*, the secondary loss rates (λ_2) are slightly slower than first-phase rates, with half-life estimates of 10-600 years. Only the Young calibration for *Macoma* favored the truncated two-phase loss models, with higher half-lives in the second phase (450-600 years; Figure 2.6). In this set of favored models, the lowest rates of loss are found in DBO1 and DBO3, with the highest rates of loss in DBO4, the opposite pattern as found in the first phase. The remaining models for *Macoma* do not show a consistent pattern across all regions. For *Nuculana*, the secondary loss rates (λ_2) are slightly slower than first-phase rates, and slower than the rates found for *Macoma*, with half-life estimates from 40-950 years (Figure 2.6). The two-phase truncated model is supported for the Young calibration in DBO1, and for the Middle calibration in DBO4 for *Nuculana*, with half-lives from 450-900 years. The remaining models for *Nuculana* excluding the Old calibration have the highest rates of secondary loss at DBO3.

The net sequestration rates (τ) from the two-phase models are consistently small (Table 8), that is the rate of change from λ_1 to λ_2 is slow or negligible in these Arctic sediments. For *Macoma*, the mean time to sequestration ($1/\tau$) is 65,000-2,000,000 years, and for *Nuculana* it is 20,000-35,000 years for supported models (Table 2.8). That is, sequestration fails to occur.

2.5 Discussion

2.5.1 Challenges of Arctic Age Dating

These results represent the first estimates of the scales of time-averaging and the rates of shell loss in Arctic seafloor sediments. However, the Arctic seafloor was methodologically challenging for these analyses.

First, the AMS calibration ages spanned the pre-bomb and post-bomb curves, returning ages on both curves, with three potential ages. These calibration ages lead to the multiple AMS calibration options (Table 2.4). Additional AMS dates are needed to stabilize the post-bomb curve and thus clarify the calibration.

Second, AAR rates for each genus were calibrated after pooling samples from both the Bering and Chukchi Seas. Because the Bering and Chukchi Seas have different bottom water temperatures with potential to affect racemization rates, this pooling of data may have contributed to the large uncertainties and the low non-parametric correlation between the D:L values and the radio-carbon estimated ages (Table 2.1). At present, we have too few AMS dates to analyze racemization rates in the two seas separately; we are in the process of dating additional specimens from both seas and also locate older shells.

Finally, although additional AMS dates will improve these analyses, AAR rates are always slower in colder waters, reducing the resolving power of the method [154, 153, 113]. This relationship is evident in the data presented here, with both *Macoma* and *Nuculana* exhibiting generally low DL ratio values: all Asp DL ratio values are <0.12, and all Glu DL ratio values are <0.05. Given slower racemization rates, calibration (correlation) becomes more challenging because of short intervals. The data presented here adds to the body of literature on the challenges of AAR dating of the skeletal remains of boreal ecosystem fauna [113].

These challenges of calibration arise from the almost-exclusively very young ages of shells in the death assemblages of all three sites within the study area: shell ages did not exceed 1600

years for either genus, regardless of the calibration model, and most shells were less than 200 years old (Table 2.7). Using truncated models — i.e., using the youngest shell to define the left edge of the shell AFD rather than an age of 0 years — was helpful in estimating loss rates for all age calibrations (gave the lowest AICc), probably a reflection of the high uncertainty in shell ages, the youngest shells being about 30 years old, and the small range of shell ages in each AFD (to 1600 years maximum).

2.5.2 Magnitude of Time-Averaging in Arctic Seabeds

For all genera, age calibrations, and regions, median shell ages range from 28-125 years with IQRs from 4-65 years (estimate of time-averaging), which is much shorter than the time-averaging estimated for bivalve dead-shell assemblages in temperate and tropical seabeds using the same methods (Table 2.9). Short windows of time-averaging in other shelf ecosystems are related to population dynamics (i.e., recent high production of shells [306]), or from taxa that are rapidly lost in the seabed (e.g., fully articulated specimens of echinoderms in the tropics [171]; Table 2.9).

Overall, dead shell assemblages from the Arctic have a much shorter window of time-averaging. The Arctic AFDs are dominated by geologically young shells <200 years old but a few older shels form a right-skewed, "L-shaped" AFDs for some age calibrations (Figure 2.3, and Figure 2.4). Maximum shell ages in the Arctic assemblages are based on a few old shells that range only up to 1600 years (Figure 2.4; Table 2.7). Given their short window of time-averaging, Arctic dead-shell assemblages provide a high-resolution source of information for ecological analysis, reflecting only the most recent few centuries of ecological history: older shells are extremely rare, despite these Arctic seabeds having similar sedimentation rates (0.1-0.5 cm/y, [52, 227]) to those of lower latitude shelves where shells within the SML commonly range up to many thousands of years old [164, 305, 10, 301]. This short window of time-averaging means that dead-shell assemblages can be an insightful and temporally sharply resolved source of retrospective information on benthic communities, especially in Arctic regions that have not been surveyed previously, or that were

inaccessible before anthropogenic climate change began. To enable further investigation of these dynamics, the sampling protocols of future expeditions here and elsewhere in the Arctic should include retaining the dead-shell assemblages of at least some benthic samples.

2.5.3 Rates of Shell Loss

Shell loss, as modeled here, is the sum of loss from all processes, including both loss from shell disintegration within the sediment surface mixed layer (SML) and loss from burial below the sediment SML. Using a one-phase model, rates of shell loss within Arctic sediment SMLs are up to 10x more rapid than they are in warm-temperate and sub-tropical seabeds (e.g., for *Nuculana*, λ = 0.0084-0.0286 vs. λ = 0.00030-0.00140 in southern California; Figure 2.7). Using two-phase models, the initial loss rates (λ_1) in the Arctic are very similar to those in temperate shelves – they are certainly not significantly higher – but the decline in rate to the second phase (λ_2) is more modest, although the error bars are large (Figure 2.8), with a decline of at most several fold rather than the two orders-of-magnitude encountered on temperate shelves.

The lack of support for a two-phase model of shell loss in Arctic death assemblages – and the very slow values of τ – indicate that the exclusively young ages of shells in these assemblages owes not to higher short-term rates of loss but to a failure of shells to sequester, i.e. to shift, as they age, to a slower rate of loss, in contrast to widespread support for the two-phase model in temperate and tropical death assemblages. τ, the net sequestration rate, is markedly slower in the Arctic, with a mean time to sequestration ($1/\tau$) for *Macoma* between 65,000-2,000,000 years, and for *Nuculana* between 20,000-35,000 years (Table 8). This contrasts with Southern California, where the mean time to sequestration is still geologically long (i.e., few shells attain sequestration) but is still much shorter than in the Arctic (for *Parvilucina* between 7000-15,000, and for *Nuculana* between 1,500-12,500 [305]). The reasons for this "failure to sequester" or "rarity of sequestration" in Arctic sediments require additional work. We suspect, however, that it is driven by slower rates or fewer pathways of diagenetic stabilization of shells within the sediment SML rather than by higher burial

and outright removal from the sediment SML: sedimentation rates in the Arctic shelves of this study are no higher than those on temperate and tropical shelves where shell AFDs have been analyzed, and the depth of penetration (and thus potential vertical advection of shells) by bioturbators is unlikely to be as deep.

The two Arctic genera that we dated have qualitatively different aragonitic microstructures, permitting a test for their effects on rates of shell loss. *Macoma* is composed of cross-lamellar aragonite outside the pallial line (the region where bivalve flesh is not attached to the shell) and complex cross-lamellar aragonite inside the pallial line; both microstructures have low organic-matrix content. In contrast, *Nuculana* shells are composed entirely of high-organic homogeneous aragonitic microstructure [296, 297]. Contrary to expectations from experimental work that high-organic content promotes shell disintegration [110], we found that *Macoma* exhibited slightly higher rates of loss than *Nuculana*. However, the rate estimates for *Macoma* and *Nuculana* are very similar, with overlapping error bars, and so this lack of differentiation between shell microstructure types may well be due to the rapid rates of loss of both types of bivalve shell.

2.5.4 Spatial Variation in Shell Loss

Aragonite Undersaturation of Overlying Waters

The saturation state of a water mass can be defined as the difference between the actual concentration of carbonate ions in water and the critical or threshold concentration of those ions below which $CaCO_3$ will dissolve [108]. The concentration of carbonate ions is determined by the quantity of dissolved CO_2 that reacts with water to create carbonate, carbonic acid, and bicarbonate [108]. The concentration of each species within the marine carbonate system is determined by the water's temperature, salinity, and pressure (the latter two are not significant factors in shelf water depths), with higher CO_2 solubility in cold waters, and therefore naturally low concentrations of calcium carbonate [86, 108]. These controlling factors help to create a strong gradient of declining carbonate saturation state with latitude, and presumably a large preservational barrier to biogenic aragonite.

The latitudinal temperature gradient is thus our first-order predictor of the postmortem persistence and thus time-averaging of shell carbonate in sediment surface mixed layers. Although calibration of AAR data is challenging in the Arctic, we in fact find that the median and maximum ages of shells are significantly younger at our Arctic sites than in counterpart tropical and temperate shelves (Figure 2.7, Figure 2.8, Table 2.7). Also, short-term loss rates in the Arctic are either 10x faster (using a one-phase model) or, using a two-phase model, are no faster than those documented by others in lower latitudes and, importantly, are less likely to be permanently sequestered (Figure, 2.7, Figure 2.8). The transition to a slower loss rate, which is widely observed in lower latitudes, is so slow in the Arctic sites as to not represent a pathway to permanent preservation at all: permanent preservation apparently requires chance deep burial below the sediment SML relatively early in the postmortem interval. These results on time-averaging and loss rates of molluscan shells represent the first quantitative field determinations of biogenic aragonite loss rates in Arctic seabeds on geologically significant time scales (ie., radiocarbon age as opposed to incubation experiments), and establish that qualitatively different dynamics of shell preservation apply there.

Within the Pacific Arctic, the relatively low aragonite saturation state decreases further for several reasons. First, anthropogenic CO_2 is particularly seasonally potent in the Arctic because this dissolved CO_2 can be trapped in the summer at the seabeds of the Bering and Chukchi Seas by the stratified water masses hat develop there [58, 249]. Second, sharp pycnoclines in the Bering and southeastern Chukchi Sea trap the CO_2 produced locally by microbial and microbenthic respiration in the seabed, increasing the p(CO_2) of bottom waters and lowering carbonate concentrations; these respiration products accumulate until bottom waters are mixed, either by storm winds in the fall and spring and/or brine injection in winter (related to sea ice formation)[58, 55]. Finally, the amount of low-carbonate water flowing northward through the Bering Strait has increased by 150% over the last 10-15 years, contributing to lower aragonite saturation states in the Chukchi Sea [58, 321].

The effects of low aragonite saturation state are especially concentrated in the DBO hotspot regions on the Alaskan Continental shelf, where biological activity – organic flux, benthic popu-

lations, respiration – are highest [58, 55]. As currents slow in the northern Bering Sea and the southeast Chukchi Sea, POM and other nutrients fall to the seabed at DBO1 and DBO3. Respiratory products from this organic matter are trapped in bottom waters by sharp haloclines and can be transported by bottom currents, or they can be reactivated into the water column from vertical mixing (i.e., brine rejection, wind driven mixing) [202, 57, 58]. This periodic trapping and release of CO_2 has created strong but episodic ocean acidification events at DBO1 and DBO3 [57, 58, 201].

DBO4, in the Northeast Chukchi Sea, is at the end of this conveyor belt and experiences the most severe seasonal aragonite undersaturation. The water that reaches DBO4 has been conditioned with both anthropogenic and respired CO_2, along with other respiratory products along its route [58, 199]. POM and nutrients are provided by inflow from the south, and from vigorous ice-edge phytoplankton communities in surface waters [58]. These two sources of POM and nutrients are trapped in DBO4 bottom waters, which in turn sinks and flows into the Arctic basin through Barrow Canyon [58].

Thus, if overlying water undersaturation from all of these processes – both expected from cold water and from the unique patterns within he Pacific Arctic – were the sole cause of shell loss, then we would expect to see the highest rates of carbonate shell loss and the shortest windows of time-averaging in DBO4, i.e., in the northeast Chukchi Sea. Contrary to this prediction, we see the highest rates of loss for *Macoma* in DBO3 in the northern Bering Sea, and the highest loss rates for *Nuculana* at DBO3 or DBO1 in the Bering Sea (depending on the calibration) (Figure 2.5, and Figure 2.6). Thus, although the Arctic shell-loss rates at all three sites are much higher than those documented at lower latitudes (Figure 2.7, and Figure 2.8), the highest loss rates within the Arctic study system are not correlated with areas of seasonal aragonite undersaturation of the overlying water, but rather with the highers 'biological activity' in the seabed (Section 2.5.4).

Seafloor Biologic Activity and Porewater Undersaturation

The Pacific Arctic DBO hotspots are home to the most productive soft bottom seafloor ecosystems in the world [318, 119] (Table 2.1). The productivity in these hotspots derives from the large amounts of POM flowing into the regions on currents from the south, plus POM flux from blooms of ice-associated microbial communities at the ice edge. In DBO1 and DBO3, most of the carbon biomass produced at the water's surface that reaches the seabed is consumed by the macrofaunal seafloor community, creating strong pelagic-benthic coupling [132, 130]. Further north at DBO4, the macrofaunal seafloor community is not as productive, leaving large amounts of POM for microbial consumption (see section 2.5.4) [57, 130, 132]. Sediment oxygen demand is also highest in the two southern sites, where bioturbation by the dense macrobenthic infaunal community would promote aerobic microbial decomposition of organics, thus increasing $p(CO_2)$ and thus porewater undersaturation (Figure 2.9).

Our observation that the shortest windows of time-averaging and highest rates of loss occur in these southern sites – DBO3 and DBO1 (Tables 2.7, Table 2.8, Figure 2.5, and Figure 2.6) – suggests that, within the cold-water Arctic study system, the effects of high organic flux and biological activity on taphonomic conditions within the seabed play a stronger role on carbonate preservation than does the saturation state of overlying water. That activity would promote aerobic microbial decomposition of organic matter (producing CO_2) and redox of the products of anaerobic microbial decomposition (such as sulfides), promoting undersaturated conditions within the sediment SML [252, 225, 243], and would likely also support larger microbial populations, which would promote maceration of biogenic carbonate (shell disintegration by loss of organic matrix, [110, 103]. Scanning electron microscopy of Arctic shells is revealing that, in fact, microbial maceration is widespread in these sediments, with negligible evidence of direct dissolution of shells (i.e., no evidence of karstic textures; Section E, [209, 163]). The pathway of shell loss seems to be through microbial attack of shell organic matrix, which releases mineral crystallites from the shell surface, which then dissolve (titrate) the undersaturated porewaters.

2.6 Conclusions

These results represent a first estimate of the scale of time-averaging for molluscan shell assemblages in polar shelves. We find that the window of time-averaging for bivalve shells on Pacific Arctic shelves is less than 1000 years, so that loss and sequestration are best characterized by a one-phase model of loss. This result contrasts with the two-phase loss models that characterize assemblages from lower latitudes and signals a failure of the shells to sequester: Arctic loss rates are up to 10 times higher than counterpart estimates for biogenic aragonite in temperate settings. Therefore, the live-dead discordance provides a temporally appropriate tool for detecting recent past changes in seafloor ecology, in addition to its improved spatial resolution using biomass as a paleoecologic currency [208]. As the Arctic continues to warm, dead-shell assemblages from regions that have never been surveyed owing to ice cover can provide a means to examine the past seafloor communities. Time-averaged assemblages from the Arctic can provide insights into how unmonitored communities are reacting to ongoing climate change. Additionally, this study increases confidence in paleobiologic investigations to analyze polar ecosystems over an expanded timeframe.

We find that shell disintegration and loss are fastest where seafloor biologic activity is greatest, indicating that the undersaturation of porewaters associated with high biological respiration may be an important factor in shell loss, rather than just the saturation state of overlying water. This finding suggests that the relative effects of seabed biology and overlying water saturation states should be examined in additional Arctic regions, such as the Barrow Canyon region (DBO5) and the Siberian Shelf, both of which are expected to experience aggressive aragonite undersaturation ($\Omega_{arag} \lesssim 1$)[58]. The porewaters of each of these regions could also be investigated to confirm the aragonite undersaturation of porewaters as proposed here.

The living macrofauna may interact with the dead shells accumulating in the sediment, by aeration of the sediment, growing of microbial communities, and the undersaturation of aragonite in porewaters. This form of taphonomic feedback should be investigated further to understand how shell disintegration could affect living communities.

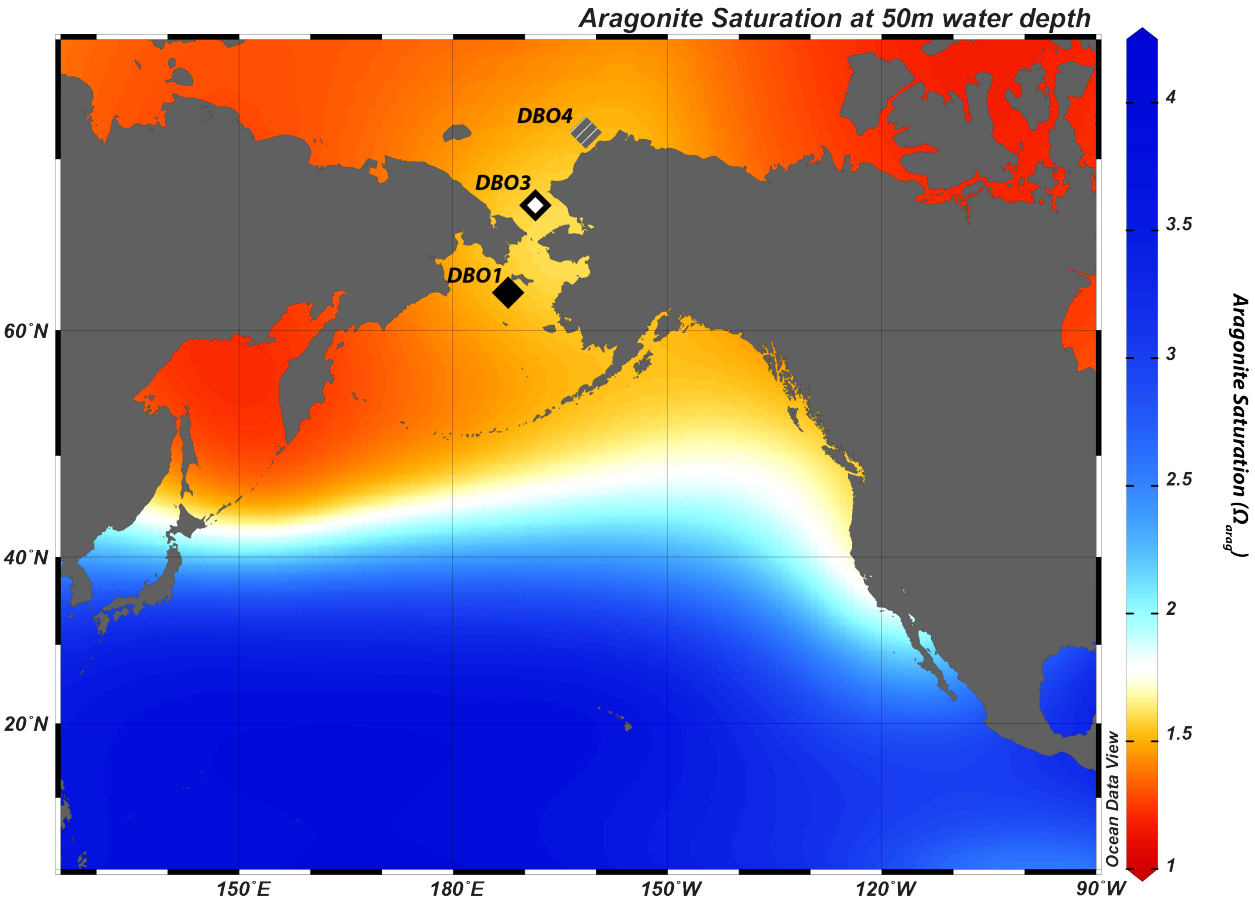

Figure 2.1: Pacific ocean aragonite saturation state (Ω_{arag}) at 50 m water depth [147], map interpolated in OceanData Viewer. Diamonds represent the locations with age-dated shells (Table 2.1, Table 2.2)

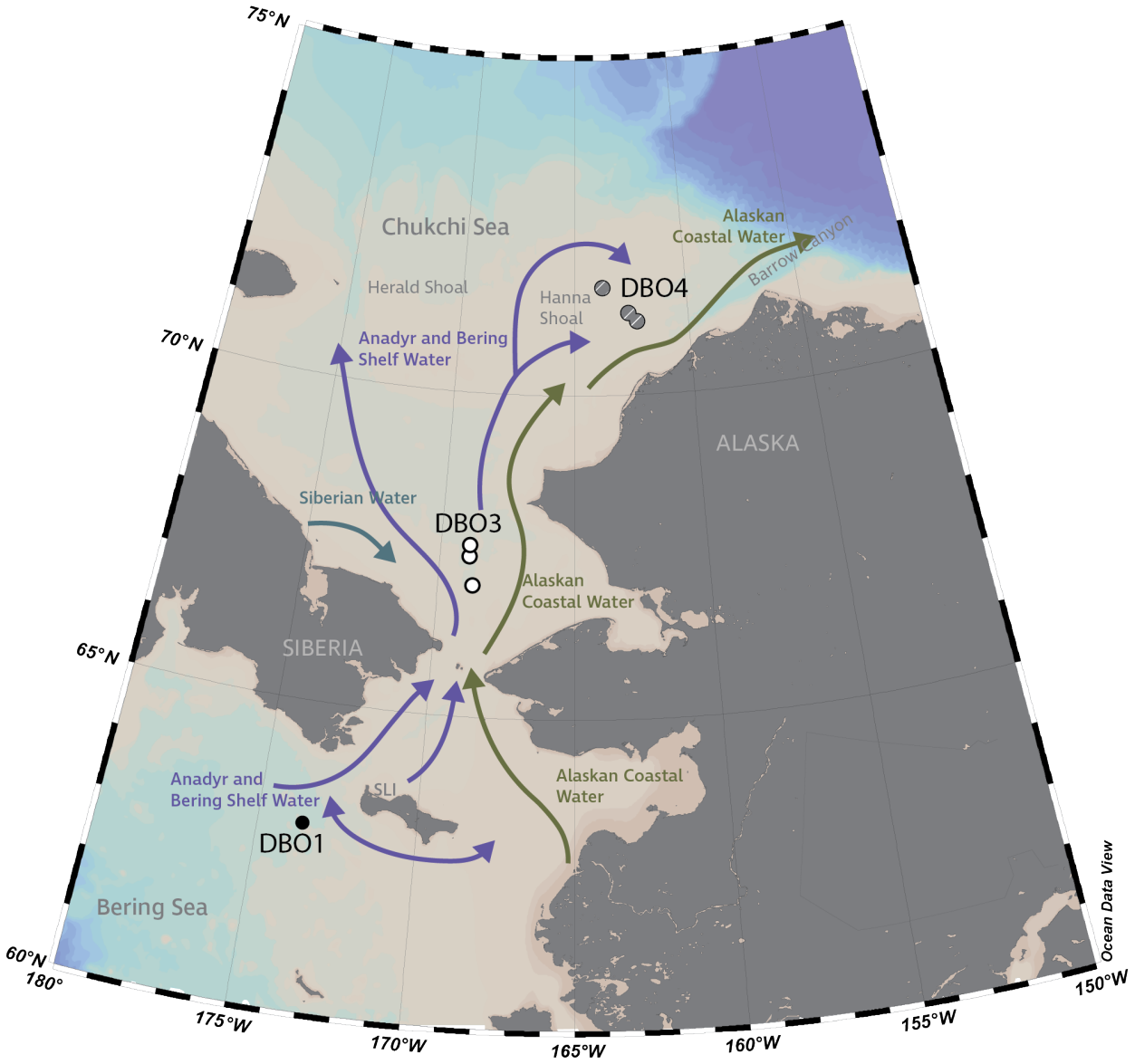

Figure 2.2: Sites sampled for dead shells, by region (Distributed Biological Observatory - DBO). Black icons - DBO1 northern Bering Sea, St. Lawrence Polynya, characterized by persistent subarctic conditions, with intermediate saturation states of overlying water and of porewater, as judged by oxygen uptake; White icons - DBO3 Southeast Chukchi Sea, recently transitioned from arctic to subartic conditions, highest rates of oxygen uptake; Striped - DBO4 Northeast Chukchi Sea; persistent Arctic conditions, lowest saturation state of overlying water. Arrows denote dominant currents: Purple - Anadyr and Bering currents, blue - East Siberian Sea current, green - Alaskan coastal current. SLI - St. Lawrence Island. Base map adapted from Ocean Data Viewer and approximate currents from [121].

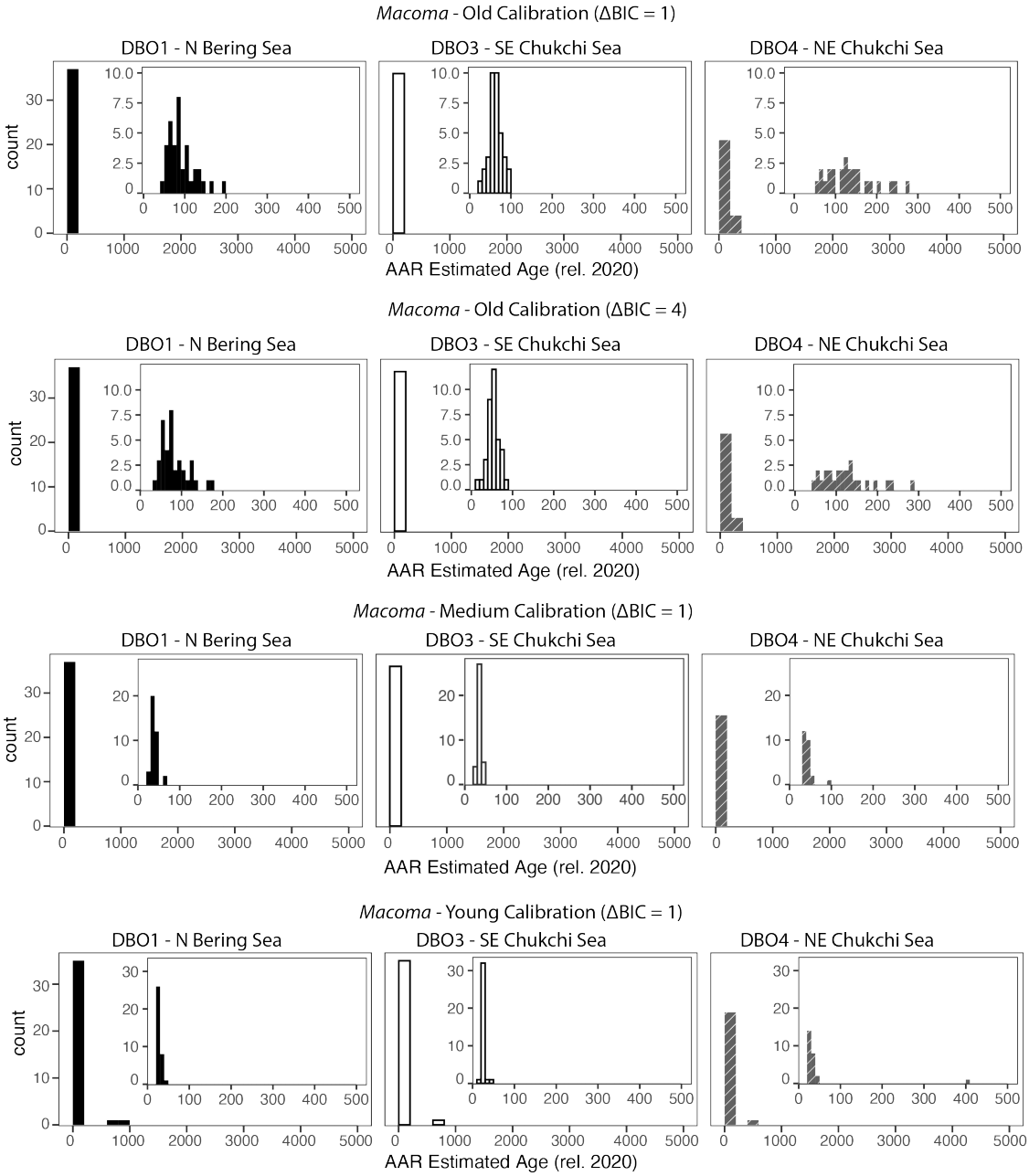

Figure 2.3: Postmortem age-frequency distributions of shells of *Macoma* from DBO1 in the northern Bering Sea (black bars), DBO3 in the SE Chukchi Sea (white), and DBO4 in the NE Chukchi Sea (striped; N denotes number of dated shells), based on four different radiocarbon-calibrations of AAR data (rows; details in Tables 2.6 and 2.7).Shell age estimates are binned into 200 year-increments in the large plots; insets display data in 10 year-increments for shells <500 years old, although such fine bins are not statistically meaningful. Most shells are very young, with only a few older shells, creating an L-shaped distribution of ages in Arctic assemblages, with little difference between calibrations.

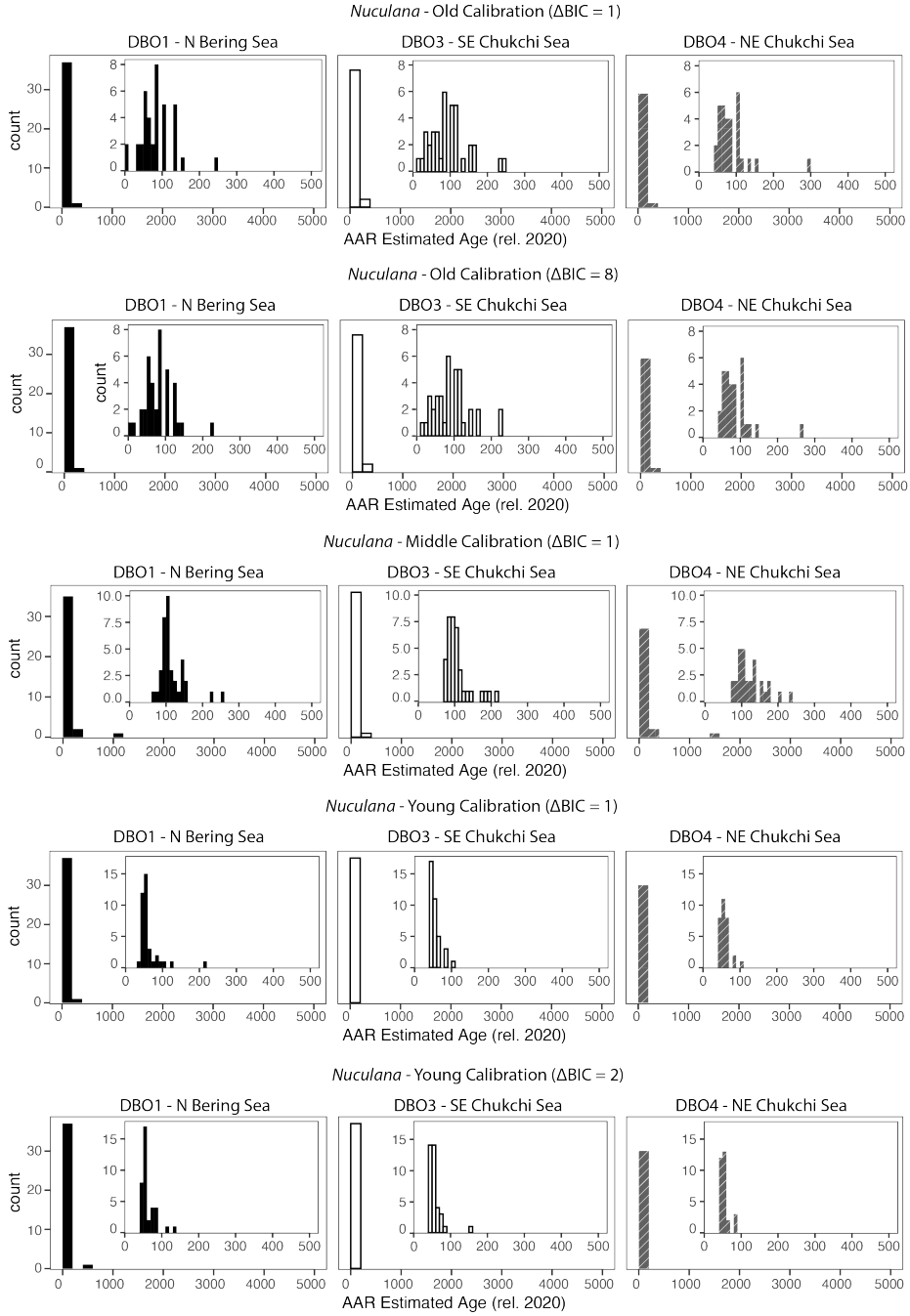

Figure 2.4: Postmortem age-frequency distributions of shells of *Nuculana*, using the same conventions as in Figure 2.3. Most shells are young, with only a few older shells, creating an L-shaped distribution of ages in Arctic assemblages, as seen with *Macoma*, but overal older ages.

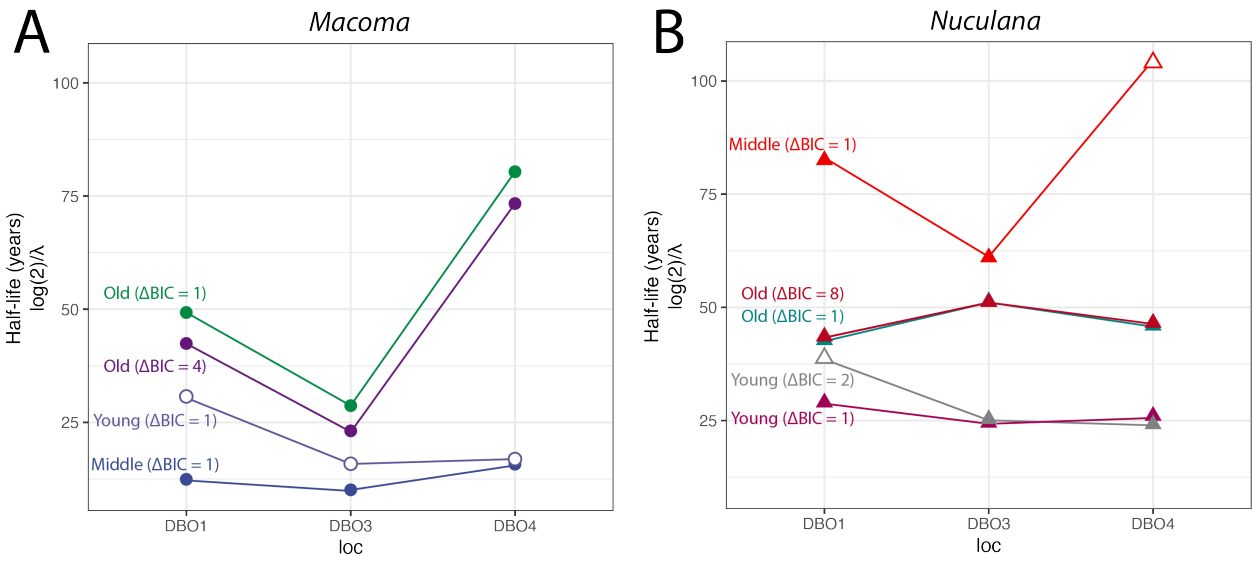

Figure 2.5: Taphonomic half-lives of shells of (A) *Macoma* and (B) *Nuculana* (years; $log(2)/\lambda$) when fitted using the one-phase truncated model in the three test regions (DBO1, 2, 3), for all calibration models (labeled lines). Filled icons indicate the favored models for the region and age calibration dataset. For *Macoma* the shortest half-lives (fastest loss rates) are at DBO3; rates are similar across all three sites for *Nuculana*, but with the lowest rates at DBO3 and DBO4.

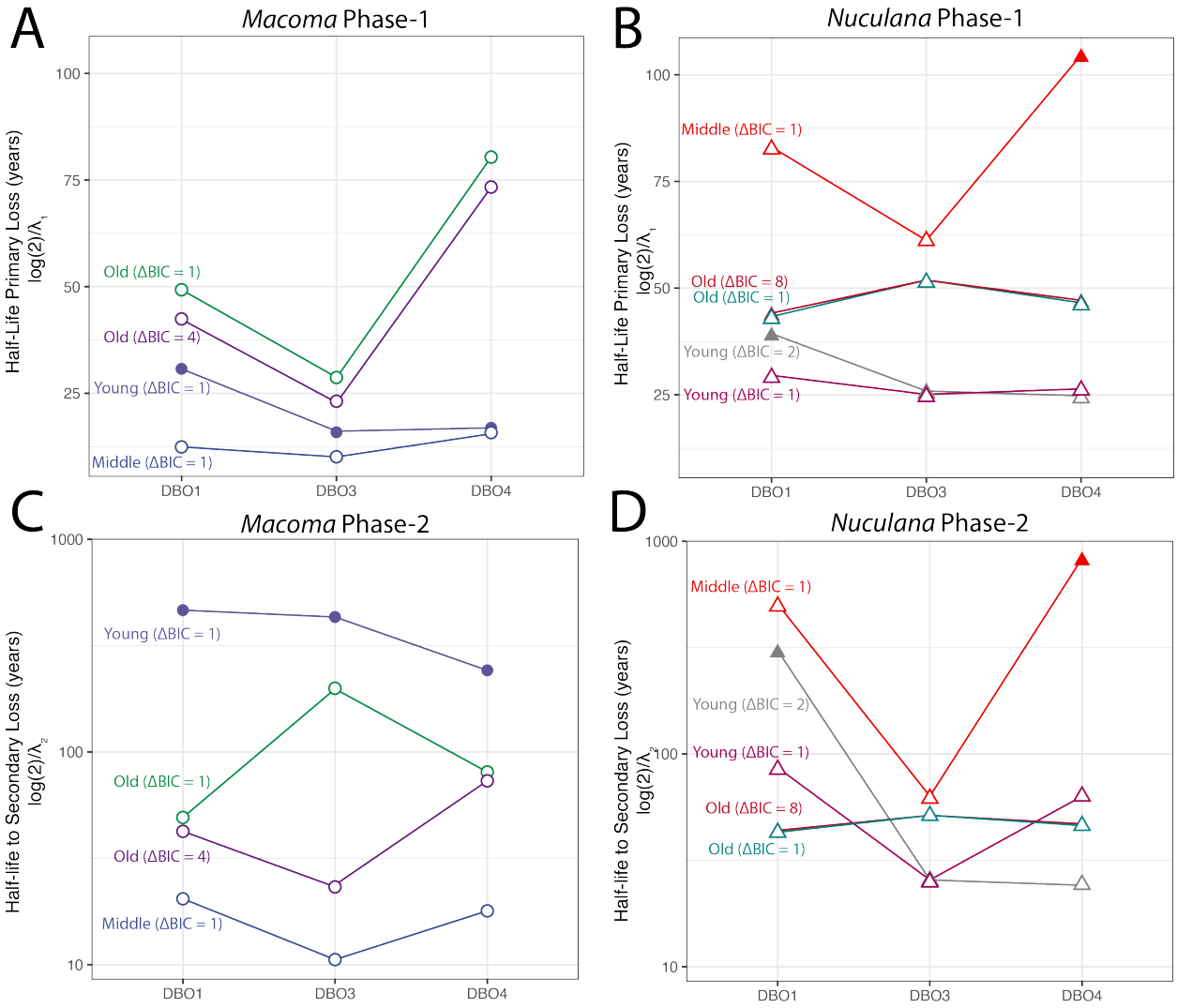

Figure 2.6: Taphonomic half-lives of shells of *Macoma* (left plots) and *Nuculana* (right plots) in the three test regions (DBO1, 3, 4)as estimated using the truncated two-phase model of shell loss within the sediment surface mixed layer (SML); loss rates plotted as half-lives (years; $log(2)/\lambda$). Top row (A, B) shows results for the initial Phase 1 of loss within the taponomically active zone (TAZ); bottom row (C, D) shows results for the subsequent Phase 2 within the sequestration zone (SZ); colored lines denote results using different calibration models (labeled). Closed icons indicate the favored model for the region and age calibration age dataset. The first phase half-lives are similar to those produced by the one-phase models (in Figure 2.5), and the second phase of loss is similar to the first-phase loss rate, i.e. with no large order-of-magnitude difference between the phases.

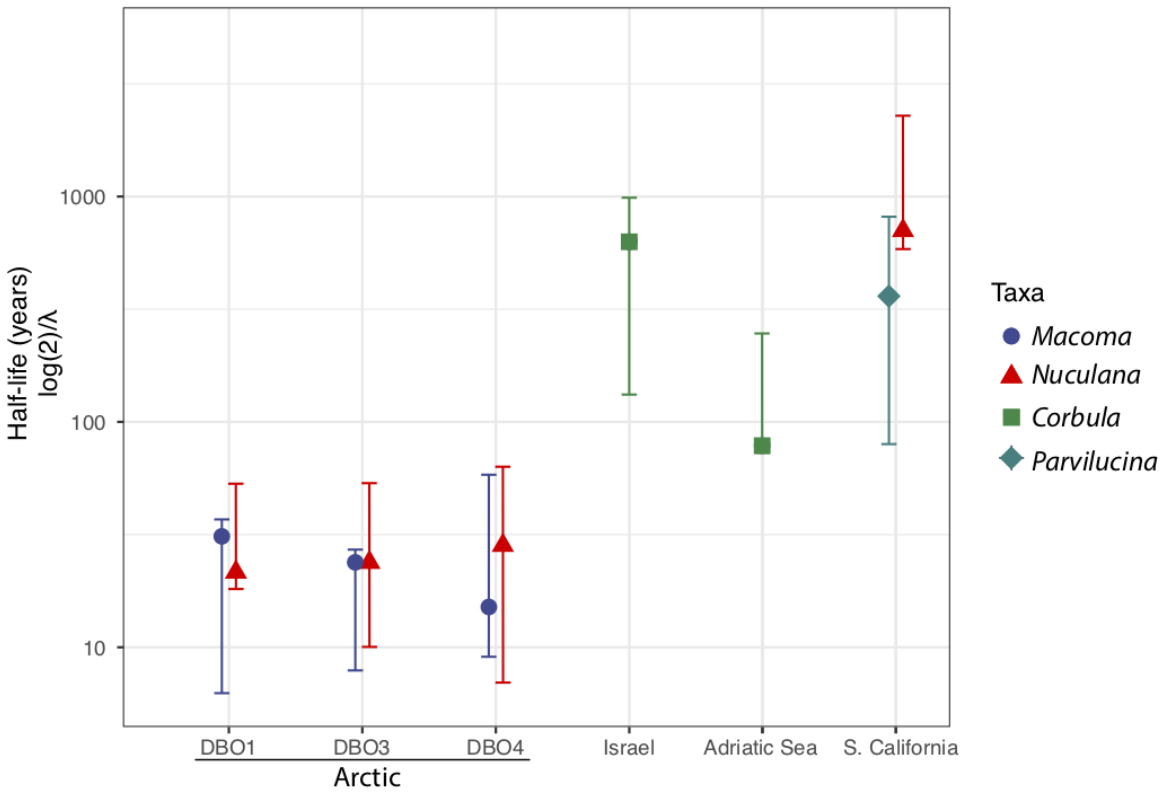

Figure 2.7: Taphonomic half-lives of aragonitic bivalve shells in the sediment surface mixed layer (SML) ($\log(2)/\lambda$) estimated using the one-phase model of loss, comparing results from the three Arctic study regions (DBO1, 3, 4; work here, Figure 2.7) with published results from three warm-temperate shelves (Adriatic Sea = [10], Mediterranean Israel = [306], and Southern California = [305]). Blue circles are *Macoma*, red triangles are *Nuculana*, green squares are *Corbula*, and teal diamonds are *Parvilucina*. Median values are represented by symbols, and bars represent the minimum and maximum reported value. Values from this study are labeled "Arctic", all other values were published in the literature. Lateral offset of vertical bars are not meaningful and are for ease of viewing only. The half-lives for aragonitic bivalve shells in the Arctic are much lower than those documented for counterpart shells on warm-temperate shelves.

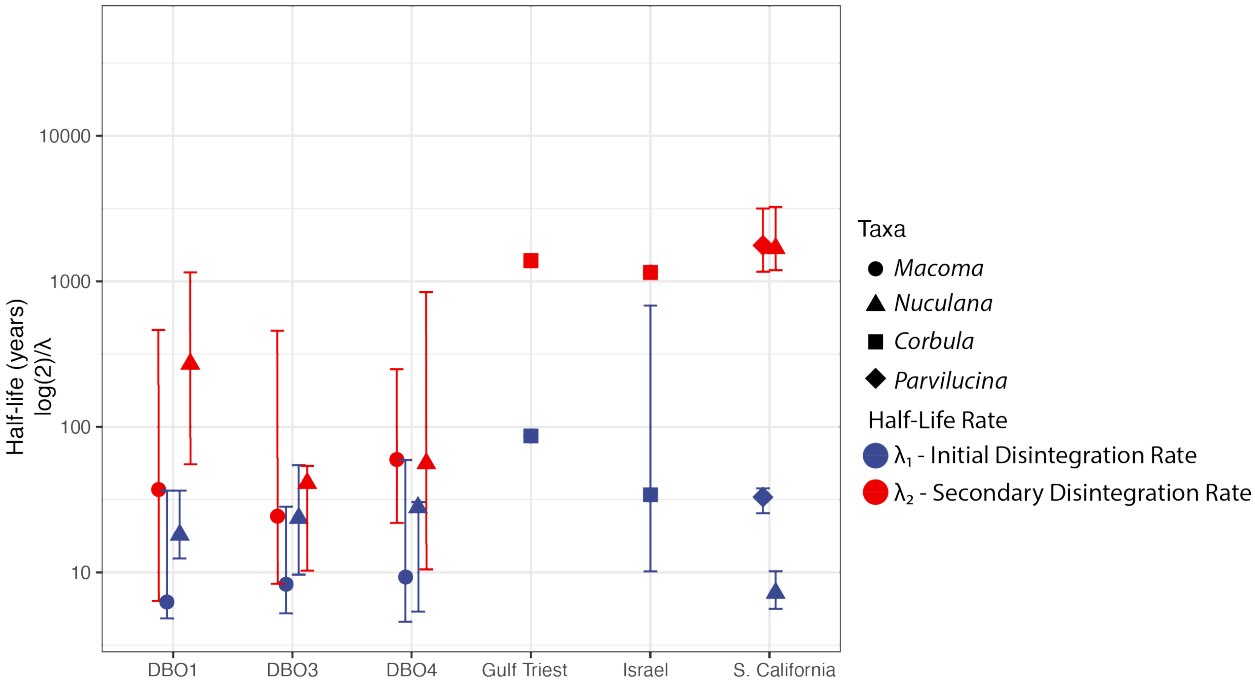

Figure 2.8: Taphonomic half-lives of shells in the surface mixed layer (SML; $\log(2)\lambda$) using the two-phase model of loss, estimated using the two-phase model of loss, comparing results from the three Arctic study regions (DBO1, 3, 4; work here) with published results from three warm-temperate shelves (Adriatic Sea = [302], Mediterranean Israel = [306], and Southern California = [305]). Blue symbols represent half-lives of phase-1 in the TAZ ($\log(2)/\lambda_1$), and red symbols represent half-lives of phase-2 in the SZ ($\log(2)/\lambda_2$). Conventions as in Figure 7. First phase half-lives are similar across all latitudes, but the second phase half-lives are much shorter in the Arctic.

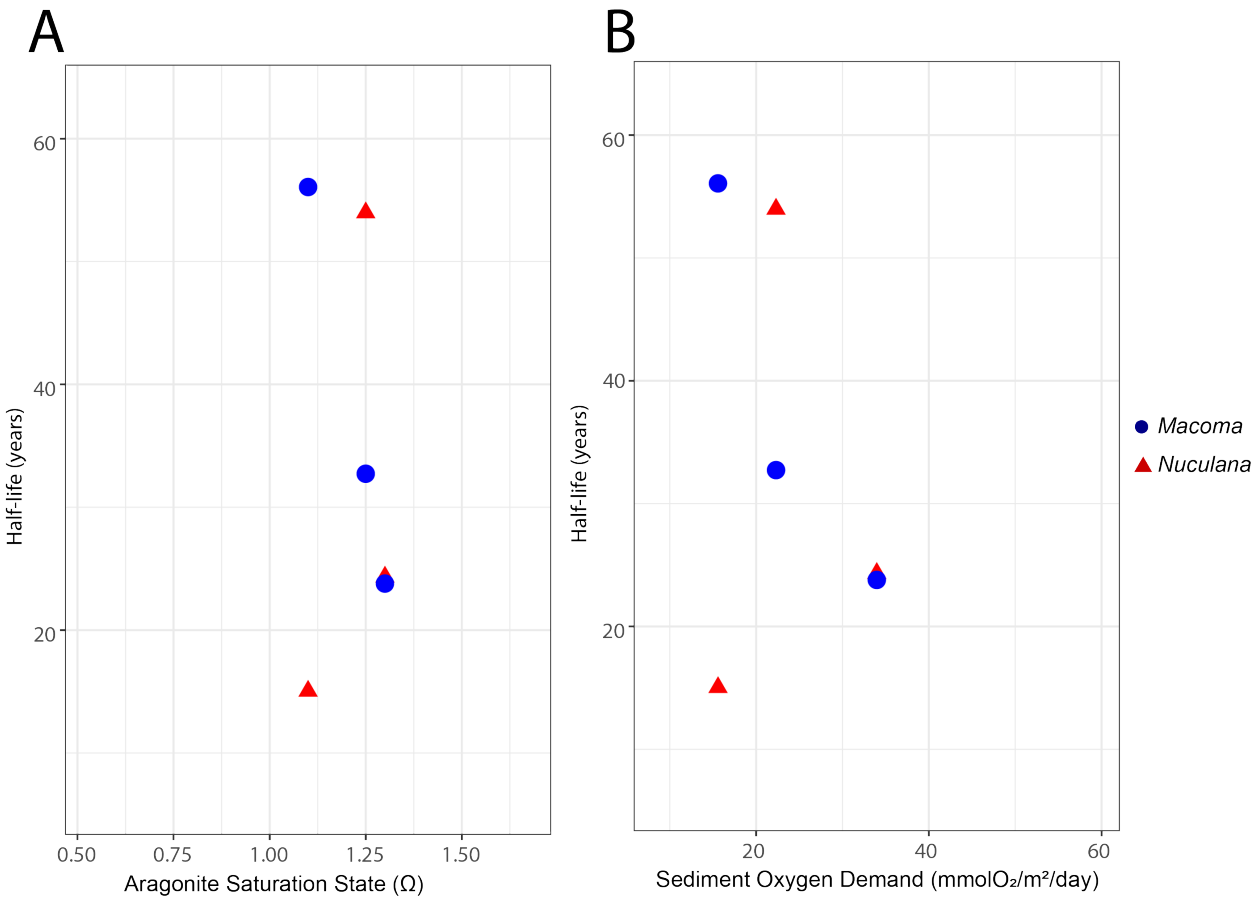

Figure 2.9: Median taphonomic half-lives of shells versus environmental measures of (A) Aragonite saturation state of the overlying bottom water (Ω_{arag}), and (b)and (b) sediment oxygen demand of the top 10 cm of the sediment (mmolO_2/m^2/day). Each dot represents the median half-life of shells from each hotspot (log(2)/λ), verses the median value of either aragonite saturation or sediment oxygen demand. Blue circles = *Macoma*, red triangles = *Nuculana*.

Table 2.1: Environmental variables from the sampled DBO regions, ordered south (DBO1) to north (DBO4). All values measured in summer from bottom water (Temperature, Ω_{arag}, Total Alkalinity), from the top 10 cm of sediment (infaunal macrofauna. Biomass and Abundance, sedimentary Oxygen Demand). Values are means, with minimum and maximum values in brackets. Sources: temperature [121], total alkalinity (TA) [203, 200, 57, 323], Aragonite saturation state (Ω_arag) [201, 241, 58, 202, 200, 323], all measures of productivity [131]. Gray shading indicates regions with lowest Ω_{arag}, and highest biological activity (Sediment oxygen demand mmolO_2/m^2/day, and infaunal macrofauna biomass gCarbon/m^2).

	Oceanography			Biology		
DBO Region	Temperature (°C)	Ω_{arag}	TA (μmol/kg)	Abundance (indiv/m^2)	Biomass (gCarbon/m^2)	Oxygen (mmolO_2/m^2/day)
DBO1	-1.64 [-1.81-0.13]	1.25 [0.5-1.4]	2175 [2150-2250]	2329 [1343-3550]	22.3 [11.5-35.4]	11.1 [3.5-19.2]
DBO3	2.20 [-1.69-10.50]	1.30 [0.5-2]	2250 [2200-2300]	8777 [1985-23,010]	34.0 [5.4-112.0]	23.8 [12.1-40.7]
DBO4	-0.70 [-1.83-6.20]	1.10 [0.5-1.6]	2250 [2000-2290]	3489 [1343-3550]	15.6 [6.15-29.0]	8.9 [5.4-12.8]

Table 2.2: Sampling year (2014 or 2015; last two digits of SWL cruise number), location, water depth, and number of age-dated dead-collected shells of two bivalve genera (total number analyzed), organized by test regions (DBO hotspots). 202 total shells were dated.

Cruise	Station	Latitude	Logitude	Depth (m)	*Macoma*	*Nuculana*
DBO1 - St. Lawrence Polynya, northern Bering Sea						
SWL14	SLIP4	63.0301	-173.4595	71	37	37
				Total	37	37
DBO3 - Southeast Chukchi Sea						
SWL14	UTN2	67.0501	-168.7291	47	33	27
SWL14	UTN4	67.5014	-168.9042	50	0	6
SWL14	UTN5	67.6705	-168.9087	50	3	4
				Total	36	37
DBO4 - Northeast Chukchi Sea						
SWL15	DBO4.2	71.1036	-162.2640	47	0	1
SWL14	DBO4.2	71.1036	-162.2640	47	6	5
SWL14	DBO4.3	71.2326	-162.6350	46	1	0
SWL14	DBO4.6	71.6182	-163.7711	42	18	24
				Total	25	30

Table 2.3: Live-collected individuals used in calibrating Amino Acid Racemization (AAR). All specimens were collected as closely as possible to the regions where dead- collected specimens were acquired. ID – UChicago lab identification number for shell.

Region	Station	Date	Latitude	Longitude	Depth (m)	Species	ID	DL Asp	DL Glu
DBO1	DBO1.1	8/5/2019	62.010	-175.060	85	*Nuculana radiata*	NR0287L	0.088	0.034
DBO1	SLIP3	7/14/2014	62.390	-174.570	71	*Macoma calcarea*	MC0101L	0.075	0.038
DBO3	DBO3.7	8/29/2017	67.783	-168.596	50	*Macoma calcarea*	MC0143L	0.086	0.043
DBO4	SE-5	8/29/2017	71.641	-160.792	49	*Nuculana radiata*	NR0104L	0.078	0.035

Table 2.4: Amino Acid Racemization (AAR) and AMS radiocarbon data from dead-collected shells used to calibrate the rate of racemization, with age estimates (years) produced using results from three models (see text) and using the regional post-bomb calibration of AMS data that was created using OxCal (for Young and Middle calibrations) and the specimens listed in Table (Young calibration excludes specimen HAO277). All calibrated ages are median ages, reported as years before 2020. ID – Uchicago lab identification number for shell.

										Young Calibration		Middle Calibration		Old Calibration	
DBO	ID	DL Asp	DL Glu	F Mod	±	Δ^{14}C (‰)	±	^{14}C age (BP)	±	Age	±	Age	±	Age	±
DBO1	MC0029C	0.118	0.049	0.9511	0.0059	-48.9	5.9	405	50	45	29-61	62	28-177	122	67-177
DBO1	MC0030A	0.114	0.046	0.9621	0.0050	-37.9	5.0	310	45	8	6-24	8	6-24	117	69-165
DBO1	MC0040A	0.112	0.047	0.9442	0.0039	-55.8	3.9	460	35	46	44-48	62	44-181	124	68-181
DBO1	MC0041C	0.110	0.047	0.9610	0.0050	-39.0	5.0	320	45	8	6-24	8	6-24	117	69-166
DBO1	MC0133C	0.102	0.047	0.9520	0.0046	-48.0	4.6	395	40	44	26-62	62	60-172	120	67-173
DBO1	MC0134C	0.108	0.049	0.9585	0.0041	-41.5	4.1	340	35	44	25-63	44	25-63	117	69-166
DBO1	MC0135C	0.103	0.047	0.9546	0.0055	-45.4	5.5	375	50	9	6-24	9	6-24	120	67-173
DBO1	MC0101L	0.075	0.038	0.958	0.007	-42.333	6.58	350	60	11	6-21	11	6-21	11	6-21
DBO3	MC0143L	0.086	0.043	0.941	0.005	-59.286	4.74	490	45	8	3-18	8	3-18	8	3-18
DBO1	NR0008C	0.115	0.046	0.9634	0.0049	-36.6	4.9	300	45	8	6-23	62	6-62	116	69-163
DBO1	NR0018C	0.122	0.051	0.9603	0.0042	-39.7	4.2	325	35	8	6-25	62	6-165	117	69-164
DBO1	NR0024A	0.111	0.046	0.9717	0.0049	-28.3	4.9	230	45	10	6-22	10	6-62	114	70-157
DBO3	NR0061C	0.104	0.045	0.9651	0.0044	-34.9	4.4	285	40	9	6-23	9	6-62	115	69-161
DBO3	NR0064B	0.111	0.045	0.9458	0.0043	-54.2	4.3	450	40	46	42-50	62	42-179	123	67-179
DBO3	NR0074B	0.112	0.043	0.9487	0.0040	-51.3	4.0	425	35	45	34-53	62	37-175	121	67-175
DBO3	NR0113A	0.107	0.046	0.9122	0.0082	-87.8	8.2	740	80	189	102-276	189	102-276	189	102-276
DBO1	NR0137B	0.115	0.044	0.9553	0.0049	-44.7	4.9	400	60	44	25-63	62	25-63	119	68-170
DBO1	NR0142A	0.119	0.047	1.0225	0.0044	22.5	4.4	MODERN		22	13-31	74	8-80	74	68-80
DBO1	NR0287L	0.088	0.034	0.988	0.006	-12.014	6.31	100	60	3	1-6	3	1-6	3	1-6
DBO4	NR0104L	0.078	0.035	0.958	0.007	-42.333	6.58	350	60	5	3-8	5	3-8	5	3-8

Table 2.5: Live-collected individuals from the Bering and Chukchi Seas used to create the regional post-bomb curve in OxCal. UAM – specimens housed in the Invertebrate Zoology Collection at the Museum of the North, University of Alaska, Fairbanks; Grebmeier – specimens collected by Jacqueline Grebmeier of the University of Maryland Center for Environmental Sciences, Chesapeake Biologic Lab. Date = collection date. Mus. Num. = the museum's identification number for the specimen. Modern = 1950. ID – Uchicago lab identification number for shell.

ID	Date	Latitude	Longitude	Collector / Mus. Num.	Taxa	F. Mod.	±	Δ^{14}C (‰)	±	^{14}C age (BP)	±
MC0101L	2014	62.390	-174.570	Grebmeier	*Macoma calcarea*	0.9577	0.0066	-42.3	6.6	350	60
NR0103L	2014	62.560	-173.549	Grebmeier	*Nuculana radiata*	0.9648	0.0039	-35.2	3.9	290	35
NR0279	1980	67.167	-172.183	UAM:Inv:2945	*Nuculana radiata*	1.0589	0.0049	58.9	4.9	Modern	
Nsp0281	1969	62.483	-174.817	UAM:Inv:3021	*Nuculana sp.*	1.1357	0.0050	135.7	5.0	Modern	
MM0285	1991	71.167	-161.917	UAM:Inv:3614	*Macoma moesta*	1.0541	0.0050	54.2	5.0	Modern	
MC0282	1973	68.600	-171.183	UAM:Inv:4093	*Macoma calcarea*	0.9392	0.0045	-60.8	4.5	505	40
MC0283	1980	67.808	-170.025	UAM:Inv:4121	*Macoma calcarea*	1.0392	0.0055	39.2	5.5	Modern	
MM0280	1970	70.300	-164.683	UAM:Inv:4209	*Macoma moesta*	1.1399	0.0070	139.9	7.0	Modern	
HA0278	1967	65.800	-168.792	UAM:Inv:4388	*Hiatella arctica*	1.0660	0.0049	66.0	4.9	Modern	
HA0277	1957	"off shore of camp at Point Barrow"		UAM:Inv:4398	*Hiatella arctica*	0.9420	0.0070	-57.9	7.0	480	60
MC0284	1986	68.498	-166.498	UAM:Inv:6663	*Macoma calcarea*	1.0391	0.0051	39.1	5.1	Modern	
CC0286	2007	68.003	-168.706	UAM:Inv:8216	*Clinocardium ciliatum*	0.9786	0.0049	-21.4	4.9	175	45

Table 2.6: Calibration statistics for the rate of amino acid racemization (AAR) based on paired radiometric and AAR analyses from 202 specimens of *Macoma* and *Nuculana*. AMS calibrations from Table 2.6(Young, Middle, Old) were modeled (first column) using methods described in [12]. $*$ = low nonparametric correlation between output age and DL. BIC = Bayesian Information Criteria. a, b, c, R_0 and d are coefficients used in calibration models (see Section 2.3.3).

Model	Amino acid	Uncertainty	ln(a)	ln(b)	c	R_0	ln(d)	BIC	ΔBIC
Old Calibration									
Macoma (ΔBIC = 1)									
APK1	Asp	Gamma	10.778	NA	0.872	0.031	2.096	88.9	0.0
CPK1	Asp	Gamma	38.541	-31.178	3.093	0.038	1.821	89.8	0.9
Macoma (ΔBIC = 4)									
APK1	Asp	Gamma	10.778	NA	0.872	0.031	2.096	88.9	0.0
CPK1	Asp	Gamma	38.541	-31.178	3.093	0.038	1.821	89.8	0.9
SPK0	Asp	Gamma	16.386	1.663	NA	0.000	2.302	90.2	1.3
TDK0	Asp	Gamma	16.270	1.655	NA	0.000	2.354	90.3	1.3
TDK1	Asp	Gamma	9.804	0.482	1.167	0.033	1.975	91.2	2.3
TDK0	Glu	Gamma	36.113	2.332	NA	0.000	2.431	91.4	2.4
SPK0	Glu	Gamma	36.403	2.341	NA	0.000	2.417	91.4	2.4
CPK0	Asp	Gamma	-0.850	3.231	NA	0.000	2.446	91.4	2.5
SPK1	Asp	Gamma	12.346	1.203	1.463	0.035	2.053	91.6	2.7
APK1	Glu	Gamma	13.506	NA	1.408	0.035	2.402	91.8	2.9
$*$ *Nuculana* (ΔBIC = 1)									

Table2.6, continued.

Model	Amino acid	Uncertainty	ln(a)	ln(b)	c	R_0	ln(d)	BIC	ΔBIC
APK1	Glu	Lognormal	13.315	NA	1.520	0.032	-2.051	107.8	0.0
∗*Nuculana* (ΔBIC = 8)									
APK1	Glu	Lognormal	13.315	NA	1.520	0.032	-2.051	107.8	0.0
TDK1	Glu	Lognormal	10.918	0.346	1.958	0.033	-2.106	120.2	1.0
SPK1	Glu	Gamma	38.601	-32.630	3.140	0.034	1.992	111.4	1.6
CPK1	Glu	Lognormal	37.135	-28.775	2.637	0.034	-2.239	109.5	2.0
SPK1	Glu	Lognormal	37.990	-32.119	3.319	0.034	-2.021	113.0	2.1
TDK1	Glu	Gamma	8.363	-0.205	2.450	0.034	2.221	118.4	3.0
CPK1	Glu	Gamma	36.455	-27.971	2.058	0.033	2.248	111.3	3.3
APK1	Glu	Gamma	12.843	NA	0.953	0.028	2.724	122.8	5.1
SPK0	Glu	Gamma	21.631	1.702	NA	0.000	3.035	116.6	8.2
TDK0	Glu	Gamma	21.472	1.692	NA	0.000	3.058	115.7	8.2
APK1	Asp	Gamma	10.778	NA	0.892	0.028	3.001	121.8	8.5
Middle Calibration									
∗*Macoma* (ΔBIC = 1)									
APK0	Asp	Lognormal	7.562	NA	NA	0.000	-0.276	81.7	0.0
APK0	Glu	Lognormal	9.171	NA	NA	0.000	-0.265	81.9	0.2
CPK0	Glu	Lognormal	38.509	-33.263	NA	0.000	-0.366	82.5	0.5
APK0	Glu	Gamma	9.570	NA	NA	0.000	2.976	82.0	0.7
APK0	Asp	Gamma	7.943	NA	NA	0.000	2.979	82.2	0.9
∗*Nuculana* (ΔBIC = 1)									
CPK0	Asp	Lognormal	-4.664	3.620	NA	0.000	-0.374	116.7	0.0
SPK0	Asp	Lognormal	20.167	2.015	NA	0.000	-0.337	119.7	0.1
TDK0	Asp	Lognormal	20.320	2.026	NA	0.000	-0.339	119.6	0.1

Table2.6, continued.

Model	Amino acid	Uncertainty	ln(a)	ln(b)	c	R_0	ln(d)	BIC	ΔBIC
APK1	Glu	Lognormal	12.165	NA	1.193	0.030	-0.328	119.4	0.3
Young Calibration									
∗*Macoma* (ΔBIC = 1)									
APK0	Asp	Lognormal	7.450	NA	NA	0.000	-0.563	77.2	0.0
APK0	Glu	Lognormal	9.060	NA	NA	0.000	-0.567	77.2	0.0
CPK0	Glu	Lognormal	38.554	-33.268	NA	0.000	-0.869	77.8	0.2
APK0	Glu	Gamma	9.367	NA	NA	0.000	2.511	77.3	0.4
APK0	Asp	Gamma	7.740	NA	NA	0.000	2.530	77.7	0.7
∗*Nuculana* (ΔBIC = 1)									
APK0	Asp	Lognormal	7.309	NA	NA	0.000	0.149	99.6	. 0.0
APK0	Glu	Lognormal	9.105	NA	NA	0.000	0.165	99.8	0.2
∗*Nuculana* (ΔBIC = 2)									
APK0	Asp	Lognormal	7.309	NA	NA	0.000	0.149	99.6	0.0
APK0	Glu	Lognormal	9.105	NA	NA	0.000	0.165	99.8	0.2
APK1	Glu	Lognormal	10.745	NA	0.557	0.024	0.044	99.9	1.4
APK1	Asp	Lognormal	8.654	NA	0.418	0.023	0.067	99.8	1.5
SPK0	Asp	Lognormal	12.176	1.430	NA	0.000	0.039	101.5	1.7
TDK0	Glu	Lognormal	15.713	1.413	NA	0.000	0.123	101.4	1.9
SPK0	Glu	Lognormal	17.014	1.507	NA	0.000	0.113	101.3	1.9

Table 2.7: Descriptive statistics for shell-age frequency distributions from each genus, calibration, age model, and test region. Red (*Macoma*) and blue (*Nuculana*) highlighting denotes the least degree of time averaging for a given calibration. IQR = Interquartile Range

Calibration	Taxon	ΔBIC Limit	DBO	Mean	SD	Median	IQR	Minimum	Maximum	Range
Old	*Macoma*	1	DBO1	92	33	84	40	41	191	150
			DBO3	62	15	63	18.25	23	94	71
			DBO4	137	58	128	65	54	279	225
		4	DBO1	82	33	72	41	35	180	145
			DBO3	54	14	54	16.5	20	87	67
			DBO4	127	60	116	65	46	283	237
	Nuculana	1	DBO1	83	44	87	50	4	241	237
			DBO3	95	53	88	65	17	243	226
			DBO4	87	48	76	39	42	296	254
		8	DBO1	84	40	89	46	6	221	215
			DBO3	95	48	90	60	20	223	203
			DBO4	88	42	79	35.75	46	267	221
Middle	*Macoma*	1	DBO1	39	8	37	8	30	67	37
			DBO3	36	4	36	6	24	42	18
			DBO4	44	13	42	10	31	97	66
	Nuculana	1	DBO1	140	155	105	35.5	61	1042	981
			DBO3	109	34	99	25	74	217	143
			DBO4	171	256	118	50.75	80	1513	1433
Young	*Macoma*	1	DBO1	65	161	27	7	21	819	798
			DBO3	44	111	25	4	18	688	670
			DBO4	45	74	30	7	24	402	378
	Nuculana	1	DBO1	63	31	53	10.75	37	214	117
			DBO3	56	14	51	10	42	107	65
			DBO4	59	14	54	10.75	44	110	66
		2	DBO1	77	88	55	20.25	45	519	546
			DBO3	58	20	53	10	41	158	117
			DBO4	56	11	51	8	46	89	43

Table 2.8: Shell loss and sequestration rates estimated following [305] and organized by age calibration used, genus, age model, and test region. Preferred Model was determined from minimum Akaike information criterion (AICc) value of the four different loss models tested (models: 1-phase, 2-phase, truncated 1- phase, and truncated 2-phase), where the truncated models (developed here) use the youngest dated shell as the left edge of the frequency distribution. Rates are: λ – One-phase loss rate; λ_1 - initial loss rate of two-phase model; λ_2 - second loss rate of two-phase model; τ – sequestration rate of two-phase model. Trun. = truncated model that uses youngest dated shell as the left edge of the frequency distribution, developed here. Log-like – log likelihood from model. Red (*Macoma*) and blue (*Nuculana*) rows are lowest TA for the calibration

Calibration	Taxa	ΔBIC Limit	DBO	Preferred Model	λ	λ_1	λ_2	τ	Log-Like	AICc
Old	*Macoma*	1	DBO1	Trun. One-Phase	0.0141	NA	NA	NA	-194.8	396.3
			DBO3	Trun. One-Phase	0.0241	NA	NA	NA	-170.1	347.0
			DBO4	Trun. One-Phase	0.0086	NA	NA	NA	-143.8	294.8
		4	DBO1	Trun. One-Phase	0.0163	NA	NA	NA	-189.2	385.2
			DBO3	Trun. One-Phase	0.0300	NA	NA	NA	-162.2	331.2
			DBO4	Trun. One-Phase	0.0094	NA	NA	NA	-141.5	290.2
	Nuculana	1	DBO1	Trun. One-Phase	0.0162	NA	NA	NA	-194.7	396.0
			DBO3	Trun. One-Phase	0.0135	NA	NA	NA	-196.3	399.3
			DBO4	Trun. One-Phase	0.0151	NA	NA	NA	-155.9	318.6
		8	DBO1	Trun. One-Phase	0.0159	NA	NA	NA	-195.3	397.4
			DBO3	Trun. One-Phase	0.0135	NA	NA	NA	-196.2	399.1
			DBO4	Trun. One-Phase	0.0149	NA	NA	NA	-156.2	319.4
Middle	*Macoma*	1	DBO1	Trun. One-Phase	0.0558	NA	NA	NA	-143.8	294.3
			DBO3	Trun. One-Phase	0.0683	NA	NA	NA	-132.6	272.0
			DBO4	Trun. One-Phase	0.0439	NA	NA	NA	-103.2	213.5
	Nuculana	1	DBO1	Trun. One-Phase	0.0084	NA	NA	NA	-219.6	446.0
			DBO3	Trun. One-Phase	0.0114	NA	NA	NA	-202.7	412.1
			DBO4	Trun. Two-Phase	NA	0.0096	0.0009	$2.9e-05$	-176.1	364.7
Young	*Macoma*	1	DBO1	Trun. Two-Phase	NA	0.0149	0.0015	$4.0e-06$	-124.4	260.8
			DBO3	Trun. Two-Phase	NA	0.2230	0.0016	$4.7e-07$	-99.8	211.5
			DBO4	Trun. Two-Phase	NA	0.1054	0.0029	$1.52e-05$	-89.1	191.3
	Nuculana	1	DBO1	Trun. One-Phase	0.0239	NA	NA	NA	-179.9	366.5
			DBO3	Trun. One-Phase	0.0282	NA	NA	NA	-169.0	344.7
			DBO4	Trun. One-Phase	0.0266	NA	NA	NA	-138.8	284.5
		2	DBO1	Trun. Two-Phase	NA	0.0238	0.0023	$5.0e-05$	-187.1	386.0
			DBO3	Trun. One-Phase	0.0274	NA	NA	NA	-170.1	347.0
			DBO4	Trun. One-Phase	0.0286	NA	NA	NA	-136.6	280.1

Table 2.9: Estimates of time-averaging based on age-dating of carbonate skeletal remains from continental shelves. Results here are only including the surface sediment increment (0-8cm, 10cm or 20cm depending on study); N - number of shells dated; $*$ - specimens not sampled randomly, thus overestimates of medians All are bivalves unless otherwise noted: Br = brachiopod, Ech = echinoid. Sources listed as in full text references.

Taxon	Latitude	Location	Environment	Sediment	Water Depth (m)	Median Age (yrs)	IQR (yrs)	Range (yrs)	N	Source
Pitar	9°N	Caribean, Panama	Shelf	Siliciclastic	4-35	375 (*)	1743	5400	15	[164, 159]
Semele	23°S	Brazil	Shelf	Siliciclastic	10	760	475	4437	38	[164, 174]
					30	964	456	4271	37	1, 3
Bouchardia (Br)	23°S	So Paulo, Brazil	Shelf	Siliciclastic	5.7-22.8	470		3195	82	[39, 169]
Leodia	25°N	San Salvador, Bahamas		Carbonate		12	2	33	30	[171]
Tecetona (Ech)	25°N	San Salvador, Bahamas		Carbonate		1058	1830	4000	30	[171]
Donax	32°N	Mediteranian, Israel	Shelf	Siliciclastic	10	671	962	4171	15	[10]
					30	1470	1344	4771	15	[10]
					40	207	292	504	15	[10]
Mactra	33°S	Southernmost Brazil	Shelf	Siliciclastic	7	663	1914	56161	20	[219]
					19	431	921	6992	20	[219]
					21	186	200	3093	20	[219]
Nuculana	34°N	Southern California	Shelf	Siliciclastic	23-58	629	4496	12712	232	[164, 305]
Parvilucina	34°N	Southern California	Shelf	Siliciclastic	19-72	36	87	10758	235	[164, 305]
Cyclocardia	34°N	Southern California	Shelf	Siliciclastic	38	2400		5900	25	[164, 174]
					89	11500		17500	25	[164, 174]
Gouldia	45°N	Adriatic Sea, Gulf of Trieste	Shelf	Siliciclastic		1200	2000	5500	60	[301]
						1100	1100	4100	59	[301]
Corbula	45°N	Adriatic Sea, Gulf of Trieste	Shelf	Siliciclastic		1000	2900	7800	50	[301]
Cerastoderma	54°N	North Sea	Shelf	Siliciclastic		5684 (*)		7839	9	[164, 99]

CHAPTER 3

NEW FRONTIERS IN ALASKAN SEAFLOOR ECOLOGY: 150 YEARS OF PACIFIC ARCTIC ECOSYSTEM CHANGE RECONSTRUCTED FROM NATURAL HISTORY COLLECTIONS

3.1 Abstract

Bivalve communities of the Bering and Chukchi Seas, which are the key food source for large populations of marine mammals and birds, are known to react quickly to climate shifts based on quantitative monitoring that began in the 1980s and focused on detecting their response to the decreasing persistence of seasonal sea-ice. However, because the effects of human-induced climate change likely started before monitoring began, historic benthic data are needed to understand the relationship between seasonal sea ice and the seafloor ecosystem and how large seafloor community reorganizations might affect higher-trophic level animals. Here, I reconstruct a 150-year history of benthic community change in the northern Bering and Chukchi Seas using natural history collections (NHCs) of bivalve prey taxa. Semi-quantitative periodic benthic surveys began in 1845 and are archived in museums, libraries, and online databases. The past geographic distributions of these bivalves can then be modeled with occurrence data to identify the southern or northern edges ("frontiers") of past populations; NHCs from the 1970s onward that overlap with the era of quantitative benthic survey data are used to evaluate the reliability of the older, pre-1970s collections. I find that, using occurrence data for seven families, bivalve communities underwent a significant reorganization in the interval between 1940 and 1960. This reorganization included (1) the expansion of Nuculanidae populations southward into the Bering Sea, and (2) the expansion of Cardiidae populations throughout the Chukchi Sea after 1940, from the BeringSea where they had previously (1900-1940) been concentrated. Frontier positions based on NHCs do not differ significantly from those based on quantitative biomonitoring during the window of 1970-2000 when both data types are available. Historic observations on bivalve family distributions inferred

from 150 years of NHCs thus indicate that the ecologic baseline inferred from the first quantitative surveys in the 1970s was at that point only a recently completed (1960s) reorganization of the benthic community; this reorganization, recognized using NHC data, had started in the 1940s, coinciding with the initial, 20th-century onset of seasonal sea ice retreat that began then. A collections-based historic perspective on benthic populations in the Arctic over the past 150 years thus reveals that the close coupling of biological and physical changes through multiple climate shifts.

3.2 Introduction

Understanding how biological communities have reacted to past and ongoing climate changes is crucial to understanding how future ecosystems might respond to new and accelerating climate shifts. However, biological monitoring often begins only after a change in the ecosystem is underway. For example, in the Bering and Chukchi Seas, marine monitoring began in the 1970s, shifting to annual and more standardized surveys in the 1980s [240, 293, 119], but instrumental records indicate that Alaskan Arctic surface air temperatures began a rapid rise as early as 1925 and that sea ice began to retreat in 1930 [240, 313, 190]. Thus some significant climate shifts of the 20th century are likely not captured by modern quantative surveys. Historic observations are thus needed to examine this major marine ecosystem through multiple warming and cooling periods to understand the future of the Pacific Arctic [143, 179, 315].Natural history collections (NHCs) from the Bering and Chukchi Seas date back to the earliest phases of post-Industrial climate shift (beginning in 1845) and range up to the present day, with the latter, 1970s-onward part of this history overlapping with modern quantitative surveys. The Pacific Arctic thus represents an excellent opportunity to test NHCs as a source of regional historic data on species occurrences over multiple intervals of rapid climate change, relevant to crucial benthivores in this ecosystem.

Once known as the most stable region on earth, the high latitudes have been undergoing strong changes in climate in recent decades, induced by rapid warming of air and water surface temperatures that have contributed to the loss of sea ice [148]. Systematic observations by the

Chesapeake Biological Laboratory Arctic Research Group (https://arctic.cbl.umces.edu/) have established strong coupling of physical and biological changes in the marine ecosystem on the open continental shelf of the Bering and Chukchi Seas (10 to 100 m) [119, 133].In the last 15 years, the northern Bering Sea and the southeast Chukchi Sea have undergone a "regime change" from an Arctic climate and ecology – characterized by a longer ice-covered season, productive benthos, and a large flux of organic carbon to the seabed from ice edge primary productivity left unconsumed by zooplankton, to a new Subarctic condition with a longer open water season, more open-water primary productivity, and a productive pelagic community, with more organic flux caught in the pelagic ecosystem [128]. The boundary between the Subarctic and Arctic regimes was in the past maintained south of St. Lawrence Island within the northern Bering Sea by a very cold ($< 1^{\circ}$C) bottom water layer [133, 119], but physical oceanographic monitoring shows that this bottom-water pool began to warm in 2014 [286]. Changes in the benthic community structure in the southeast Chukchi Sea since 1990's indicates that Arctic benthic communities are under transition in the Northern Bering Sea, and the Southeastern Chukchi Sea. This regime change is driven by accelerated climate change, and seasonal sea ice retreat.

Primary productivity along the sea-ice edge provides abundant organic carbon to the seafloor, which in turn supports a diverse, abundant, and productive (high biomass) benthic community, dominated by infauna such as bivalves, polychaetes, and arthropods [119, 132, 130]. Without a consistent seasonal cycle of sea ice formation and break-up, the amount of carbon delivered to the benthos changes both in source and amount, forcing benthic populations to find a new environment during the next generation, or to adapt to the new carbon delivery. This physical-biological coupling found in the Pacific Arctic region creates a strong trophic reaction to sea ice changes within the ecosystem, with ice-associated marine benthivores such as the Pacific walrus (*Odobenus rosmarus divergens*) and spectacled eiders (*Somateria fischeri*) depending on both the ice itself (resting habitat) and he infaunal prey communities linked to the ice edge [119, 182, 184, 187, 277] (See Appendix F, and Appendix G for review).

Natural history collections (NHCs) can offer an unparalleled source of historic ecological information over multiple past changes in climate, as shown by many past studies [149, 175, 116, 248, 244, 180, 141, 198, 264, 265]. Even qualitative from NHCs have the power to reveal relationships between biology and climate change owing to the fundamental place-and-date data they archive on species' occurrences [248, 149]. These NHC data can now be extracted and digitized for new, ecological applications [248, 265, 149, 264, 198].The North Pacific Arctic is an ideal area to bring NHCs to bear on the early effects of postindustrial climate change, as it has been the focus of prolonged scientific interest, starting with the exploratory marine surveys of Bering and Stellar to the coasts of Kamchatka and Siberia in 1733-1743 [151, 28]. Here I present bivalve occurrence data of gathered from Pacific Arctic NHCs (2587 data points), as a rough time series from 1865 to 2000, in 20 year time increments.

Using NHC records, I will address the following questions in this chapter:

1. Can species occurrence (presence-absence) data from NHCs reliably reconstruct the geographic distribution of key benthic prey taxa of the Arctic open-continental shelf, using recent quantitative surveys as a benchmark?

2. How have seafloor communities changed over the last 150 years?

I find that the NHCs of the Pacific Arctic provide reliable, interdecadal-scale information on historic changes in seafloor ecology, drawing on the more than 4000 museum lots available for analysis. I also present a new model to estimate one edge — one frontier – of a taxa's geographic distribution, i.e., the descending limb of a unimodal global distribution, or the local minima of an assumed bimodal global distribution. From this "frontiers" model, I find a significant and previously unsuspected shift in the distribution of bivalve populations in the 1940-1960 interval, coincident with an independently known region-wide shift in the timing of seasonal sea ice retreat.

3.3 Methods

3.3.1 Data Collection

Study Region

Analyses focus on the northern Bering and Chukchi Seas, between 61°N and 73°N, and between 180° and 155°*W* (Figure 3.1). These geographic limits correspond to those of modern surveys in the Pacific Arctic Region, such as the Distributed Biological Observatory (https://dbo.cbl.umces.edu/), with the southern boundary (61°N) at the interface between the northern Pacific-influenced Arctic ecosystem and the Subarctic southern ecosystem within the Bering Sea, and the northern boundary is at the northern edge of the Arctic continental shelf (73°N). The eastern boundary (155°W)) is Point Barrow, to exclude taxa endemic to the Beaufort Sea, and the western boundary is political, set by the US-Russia boundary (180°W) that serves as the usual limit of modern American and Canadian oceanographic surveys.

Target Taxa

A subset of seven bivalve families was selected for analysis, focusing on important prey taxa of either Pacific walrus or spectacled eiders (Table F.1, and Table G.1). Dominant prey for the walrus are large bodied suspension feeding bivalves including Cardiidae (specifically the genus *Serripes*) and Myidae, as well as smaller bivalves of various feeding guilds including Tellinidae (facultative deposit feeder), Hiatellidae (nestling suspension feeder), and Yoldiidae (infaunal generalist deposit feeder) [88, 277, 210, 89, 300]. Dominant prey for the spectacled eiders are the Nuculanidae and Nuculidae (both infaunal subsurface deposit feeders), and Tellinidae. Analyses here focus on Nuculanidae, Nuculidae, Tellinidae, Myidae, Cardiidae, Hiatellidae, and Yoldiidae.. The taxonomy in NHCs is complicated, particularly for old lots; therefore, before analysis, all species and genera identifications based on the specimen label were checked against and upgraded to the latest. . .

were checked against the specimen, and upgraded to the latest accepted taxonomic identification following WoRMS [54]. To minimize taxonomic misidentification with these records, only family-level taxonomy was used.

Natural History Collections

Bivalve occurrence data were collected from four Invertebrate Zoology collections; National Museum of Natural History, Smithsonian Institution, Washington, the California Academy of Sciences, San Francisco California; the Museum of the North, University of Alaska, Fairbanks Alaska; and the Russian Academy of Sciences (RAS), St. Petersburg (Table 3.1). At each museum, all Arctic taxa were searched for relevant collections. A museum lot – a separate collection event defined by the museum - was recorded if it was collected in the Pacific Arctic region, including the Bering Sea, and the Chukchi Sea, whether in Alaska or Siberia.

Overall, I acquired data on 4293 museum lots for possible analysis (Table 3.1). Acquiring and confirming these data included collaborating with respective collection curators and my updating their digital catalogs. The collection date and location could not be conclusively established for all lots based on museum labels alone, but such data could still be included for many lots as an "estimate" or could be estimated from secondary sources such as cruise reports (e.g., [67]). For analysis, the total set of museum lots was narrowed to only those bivalve lots that had been collected (1) on the open continental shelf (>10 m water depth) (2) a collection date known within a narrow range (set at < 15 years) and (3) and (3) a collection location that was north 61°N and between 180o and 155°W, , i.e. within the study area, which was set to overlap the geographic range of most modern (1970s-onward) oceanographic surveys. In older lots and labels, locations were often reported only in terms of a land feature and water depth, requiring *post hoc* georeferencing with some amount of uncertainty. That uncertainty is estimated to be 10 nautical miles and is denoted by "Estimated" in the database. This uncertainty on the estimated location could not be incorporated in these analyses.

The final analytical dataset contains 2587 museum lots, which ranged in collection date from 1845 to 2000 (Table 3.2). These lots reflect sampling effort at 921 "stations", which are unique combinations of sampling year, latitude, and longitude (Table 3.1, and Figure 3.2). Lots collected after 1999 were excluded from analysis because they were very few (only three between 2000-2012, across all museums visited).

To compile this data set, museum labels were transcribed verbatim, translated if needed, and used to determine collection date, original collection report (e.g., the expedition, or the museum's accession number), and collection location (latitude and longitude if available, or place name). Each museum lot was assigned a unique number in a master database. Each bivalve individual was tallied (to build abundance data), measured for body size (to build data on biomass, g Carbon; [207]), and examined to determine if it had been collected alive or dead (live collection inferred from articulated valves, adhering flesh, or archived in alcohol).

Only presence-absence occurrence data are analyzed here, and both live collected and dead-collected lots are used in these analyses. 435 lots contained only "dead" collected individuals. In the RAS collections, 555 lots (20%, Table 3.1) were not physically accessible, that is I could not examine the specimen and its label directly. Data were thus collected from these lots based on my translation of mostly hand-written entries in museum ledgers, which consistently included latitude and longitude information as well as collection data. These lots thus represent valuable data that would otherwise be entirely inaccessible but have the disadvantage in that they could not be scored for specimen abundance, body size (biomass), or live versus dead status at the time of collection. Despite the uncertainty of the unexamined lots, they were included in the analysis: many of these specimens are in the oldest lots.

Modern Survey Data

Survey data on animal occurrences were gathered from online data repositories covering the last 50 years, including NSF Arctic Data Center (https://Arcticdata.io/), NOAA National Centers for

Environmental Information, and newer data shared by Prof. Jacqueline Grebmeier, the lead scientist on many research cruises over the past several decades [135, 81, 76, 75, 146, 82, 320, 206, 4, 5, 3]. As with the NHC data, all species and genus identifications were aggregated to family, using WoRMS [54].Because analyses incorporated only occurrence (presence-absence) data, only station location data were used: differences in gear between these modern and historical collections that would affect data on abundance and biomass were ignored. Overall, the data set based on modern surveys spans 1970-2016, thus overlapping with the NHC data for about 40-50 years.

3.3.2 Data Analysis

Modelling Frontiers of Geographic Distribution

The geographic extent of bivalve occurrences at any given moment in time – here, the northern or southern edge of a population of a given family, can be modeled as a "frontier", that is a sloping front beyond which bivalves are less likely to live. A new model is developed here in order to accommodate the inconsistent nature of the data from NHCs, and to use occurrence- rather than abundance-based data: occurrence data cannot be used with dynamical models such as the reaction diffusion models [282].

If y_i represents the presence or absence of a bivalve family (1 or 0) at a given latitude x_i, then bivalve presence could be modeled with a simple regression:

$$y_i = \beta_0 + \beta_1 x_i + \epsilon, \tag{3.1}$$

where β_0 and β_1 are coefficients in a linear regression scaling bivalve presence or absence to latitude and a "noise" factor (ϵ). The *expected* value of occurrence ($E(y_i)$) at a given latitude (x_i) is equivalent to the *probability* of occurrence and can be written as:

$$E(y_i) = \beta_0 + \beta_1 x_i \tag{3.2}$$

This model for the latitudinal distribution of bivalve occurrences can be used to model the expected number of occurrences per latitude if sampling of bivalves had been uniform over time. However, museum lots were collected over decades to century timescales, with erratic spacing in time and space and by a variety of researchers with differing goals and collection strategies, thus creating an inherently non-uniform sampling scheme [248, 244, 265, 270]. Therefore, a model that assumes uniform sampling is insufficient to capture the dynamics of the Pacific Arctic seabed. Instead the probability of occurrence is more appropriately modeled as a Poisson process, which describes a random pattern of points in a mathematical space. The Poisson process used here models a sequence of random latitudes where a family of bivalve occurs, as follows.

$$E(y_i) = \pi_i = -1 - exp{-\lambda(x_i)} \tag{3.3}$$

where $\lambda(x_i)$ is the intensity of the Poisson process at a given latitude (x_i). This intensity serves as a linking function for a generalized linear model of $E(y_i)$ where

$$\lambda(x_i) = exp{\beta_0 + \beta_1 x_i} \tag{3.4}$$

An exponential function was chosen to model the bivalve occurrences as this model estimates one edge of the family distribution, i.e., the descending limb of a unimodal global distribution, or the local minima of an assumed bimodal global distribution. Therefore, the Poisson process can be written as [319]:

$$log(-log(1 - \pi_i)) = \beta_0 + \beta_1 x_i \tag{3.5}$$

In this approach, the occurrence of bivalves is modeled as a Poisson process with the intensity $\lambda(x) = exp(\beta_0 + \beta_1 x)$, which characterizes the complex data of the bivalve distributions as a single number, namely the ”frontier”:

$$\phi = -\beta_0/\beta_1 \tag{3.6}$$

The frontier (ϕ) measured as a latitude beyond which bivalves are less likely to be sampled. Here we focus on the latitudinal gradient in the Alaskan Arctic; however, future work will include longitudinal variation. The latitude of this frontier is determined by the latitude where the intensity (Eqn 4) decreases below some threshold value (λ_1). The magnitude of paired β_0, and β_1 values determines the shape of the curve depicting variation in occurrences with latitude (Eqn 4). The steeper the slope of intensity, the faster bivalve occurrences decrease at the frontier, i.e. the more distinct the edge of the latitudinal distribution. The signs of β_0, and β_1 determine the direction of the frontier (northward with positive β_0 and negative β_1 or southward with negative β_0 and positive β_1).

Figure 3.3 shows hypothetical examples of different paired values of β_0, β_1 within this model framework, and the resulting intensity curves (Eqn 4). The threshold intensity (λ_1) was set equal to 1, and so in these examples the frontier is defined as the latitude where the curve intersects with an intensity of 1.

Modelling Temporal Data

To model latitudinal shifts of frontiers over time, all bivalve data were binned into seven 20-year time bins for analysis, with the first bin representing all samples "before 1880" and 20-year bins thereafter (Figure 3.2). To estimate the frontiers for the total number of time increments (τ), T_i denotes the ith time increment, with each observation year (t) falling within a time increment (i). The frontier model can then be modified to allow for separate intercepts in latitude coefficients for each time interval (i.e., β_{0i} and β_{1i}). This model can be written as follows:

$$\log\big(-\log(1-\pi(x,t))\big) = \sum_{i=1}^{\tau}\big(\beta_{0i}I\{t \in T_i\} + \beta_{1i}I\{t \in T_i\}x\big) \quad \text{(Model 1)} \tag{3.7}$$

The number of parameters is 2τ, twice the number of time increments because each increment has a β_0 and β_1. I is an indicator variable denoting the particular time increment (T_i) the station collection year (t) is in, and therefore what parameters (β_{0i} and β_{1i}) to use.

This full model (Model 1) was tested against a "reduced model" in which the latitude coefficient denoting slope (β_1) is constant in time ($\beta_1(t) = \beta_1$):

$$\log\big(-\log(1-\pi(x,t))\big) = \sum_{i=1}^{\tau}\big(\beta_{0i} I\{t \in T_i\}\big) + \beta_1 x \quad \text{(Model 2)} \tag{3.8}$$

A likelihood ratio test was used to test the null hypothesis that $\beta_{1i} = \beta_1$ for all i, in other words that the reduced model is sufficient. If the result is significant, then the null is rejected, and Model 1 must be used. If the result is not significant, then the null cannot be rejected and so Model 2 may be used. Here I test for significance at the 95% level, in which case p-values < 0.05 are significant. All these models assume that the observations in successive years are independent, and that a lack of occurrence at a latitude is the same as the bivalve being known not to live at that station (i.e., not be present at that place in that time increment).

Confidence Intervals for Frontiers

To estimate the 95% confidence intervals of the frontier I employed Fieller's method, which allows for confidence intervals to be calculated from a ratio of two means [96]. This method uses the estimated co-variance matrix for β_0 and β_1 to estimate the confidence intervals of the frontier ($\phi = -\beta_0/\beta_1$). Fieller's estimates were accompanied by nonparametric bootstrapping (10,000 simulations) to provide confidence intervals both for frontiers and for intensity estimates.

Intensity Thresholds (λ_1)

Three types of intensity thresholds were used to find the frontier (Table 3.4). First, the intensity for all families was set to a constant value at 0.2, the "constant threshold" (C). Second, for each family the median intensity of each family was used, the "midpoint threshold" (MP). Third, for each family and each time increment, the minimum and maximum intensity was found, and a value was chosen that overlapped with the most time increments, the "By Period Threshold" (BP).

Survey Data Analysis

Quantitative "survey data" produced in 1970-2016 were used to test the NHC data in two simple ways. First, the survey data were run through the same Poisson Process model as the NHC data (Section 3.3.2) in order to generate frontier latitudes. Frontier latitudes were considered to match if the museum-estimated frontier was within the confidence interval of that of the survey data and if the sign of the slope of the frontier matched (e.g., both recognized a north- facing frontier), or, alternatively, neither dataset detected a frontier within the geographic bounds of the analysis. Only frontiers from the same type of intensity threshold were compared (e.g., Frontier MP of survey vs. Frontier MP of Museum), and the constant intensity threshold was set to 0.2, the same as the NHC models (Table 3.5). Running the survey data through the model is an important test, because even a quantitative survey focuses on some but not all parts of the study area, here with particular focus on biomass hotspots. Second, for each 20-year time interval, the observed latitudes of bivalve family occurrences (simple histograms) were compared between the NHC data and the survey data using a two-sample Kolmogorov-Smirnov test. If the two samples were randomly sampled from identical populations, then I would expect their frequency distributions of latitude to be similar, i.e. that the NHC data would provide an adequate substitute for survey-generated occurrence data. Therefore, if the p-value is small (<0.05), then the null hypotheses is rejected: the two samples are from different distributions, and NHC data are not a good proxy for geographic occurrence.

3.4 Results

3.4.1 Overall Sampling using NHCs

NHCs examined for this study yielded a total of 2587 museum lots, that had both collection date and location metadata of sufficient resolution and were collected on the Bering and Chukchi Sea continental shelves, within the bounds of the study. The oldest historic lots were collected in 1845 CE in the Bering Straits (RAS lots 100307 and 100308 of *Macoma balthica*), and the youngest

lots used in the analysis were collected in 1999 in the Bering Sea (RAS lots 101783-101785 of *Musculus corrugotus* and 101858-101861 of *Musculus niger*).

Sampling technology and strategies changed over time. For example, Figure 3.4 contours the changing density of shelf stations. From 1845 to 1900, sampling was concentrated around the Bering Strait and near coasts. Sampling from 1900 to 1940 expanded into the northwest Chukchi and northern Bering basins and away from coastlines. The 1940-1960 interval was a period of intense sampling around Point Barrow, related to the establishment of the Naval Arctic Research Laboratory after World War II.

Collectors also used a variety of sampling gear: the majority of museum lots were collected using trawl, dredge, or grabs (Petersen and van Veen) that sample the surface 15-20 cm of muddy sediment. All seven of the bivalve families targeted here were encountered in each of the 20-year time increments (Table 3.3, Figure 3.5), with fairly consistent representation of families over time. This pattern suggests that collection is not taxonomically biased over time, but some bias from collection gear persists. Most notably, deep-burrowing bivalves, such as *Mya arenaria* within Myidae, and bivalves that prefer rocky or pebbly habitats, such as *Hiatella arctica* within Hiatellidae, are expected to be under-sampled and in fact, only small numbers of lots of Myidae and Hiatellidae are available for analyses (Table 3.3).

3.4.2 Model Selection

For each of the families, the goodness of fit between Model 1 and Model 2 was tested using a likelihood ratio test (Table 3.6). This test revealed that the full model (Model 1) must be used for the Cardiidae, Nuculanidae, Nuculidae, and Yoldiidae, whereas the reduced model (Model 2) can be used for Hiatellidae, Myidae, and Tellinidae. Consequently, only the results of the favored model will be presented for each family.

Hiatellidae and Myidae have the fewest occurrences of all families (Table 3.3; 104 and 42 stations, respectively), and this probably explains their lack of support for Model 1 (i.e., too

few data points per 20-year increment to identify frontiers). The lack of support for Model 1 by Tellinidae, on the other hand, may be rooted in their biology, since his family is very well sampled and not prone to the same collection (gear) biases as Hiatellidae and Myidae (Table 3.3, 188 stations). Tellinidae are generalist, facultative deposit feeders, and today (2000-2016) occur throughout the region in consistently high abundance.

3.4.3 Bivalve Frontiers

Overall, frontiers are identified consistently from 1900-1960 for the families favoring Model 1, as these time intervals hold the most stations. Most of these frontiers are south-facing, meaning that boundaries identify latitudes south of which the bivalve family is unlikely occur (Table 3.6, and Table 3.6). Among families favoring Model 2, few frontiers were identified during this same period, which is likely due to the low-density sampling of Hiatellidae and Myidae and the widespread distribution of the heavily-collected Tellinidae. Very few frontiers are found more recently than 1980 for any model.

A lack of an identified frontier does not indicate a lack of information using this model. If no frontier is found for a time interval despite a sufficient number of occurrences, then that bivalve family may simply occur throughout the region rather than concentrated in only one part of it.

For all models, the intensity thresholds were set using three different approaches (see Section 3.3.2, Table 3.4). Of these, the MP intensity threshold method often produced the highest intensity thresholds (except Myidae), while the C and BP intensity threshold methods often found threshold intensities at 0.2. Differences among frontier estimates as a function of the threshold value are usually small and within confidence interval estimates. The choice of threshold intensity nonetheless significantly affects the latitude of the frontiers presented below.

Cardiidae - Model 1

Cardiidae occurrences yield intensities whose maxima range from 0.06 to 0.82, and five curves slope to the south and two to the north (Figure 3.7, Table 3.6). Model 1 identified a persistent frontier at 67.5°N in 1900-1940 using the BP and the C intensity threshold. The MP intensity threshold yielded one frontier at 65.2°N in 1900-1920 (Figure 3.7, Table 3.6). All three intensity thresholds resulted in similar frontiers in 1900-1920, but the MP frontier (in 1920-1940) is outside of the study area and its confidence intervals do not overlap with the BP and C estimates. The two C and BP frontiers do not change location between the two time intervals, but these frontiers are north-facing, unlike the majority of frontiers found for other bivalve families. These north-facing frontiers are in the opposite direction to that expected from sampling bias – i.e., low sampling in the Bering Sea should create south-facing frontiers – and suggest that this southern boundary for Arctic Cardiidae species is real.

Hiatellidae - Model 2

Hiatellidae bivalve intensities range from 0.06 to 0.42, with southern sloping intensity curves(Figure 3.8, Table 3.6). Model 2 found two frontiers, at 65.1°N in 1880-1900, and 69.2°N using the MP intensity threshold and only that threshold, which is the highest intensity threshold tested for Hiatellidae (Table 3.4). For most intervals, the Hiatellidae intensity curves are relatively flat, with low overall intensities, making it difficult to define a frontier using this method. Intervals from 1920-1940 and 1940-1960 have large enough sample sizes to confidently define a frontier, but the majority of the 1940-1960 stations are around the Barrow Canyon, limiting the power of the method. Low occurrences of Hiatellidae in the other time intervals (<15 occurrences) are unlikely to identify a frontier.

Myidae - Model 2

Myidae bivalve intensities range from 0.01 to 0.18, with southern sloping intensity curves (Figure 3.9, Table 3.6). Model 2 did not detect any significant frontiers at any intensity threshold. The Myidae intensity curves are low and flat, and the number of occurrences in each time interval is low (<15 occurrences); therefore, this model is unlikely to capture frontiers for this family without more data.

Nuculanidae - Model 1

Nuculanidae bivalve intensities range from 0.06 to 0.75, with six southern sloping intensity curves and one northern sloping intensity curve (Figure 3.10, Table 3.6). Model 1 found five significant frontiers using the BP and C intensity thresholds, including 68.3°N before 1880, 69.4°N in 1900-1920, 63.5°N in 1920-1940, 70.1°N in 1940-1960, and at 61°N in 1980-2000. The frontiers shifted south significantly from 1900-1920 to 1920-1940, and north again in 1940-1960. These shifts coincide with southern and northern shifts in Nuculidae, another deposit-feeding bivalve group. Sample sizes for Nuculanidae were low before 1920, and so frontiers before 1920 might not be reliable reflections of biology. Using a different intensity threshold strongly affects the frontier estimate. The MP threshold moves the estimated frontier to the very edge of the domain in many cases (e.g., a 1900-1920 frontier at 71.3°N, Table 3.4). The high MP intensity threshold (0.41) means that it intersects most intensity curves at high intensity and steep slopes (Figure 3.10); therefore, this intensity threshold may be too high to capture a genuine frontier.

Nuculidae - Model 1

Nuculidae bivalve intensities range from 0.04 to 0.72 with three southern sloping intensity curves and three northern sloping intensity curves (Figure 3.11, Table 3.6). Model 1 detected three frontiers using BP and C intensity thresholds, including 66.3°N in 1900-1920, 61.4°N in 1920-1940, and

69.1°N in 1940-1960. The frontiers shift north significantly from 1920-1940 to 1940-1960. This shift coincides with shifts from the Nuculanidae family (Section 3.4.3). Sample sizes for Nuculidae were low before 1900, and so those early frontiers might not be reliable reflections of biology. Using a different intensity threshold strongly affects the frontier estimate, as also found in Nuculanidae. However, the pattern from 1920-1960 previously described is maintained when using the MP threshold, with the frontier shifting from 67.5°N in 1920-1940 to 71.5°N in 1940-1960.

Tellinidae - Model 2

Tellinidae bivalve intensities range from 0.06 to 0.58, with southern sloping intensity curves (Figure 3.12, Table 3.6). Model 2 found two frontiers using the MP intensity threshold, at 63.2°N in 1900-1920, and at 69.5°N in 1960-1980. Frontiers were detected only using the MP intensity threshold, which is the highest intensity threshold tested for Tellinidae (Table 3.4). Although the Tellinidae has relatively high intensity with many occurrences, the curves are relatively flat, making it difficult to define a frontier using this method. Tellinidae is a generalist (facilitative deposit feeder) and is expected to occur throughout the region in high abundance. Probably due to their flexible life habit, they may not have a frontier to identify within the study system, i.e. the analysis yields a correct result of 'no frontier'.

Yoldiidae - Model 1

Yoldiidae bivalve intensities range from 0.03 to 1.09 with four southern sloping intensity curves and three flat curves (Figure 3.13, Table 3.6). Model 1 yielded one frontier, in 1940-1960, at 69°N using the C and BP thresholds and at 71.5°N using the MP threshold. Thus, the intensity threshold strongly affected the frontier estimate, as also found in Nuculanidae. The higher intensity threshold pushes the frontier estimate to the edge of the domain (71.5°N in 1940-1960). After 1960, Model 1 does not identify more frontiers for Yoldiidae. The 1940-1960 frontier for Yoldiidae is in a similar location as other deposit feeders, Nuculanidae and Nuculidae. However, since Yoldiidae are more

flexible surface and subsurface deposit feeders, they may not have a frontier to identify within the study system in other intervals.

3.4.4 Comparison of Museum and Survey Data

When the frontier model is applied to the occurrence data acquired from modern surveys (1960-2000), the Poisson intensity values are consistently higher than those found with the NHC data, most likely due to the larger number (higher density) of stations for the survey data than for the NHCs. Using survey data, the Cardiidae, Hiatellidae, and Myidae families supported Model 2, and all other families used Model 1 (Table 3.6). Higher intensities lead to higher MP and BP thresholds for all families, while the C threshold was held to 0.2 (Table 3.5). For all families, the survey models found no frontiers in the 1960-1980 interval, which is the same pattern as the NHC data. The lack of frontiers in this time interval may thus reflect seafloor biology rather than an error in the occurrence data or model. For 1980-2000, the survey data yielded significant frontiers for Cardiidae, Nuculanidae, and Yoldiidae, of which none were found in the NHC data, but the other three families matched between the survey and NHC data. Thus, overall, of the seven families compared in the two time increments and three intensity thresholds (42 pairwise comparisons), the museum and survey data agreed in 31 cases.

In addition to analyzing the overlapping time intervals, the survey data from 2000-2015 were included in the model analyses. This time interval yielded reasonable frontiers for all families (Table 3.6), and the largest number of occurrences found in the study (all families .100 occurrences). All frontiers found, except Yoldiidae, are southern-facing frontiers. Yoldiidae holds the only northern facing frontier at 67.2°N using the Frontier BP intensity threshold. The frontiers found here are strongly affected by the frontier intensity threshold used (e.g., Tellinidae MP Frontier 66.4°N vs BP frontier 71.5 °N). The frontiers in this time interval serve as an additional test of the model, as they can be compared to established changes in the Arctic seafloor ecosystem (see Section 3.5). However, 2000-2020 is characterized by rapid change and a 20-year interval may be too coarse to

discern all ecologic changes in the region.

For 1960-2000, when both museum and survey data are available, the latitudes of bivalve family occurrences derived from those two sources were compared using a simple two-sample Kolmogorov-Smirnov test. If the two samples were randomly sampled from identical populations, then I expect the frequency distributions of occurrences with latitude to be similar. Thus, for p-values <0.05, the null hypothesis of no difference was rejected. This test only examines the "hits" within a bivalve family – the latitudes of positive occurrences in the survey and NHC data. The test does not analyze the "known misses" available in the data – stations with no occurrences of a given taxon despite the presence of other bivalves. This Kolmogorov-Smirnov test also assumes random and thus comparable sampling of the region by both data sources, which is arguably violated by each data source. Despite these issues, museum and survey data are not significantly different for five of seven families in 1960-1980 (exceptions are Cardiidae and Yoldiidae) whereas the two data sources are significantly different for all but Yoldiidae in 1980-2000 (Table 3.9). Filtering out those lots with only dead-collected shells, and lots only from RAS ledgers and not a physical examination, Nuculidae in 1980-2000 is found to be not significantly different, while all other results remain the same.

3.5 Discussion

3.5.1 Caveats for NHC data

NHCs pose both an opportunity and a challenge for historical ecology research. Here, I present the results of the largest compilation of Arctic bivalves ever assembled from NHCs, building a database of species-level occurrence data and place-time-depth metadata from a combination of archived specimens and original cruise and museum ledgers. Although NHCs hold unique historical data, they can still present challenges for biologic and paleobiologic analyses, with three considered here.

First, despite an exhaustive inventory, the number of data points may still not provide sufficient

power to test for changes in geographic distributions. In the present study, more data would always be better. However, the analyses here are based on a very large database (2587 occurrences), with an average of 50 occurrences per family per 20-year time increment, and thus constitute much more than anecdotal observations such as northern-most and southern-most known specimens. This dataset required acquiring data from offline sources – visiting museums in-person to examine specimen labels and ledgers – and transforming qualitative georeferencing information into latitude and longitude coordinates for many records. This effort yielded data on bivalve occurrences throughout their range within the Arctic study area, permitting statistical analysis of the (former) edges of their populations. This dataset thus constitutes a far more robust basis for evaluating variation over time than the range end-point data that NHCs might ordinarily be used for.

Second, because NHCs can reflect haphazard or opportunistic collection of specimens over time [248], and are not exclusively the products of systematic efforts, the time series of species occurrences extracted from such collections might have significant temporal or spatial bias. The bias created by the uneven collecting of any single effort, however, is minimized by summing the collections from many different surveys and expeditions. Figure 3.4, Table 3.2, and Table 3.1 describe the spatial and temporal variation in bivalve occurrences that exist in the data from NHCs. These patterns include shifting hotspots in sampling effort, and thus an uneven spatial grid of stations for analyses, much as modern surveys focus on particular hotspots. The Poisson model was developed to overcome this reality of uneven data availability across the study area in any given time increment, and the variation over time in the spatial pattern. In detail, such temporal variation in benthic sampling reflects the history of federal (both US and Russian) and academic interests in the Arctic (for history, see Appendix H).

Third, museums – and curators – can have different priorities and resources for taxonomic groups and collecting areas, and some can be biased against (or simply cannot accommodate) "redundant" specimens, i.e., lots that differ from others only in the date of collection and/or the locality within a given region. Therefore, museum holdings might have a surplus of one or more families relative

to others. The data presented here do not show clear evidence of taxonomic bias among museums (similar total number of families; Table 3.1), or obvious trends in family occurrences over time (Figure 3.6, Table 3.3). The relative scarcity, both in NHCs and survey data and across all time intervals, of deep-burrowing bivalves such as Myidae and pebble-nestling bivalves such as Hiatellidae, likely does reflect sampling bias related to gear, not archival bias. Upgrading these occurrence data with information on specimen abundances per station and/or body size or biomass data would help illuminate any pervasive taxonomic collection biases. However, the results appear to be robust to sampling and other collection-related biases.

3.5.2 Model Caveats

The frontier model presented here models an edge of bivalve occurrences, beyond which the target bivalve family is unlikely to occur. This model has two significant assumptions about bivalve distributions.

First, the model assumes a unimodal distribution of occurrences and tests for the existence of a single frontier of that biogeographic range, whereas a taxon might have a multi-modal distribution with more than one frontier within the study region. Therefore, failure to detect a frontier might indicate a different biologic structure rather than a failure of the model given the data. Alternatively, the northern (or southern) edge of a taxon's range might lie outside the domain of the study area. In this instance, given a reasonable number of occurrences exist in that interval, failure to detect a frontier could simply mean that the bivalve occurs throughout the region.

Second, the model assumes that if a bivalve was not sampled in a location during a time interval then it did not live at that location, that is, "zero occurrences" are as meaningful as positive occurrences. Thus, the model uses both presences and absences to estimate an intensity in a mathematical space, rather than exclusively using occurrence data to estimate a probability of occurrence. This assumption does not consider that sampling of the seafloor is incomplete, and that grabs and dredges sample small sections of the seafloor and can easily miss populations of

taxa. Adding more NHCs to this data set will thus improve these estimates of intensity, and so improve the estimation of frontiers, by better describing the heterogeneity of bivalve occurrences on the seafloor.

The results of this model also could be improved by closer discrimination of live versus dead occurrences. Occurrences based on dead-collected specimens may erroneously extend the range of living population during that time interval (or increase its intensity) and thus will tend to broaden ranges and decrease the likelihood of recognizing a frontier. Dead-only occurrences from 1980-2000 revealed the existence of a frontier for Nuculidae, that was otherwise undetected (see Section 3.4.4).

This model currently only examines variation along latitude: examining variation along longitude would improve it, possibly revealing mode dynamics within the Alaskan Arctic system. In addition to the shifts identified here, adding data about the longitudinal variation in species occurrences would help identify changes that might be related to a strong nutrient gradient that exists today between the Alaskan Coastal Current and the open shelf waters of the Chukchi Sea [130, 94]. This nutrient gradient creates a sharp boundary in community composition under these two different water masses, with the nutrient-poor waters of Alaskan Coastal Current supporting many sea urchins and slow-growing bivalves (e.g., Astartidae), and the open-shelf waters supporting more productive and faster growing bivalves (e.g., Cardiidae) [130, 94]. Future work will examine longitudinal changes within the Chukchi Sea given that this nutrient gradient appears to exert significant control on seafloor assemblage composition.

3.5.3 Shifting Seafloor Ecology

The seven bivalve families targeted here were grouped by their life habits and functions within the benthic community. Cardiidae, Myidae, and Hiatellidae are all suspension-feeding bivalves (at various sediment depths); Nuculanidae and Nuculidae are both obligate subsurface deposit-feeding bivalves; Yoldiidae are generalist deposit-feeding bivalves (both surface and subsurface);

and Tellinidae are facultative surface deposit-feeding bivalves (mix of suspension and deposit-feeding). The following sections will discuss the frontiers found for these different bivalve families by feeding guild.

Suspension-Feeding Bivalves – Cardiidae, Hiatellidae, Myidae

All suspension feeding bivalves in the Pacific Arctic depend on receiving ”fresh” organic carbon year round, which is here supplied by planktonic productivity along the ice edge [155, 312, 316, 40, 17, 317, 168]. Cardiidae and other suspension feeding bivalves in the study area are found in relatively sandy sediments with low sediment organic carbon [183, 181, 130]. Therefore, the shifting positions of the frontiers of suspension feeders found here (Cardiidae, Hiatellidae) is probably an ecologic change in response to a change in patterns of carbon deposition.

Very few frontiers were identified for the suspension feeding bivalves(Table 3.6, Table 3.6). For Myidae and Hiatellidae, this lack of frontiers likely reflects their low occurrences despite sampling effort (Table 3.3) [300, 34, 229, 252, 130]: adult Myidae are expected to be difficult to collect because of their deep burrows (15-20 cm) and Hiatellidae because of their preference to nestle on pebbly or rocky substrata where grab samplers commonly fail. These results suggest that a taxon must have more than 15 occurrences per time period, and more than 104 occurrences total, for the model to detect a spatial frontier in its distribution (Table 3.3).

Shallowly-burrowing Cardiidae, on the other hand, have more overall occurrences, exhibit frontiers, and are the only bivalves with north-facing frontiers (Table 3.6). From 1900-1940 Cardiidae were concentrated in the northern Bering Sea, and from 1940 onward, there are no discernible frontiers (the family occurred throughout the entire study area). Their early 20th-century north-facing frontiers are opposite to the expectation from sampling biases alone because the Chukchi Sea is consistently more densely sampled than is the Bering Sea: an absence from the Chukchi Sea is difficult to produce artificially.

Modeling of the modern survey data shows Cardiidae to be present further north within the

Chukchi Sea and have a south-facing frontier in the Bering Strait (66.1°N) in 1980-2000 and the northern Bering Sea (61.9°N) in 2000-2020 (Table 3.6). The confidence intervals of these frontiers overlap; therefore, there is not a significant spatial shift. The NHC data did not record the frontier in 1980-2000, despite sufficient sampling in this time interval (42 occurrences). From 1980-2020 the Cardiidae populations have gone through large "booms and busts", with large populations springing up and for a short period when there is their preferred level of carbon delivery in the region [131, 93, 119].From 1970-2020, large populations of *Serripes* were often found in the Bering Sea, and in 2004 they began to become dominant in the southeastern Chukchi Sea as well, until their decline from 2017-2020 [131, 93, 293]. These reports do not completely agree with the observed frontiers and highlight how abundance data, and finer time intervals could identify rapid shifts as expected with Cardiidae.

Subsurface deposit-feeding Bivalves – Nuculanidae, Nuculidae

In general, Nuculidae and Nuculanidae throughout the Pacific Arctic are most often associated with fine sediment and abundant seafloor organic carbon [183, 184, 130, 316]. Nuculanidae and Nuculidae both grow well while feeding off detrital carbon [183, 184, 130, 316], and the subsurface deposit feeders can dominate a region when large quantities of organic carbon are consistently delivered, as in the northern Bering Sea from 1980-2008 [131]. The largest populations of obligate subsurface deposit-feeding bivalves occur in the St. Lawrence Island polynya, an ice-free patch of sea during winter, south of St. Lawrence Island in the Northern Bering Sea that is consistently fed by ice edge, and open water algae throughout the year [183, 130, 317]. As sea ice retreats, this source of abundant carbon is threatened, by a change in the sub-ice circulation (Anadyr Gyre) and a change in the quality and quantity of carbon delivered near the polynya.

The south-facing frontiers of Nuculanidae and Nuculidae shifted north significantly between 1920-1940 and 1940-1960, from the northern Bering Sea (63.5°N, and 61.4°N in 1920-1940) to the Chukchi Sea (70.1°N and 69.1°N in 1940-1960; Figure 3.11, Figure 3.10, Table 3.6). Because

both bivalve families are well sampled (Nuculidae 205 occurrences, Nuculanidae 196 occurrences, Table 3.3), are members of the same feeding group, and experience the same shift in the frontier. In the interval 1960-1980, both Nuculanidae and Nuculidae have too few occurrences to discern frontiers (both <= 15). In 1980-2000, with sufficient sample sizes, no frontier could be found for Nuculidae, while Nuculanidae had one south-facing frontier at 61 °N (C and BP) or 67.4 °N (MP). These results indicate that after 1960, Nuculanidae and Nuculidae spread throughout the region again.

Modeling of the modern survey data revealed two reasonable frontiers for Nuculanidae at 67.9°N in 1980-2000 and 67°N in 2000-2020 and one for Nuculidae at 67.9°N in 2000-2020 (Table 3.6). Based on monitoring data, biologists reported large populations of Nuculanidae and Nuculidae in the northern Bering Sea, associated with the St. Lawrence Island polynya (DBO1 [131]), and that these families were the most abundant of all bivalve taxa in this region from the 1980s to 2008 [131, 184, 121]. During the 2008-2015 interval, however, the northern Bering seafloor underwent a significant transition from dominance by these subsurface deposit-feeding bivalves to more generalist bivalves (Tellinidae, and Yoldiidae) [131, 111]. This transition coincides with the frontiers identified during 2000-2020 by modeling the survey-based data, but not the Nuculanidae frontier identified in 1980-2000. While the most abundant populations occur in the Northern Bering Sea, the family is widespread and could have higher occupancy in the Chukchi Sea rather than the Bering Sea, resulting in Chukchi Sea frontiers.

Generalist Bivalves – Yoldiidae, Tellinidae

Yoldiidae and Tellinidae are identified as generalist bivalves in this study and are grouped because of their functional flexibility and similar diet of available seafloor organic carbon [181, 155]. Yoldiidae, and notably the abundant Pacific Arctic species *Yoldia hyperborea*, are deposit-feeding bivalves that can feed both at the surface of the sediment-water interface (in response to high organic deposition) as well as subsurface [300, 258, 289]. Tellinidae, particularly *Macoma* spp. that are

abundant in the Pacific Arctic, use both suspension-feeding and surface deposit-feeding depending on the delivery of carbon.

Modeling the NHC data revealed very few frontiers for either family, despite their both having many occurrences (183 occurrences Yoldiidae, 188 occurrences Tellinidae, able 3.3, Table 3.6, Table 3.6, Figure 3.12, Figure 3.13). Yoldiidae yielded only one frontier, and it was south-facing in the North Chukchi Sea (69°N) during 1940-1960. This frontier is similar to those identified during the 1940-1960 interval among the subsurface deposit feeders (Section 3.5.3) and further strengthens the idea that these frontiers reflect an ecological response of bivalves, especially the deposit-feeding guilds rather than being artifacts of a change in sampling. Tellinidae yields frontiers when the (low) MP intensity threshold is used. The intensity curves in most time intervals are relatively flat for both families: they occur consistently almost everywhere (Figure 3.12, Figure 3.13). Given that both families are generalists, the inability of modeling to detect a frontier within the study system is very likely a correct result.

Using survey data, several frontiers were identified for these families: in 1980-2020 for Yoldiidae – both a south-facing frontier at 69.9°N and a north-facing frontier at 67.2°N – and for Tellinidae a north-facing frontier in 1960-1980 at 70.3 °N and in 2000-2020 a south-facing frontier at 66.4°N in the near the Bering Strait (Table 3.6). These frontiers are consistent with isolated reports that Tellinidae dominated the northern Bering Sea before 1980 [293],with that role replaced by Nuculanidae and Nuculidae from 1980-2008, and with a resurgence of Tellinidae from 2008 onward [131, 111]. Tellinidae should be examined for more complex multi-modal distributions, as Tellinidae population centers of the southeastern Chukchi Sea were expanding south while those of the northern Bering Sea were contracting north across a seafloor of heterogeneous grain size and organic carbon input [111]. Yoldiidae are less abundant than Tellinidae in the Pacific Arctic and shifts in their populations have not been as thoroughly characterized; therefore, this model and NHC dataset provide an opportunity to examine the Yoldiidae response to climate shifts.

3.5.4 Sea Ice and Seafloor Ecology

The Arctic seafloor is connected to the seasonal sea ice cycle through pelagic-benthic coupling, with about 70% of water column productivity settling to the seafloor and consumed by the benthic community [132, 130]. Productivity is closely linked spatially to the ice edge, where sunlight can reach primary producers through thin ice and open water [104]. Therefore, the shifts in seafloor ecology described in the previous section should be examined in tandem with historical sea ice data. Figure 3.14 displays a time series of the month of the breakup of sea ice from the Historical Sea Ice Atlas, a gridded, monthly, sea ice concentration data set from 1850 to 2017 [6].The month of the breakup was the first month of the year during which the sea ice concentration dropped below 15% [49, 104]. Starting in 1940, sea ice in the region began to retreat one to two months earlier, a change that was likely related to the rapid rise in Arctic surface air temperatures observed as early as 1925 [240, 313, 190]. This period of sea ice transition started before the onset of ecosystem monitoring (1970s) but is overlapped by the time series of NHC data developed here. Over the period 1940-1960 when the Atlas data indicates that sea-ice started to break up much earlier (Figure 3.14), the NHC data identify four major changes in community structure:

1. Cardiidae (suspension feeders) lose their formerly consistent north-facing frontier at 67.5°N and transitions to a state with no identifiable frontier;

2. Nuculanidae and Nuculidae (subsurface deposit feeders) both shift their south-facing frontiers northward, from the northern Bering Sea (63.5°N and 61.4°N) into the Chukchi Sea (70.1°N and 69.1°N), after which no frontiers can be identified; and

3. Yoldiidae develops a south-facing frontier at 69°N, after exhibiting no frontiers in the previous decades (1920-1940)

In contrast, no frontiers could be identified for any family in the interval 1960-1980, by which time the early break-up date had stabilized across the region, and very few frontiers were found for any family, using either the NHC or the survey data. Using this model, a lack of a frontier does not

mean a lack of information: instead, if the family exhibits a sufficient number of occurrences across the region (i.e., Tellinidae, Yoldiidae), it most likely simply occurred throughout the region rather than being concentrated in only one part of it.

Given the similarities among feeding guilds and the NHC and survey datasets in the time at which frontiers appear and their directions of movement, and given the coincidence of these changes with a major and rapid change in the timing of sea ice break up, the NHC-based analyses reveal a previously unreported reorganization of seafloor communities in the 1940s and 1950s, several decades before the shelf-wide quantitative survey began in 1970. This mid-20th-century reorganization entailed the northward expansion of populations of suspension feeders from the Bering Sea to the entire region, and the nortward contraction of obligate deposit feeders to the Chukchi Sea. It closely resembles the ecological "regime change" that is associated with a late 20th-century phase of rapid sea-ice retreat and recognized using monitoring data [133, 119]. The NHC-based evidence presented here of a rapid mid-20th century shift also indicates that the benthic conditions sampled quantitatively in the 1970s-80s and thought to be a stable baseline were instead a more recently established state. Finally, the existence of two phases of rapid ecological reorganization within the 20th-century suggests that benthic community change in the Arctic during anthropogenic climate warming has proceeded as a series of punctuated changes, implying (a) less inertia to change than previously assumed (i.e. a few decades of stability) and (b) that the well-documented and understood late-20th century reorganization was not unprecedented but rather part of a pattern of repeated and relatively sudden reorganizations.

3.6 Conclusions

This study is based on the analysis of 2600 museum lots of bivalves from the Bering and Chukchi shelves, drawn from >4000 available lots, and represents the largest compilation of Arctic NHCs and first attempt to inform the historical ecology of this region. This study represents one sliver of what NHC's have to offer Arctic researchers: adding additional taxa, body size information,

and abundances gained from NHCs could all further inform on the history of the Arctic. The bivalve families targeted here are important prey items for benthivores, most notably the walrus and spectacled eiders, and thus it would now be worth looking for changes in these key consumer populations beginning in 1940 to further understand the future of this complex ecosystem. The frontier model presented here is a novel method to estimate a single geographic boundary within the preferred habitat of a taxon (here, of bivalve taxa), and has been applied to uncover how seafloor ecology has shifted over the last 150 years. Further work should resolve longitudinal gradients, the location of highest abundance in the region, and the relationship between the environment and the seabed ecology.

From this model, I identify three major changes in the distribution of infaunal bivalves between 1940 and1960. This represents a significant change in benthic community structure, andcoincides with a regional shift to an earlier seasonal break-up of sea ice. Between 1940 and 1960:

From this model, I identify three major changes in community structure from 1940-1960, coincident with earlier sea ice break up across the region:

1. Cardiidae (suspension feeders) lose their formerly consistent north-facing frontier at 67.5°N and transition to a state with no identifiable frontier by occupying the entire study area;

2. Nuculanidae and Nuculidae (subsurface deposit feeders) both shift their south-facing frontiers northward, from the northern Bering Sea (63.5°N and 61.4°N) into the Chukchi Sea (70.1°N and 69.1°N), after which no frontiers can be identified; and

3. Yoldiidae develops a south-facing frontier at 69°N, after exhibiting no frontiers in the previous decades (1920-1940).

In contrast, no frontiers could be identified for any of the seven families tested in the interval between 1960-1980. By 1960 the new-early sea-ice break-up date had stabilized across the region. After 1960, the seven bivalve families examined here were spread throughout the region rather than organized behind a single frontier. The existence of this rapid ecological reorganization, within

two decades of the mid-20^{th} century, implies that the Arctic seafloor has undergone repeated, relatively sudden community shifts. Moreover, what was previously thought of as a baseline in the 1970s based on quantitative surveys and biological monitoring, may represent a relatively recent community reorganization in response to an earlier onset of anthropogenic climate change. As sea ice continues to retreat and Arctic warming continues to accelerate, the results presented here offer the opportunity to add long-term benthic data to new models that can examine the future function of a new Arctic ecosystem, and the future of higher trophic-level prdators.

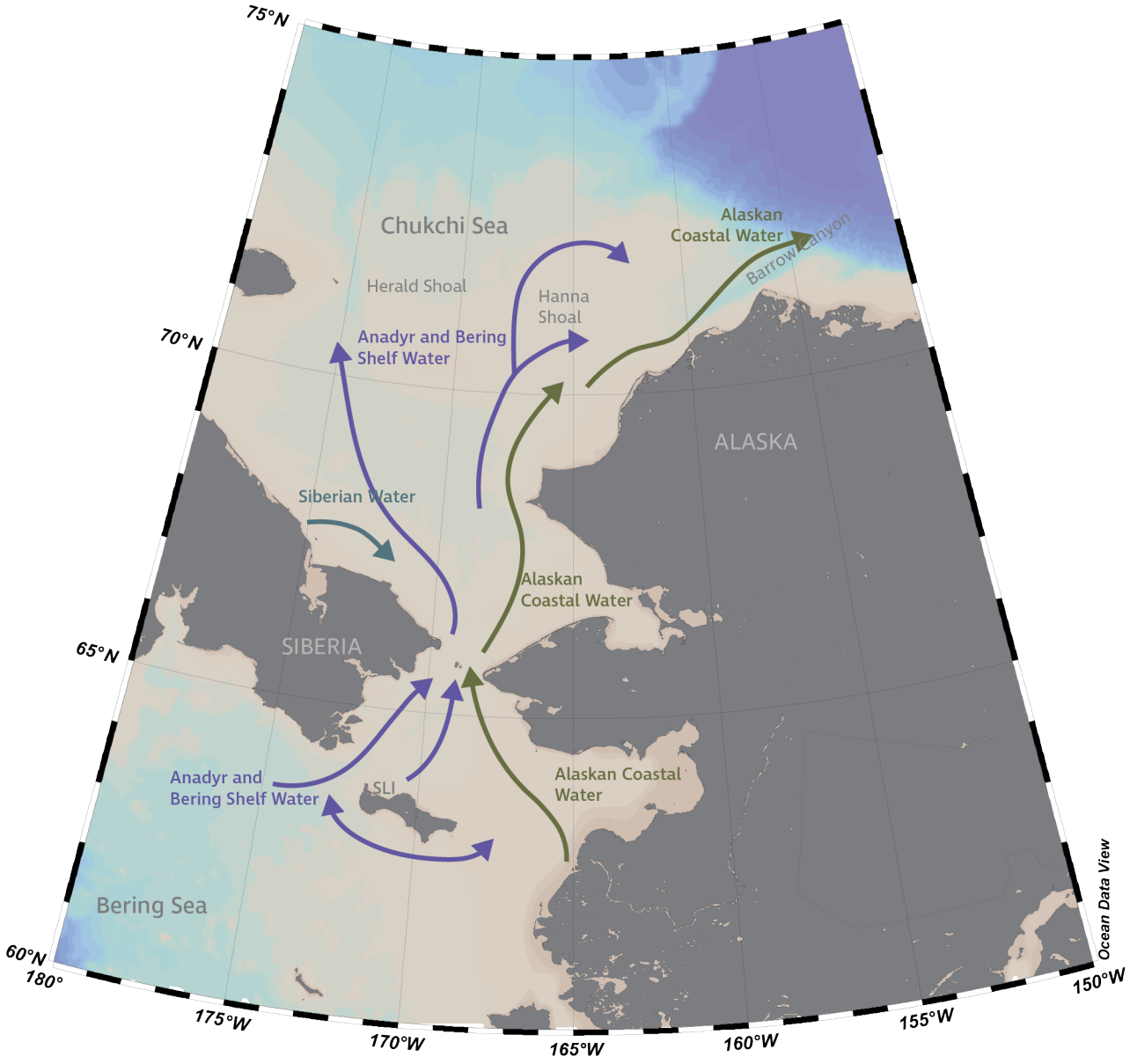

Figure 3.1: Map of the Pacific Arctic region used in this study. Arrows denote dominant currents: purple Anadyr and Bering currents, blue Siberian current, green Alaskan coastal current. SLI St. Lawrence Island. Base map adapted from Ocean Data Viewer and approximate currents from [121]

.

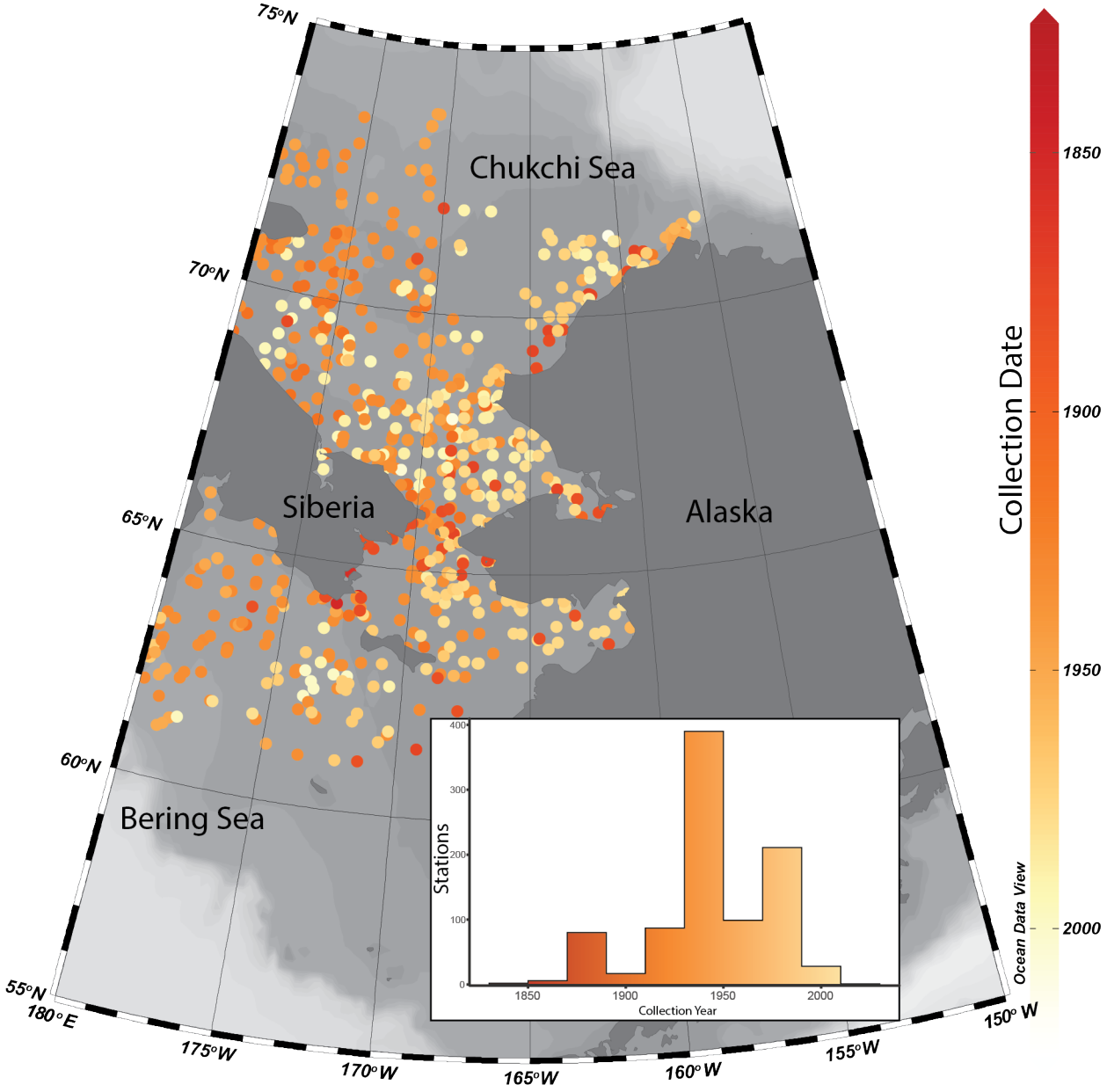

Figure 3.2: All museum lots used in these analyses. Darker colors correspond to older collection age. Inset shows histogram of stations (unique latitude, longitude, date combinations) used in these analyses

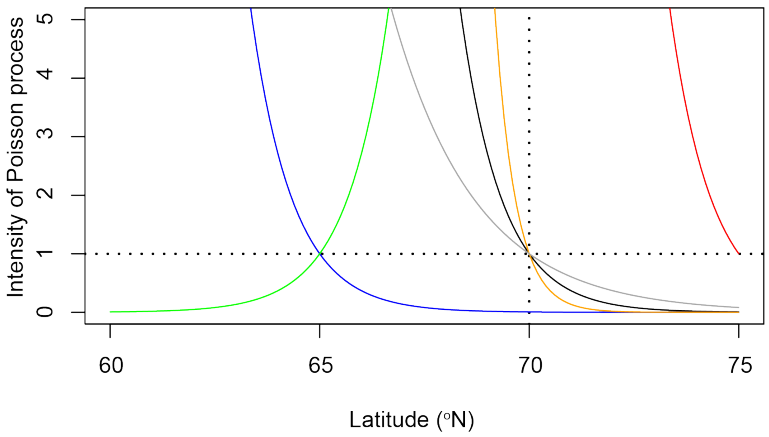

Line Color	β_0	β_1	Frontier	Direction
Red	75	-1	75	N
Black	70	-1	70	N
Blue	65	-1	65	N
Green	-65	1	65	S
Orange	140	-2	70	N
Gray	35	-0.5	70	N

Figure 3.3: Examples of modeled frontiers, including β_0, and β_1 values. Location of frontier determined when intensity threshold ($\lambda(x) = 1$) crosses curve. The Direction of the frontier (N = North, S = South) is determined by the sign of the β_0, and β_1 values, indicating if the intensity is lower to the north or south of the frontier.

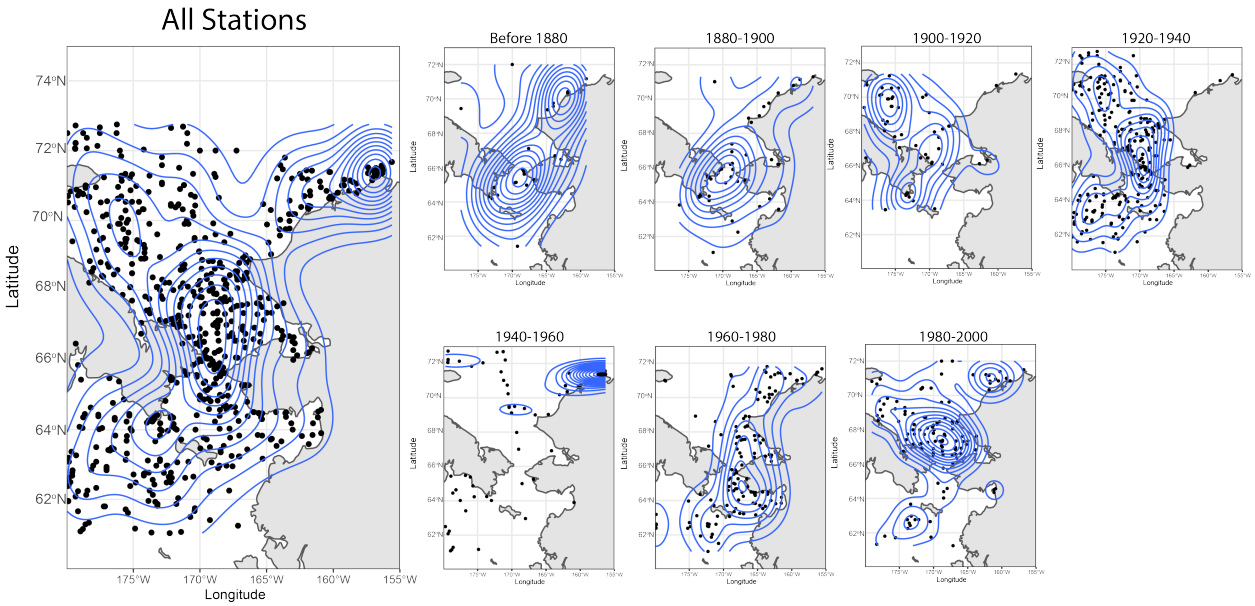

Figure 3.4: Kernel density maps of all stations, and split by 20-year time interval. From a 2-dimensional kernel estimate from from bivariate normal kernels (function in MASS::kde2d) estimated independently for each time-interval, with the bandwidth estimated from the data for each time-interval (with R function bandwidth.nrd).

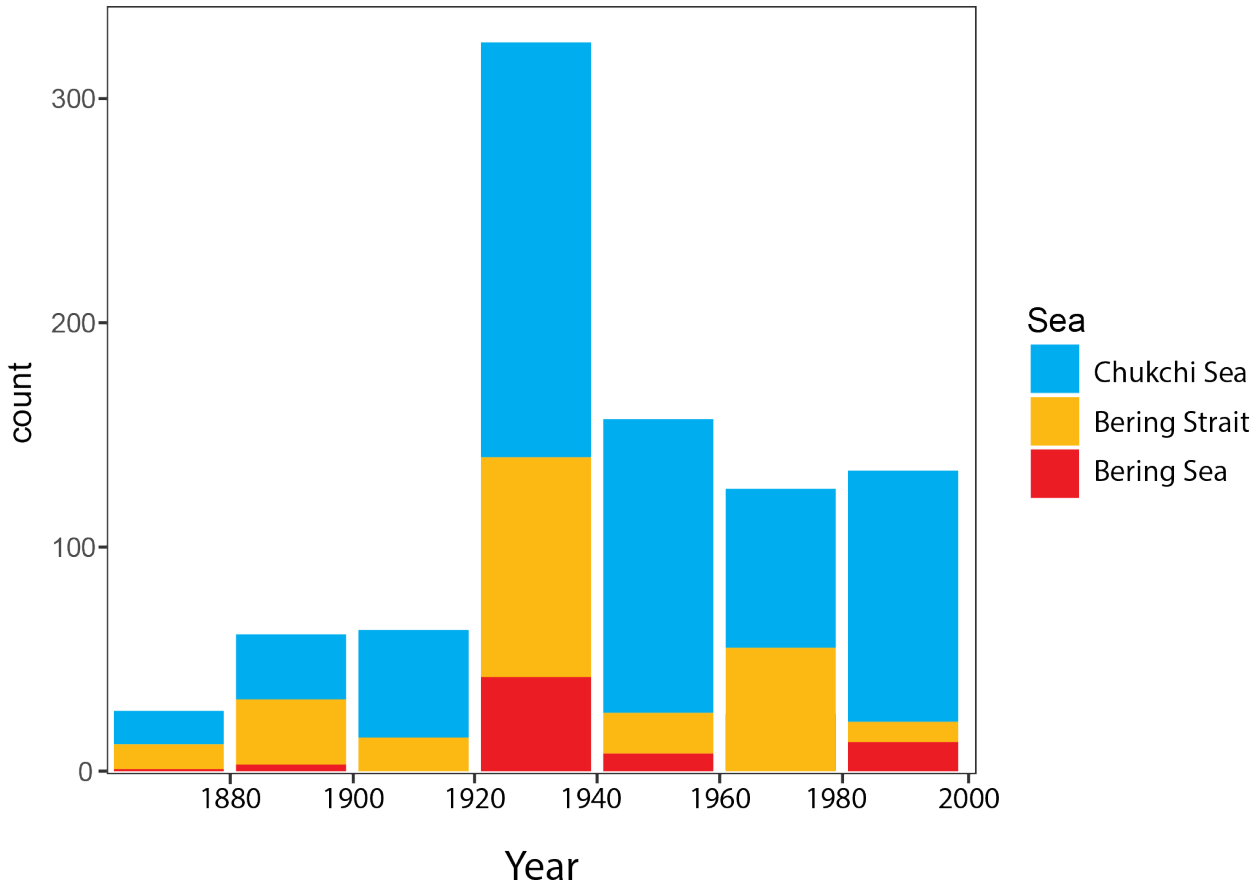

Figure 3.5: All stations (unique latitude, longitude, date combinations) used in these analyses, color coded by region (Chukchi Sea, Bering Straits, Bering Sea)

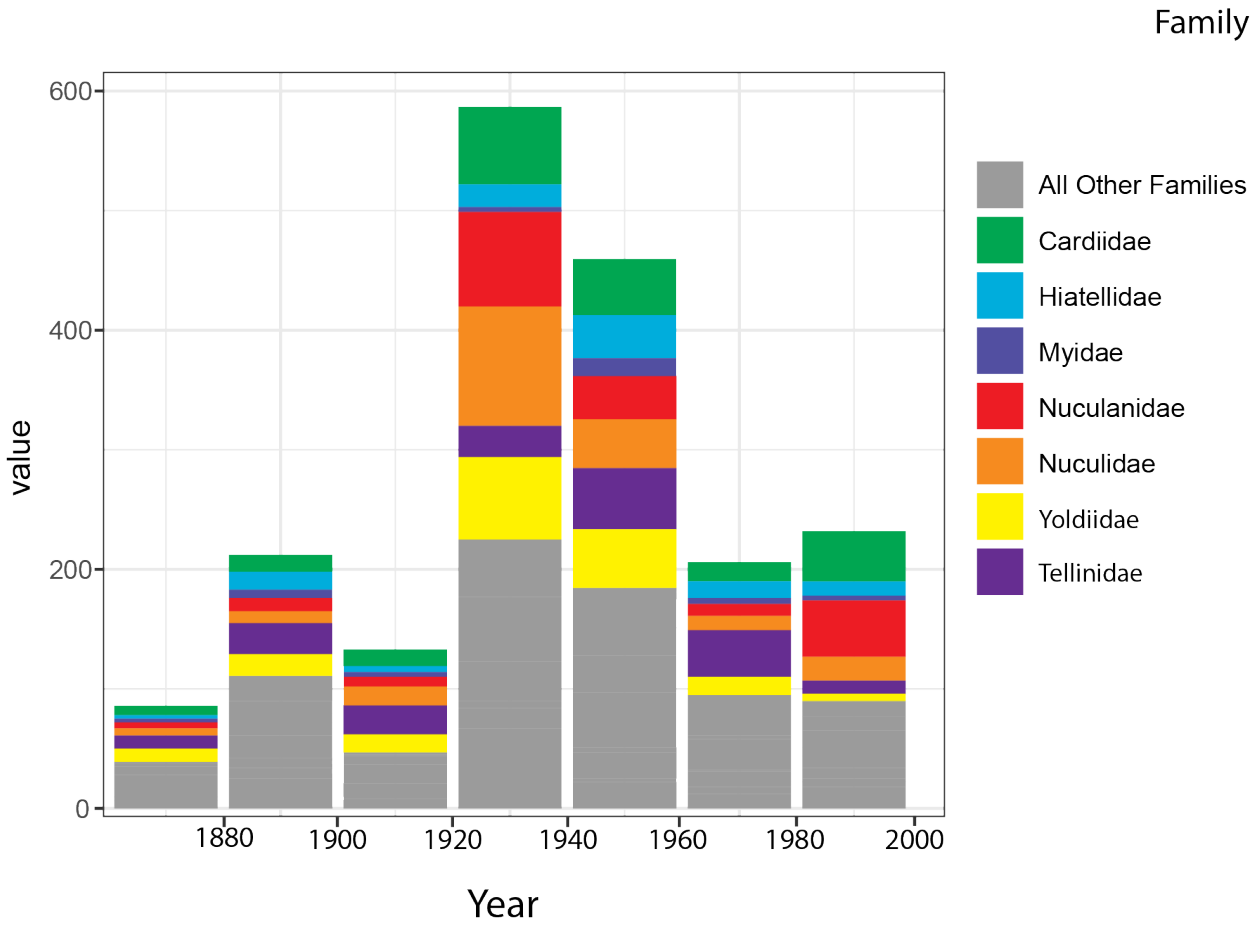

Figure 3.6: All lots used in these analyses, color coded by Bivalve family, target families in color, all other in gray

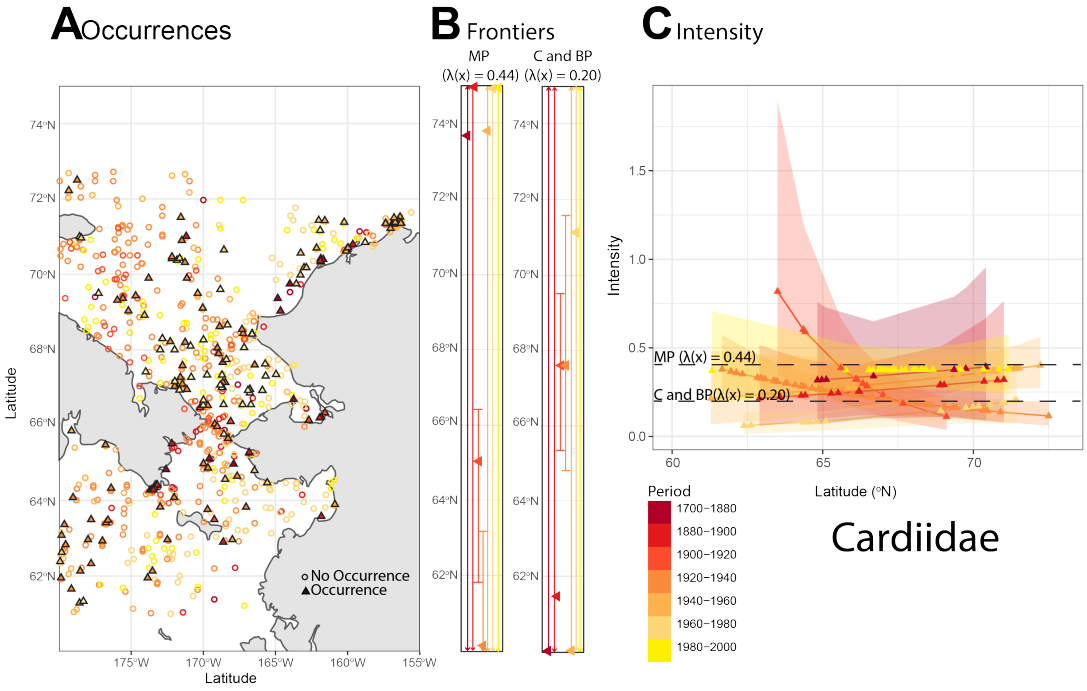

Figure 3.7: Results of Cardiidae Model 1. A) All occurrences of Cardiidae (triangles) color coded by time interval with darker colors represent older periods, and open circles are stations without Cardiidae occurrences. B) Triangles are the frontier estimates from MP, BP and C intensity thresholds with bootstrapping confidence intervals. If symbol is on the left or right margin the frontier estimate is outside the sampling domain. Error bars that exceed the sampling domain are denoted with arrows. C) intensity curves from Model 1 with intensity thresholds (C, MP, and BP) marked with dashed lines (Table 3.4). Shaded envelopes around intensity curves represent bootstrapping confidence interval estimates of the intensities.

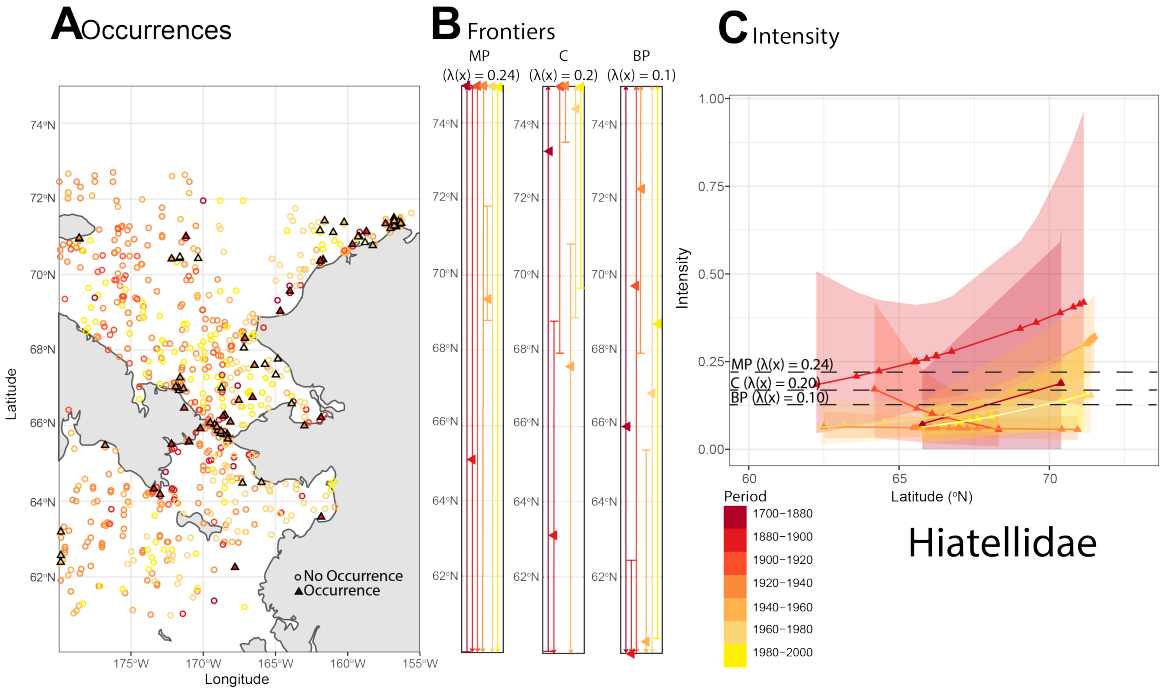

Figure 3.8: Results of Hiatellidae Model 2. A) All occurrences of Hiatellidae (triangles) color coded by time interval with darker colors represent older periods, and open circles are stations without Hiatellidae occurrences. B) Triangles are the frontier estimates from MP, BP and C intensity thresholds with Fieler's confidence intervals. If symbol is on the left or right margin the frontier estimate is outside the sampling domain. Error bars that exceed the sampling domain are denoted with arrows. C) intensity curves from Model 2 with intensity thresholds (C, MP, and BP) marked with dashed lines (Table 3.4).Shaded envelopes around intensity curves represent bootstrapping confidence interval estimates of the intensities.

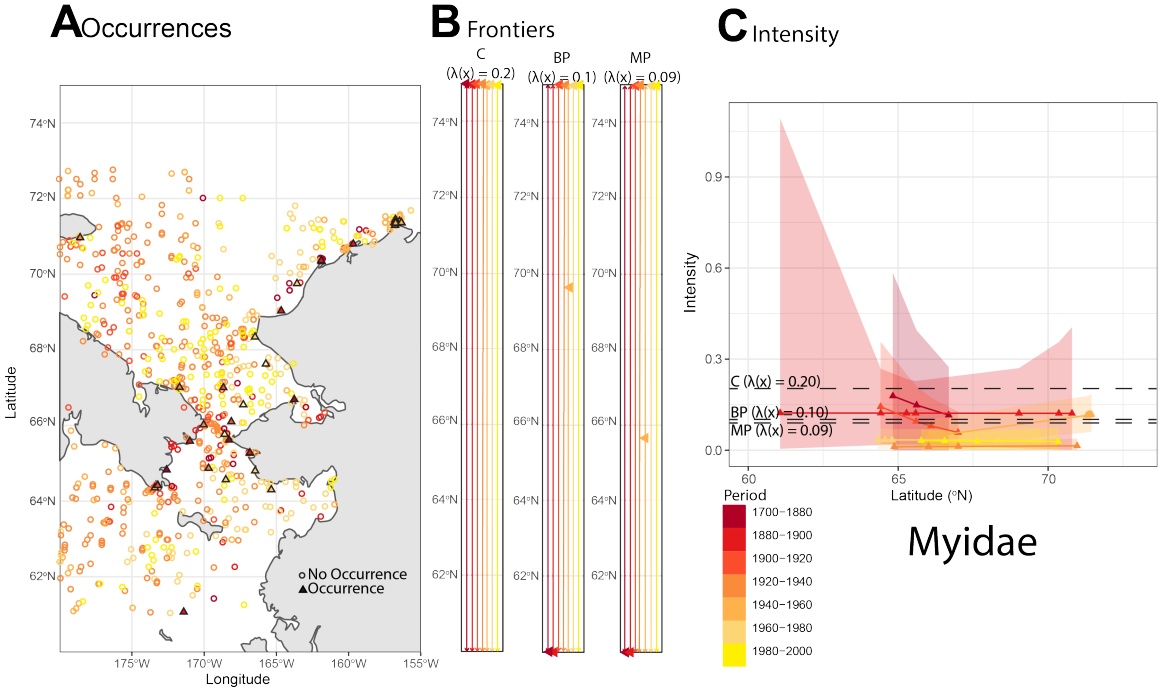

Figure 3.9: Results of Myidae Model 2. A) All occurrences of Myidae (triangles) color coded by time interval with darker colors represent older periods, and open circles are stations without Myidae occurrences. B) Triangles are the frontier estimates from MP, BP and C intensity thresholds with Fieler's confidence intervals. If symbol is on the left or right margin the frontier estimate is outside the sampling domain. Error bars that exceed the sampling domain are denoted with arrows. C) intensity curves from Model 2 with intensity thresholds (C, MP, and BP) marked with dashed lines (Table 3.4). Shaded envelopes around intensity curves represent bootstrapping confidence interval estimates of the intensities.

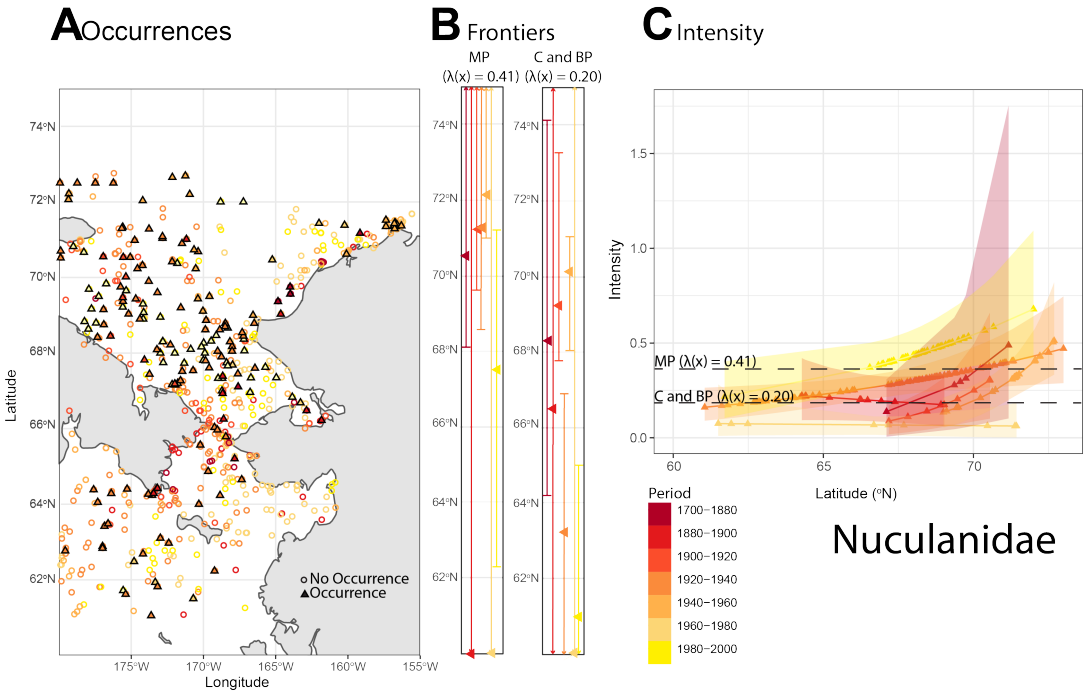

Figure 3.10: Results of Nuculanidae Model 1. A) All occurrences of Nuculanidae (triangles) color coded by time interval with darker colors represent older periods, and open circles are stations without Nuculanidae occurrences. B) Triangles are the frontier estimates from MP, BP and C intensity thresholds with bootstrapping confidence intervals. If symbol is on the left or right margin the frontier estimate is outside the sampling domain. Error bars that exceed the sampling domain are denoted with arrows. C) intensity curves from Model 1 with intensity thresholds (C, MP, and BP) marked with dashed lines (Table 3.4). Shaded envelopes around intensity curves represent bootstrapping confidence interval estimates of the intensities.

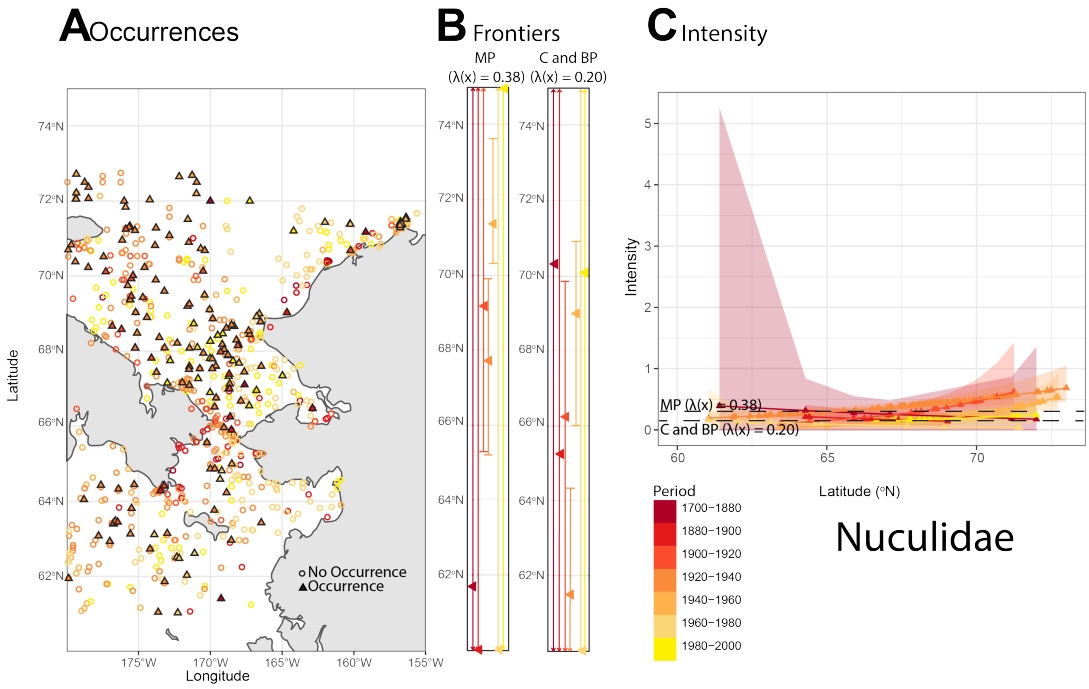

Figure 3.11: Results of Nuculidae Model 1. A) All occurrences of Nuculidae (triangles) color coded by time interval with darker colors represent older periods, and open circles are stations without Nuculidae occurrences. B) Triangles are the frontier estimates from MP, BP and C intensity thresholds with bootstrapping confidence intervals. If symbol is on the left or right margin the frontier estimate is outside the sampling domain. Error bars that exceed the sampling domain are denoted with arrows. C) intensity curves from Model 1 with intensity thresholds (C, MP, and BP) marked with dashed lines (Table 3.4). Shaded envelopes around intensity curves represent bootstrapping confidence interval estimates of the intensities.

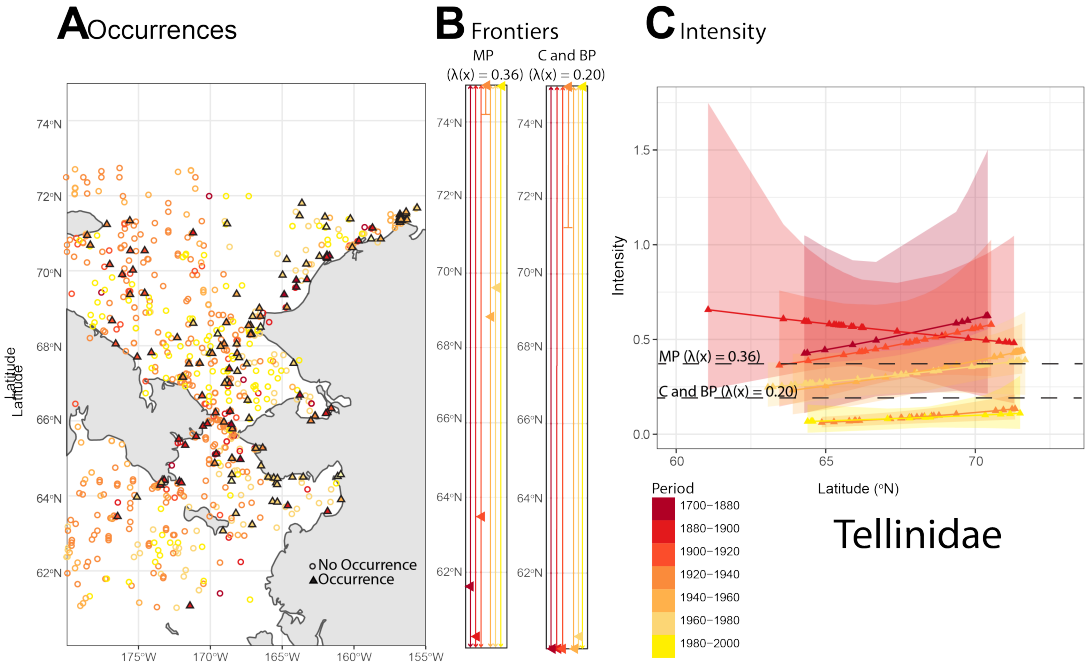

Figure 3.12: Results of Tellinidae Model 2. A) All occurrences of Tellinidae (triangles) color coded by time interval with darker colors represent older periods, and open circles are stations without Tellinidae occurrences. B) Triangles are the frontier estimates from MP, BP and C intensity thresholds with Fieler's confidence intervals. If symbol is on the left or right margin the frontier estimate is outside the sampling domain. Error bars that exceed the sampling domain are denoted with arrows. C) intensity curves from Model 2 with intensity thresholds (C, MP, and BP) marked with dashed lines (Table 3.4). Shaded envelopes around intensity curves represent bootstrapping confidence interval estimates of the intensities.

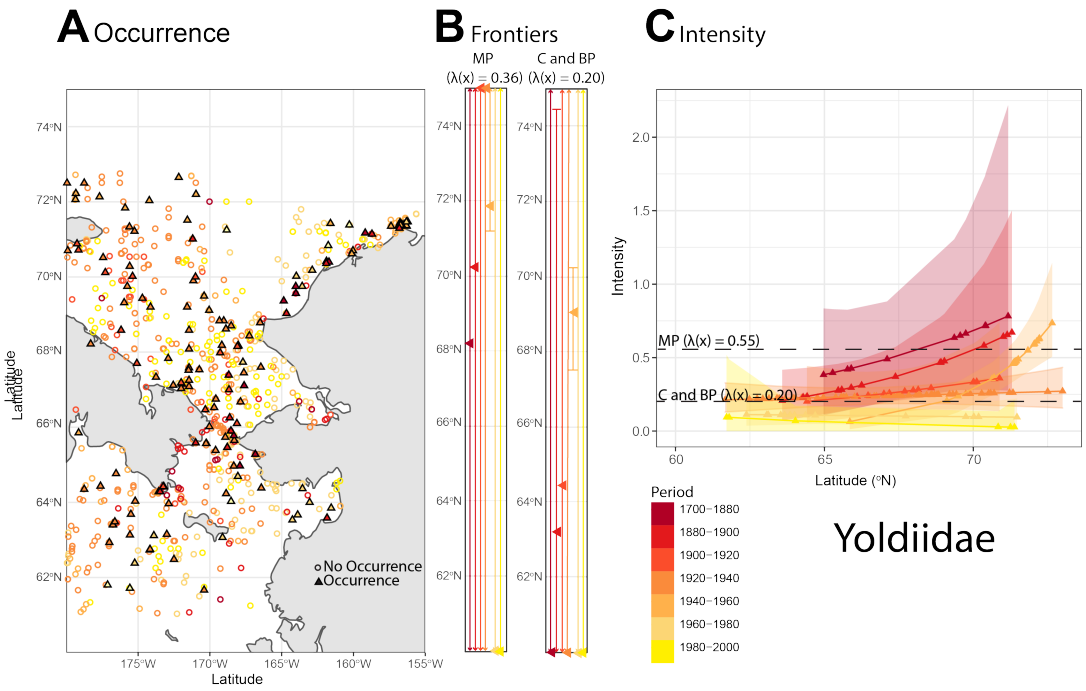

Figure 3.13: Results of Yoldiidae Model 1. A) All occurrences of Yoldiidae (triangles) color coded by time interval with darker colors represent older periods, and open circles are stations without Yoldiidae occurrences. B) Triangles are the frontier estimates from MP, BP and C intensity thresholds with bootstrapping confidence intervals. If symbol is on the left or right margin the frontier estimate is outside the sampling domain. Error bars that exceed the sampling domain are denoted with arrows. C) intensity curves from Model 1 with intensity thresholds (C, MP, and BP) marked with dashed lines (Table 3.4). Shaded envelopes around intensity curves represent bootstrapping confidence interval estimates of the intensities.

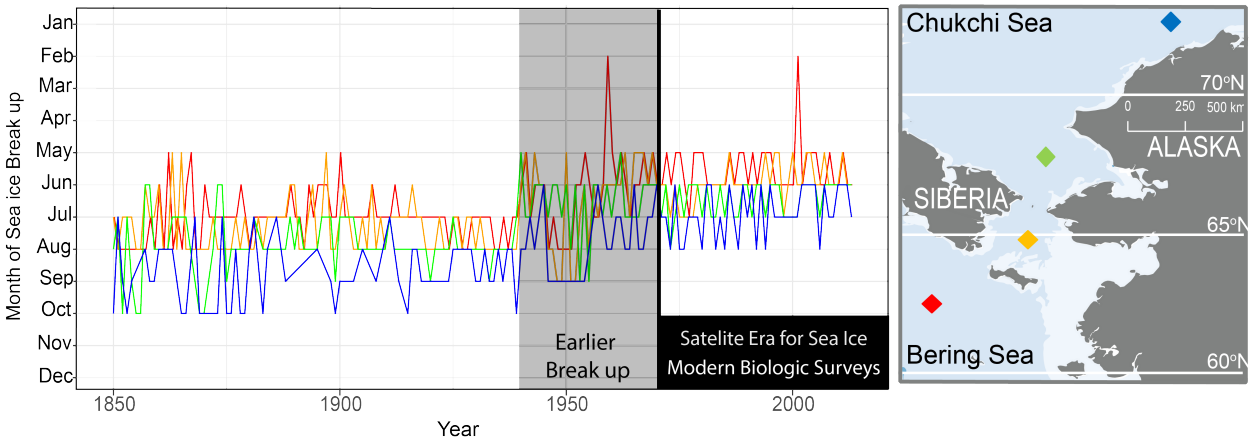

Figure 3.14: Timeseries of the month of sea ice break up (left graph) for four subregions in the study area (right map), with monthly resolution for the last 150 years; data from the Historic Sea Ice Atlas [139]. red lines = northern Bering Sea, orange = Bering Strait, green = southern Chukchi Sea, and blue = northern Chukchi Sea. Month of break up was defined as the first month with 15% ice cover. During the 1940's, sea ice started to break up significantly earlier breakup across the entire region, and a new normal was established by the 1960s. Black bar indicates first shelf-wide biologic surveys, and the advent of satellite based measurements for sea ice concentration.

Table 3.1: Summary of all bivalve lots that were examined in museums

Museum	Total Lots	Bering Sea Lots	Chukchi Sea Lots	Families
California Academy of Sciences	360	84	276	19
Smithsonian Institution	836	242	594	21
Russian Academy of Sciences	1258	383	875	19
Museum of the North (UAF)	197	63	134	21

Table 3.2: Summary of all NHC lots analyzed in this study. *Sufficiency of date information includes both lots for which a single collection year is available and lots with <15 years of possible collection years

Total Lots	4293
Subtotal of Lots with sufficient date information*	3992
Intertidal Lots (<10 m)	352
Shelf Lots	3640
Subtotal of shelf lots in the Study Region	2587
Unique sampling locations – "Stations"	921

Table 3.3: NNumber of stations in each time period, with occurrences for each family

Family	before 1880	1880-1900	1900-1920	1920-1940	1940-1960	1960-1980	1980-2000	Total Occurrences
Infaunal Suspension Feeder								
Cardiidae	8	14	14	65	47	16	42	206
Myidae	3	7	4	4	15	5	4	42
Nestling Suspension Feeder								
Hiatellidae	3	15	5	19	36	14	12	104
Subsurface Deposit Feeder								
Nuculanidae	5	11	8	79	36	10	47	196
Nuculidae	6	10	16	100	41	12	20	205
Surface and Subsurface Deposit Feeder								
Yoldiidae	11	18	15	69	49	15	6	183
Infaunal Facultative Deposit Feeder								
Tellinidae	11	26	24	26	51	39	11	188
Total Occurrences	47	101	86	362	275	111	142	1124
Total Stations	27	61	63	325	157	151	134	918

Table 3.4: Intensity thresholds chosen for the frontier using for NHC data. C = Constant intensity, MP = mean intensity, BP = by period intensity, estimated from choosing the intensity that overlapped with the most time increments

		Intensity Threshold		
Family	Model	C	MP	BP
Cardiidae	1	0.20	0.44	0.20
Myidae	2	0.20	0.09	0.10
Hiatellidae	2	0.20	0.24	0.10
Nuculanidae	1	0.20	0.41	0.20
Nuculidae	1	0.20	0.38	0.20
Yoldiidae	1	0.20	0.55	0.2
Tellinidae	2	0.20	0.36	0.20

Table 3.5: Intensity thresholds chosen for the frontier using biologic survey data. C = Constant intensity, MP = mean intensity, BP = by period intensity, estimated from choosing the intensity that overlapped with the most time incrementss

		Intensity Threshold		
Family	Model	C	MP	BP
Cardiidae	2	0.2	0.528493804	0.53
Hiatellidae	1	0.2	0.088093219	0.005
Myidae	2	0.2	0.193291026	0.16
Nuculanidae	2	0.2	0.810680539	0.5
Nuculidae	1	0.2	4.145614309	1.86
Yoldiidae	1	0.2	1.071752298	1.382
Tellinidae	1	0.2	3.115191446	1.9

Table 3.6: Results of likelihood ratio test between Model 1 and Model 2. p-values <0.05 indicate that Model 1 must be used.

Family	Likelihood Ratio	p-value
Cardiidae	19.707	0.003
Myidae	6.2155	0.399
Hiatellidae	9.534	0.143
Nuculanidae	13.1352	0.041
Nuculidae	15.2741	0.018
Yoldiidae	17.2250	0.008
Tellinidae	2.5242	0.866

Table 3.7: Frontier estimates using Model 1, with bootstraping estimates for confidence intervals, and different values of intensity corresponding to Table 3.4, gray shading highlights reasonable frontiers with at least one bound of the confidence intervals within the study region.

Family	Time Increment	#	Dirrection	Frontier C (°N)	Frontier MP (°N)	Frontier BP (°N)
Cardiidae Infaunal Suspension	before 1880	8	S	52.5 (-9.6, 141.9)	73.5 (24.6, 107.8)	52.5 (-9.6, 141.9)
	1880-1900	14	S	61.4 (19.5, 111.8)	77.5 (2.8, 138.6)	61.4 (19.5, 111.8)
	1900-1920	14	N	67.5 (65.4, 69.3)	65.2 (62.6, 66.6)	67.5 (65.4, 69.3)
	1920-1940	65	N	67.5 (64.8, 71.6)	60.3 (45.3, 63.2)	67.5 (64.8, 71.6)
	1940-1960	47	S	60.1 (-38.8, 147.8)	73.8 (35.8, 111.8)	60.1 (-38.8, 147.8)
	1960-1980	16	S	71.3 (39.7, 104)	77.3 (-2.3, 142.6)	71.3 (39.7, 104)
	1980-2000	42	S	-179.1 (-144.3, 304)	128.7 (7.2, 131)	-179.1 (-144.3, 304)
	before 1880	5	S	68.3 (64.1, 74.1)	70.6 (68, 81.8)	68.3 (64.1, 74.1)
	1880-1900	11	N	66.4 (29.7, 108.6)	52.5 (-43.6, 181.8)	66.4 (29.7, 108.6)

Table 3.7 continued

Family	Time Increment	#	Dirrection	Frontier C (°N)	Frontier MP (°N)	Frontier BP (°N)
Nuculanidae Subsurface Deposit	1900-1920	8	S	69.4 (67.7, 73.3)	71.3 (69.6, 78.4)	69.4 (67.7, 73.3)
	1920-1940	79	S	63.5 (51.6, 66.6)	71.4 (68.6, 85.1)	63.5 (51.6, 66.6)
	1940-1960	36	S	70.1 (68.8, 71.2)	72.1 (71.2, 73.5)	70.1 (68.8, 71.2)
	1960-1980	10	S	8.4 (-54.7, 192.9)	-30.1 (-139, 281.3)	8.4 (-54.7, 192.9)
	1980-2000	47	S	61 (37.2, 65.2)	67.4 (62.2, 71.3)	61 (37.2, 65.2)
Nuculidae Subsurface Deposit	before 1880	6	N	70.3 (36.3, 97.5)	61.8 (36, 94.9)	70.3 (36.3, 97.5)
	1880-1900	10	N	65.1 (33.2, 97.7)	57.9 (-20.9, 141.4)	65.1 (33.2, 97.7)
	1900-1920	16	S	66.3 (56.3, 69.9)	69.1 (65.4, 76.3)	66.3 (56.3, 69.9)
	1920-1940	100	S	61.4 (52.5, 64.4)	67.5 (65.3, 69.9)	61.4 (52.5, 64.4)
	1940-1960	41	S	69.1 (66, 70.8)	71.5 (70.4, 73.5)	69.1 (66, 70.8)
	1960-1980	12	N	59.6 (-1.6, 119.9)	55 (-49.5, 169.8)	59.6 (-1.6, 119.9)

Table 3.7 continued

Family	Time Increment	#	Dirrection	Frontier C (°N)	Frontier MP (°N)	Frontier BP (°N)
	1980-2000	20	S	70.1 (51.3, 93.4)	76.6 (13.2, 153.6)	70.1 (51.3, 93.4)
Yoldiidae Generalist Deposit	before 1880	11	S	59.3 (17.9, 134.4)	68.2 (51.4, 85.9)	59.3 (17.9, 134.4)
	1880-1900	18	S	63.3 (42.8, 74.5)	70.1 (53.8, 88.1)	63.3 (42.8, 74.5)
	1900-1920	15	S	64.3 (30.5, 99)	75.8 (-6.1, 146.9)	64.3 (30.5, 99)
	1920-1940	69	S	58.6 (-5, 128.6)	106.9 (-211.5, 391.5)	58.6 (-5, 128.6)
	1940-1960	49	S	69 (67.4, 70.2)	71.5 (70.4, 73.5)	69 (67.4, 70.2)
	1960-1980	15	NA	32.2 (-52.3, 165.8)	-22 (-227.1, 352)	32.2 (-52.3, 165.8)
	1980-2000	6	N	55 (-1.7, 143.6)	48 (-56.5, 186.2)	55 (-1.7, 143.6)

Table 3.8: Frontier estimates using Model 2, bootstrapping estimates confidence intervals, and different values of intensity corresponding to Table 3.4, gray shading highlights reasonable frontiers with at least one bound of the confidence intervals within the study region.

Family	Time Increment	#	Direction	Frontier C (°N)	Frontier MP (°N)	Frontier BP (°N)
Hiatellidae Nestling Suspension	before 1880	3	S	89.8 (76.6, 154.9)	75 (62.6, 103.7)	66 (45.9, 81.2)
	1880-1900	15	S	80 (73.1, 117.2)	65.1 (54, 71.1)	56.2 (23.4, 62.5)
	1900-1920	5	S	93.6 (80.6, 167.8)	78.8 (69.6, 113.6)	69.8 (59.2, 85.8)
	1920-1940	19	S	96.3 (83.7, 177.4)	81.5 (74.6, 121.2)	72.5 (67.9, 88.7)
	1940-1960	36	S	84.1 (77.8, 122.7)	69.2 (62.1, 73.1)	60.3 (30.6, 65.4)
	1960-1980	14	S	90.9 (80.1, 158.1)	76 (70.2, 102.7)	67.1 (58.8, 74.9)
	1980-2000	12	S	92.4 (81.2, 161.4)	77.5 (71.3, 106)	68.6 (60.4, 77.7)
	before 1880	3	S	237.9 (-Inf, 48) U (82.3, Inf)	50.5 (-Inf, Inf)	54.6 (-Inf, Inf)

Table 3.8 continued

Family	Time Increment	#	Direction	Frontier C (°N)	Frontier MP (°N)	Frontier BP (°N)
Myidae – Deep-Infauna Suspension	1880-1900	7	S	234.3 (-Inf, 45.8) U (83, Inf)	46.8 (-Inf, Inf)	50.9 (-Inf, Inf)
	1900-1920	4	S	284.6 (-Inf, 40.6) U (88.6, Inf)	97.1 (-Inf, Inf)	101.2 (-Inf, Inf)
	1920-1940	4	S	416.6 (-Inf, 21.7) U (102.5, Inf)	229.1 (-Inf, 47.8) U (81.6, Inf)	233.2 (-Inf, 47.2) U (82.1, Inf)
	1940-1960	15	S	253 (-Inf, 46.4) U (88.7, Inf)	65.5 (-Inf, Inf)	69.6 (-Inf, Inf)
	1960-1980	5	S	336.5 (-Inf, 31.9) U (93.7, Inf)	149 (-Inf, 60.1) U (70.7, Inf)	153.1 (-Inf, 59.2) U (71.5, Inf)
	1980-2000	4	S	346.1 (-Inf, 32.2) U (95.6, Inf)	158.7 (-Inf, 60.9) U (72.1, Inf)	162.8 (-Inf, 59.9) U (73, Inf)
	before 1880	11	S	77.6 (68.3, 122.3)	61.7 (30.2, 71.5)	52.7 (-12, 62.8)
	1880-1900	26	S	76 (69.6, 115.1)	60.2 (29.6, 66.3)	51.1 (-14.7, 59.6)

Table 3.8 continued

Family	Time Increment	#	Direction	Frontier C (°N)	Frontier MP (°N)	Frontier BP (°N)
Tellinidae Facultative Deposit	1900-1920	24	S	79 (72, 126.7)	63.2 (40.1, 69.6)	54.1 (-3.2, 61.9)
	1920-1940	26	S	105.6 (88, 260.9)	89.7 (78.8, 181.2)	80.7 (73.1, 136)
	1940-1960	51	S	84.6 (77.5, 143.1)	68.8 (57.8, 73.9)	59.7 (15.2, 65.5)
	1960-1980	39	S	85.4 (76.4, 160.8)	69.5 (64.1, 84.1)	60.4 (31.9, 65.5)
	1980-2000	11	S	105.9 (87.7, 260.8)	90.1 (78, 181.7)	81 (71.5, 137.3)

Table 3.9: Results of two-way Kolmogorov-Smirnov tests comparing the latitudes of occurrences of bivalve families from Museum and Survey Data. Gray shading indicates significant p-values (<0.05), and that both museum and survey data could be sampled from the different distribution.

	1960-1980				1980-2000			
Family	Museum Occ.	Survey Occ.	D-Value	p-value	Museum Occ.	Survey Occ.	D-Value	p-value
Cardiidae	16	102	0.4743	0.004	42	371	0.5831	1.4e-11
Hiatellidae	14	18	0.2619	0.653	12	122	0.4522	0.022
Myidae	5	57	0.3895	0.488	4	209	0.6794	0.053
Nuculanidae	10	167	0.2341	0.679	47	889	0.7101	2.2e-16
Nuculidae	12	211	0.3444	0.135	20	1539	0.6811	2.22e-08
Yoldiidae	15	101	0.4416	0.012	6	1123	0.4501	0.178
Tellinidae	39	221	0.1991	0.144	11	1403	0.5138	0.006

Table 3.10: Frontiers found using the Poisson process model with modern biologic survey data. Green cells are a match between the frontiers found here and the frontiers found in the NHC data, orange cells do not match. Confidence intervals are determined from bootstrapping estimates. Bold font indicates a frontier that is considered "reasonable" (within the study bounds with at least one confidence interval within bounds). N is the number of stations with occurrence of the family in that time interval.

Family	Interval	N	Model	Direction	Frontier MP (°N)	Frontier BP (°N)	Frontier C (°N)
Cardiidae	1960-1980	57	2	S	64.5 (28.5, 101.1)	64.5 (29.8, 105.7)	57 (51.4, 60.4)
	1980-2000	102	2	S	**66.1 (63.4, 68.7)**	**66 (63.3, 68.5)**	58.5 (53.5, 61.4)
	2000-2020	371	2	S	**61.9 (57.4, 64.6)**	**61.9 (57.1, 64.6)**	54.4 (45.3, 58.7)
Hiatellidae	1960-1980	3	1	S	**61.6 (-Inf, 62.9)**	**64.7 (63, 66.4)**	59 (-Inf, Inf)
	1980-2000	18	1	N	**68 (61.8, 79.1)**	47.4 (-65.9, 95.3)	85.4 (-Inf, Inf)
	2000-2020	122	1	S	**68.8 (65.3, 70.9)**	103.7 (91.8, 146)	39.3 (-Inf, Inf)

Table 3.10 continued

Family	Interval	N	Model	Direction	Frontier MP (°N)	Frontier BP (°N)	Frontier C (°N)
Myidae	1960-1980	22	2	S	61.6 (34.8, 94.1)	67.3 (37.1, 94.4)	11.7 (-Inf, Inf)
	1980-2000	57	2	S	75.1 (-73.9, 179)	80.9 (-115, 265)	25.2 (-Inf, Inf)
	2000-2020	209	2	S	**60.3 (46.3, 67.4)**	**66.1 (59.1, 70.2)**	10.4 (-Inf, Inf)
Nuculanidae	1960-1980	24	2	S	41.8 (-100.8, 224)	49.4 (-43.9, 171.5)	38.5 (21.4, 47.4)
	1980-2000	167	2	S	71.2 (40.3, 119.9)	78.8 (-6, 185.6)	**67.9 (65.4, 71)**
	2000-2020	889	2	S	**70.3 (69.2, 71.3)**	77.9 (75, 81.6)	**67 (64.6, 68.3)**
Nuculidae	1960-1980	97	1	N	80.3 (6.3, 163.8)	69.7 (45, 98.6)	61.4 (-Inf, Inf)
	1980-2000	211	1	S	-289.2 (-391.3, 504.4)	71.1 (30.6, 104.6)	350 (-Inf, Inf)
	2000-2020	1539	1	S	**67.9 (65.3, 69.7)**	76.3 (74, 81.2)	82.8 (-Inf, Inf)

Table 3.10 continued

Family	Interval	N	Model	Direction	Frontier MP (°N)	Frontier BP (°N)	Frontier C (°N)
Yoldiidae	1960-1980	102	1	N	-174.4 (-28.5, 154.9)	61.6 (34.7, 93.4)	-238.7 (-Inf, Inf)
	1980-2000	101	1	S	**69.9 (68.8, 71.5)**	**71 (69.8, 73)**	69.6 (-Inf, Inf)
	2000-2020	1123	1	N	72.9 (71.4, 76.9)	**67.2 (62.7, 68.9)**	74.4 (-Inf, Inf)
Tellinidae	1960-1980	115	1	N	**70.3 (65.8, 92.4)**	**64.4 (59.2, 68.5)**	56.8 (-Inf, Inf)
	1980-2000	221	1	S	58.2 (-1.7, 115.6)	69.8 (43.1, 101.1)	84.9 (-Inf, Inf)
	2000-2020	1403	1	S	**66.4 (64.8, 67.6)**	**71.5 (70.9, 72.3)**	78.1 (-Inf, Inf)

APPENDIX A

ABBREVIATIONS

Table A.1: Abbreviations used throughout text. See text for additional explanation.

Abbreviation	Explanation
AAR	Amino Acid Racemization
AFD	Age Frequency Distribution
AICc	Akaike information criterion
AMS	Accelerated Mass Spectrometer
Asp	Aspartic Acid
ARG	Arctic Research Group
BIC	Baysean Information Criteria
BP	By Period Intensity Threshold
C	Constant Intensity Threshold
CCA	Canonical Correspondence Analysis
CCGC	Canadian Coast Guard Cutter
CE	Common Era
C:N	Carbon to Nitrogen ratio
CPK	Constrained Power-law Kinetics
CSESP	Chukchi Sea Environmental Studies Program
DBO	Distributed Biological Observatory
DCA	Detrended Correspondence Analysis
DL Ration	left- (“L”) and right-handed (“D”) amino acid isomers
gC	grams Carbon (in reference to biomass)
Glu	Glutamic acid

TableA.1, continued

Abbreviation	Explanation
IQR	Interquartile Ranges
JC	Jaccard-Chao
MAPS	Mid-American Paleontology Society
MP	Mid-point Intensity Threshold
NHC	Natural History Collection
NMDS	Non-metric Multidimensional Scaling
NOAA	National Oceanic and Atmospheric Administration
NSF	National Science Foundation
OA	Ocean Acidification
OW	Overlying water
PRF	Petroleum Research Fund
PacMARS	Pacific Marine Arctic Regional Synthesis
RAS	Russian Academy of Sciences
SEM	Scanning Electron Microscope
SML	Sediment Surface Mixed Layer
SPK	Simple Power-law Kinetics
SWL14	Sir Wilfred Laurier cruise in 2014
SZ	Sequestration Zone
TA	Total Alkalinity
TAZ	Taphonomically Active Zone
TDK	Time-Dependent Reaction Kinetics
TINRO	Pacific Scientific Institute of Ichthyology
TOC	Total Organic Carbon
TON	Total Organic Nitrogen

TableA.1, continued

Abbreviation	Explanation
UAF	University of Alaska, Fairbanks
USCGC	United States Coast Guard Cutter

[]

APPENDIX B

ESTIMATING FOSSIL BIOMASS FROM SKELETAL MASS IN MARINE INVERTEBRATES

B.1 Abstract

Palaeoecology uses the numerical abundance and the occurrence of species to evaluate the dynamics of past communities, but biomass–the quantity of soft tissue -– is the critical currency needed to capture the flow and role of nutrients in modern ecosystems. Acquiring biomass data from fossil assemblages has, however, remained challenging, thus limiting the analysis of net secondary production in palaeocommunities.Prior models relate shell size or shell biovolume to fossil biomass. These models neglect shell fragments and, moreover, use units of biovolume (cm^3) that are not directly related to those of biomass (g), making the models difficult to tune and the coefficients highly specific. To remedy these shortcomings, I evaluate skeletal mass as a means of estimating the soft tissue biomass of fossil taxa, using ratios among biomass, skeletal mass and the total wet mass of living representatives of extant species, so that skeletal mass alone can be used to estimate grams of organic biomass. Data on total wet mass,organic carbon mass, and shell mass were acquired from more than 80 live-collected individuals from eight families in three major, shelly macrobenthic groups (Mollusca, Brachiopoda, Arthropoda) and supplemented with counterpart data from the literature to increase taxonomic breadth. This new shell-mass model provides more accurate and precise biomass estimates than models based on the linear dimensions of shells,expanding our ability to examine the interplay between organisms and their environments.

B.2 Summary

This appendix points to the published manuscript of [207], available online at doi: 10.1111/let.12314, and files can be found in the online supplement in the file:

Appendix B_Meadows_Biomass_Lethaia.zip.

APPENDIX C

SWL14 DEAD BIVLAVLE DATA - FAMILY LEVEL

Appendix contains the full dataset for Chapter 1, available in the online supplement in the file: ***Appendix C_SWL14_FAMILY_Dead Collected_Bivalve Taxa.zip***.

APPENDIX D

AGE DATING MODEL OUTPUT

Appendix contains the full dataset and all model output for Amino Acid Calibration found in Chapter 2, available in the online supplement in the file:

Appendix D_AAR_ALASKA_Bivalve_Meadows_Kidwell.zip.

APPENDIX E

SEM EVIDENCE OF POST-MORTEM SHELL MICROSTRUCTURE CHANGE

Experiments have shown that the disintegration of aragonitic shells is accelerated by the microbial communities' presence, regardless of water saturation [110]. To establish the process of shell disintegration in Arctic shells, we treated live-collected *Macoma* shells to reagents of known effect: bleach (NaClO) to remove the organic matrix, simulating microbial maceration, and acetic acid to remove mineral crystallites, simulating dissolution (Figure E.1). Experiments were designed with to mimic the methods of studies investigating the crystallographic structures of biogenic carbonates [85, 15, 42, 310, 110]. The resulting textures were compared to microstructure textures of dead collected *Macoma* shells. These reagents yield different textures based on what phase of the shell was removed – mineral or matrix (Figure E.1 top row). SEM images of dead-collected *Macoma* reveal damage that is most consistent with loss of organic matrix and not with preferential loss of the mineral phase (Figure E.1 bottom row, left and center images). We observed no "karstic" or "needle-like" textures created from the chemical dissolution of aragonite, but instead saw gaps between crystallites where the organic matrix would have originally been. We also observed syntaxial deposition of carbonate on top of the original bivalve microstructure (Figure E.1 bottom right image).

The results presented here indicate that the rapid shell loss seen in the Arctic is mediated by the biology at the seafloor, particularly the bioturbation to promote aeration of the sediment and the microbial activity in the sediment to strip the shells of organic material. Undersaturated waters – porewaters, overlying waters, or both – almost certainly contribute to high rates of shell loss from the seabed, but only after the aragonite crystallites (mineral phase of the shell) have been released from the microstructure by the loss of organic matrix through a process of microbial maceration, and not through the direct dissolution of crystallites while they are still part of the shell microstructure.

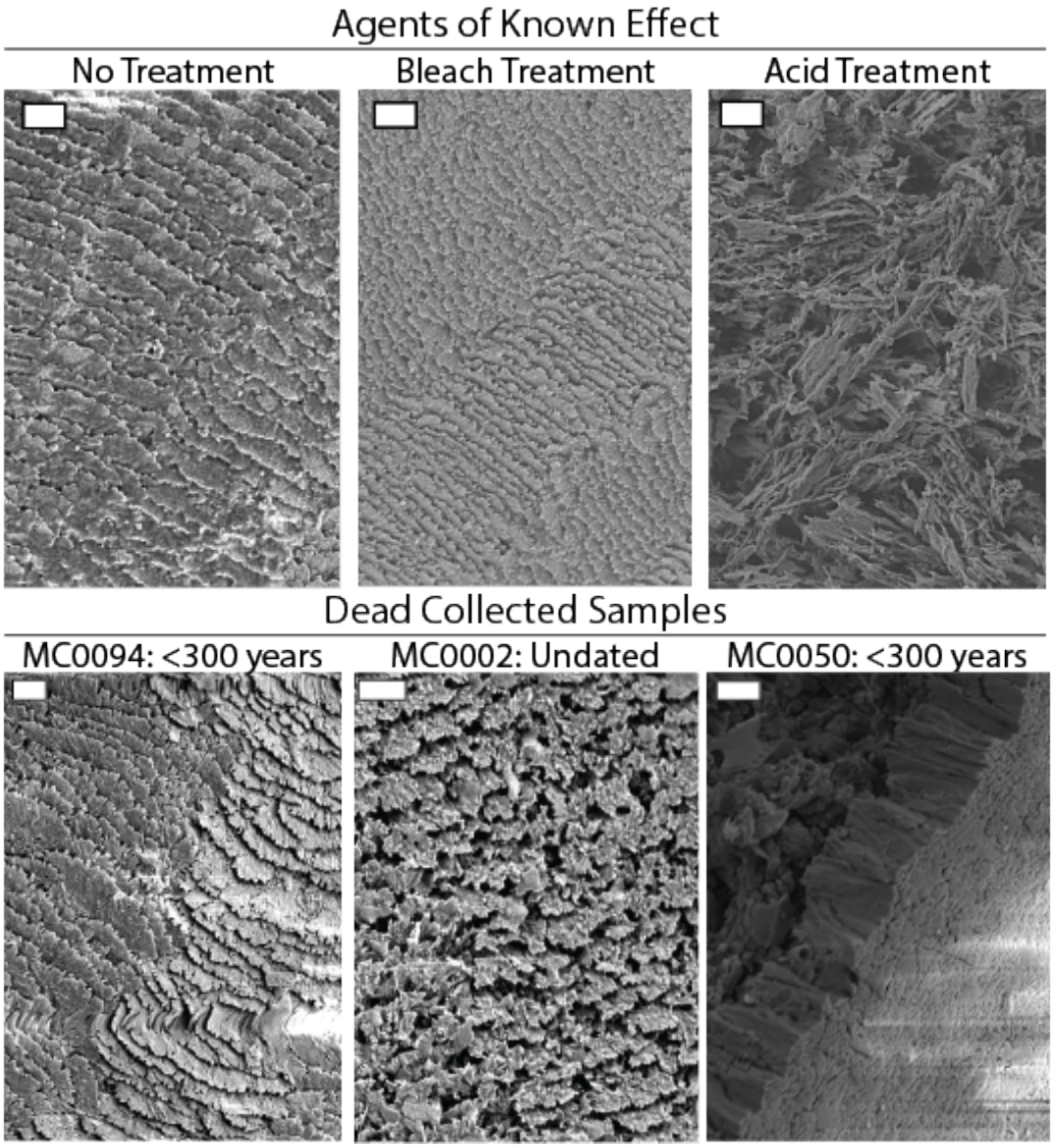

Figure E.1: Scanning Electron microscope images of the interior surfaces of *Macoma* shells, which are characterized by cross-lamellar aragonitic microstructure. Top row: Live-collected shells without treatment (left), after exposure to bleach (10% NaClO) to preferentially remove organic matrix (middle), and after exposure to acetic acid (10%, pH = 4) to preferentially remove mineral crystallites (right). Bottom row: Dead-collected shells exhibit damage consistent with loss of organic matrix rather than dissolution of mineral crystallites (left and middle images), and some acquire a thin prismatic crust (right image, unknown mineralogy); AAR-estimated shell ages. Scale bars are 1 μm long (8000x magnification, uncoated specimens).

APPENDIX F

PACIFIC WALRUS - *ODOBENUS ROSMARUS DIVERGENS*

F.0.1 Life History

The Pacific walrus (*Odobenus rosmarus divergens*) is a major predator of the macrobenthos, diving down from the ice flows of the Bering and Chukchi Seas. The goal of a feeding walrus is to fill its stomach twice per day [88, 89, 252, 191]. Depending on the size of the walrus and the density of benthos on the seafloor, each walrus thus eats between 6 and 9 seafloor individuals per minute of a feeding dive [88], with a total of about 50 individuals per dive, and from 4000-6000 individual benthic animals per walrus per day to fill to reach their metabolic demands [252, 88, 152]. Throughout the season an individual walrus can consume 180-240 kg of benthic biomass per day, which means that 250,000 walrus (estimated population size) of Pacific walrus consumes 2.53% of the standing stock biomass of the Bering and Chukchi Sea benthos each year [88]. Walrus predation is concentrated along the coasts and along the ice edge of the Bering and Chukchi shelf between 10 and 80 m water depth (120m maximum), predominantly south of St. Lawrence Island in the winter and into the Chukchi Sea along ice leads in the summer, that is relatively near to ice or shoreline resting (haul-out) grounds [87, 88].

While hunting for prey, walruses excavate a track of pits as much as 0.2m into the sediment [252, 34, 229]. These excavations vary in length but average 0.4 m across [252]. A single walrus is estimated to affect 260-400 m^2 of seabed per day, and an entire population can disturb 3000-5000 km^2 (or 2-3% of Bering and Chukchi seabed) in a 5-month season [252]. The feeding traces are large enough to be detected with side-scan sonar, like the feeding scars of gray whales, creating an undulating soft sediment seabed of both undisturbed and excavated muddy sediment [222, 150]. This large scale bioturbation has been suggested as contributing to the extremely high benthic productivity on the Pacific Arctic Shelf, by releasing nutrients during feeding and creating habitat heterogeneity [252]. It is estimated that benthic-feeding marine mammals disturb the entirety of

the Bering and Chukchi Shelf every 3 years [221]. Walrus diets are wide and varied, including every phylum of macrobenthic invertebrate and also, opportunistically, birds and seals encountered while feeding [187, 277, 79, 188, 88]. The diets of walrus are therefore considered to be a sampling of available large-bodied seafloor prey, rather than a highly selective diet [88]; therefore, as benthic taxa in feeding grounds shift, so do the diets of the Pacific Walrus [195, 324, 45].

Although able to subsist on many prey animals, the stomachs of walrus are often "filled with clams" [176], even when considering that stomach contents hold their own biases towards digestively robust tissues [276]. In the Bering Sea, large deep-burrowing bivalves can compose up to 80% of the food items in stomachs, and can be found in nearly all of walrus stomachs (75-100%; Table F.1).The most common bivalve taxa include *Serripes*, *Mya*, and *Hiatella*, the last of which are swallowed whole[277, 276, 89, 88, 210]. There are fewer observations in the Chukchi Sea, but walruses there appear to eat more gastropods, polychaetes, and other fleshy worms, in accordance with the Chukchi's Arctic, as opposed to subarctic, benthic communities.

Throughout the year, walrus follow the ice edge, which in January is in the Bering Sea (St. Lawrence Island) and Bristol Bay (Figure F.1A) [88, 176]. Winter (January-March) is also the mating season, leading to births 14 months later in spring; therefore, ice and adequate haul-out locations allow for proper feeding [88, 191]. As the ice breaks up, many walrus follow the ice floes northwest into the central Chukchi Sea, and along the Alaskan coastal current in the eastern Chukchi Sea, while large populations of males are found in the Bering Sea near Round Island [88]. Walrus spend June-September in the Chukchi Sea where the ice edge overlaps with the continental shelf and productive feeding grounds [88, 27]. September marks the end of summer and the beginning of a southern migration back to the Bering Sea, again following the ice edge [88].

Before commercial exploitation the walrus population was thought to be nearly 300,000 individuals, at the estimated carrying capacity of the Bering and Chukchi Seas, and herds were described as "innumerable" by the first whalers in 1849 (Figure F.2) [176, 88, 252, 269, 139]. Walruses have a 2000-year history in the culture of people living in the Bering and Chukchi Seas [176, 139].

Commercial harvest of walrus began during the search for biogenic oil in the Bering and Chukchi Seas, with the first commercial whaling expedition in the Chukchi Sea led by Captain Thomas W Roys in 1849 [269, 16, 31]. Walruses were hunted on the ice while waiting for the ice to retreat into the Chukchi Sea, and the hunters then followed whales further north [269]. This mid-19th-century harvest was extensive and thought to have entirely crashed the Pacific Walrus population with excessively large takes (nearly 80,000 walruses harvested in 1880) [285, 192] (Figure F.3). Regulation of Alaskan marine mammal commercial harvest began as early as 1806 by the Russians to protect fur seals, but walruses were not fully protected from commercial exploitation until 1985 [263].Following this 1806 regulation, the Americans and the international community began restricting the hunting of whales and other marine mammals in 1905. Increasing regulation and monitoring culminated in the Marine Mammal Protection Act in 1972, with sustainable subsistence harvests being managed beginning in 1985 [263]. Through conservation and more sustainable harvesting practices, Pacific Walrus populations recovered from a low of around 80,000 individuals in 1960 to about 250,000 in 1980 [90] (Figure F.2, Figure F.3). The walrus population declined after 1980, owing to human hunting, and declining sea ice, and petitions for international cooperation and protection were issued in the 1980's, during the Cold War [91, 80]. After further protection and sustainable harvesting, the population of Pacific Walrus seems to have rebounded to nearly 300,000 individuals by 2014 [191]. Walrus were nominated for consideration for protection under the Endangered Species Act in 2008, and Pacific walrus were nominated in 2011, but no formal habitat protection has been undertaken [106]).

With a shorter season of sea ice, walruses are losing both resting grounds and suitable feeding grounds [184, 124, 324]. This stress has led to mass mortality events on the coast of Siberia and Alaska, mass mortality at haul out locations, and a change in the location of walrus herds [191, 307, 97]. The specific, ice-edge habitat needs of walrus make it possible to estimate the carrying capacity with 1980's sea ice at about 300,000 individuals [91, 144, 184, 145]. However, the future of walruses is uncertain. Historic data is needed to understand how walrus populations

are affected by changes at the seabed and would create better projections of the future changes in walrus population [144, 184]. The future of the walrus populations will have long reaching effects on the marine community, and the people of Alaska who depend on marine resources [278, 191, 192, 176, 252].

F.0.2 Potential Reaction to Historic Seafloor Community Change:

Of the known prey taxa of walrus, this study can provide reliable data about the Cardiidae (*Serripes*) bivalve. The expansion of Cardiidae from the Bering Sea to the entire region in the 1940s-60s likely increased the size of the feeding grounds of some walrus herds (e.g., [189, 88]). Acquiring additional data about longitudinal variation in bivalve species occurrences within this region would help identify changes in the summer feeding grounds of walrus, which are spread widely across the Alaskan continental shelf, and on ice floes created along the Alaskan Coastal Current in the Chukchi Sea [88]. Because walrus are generalist feeders of sessile macrobenthos and search for seabeds with abundant fauna, the NHC bivalve database developed could help identify the location of past hotspots of biomass, such as those hotspots currently being monitored as within the DBO [215, 277, 88].

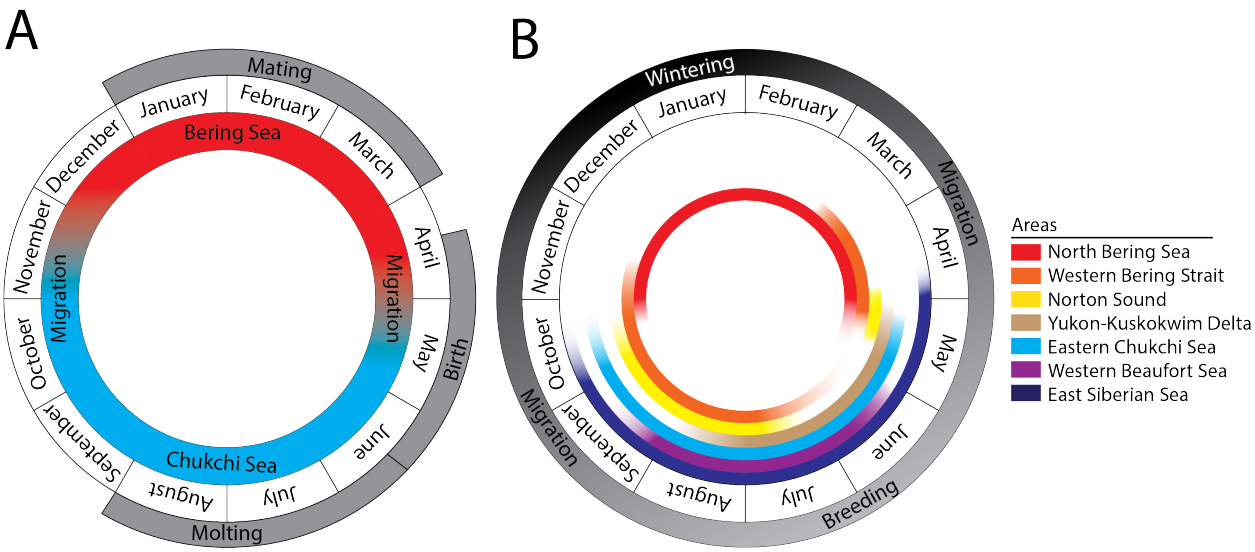

Figure F.1: Life history diagrams of Pacific walrus (A), and spectacled eider (B). Figure altered from (A) [176] and (B) [275].

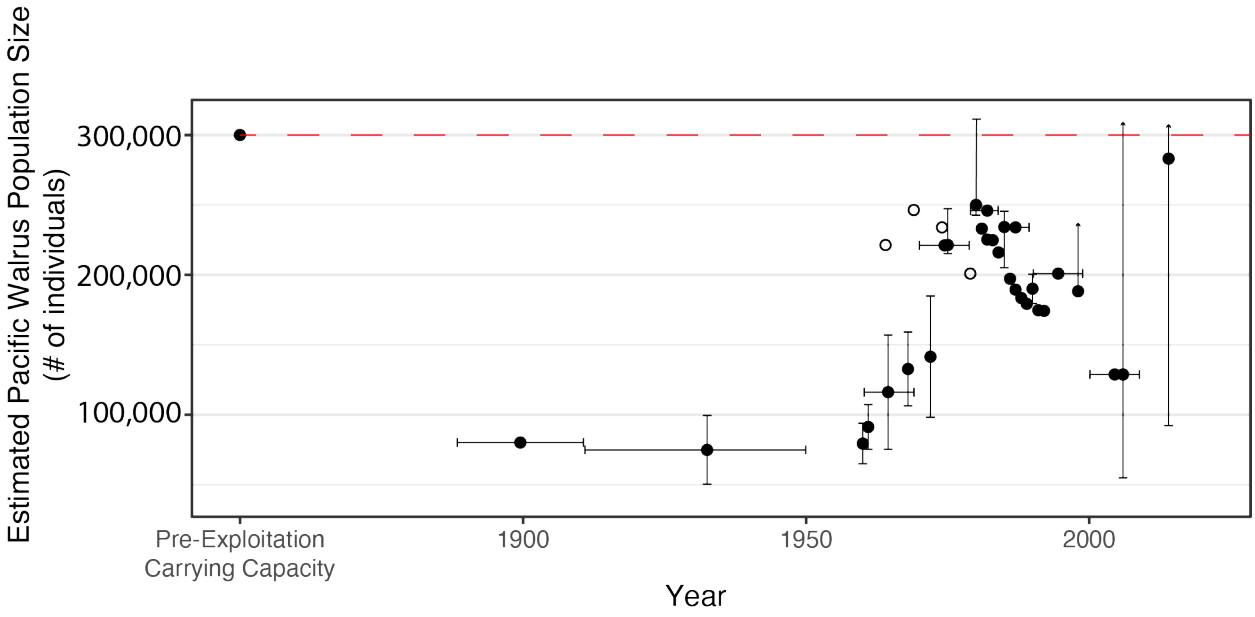

Figure F.2: Estimated walrus population size. Pre-Exploitation population size and estimated carrying capacity are marked with a black dot to the left and a dashed red line. Estimates of population are plotted as black dots with vertical error bars indicating minimum and maximum values reported for that year if more than one value was reported, or 95% confidence intervals for the 2014 and 2006 data points from the most recent census of Pacific Walrus [191, 106]. Open circles are reported from [18] and held the caveat that they should not be used to infer trends. Horizonal error bars represent data averaged over multiple observing years represent the minimum and maximum year in that range (MacCracken 2012). Data collected from [191, 192, 106, 284, 114, 90, 91]. Due to differences in methods and the difficulty in capturing all walrus in surveys, these population estimates are subject to several caveats and are not particularly reliable to infer precise trends [18].

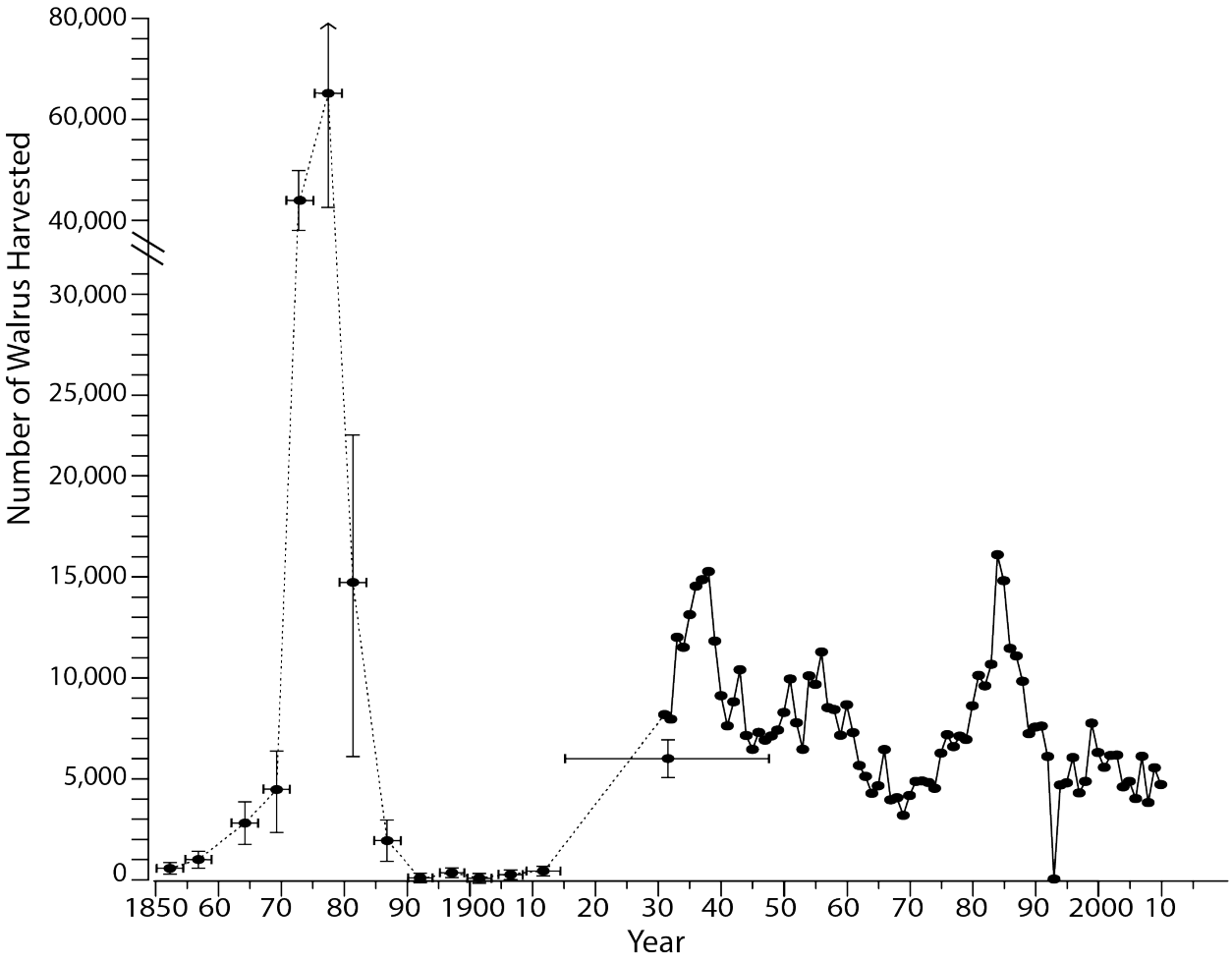

Figure F.3: Number of walrus harvested from 1850-2015. Data gathered from the following sources. 1849-1909: [32], 1960-2011:NOAA Pacific Walrus Stock Assessment (2014), 1650-2009 (not all plotted): [192], 1930-2000: [107]. Horizontal bars represent the range of years over which data were averaged by [32], to attain the mean (dot) and standard deviation represented by the vertical bars.

Table F.1: Summary of the prey of Pacific walrus based on the literature. Taxa are reported to the genus level when possible. Average percent occurrence was calculated from the mean of reported percent occurrence of that taxa. Data based on DNA analysis are tabulated separately (in parentheses). X = Found in stomachs but not in sufficient quantities to be tabulated as % occurrence. The type of observation: SC = Stomach Contents, F = Feces, PCR = DNA from feces or GI tracts, D = Detritus on ice/resting area. "Year Range" is oldest past and most recent years in which a prey taxon was documented in the walrus' diet.

TAXA	Mean % Occ., Bering Sea	Mean % Occ., Chukchi Sea	Observation Type	Years	Source
POLYCHAETA	78	97	SC	1934-1991	[88, 277, 87]
Lumbrineris	7 (94)	X	SC, PCR	1952-2018	[88, 277, 195]
Aphrodita		X	SC	1952-1991	[277]
Nephtys	25	X	SC	1952-2007	[88, 277, 210, 89]
Phyllodoce	X		SC	1952-1991	[277]
Arenicola	8	X	SC	1952-1991	[277, 210]
Maldanindae	10	X	SC	1952-1991	[277, 210]
Maldane	X	X	SC	1952-1991	[277]
Brada	5	X	SC	1952-1991	[277, 210]

Table F.1 continued

TAXA	Mean % Occ., Bering Sea	Mean % Occ., Chukchi Sea	Observation Type	Years	Source
Flabelligera	X	X	SC	1952-1991	[277]
Pectinaria	4		SC	1952-1991	[277, 210]
Terebellidae	X	X	SC	1952-1991	[277]
Terebella	X		SC	1952-1991	[277]
Owenia		X	SC	1952-1991	[277]
Echiurus	42 (58)	26	SC, F, PCR	1934-2015	[88, 277, 210, 195, 89, 87]
BRACHIOPODA	X		SC	1952-1991	[277]
BRYOZOA	1	X	SC	1952-1991	[277, 210]
CNIDARIA	11	35	SC	1952-1991	[277]
Scyphozoa	10		SC	1952-2007	[277, 210]
Anthozoa	X	X	SC	1952-1991	[277]
Alcyonacea	X		SC	1952-1991	[277]
Pennatulacea		X	SC	1952-1991	[277]
Actiniaria	9	X	SC	1952-2007	[277, 210]
Metridium	X		SC	1975	[88]
CRUSTACEA	19	X	SC	1952-2007	[277, 210]
CIRRIPEDIA	X	X	SC		
Balanus	11		SC	1952-2007	[277, 210, 89]
Thoracica	X	X	SC	1952-1991	[277]

Table F.1 continued

TAXA	Mean % Occ., Bering Sea	Mean % Occ., Chukchi Sea	Observation Type	Years	Source
AMPHIPODA	20	52	SC	1956-1991	[88, 277, 210]
Ampelisca	7	X	SC	1972-1985	[88, 210, 89]
Byblis	3		SC	1982	[210]
Lembos	3		SC	1976	[89]
Protomedeia	1		SC	1980	[210]
Hippomedon	4		SC	1975-1980	[210, 89]
Anonyx	9		SC	1975-2007	[210, 89]
CUMACEA	X	X	SC	1952-1991	[277]
Diastylis		X	SC	1952-1991	[277]
DECAPOD	21	67	SC	1956-2007	[88, 277, 210]
Erimacrus	X (27)		PCR	2014-2018	[195]
Argis	12		SC	1974-2007	[210, 89]
Sabinea	5		SC	1985	[210]
Sclerocrangon		15	SC	1952-1975	[88, 89]
Cragonidae	35 (14)		SC, PCR	1957-2015	[88, 195]
Chionoecetes	40		SC, F	1972-1985	[88, 210, 89, 87]
Hyas	32 (15)		SC, PCR	1952-2015	[88, 210, 195, 89]

Table F.1 continued

TAXA	Mean % Occ., Bering Sea	Mean % Occ., Chukchi Sea	Observation Type	Years	Source
Pagurus	21 (79)		SC, PCR, D	1972-2015	[88, 210, 195, 89, 87]
ECHINODERMATA	X	X			
HOLOTHUROIDEA	X	X	SC	1952-1991	[88, 277]
Cucumaria	39 (34)	12	SC, PCR	1934-2018	[88, 277, 210, 195, 89]
Thyonidium	32	X	SC	1974-1980	[88, 210]
Stolus	X	X	SC	1952-1991	[277]
Psolus	8		SC	1952-1991	[277, 210, 89]
Molpadia	X	X	SC	1952-1953	[88]
OPHEROIDEA		X	SC	1952-1991	[277]
Ophiura		X	SC	1952-1991	[277]
MOLLUSCA	X	X	SC	1962	[88]
Shell	16		SC	1982-1985	[210]
BIVALVIA	84	89	SC	1952-2007	[277, 210]
Musculus	X		SC, D	1952-1972	[88, 277]
Mytilus		X	SC	1952-1991	[277]
Cardiidae	X	X	SC	1952-1991	[277]
Clinocardium	23 (24)		SC, PCR	1952-2018	[88, 277, 210, 195, 87]

Table F.1 continued

TAXA	Mean % Occ., Bering Sea	Mean % Occ., Chukchi Sea	Observation Type	Years	Source
Serripes	74 (19)	64	SC, PCR	1934-2018	[88, 277, 210, 195, 87, 89]
Cartididae	X	X	SC	1952-1991	[277]
Cyclocardia	X	X	SC	1952-1991	[88, 277, 195, 89]
Hiatella	25	6	SC	1952-1991	[88, 277, 195, 89]
Panomya	52		SC	1985-2007	[210, 87]
Mactromeris	20	1	SC	1952-1991	[277]
Spisula	17 (39)		SC, PCR	1980-2018	[88, 210, 195]
Mya	70 (88)	37	SC, PCR	1934-2018	[88, 277, 210, 210, 195, 89]
Siliqua	X (39)	X	SC, PCR	1952-2018	[277, 195]
Tellinidae	29	X	SC	1952-1991	[277, 210, 89, 87]
Macoma	X (59)	X	SC, PCR, D	1934-2018	[88, 277, 195]
Tellina	86	X	SC, PCR	1952-2018	[88, 277, 195]

Table F.1 continued

TAXA	Mean % Occ., Bering Sea	Mean % Occ., Chukchi Sea	Observation Type	Years	Source
Thyasira	1	X	SC	1952-1991	[88, 277, 210]
Liocyma	3		SC	1952-1991	[277, 210]
Nuculana	X (12)	X	SC, PCR	1952-2015	[277, 195]
Nucula	2 (27)	X	SC, PCR, F	1952-2018	[88, 277, 210, 195, 89]
Yoldia	13	31	SC	1952-1991	[88, 277, 210, 89, 87]
GASTROPODA	57	99	SC	1952-2007	[277, 210]
Eggs	X	X	SC	1952-1991	[277]
Boreoscala	X	X	SC	1952-1991	[277]
Epitonium	3		SC	1980	[210]
Turritella	X		SC	1952-1991	[277]
Onchidiopsis	16	X	SC	1952-1991	[277, 210]
Naticidae	29	X	SC	1952-1991	[277, 210]
Euspira	X (69)		PCR	2017-2018	[195]
Natica	36	96	SC, F	1952-1991	[88, 277, 195, 89, 87]
Polinices	60	96	SC, F	1952-2007	[88, 277, 195, 89, 87]
Velutina	X		SC	1952-1991	[277]

Table F.1 continued

TAXA	Mean % Occ., Bering Sea	Mean % Occ., Chukchi Sea	Observation Type	Years	Source
Buccinum	42 (13)	33	SC, PCR, F	1952-2015	[88, 277, 210, 195, 89, 87]
Clinopegma	X	X	SC	1952-1991	[277, 87]
Buccinidae	43		SC	1985	[210]
Neptunea	63 (54)	90	SC, PCR, F	1952-2018	[88, 277, 210, 195, 89, 87]
Margarites	8 (34)	X	SC, PCR	1952-2018	[88, 277, 210, 195]
Solariella	4		SC	1952-1991	[277, 210]
Nudibranchia	8		SC	1952-1991	[277, 89]
CEPHALOPODA	X	X			
Octopoda	5	23	SC	1952-1991	[277, 210, 89, 87]
NERMERTEA	9	X	SC	1952-2007	[277, 210]
PORIFERA	X				
Tethya	X		SC	1949-1959	[88]
PRIAPULIDA	X	X			
Priapulus	48 (68)	61	SC, PCR	1934-2018	[88, 277, 210, 195, 89, 87]

Table F.1 continued

TAXA	Mean % Occ., Bering Sea	Mean % Occ., Chukchi Sea	Observation Type	Years	Source
SIPUNCULA	23	25	SC	1952-1991	[88, 277, 210]
Golfingia	31 (69)		SC, PCR	1974-2018	[88, 210, 195, 89]
TUNICATA	6	50	SC	1952-1991	[88, 277, 195, 89]
ASCIDIACEA	14		SC	2007	[210]
Halocynthia	X		SC	1952-1991	[277]
Pelonaia	6	X	SC, F	1934-1991	[88, 277, 210, 89]
Styela	X (87)		PCR	2014-2018	[195]
VERTEBRATA	X	X			
AVES	X		SC	1952-1991	[277]
Cepphus	X		SC	1952-1991	[277]
Phalacrocorax	X		SC	1952-1991	[277]
MAMMALIA	X	X			
Pinnipedia	X	X	SC	1952-1991	[277]
Erignathus	1		SC	1952-1991	[277]
Phoca hispida	X	X	SC	1952-1991	[277]
Phoca largha	X		SC	1952-1991	[277]
ACTINOPTERYGII	5	X	SC	1952-1991	[277, 210]

Table F.1 continued

TAXA	Mean % Occ., Bering Sea	Mean % Occ., Chukchi Sea	Observation Type	Years	Source
Ammodytes	15 (38)		SC , PCR	1952-2015	[277, 210, 195]
Anisarchus	X (37)		PCR	2014-2018	[195]
Lumpenus	X (60)		PCR	2014-2015	[195]
Acantholumpenus	21		PCR	2014-2018	[195]
Eumesogrammus	X (27)		PCR	2014-2015	[195]
Microstomus	X (37)		PCR	2014-2015	[195]
Parophrys	X (51)		PCR	2014-2015	[195]

APPENDIX G

SPECTACLED EIDERS - *SOMATERIA FISCHERI*

G.0.1 Life History

The spectacled eider winters in the St Lawrence polynya in the northern Bering Sea, resting on ice and diving up to 80 m to retrieve bivalves from the seafloor [236]. The duck wintering ground was a mystery until 1990s with the advent of sufficiently small GPS tags for tracking their migration [235, 234]. The ducks visit the polynya southwest of St. Lawrence Island, which is also frequented by walruses and home to diverse and abundant seafloor communities [121, 187, 186].

While in the Bering Sea, spectacled eiders eat the largest size classes of infaunal deposit feeding bivalves, especially *Nuculana*, along with some *Enucula* and *Macoma* (Table G.1) [186].Bivalves, and particularly these species of bivalves, are found in the stomachs almost all spectacled eider stomachs examined (80% occurrence), and constitute all or nearly all of the diet in the few stomachs that could be examined [186, 230, 237, 236].SThe preferred prey item is *Nuculana radiata* in the 18-24 mm size class, which provide the most nutrition (soft tissue) per individual and represent 30% by mass of stomach contents [186, 259]. Overall, in order to provide successful dives the seafloor must have at least 90 bivalves/m^2 with broken and open sea ice above [186, 182, 184].

After winter, the large population of spectacled eiders that assembled in the northern Bering Sea migrate to several breeding and molting areas (Figure F.1B) [23, 98, 234, 275, 267, 274]. These areas include both Alaska and Siberia, with the larger populations of birds in Siberia and particularly at the Indigirka River Delta [274, 140, 167, 236, 275, 232]. The Yukon-Kuskokwim Delta in Alaska is the largest breeding ground for spectacled eiders within Alaska, and is protected land for the spectacled eider [83, 290]. When not on-land breeding and tending their young, spectacled eiders occur in eight important areas (identified by [275] (Figure F.1B):

Pre/Post-Breeding Migration (mid-March-early May and mid-July-mid-November):

1. western Bering Strait within approximately 60 km of the coast of the eastern Chukotka

Peninsula, Russia;

2. eastern and southern Norton Sound in the northeastern Bering Sea;

Pre-Breeding Staging (Early-mid-May) and during Breeding:

3. Yukon-Kuskokwim Delta and adjacent marine areas within approximately 20 km of the coast of western Alaska;

Pre-Breeding Staging, Breeding and Molt (sporadically May-September):

4. eastern Chukchi Sea within approximately 70 km of the coast of northern Alaska;

5. East Siberian Sea within 200 km of the coast of northern Russia;

During Breeding only:

6. western Beaufort Sea within approximately 30 km of the coast of northern Alaska;

Wintering (November-mid-February):

7. northern Bering Sea within approximately 200 km of the southern coast of St. Lawrence Island.

The wintering area of the St. Lawrence Island polynya is well-connected to each breeding ground, and may be the where pair bonding occurs before the mating season [275]. This migration pattern has been observed since the 1800's and early 1900's, when large populations of Eiders in Siberia and few observations in Alaska were also mentioned [62, 63, 36, 273, 48, 72].

With this large population of birds spread over the Russian-American border, it is difficult to estimate the full population size, even when they are on land and easier to survey. While in the northern Bering Sea, they occupy an open patch of sea (polynya) that is completely surrounded by ice. Nonetheless, observers on icebreaker cruises and aerial surveys have estimated the wintering population to be nearly 350,000 individuals (Figure G.1) [50, 235**?** , 178].107].The population of

spectacled eider today is relatively stable; however, from 1952-1993 the spectacled eiders breeding at the Yukon-Kuskokwim Delta declined 96%, prompting protection under the endangered species act [98, 290]. The Yukon-Kuskokwim Delta has been extensively monitored since then, with the cause of the decline largely unknown but likely related to lead and heavy metal poisoning [83, 101, 100, 117].

Spectacled eider populations are currently stable but vulnerable, due to the loss of sea ice, changing seafloor food dynamics, and the exploitation of their habitat for hunting, fishing, and mining, and development [267, 274, 100]. Most worryingly, ecologically similar benthic-feeding birds such as King Eiders have experienced mass mortality events in the Bering and Chukchi Seas due to heat, starvation, and harmful algal toxins [22, 314, 262, 309], and parasites and high levels of heavy metals have recently been observed in spectacled eiders [185, 254]. The future of eiders is uncertain, but the most pressing need is for protection of the northern Bering Sea wintering area (i.e. the St. Lawrence Island polynya), as well as areas where the ducks might winter in the future as sea ice continues to disappear [184, 124].

G.0.2 Potential Reaction to Historic Seafloor Community Change

The NHC analysis here found that Nuculanidae and Nuculidae bivalves shifted their frontiers from the northern Bering Sea (63.5°N and 61.4°N) to the Chukchi Sea (70.1°N and 69.1°N) in 1920-1960 before expanding southward back throughout the region. Because Nuculanidae are the preferred prey of spectacled eider, a decline of Nuculanidae in the northern Bering Sea in 1920-1960 would negatively affect the body condition and health of the spectacled eider population [186, 259]. This change in the seabed community would have a disproportionately large effect on spectacled eiders because nearly the entire population winters at the Saint Lawrence Island polynya (350,000 individuals) before dispersing to multiple breeding grounds in the spring/summer (Figure G.1) [50, 235, 178].

The preferred prey item is the 18-24 mm size class of *Nuculana radiata*, which combines the

nutrition and high density at the seabed (30% by mass of stomach contents) [186, 259]. Overall, successful foraging require that the seafloor has at least 90 bivalves/m^2 and that the sea surface is characterized by broken and open sea ice [186, 182, 184]. Given these strict requirements, spectacled eider offer the opportunity to expand the NHC dataset to include information on abundance, biomass, and body size, to greatly improve models of eider health.

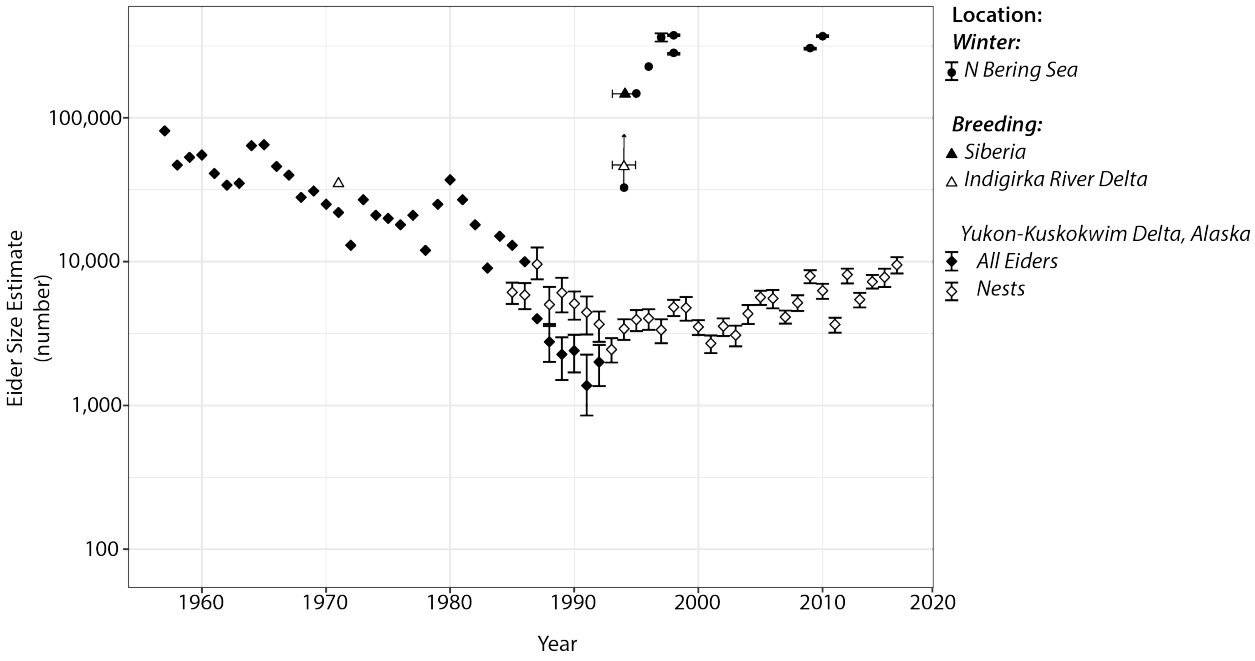

Figure G.1: Spectacled eider population estimates from various wintering and breeding locations. Wintering estimates in the northern Bering Sea represent estimates of nearly the entire population of spectacled eiders (near 350,000 individuals). In breeding areas, only displaying estimates for all Siberia (closed triangle), the Indigrka River delta (open triangle), and the Yukon-Kuskokwim Delta in Alaska (diamonds). There are very few estimates of spectacled eider population sizes in Siberia although it is thought to be the largest breeding ground. Within the Yukon- Kuskokwim Delta two types of data are presented, counts of all Eider species individuals (closed diamonds) and counts of spectacled eider nests (open diamonds). The majority of birds at the Yukon- Kuskokwim Delta are spectacled eiders [98]. Sources of data include [167, 290, 140, 235, 178, 98]. Due to differences in methods and the difficulty in capturing all eiders in surveys, these population estimates are subject to several caveats and are not particularly reliable to infer precise trends.

Table G.1: Summary of the prey of spectacled eider while wintering in the northern Bering Sea; all data from stomach contents. Taxa are reported at the lowest possible level, based on identifiable remains. Percent occurrence in stomach contents reported when present, as well as percent of stomach contents where the taxon is the sole taxon present in the stomach contents, and the percent of the stomach contents that the taxon occupies (by mass from [230]). "Year Range" is the oldest past and most recent years in which a prey taxon was observed to be part of the duck's diet

TAXA	% Occ, Bering Sea	% Sole Taxon	% of Diet (by mass)	Year	Source
ALGAE					[236]
PROTOZOA					[236]
BRYOZOA					[236]
CRUSTACEA	30.6	11.1		1987-1992	[236, 237, 186]
MALACOSTRACCA			13.1 ± 64.9		[230]
DECAPODA					
Majidae	5.6	0		1987-1992	[236, 237]
Chionocetes sp.	19.4	11.1		1987-1992	[236, 237, 186]
Dermaturus mandtii	2.8	0			[236, 237]
Hyas sp.	2.8	0		1987-1992	[236, 237]
CIRRIPEDIA			0.1 ± 0.4		[230]
Balanidae	8.3	0		1987-1992	[236, 237]
ECHINODERMATA					
ASTEROIDEA			0.1 ± 0.4		[236, 230]
ECHINOIDEA			0.3 ± 1.5		[230]
Echinarachnius parma					[236]
MOLLUSCA	100	88.9		1987-1992	[237]
BIVALVIA	80	48	86.2 ± 68.2	1987-1992	[236, 186, 230]
Macoma brota	40	12		1987-1992	[236, 237]
Macoma calcarea	40	8		1987-2001	[236, 237, 186]
Macoma lama	16	0		1987-1992	[236, 237]
Macoma spp.	12	36		1987-1992	[236, 237, 186]
Panomya spp.	4	0		1987-1992	[236, 237]
Musculus spp.					[236]
Mytilus edulis					[236]
Ennucula tenuis		9		2001	[186]
Nuculana radiata		28		2001	[186]
Megayoldia traciaeformais	4	0		1987-1992	[236, 237]
Yoldia spp.	16	0		1987-1992	[236, 237]
GASTROPODA	20	0	0.1 ± 0.7	1987-1992	[237, 186, 230]
Natidicae	8	0		1987-1992	[236, 237]
Trichotropis sp	12	0		1987-1992	[236, 237]
Trochidae					[236]
VERTEBRATA					
ACTINOPTERYGII			0.1 ± 0.4		[230]
Cottidae					[236]
Gadidae	2.8	0		1987-1992	[236, 237]
Ampeliscidae	5.6	0		1987-1992	[236, 237]
Lysianassidae	8.3	0		1987-1992	[236, 237]

APPENDIX H

HISTORIC EXPLORATION AND SURVEYS OF THE PACIFIC ARCTIC

Alaskan and Siberian colonial exploration began with Bering's and Steller's "Second Expedition" to Kamchatka and Siberia in 1733-1743, which was an effort by Russia to prospect the sea and mineral resources of the Pacific Arctic (Figure H.1, Table H.1, and Table H.2) [151, 28]. This expedition began Russia's economic use of the ecologic resources of the region and colonization of the region starting in 1733 (see [151] for full accounting of regional extinctions and depletions of marine mammals). The first Russian Settlement in Alaska was established in 1784 at Three Saints Bay, on Kodiak Island [8], and Alaska became a colony of Russian America in 1799 [28]. Russia's foothold in America was used to exploit the fur seals, otters, whales, and other marine mammal resources as well as grow their empire via trade with and subjugation of the Indigenous American people [151, 28]. During this second half of the 18th century, the Stellar sea cow was hunted to extinction and all other economically valuable marine mammals faced total extirpation by 1800, particularly in the Aleutian Islands [151]. The Russian economic domination in the Pacific Arctic led to a treaty with the United States that granted Russia exclusive trading rights north of 54°40'N, including all of the Bering and Chukchi Seas [151, 212].

During Russian Colonial rule (1733-1842), other European expeditions prospected for the Northwest Passage from the east and for varied economic resources within Alaska [47, 26, 233], including several ill-fated voyages and rescue attempts [19, 250]. These 18th and early 19th century expeditions also mark the beginning of widespread interest in the Arctic as a natural system, and a theory that there was another new world at the top of the globe for whomever could break through the ice [78, 217, 261].

US presence and exploitation of Alaskan marine resources began upon Russia's withdrawal from the region beginning in 1842 (Table H.2) [220], related to re-focusing of political economic attention on Europe. Whaling began in 1848, when Captain Royce on board the Superior described bowhead whales for the first time [269, 32, 31]. The discovery of abundant blubber- and oil-producing

marine mammals drew American whalers and explorers into the area, along with US military exploration by the 1870s, using ships repurposed from the Civil War [21, 217, 136, 137, 280, 291]. Knowledge of marine resources in Alaska was slow through this early phase of US exploration, but this changed in the 1860's with a new era of scientifically-focused expeditions ushered in by William Healy Dall of the Smithsonian Institution. Dall's work with the joint Russian-American Telegraph Expedition in 1865-67 was a logistical failure – they failed to establish a telegraph line between Russia and America – but a scientific success [**?** 61, 280, 62], allowing Dall to spend two years in Alaska systematically documenting the biodiversity and geology of the territory (green symbols in Figure H.1) [280, 67, 64], on behalf of the US Coast Survey, the Smithsonian Institution, and the US Geological Survey [280]. This work marked the transition from haphazard and largely opportunistic exploration, to systematic, purposeful surveys and documentation of Alaska's natural resources [70, 73, 71, 280, 322]. Dall created guides for the collection of marine invertebrates [68], as well as detailed taxonomic treatments of fossil and extant mollusks [64, 72, 69, 66], and became the foremost expert on Alaskan ecosystems during the American colonization period [280].

Much of the active scientific investigation of Alaska was determined by US Military and economic interests, which provided marine access [214]. Alaska was purchased from Russia by the US in 1867 [279, 220], and then ruled through martial law by the US Army, Department of Treasury, and Navy until the formation of a civil government in 1884 [220, 214, 1]; statehood was not achieved until 1959. The scientific work described here thus often occurred in tandem with military action against the indigenous people of Alaska (see [214] for more). Ships of the US Revenue Cutter Service were the primary means of both patrolling and studying Alaska [294, 217, 136, 137]. Military-sponsored science in Alaska established the Naval Petroleum Reserve No 4 (1923-Present; in the North Slope from Icy cape to Prudhoe Bay), established the US Arctic Naval Research Laboratory (1947-1966; Point Barrow), and prompted ecologic investigations prior to military experiments throughout the region (e.g., nuclear weapons as excavation tools) [16, 255]. At the same time, the Russian government established the Pacific Scientific Institution of

Ichthyology (TINRO) on the western shore of the Siberian and Chukchi Seas and began purposeful investigations of the Siberian Arctic [16]. The establishment of the US Arctic Research Laboratory at Point Barrow in 1947 and the Russian TINRO survey of Northwestern Chukchi Sea in 1932-33 marked a transition to more quantitative, fully modern surveys of marine resources, but with the first modern ecologic survey of the continental shelf was not undertaken until 1970, led by Samuel S. Stoker and colleagues from the University of Alaska (focused on both the Bering and Chukchi Sea Sea) [293].

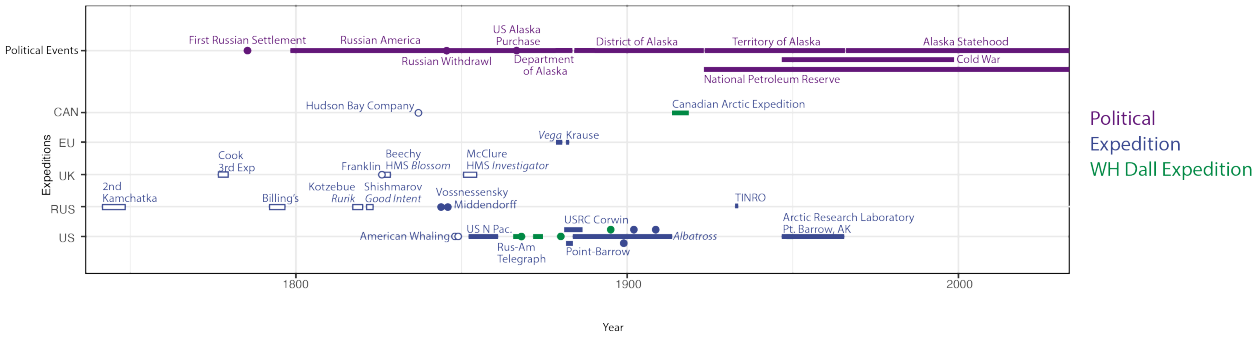

Figure H.1: Timeline of Alaskan Exploration with Relevant Collections. Single and multi-year events are represented by dots and bars. Purple represents names of political or governmental states in Alaska, such as Russian rule of America. Blue denotes expeditions to Alaska by various countries (CAN = Canada, EU = European nations, UK = Britain and United Kingdom, RUS = Russia, US = United States), and green denotes field expeditions by WH Dall. Other notable expeditions are labeled separately. Open shapes represent expeditions with reports of relevant sampling but are not presented in this study.
Explanations: American Whaling = First American Whaler N of the Bering Strait (Capt. Royce, Superior), US N Pac = United States North Pacific Exploring Expedition, Rus-Am Telegraph = Russian American Telegraph Expedition (aka Western Union Telegraph Expedition, Collins Expedition), Point-Barrow = International Point Barrow Research Expedition, TINRO = Pacific Scientific Institution of Ichthyology Surveys, Albatross = US Fishing Commission Pacific Surveys from the USFC Albatross.

Table H.1: Near comprehensive list of expeditions to Alaska. Expedition dates range from 1733 to 1966. Expeditions are organized by leading country and date. US expeditions are subdivided into categories of "Oceanographic", "Geologic" and "Other". Meta data include the date, name of leader(s), expedition name or =ship used, the stated primary purpose(s) of the expedition, and source of information. NA = not available

Date	Leader	Expedition/Ship Name	Purpose	Source
		CANADA		
1837	Dease, Simpson	Hudson Bay Company	Prospecting	[256]
1913-18	Dall, Kindle	Canadian Arctic Expedition	Scientific	[71, 166]
1887-88	Dawson, Oglvie, McConnell	Boundary between Canada and Alaska	Prospecting	[77, 280]
		EUROPE		
1865	Lambert		Scientific	[16]
1878-80	Nodenskiold	*Vega*	Exploratory	[16, 226, 26]
1881-82	Krause, Krause	Krause Expedition	Scientific	[280, 173]
		BRITAIN AND THE UNITED KINGDOM		
1776-79	Cook	3rd Expedition	Scientific, Exploratory	[256, 16, 233, 47]
1825-28	Beechey	HMS *Blossom*	Exploratory	[256, 16, 26]

TableH.1, continued

Date	Leader	Expedition/Ship Name	Purpose	Source
1826	Franklin	Mackenzie River Expedition	Exploratory	[256]
1850-54	McClure	HMS *Investigator*	Exploratory	[16, 250, 19]
		RUSSIA		
1733-43	Bering, Stellar	Second Kamchatka Expedition	Exploratory	15, [28]
1789-95	Billings	Billings Expedition	Exploratory	[151, 268]
1815-18	Kotzebue	*Rurik*	Prospecting	[16, 311]
1819-21	Shishmaryov	*Good Intent*	Scientific	[16, 311, 20]
1842	Vossnessensky	NA	Scientific	[16, 211]
1843-44	Middendorff	NA	Scientific	[16, 211, 295]
1932-33	NA	Pacific Scientific Institution of Ichthyology (TINRO)	Scientific	[16]
		UNITED STATES OF AMERICA		
		Oceanographic Expeditions		
1848	Royce	*Supperior*, Whaling	Prospecting	[256, 16, 31, 269]
1849	Pullen	NA	Prospecting	[256]
1852-61	Ringgold, Rodgers, Stimpson	US North Pacific Exploring Expedition	Exploratory, Scientific	[291, 292, 260]

TableH.1, continued

Date	Leader	Expedition/Ship Name	Purpose	Source
1865-67	Kennicott, Dall	Russian American Telegraph Expedition	Scientific, Prospecting	[280, 61, 62]
1867-68	Dall	Solo remains in AK	Scientific	[280, 64, 67, 62]
1867	Davidson	*Lincoln*	Prospecting	[280, 279]
1868	Minor	USRC *Wayanda*	Prospecting	[280, 20, 294]
1871-74	Dall	US Coast Survey	Scientific	[280, 64, 67, 63]
1879-81	De Long	USS *Jeannette*	Exploratory	[217, 78]
1880	Bean and Dall	US Coast Survey, 10th Census, Yukon	Scientific	[16, 64, 25]
1880	Dall, Baker	US Coast Survey	Scientific	[280, 64, 66, 65]
1881-86	Healy, Muir, Stoney, McLenegan	USRC *Corwin*	Military, Scientific	[256, 280, 16, 217]
1881-83	Ray, Murdoch	Point Barrow Expedition	Scientific	[256, 253, 74, 196]
1883-1913		USFC *Albatross*	Scientific	[196, 7]
1902	Kindle	USRC *Thetis*	Scientific	[165]
1908	Kindle	*Umatilla*	Scientific	[165]
1924	Bartlett	*Effie M. Morrissey*	Scientific	[16]

TableH.1, continued

Date	Leader	Expedition/Ship Name	Purpose	Source
1958-59	McLaughlin	King Crab Investigation, Bureau of Commercial Fisheries	Scientific	[204]
1948-50	MacGinitie	Arctic Research Laboratory	Scientific	[142, 193]
		Geologic Expeditions		
1889-90	McGrath, Turner	US Coast and Geodetic Survey	Scientific	[280, 266]
1895	Dall, Becker	US Geological Survey	Scientific	[280, 69]
1898	Spurr	US Geological Survey	Scientific	[280]
1898	Spurr, Post	US Geological Survey	Scientific	[280]
1900	Barnard, Brooks, Peters, and Mendenhall	US Geological Survey	Scientific	[280]
1901	Peters, Schrader	US Geological Survey	Scientific	[256]
1906-14	Leffingwell, Anderson	US Geological Survey	Prospecting	[256]
1908-18	Stefansson	US Geological Survey	Prospecting	[256]
1923	Paige	US Geological Survey	Scientific	[256, 231]
1924	Smith, PS	US Geological Survey	Scientific	[256]
1925	FitzGerald	US Geological Survey	Scientific	[256]
1926	Smith, PS	US Geological Survey	Scientific	[256]
1951	Malkin	US Geological Survey	Scientific	[194]
1958	Scholl, Sainsbury	US Geological Survey	Scientific	[271]
		Other Expeditions		

TableH.1, continued

Date	Leader	Expedition/Ship Name	Purpose	Source
1890-91	NA	Leslie Illustrated Newspaper Expedition	Exploratory	[280, 56]
1899	Harriman	SS *George W Elder*	Exploratory	[60, 2]
1912	NA	International Boundary Commission	Prospecting	[256]
1947	NA	USS *Nereus*	Military	[16, 177]
1947	NA	USS *Burton Island*, BAREX47	Military	[256, 16]
1947-66	NA	Arctic Research Laboratory, Point Barrow	Scientific	[255]

Table H.2: List of historic political and governing events in Alaska.

Date	Event	Sources
	RUSSIAN AMERICA	
1733	Russian Colonialization	[280, 151, 28]
1784	First Russian Settlement in AK	[8]
1799	Incorporation of Alaska as a Russian Colony	[28]
1824	Russo-American Treaty, Russians hold exclusive trading rights north of 54 40°N	[151, 212]
1842	Russian withdrawal from Alaska began	[8, 220]
	UNITED STATES OF AMERICA	
1865	Last Shot of Civil War, CSS *Shenandoah*, Bering Sea	[21]
1867	Purchase of Alaska by the United States (Seward's Folly)	[280, 1, 220]
1867-84	Department of Alaska	[280, 220, 214]
1867-77	Period of Army Rule	[280, 220, 214]
1877-79	Period of Treasury Department Rule in Alaska, Enforcement by the US Revenue Cutter Service (Coast Guard)	[280, 220, 214]
1879-84	Period of Naval Rule in Alaska	[280, 220, 214]
1880	The 10th US Census, First Census of Alaska (Petrov)	[280, 238]
1884	Alaska's First Organic Act	[280, 1, 220, 214]
1884-1912	District of Alaska	[280, 1, 220, 214]
1912-59	Territory of Alaska	[220, 214]
1923-2020	Naval Petroleum Reserve No. 4, established and active Geologic Surveys	[256]
1959-2020	State of Alaska	[214, 220]

APPENDIX I

FULL SPECIES LIST IN ARCTIC BIVALVE NATURAL HISTORY COLLECTIONS

Below is a list of all the species reported in the NHC collections presented here. Species are grouped into families, with families are arranged by relationship to one another. Species names may be out of date because of the age of the collections presented here. Species are arranged alphabetically. ∗ = not a fully accepted name.

BIVALVIA (Class)

AUTOBRANCHIA (Subclass)

HETEROCONCHIA (Infraclass)

ARCHIHETERODONTA (Subterclass)

CARDITIDA (Order)

CRASSATELLOIDEA (Superfamily)

ASTARTIDAE (Family)

Astartidae indet.

Astarte sp.

Astarte (Nicamia) warhami	*Astarte warhami*
Astarte banksii	*Astarte montagui*
Astarte borealis	*Astarte borealis*
Astarte borealis v. placenta	*Astarte borealis*
Astarte borealis var sibirica	*Astarte borealis*
Astarte crenata	*Astarte crenata*
Astarte esquimalti	*Astarte esquimalti*
Astarte montagui	*Astarte montagui*
Astarte montagui (Leach)	*Astarte montagui*

Astarte montagui var fabula	*Astarte warhami*
Astarte montagui var striata	*Astarte montagui*
Astarte montagui var vernicosa	*Astarte montagui*
Astarte montagui var warhami	*Astarte warhami*
Astarte montegui (Dilwyn)	*Astarte montagui*
Astarte rollandi	*Astarte arctica*
Astarte varhami	*Astarte warhami*
Astarte vernicosa	*Astarte vernicosa*

CARDITOIDEA (Superfamily)

CARDITIDAE (Family)

Carditidae indet.

Astarte crassidens	*Crassicardia crassidens*
Cardita granulata s. sp. rjalinivae	*Cardita sp.*
Crassicardia crassidens	*Crassicardia crassidens*
Cyclocardia sp.	
Cyclocardia crassidens	*Crassicardia crassidens*
Cyclocardia crebicostata	*Cyclocardia crebicostata*
Cyclocardia ovata	*Cyclocardia ovata*
Cyclocardia rjabininae	*Cyclocardia rjabininae*
Cyclocardia ventricosa ovata	*Cyclocardia ventricosa*
Venercardia (Cyclocardia) borealis var. novangliae	*Cyclocardia borealis*
Venericardia (Cyclocardia) borealis v. ovata	*Cyclocardia ovata*
Venericardia (Cyclocardia) crassidens	*Crassicardia crassidens*
Venericardia (cyclocardia) crebicostata (Krause)	*Cyclocardia crebicostata*
Venericardia (Cyclocardia) paucicostata	*Cyclocardia sp.*
Venericardia (Cyclocardia) ventericosa	*Cyclocardia ventericosa*

Venericardia (Cyclocardia) ventricosa	*Cyclocardia ventericosa*
Venericardia granulata	*Cyclocardia granulata*
EUHETERODONTA (Subterclass)	
IMPARIDENTIA(Superorder)	
CARDIIDA(Order)	
CARDIOIDEA(Superfamily)	
CARDIIDAE (Family)	
Cardiidae indet.	
Cardium californense	*Keenocardium californiense*
Cilartocardium ciliatum	*Cilartocardium ciliatum*
Cilartocardium cil. ciliatum	*Cilartocardium ciliatum*
Ciliantocardium cil techuktchiuse	*Cilartocardium cil. tchuktchense*
Ciliatocardium cil dawsoni	*Cilartocardium ciliatum*
Clinocardium blandum	*Keenocardium blandum*
Clinocardium californien	*Keenocardium californiense*
Clinocardium californiense	*Keenocardium californiense*
Clinocardium ciliatum	*Cilartocardium ciliatum*
Clinocardium fucanum	*Keenocardium blandum*
Clinocardium nuttallii	*Clinocardium nuttallii*
Keenocardium californiense californiense	*Keenocardium californiense*
Serripes (Yangudiuella) notablis	
Serripes gr. beringianus	*Serripes groenlandicus*
Serripes gr. groenlandicus	*Serripes groenlandicus*
Serripes groenlandicus	*Serripes groenlandicus*
Serripes laperousii	*Serripes laperousii*
Serripes notablis	*Serripes notablis*

TELLINOIDEA (Superfamily)	
TELLINIDAE (Family)	
Tellinidae indet.	
Macoma sp.	
Macoma balthica	*Macoma balthica*
Macoma brota	*Macoma brota*
Macoma calcarea	*Macoma calcarea*
Macoma calcarea var. soot-zyem	*Macoma calcarea*
Macoma crassula	*Macoma crassula*
Macoma inquinita	*Macoma inquinita*
Macoma krausei	*Macoma moesta*
Macoma lama	*Macoma lama*
Macoma loveni	*Macoma loveni*
Macoma middendorffii	*Macoma middendorffii*
Macoma moesta	*Macoma moesta*
Macoma obliqua	*Macoma obliqua*
Macoma planiscula	*Macoma lama*
Tellina lutea	*Megangulus luteus*
MYIDA (Order)	
MYOIDEA (Superfamily)	
MYIDAE (Family)	
Myidae indet.	
Mya sp.	
Mya (Mya) pseudoarienaria	*Mya pseudoarienaria*
Mya japonica	*Mya japonica*
Mya pseudoarenaria	*Mya pseudoarienaria*

Mya pseudoaria	*Mya pseudoarienaria*
Mya truncata	*Mya truncata*
Mya uzenensis	*Mya uzenensis*
PECTINIDA (Order)	
PECTINOIDEA (Superfamily)	
PECTINIDAE (Family)	
Pectinidae indet.	
Chlamys behringiana	*Chlamys behringiana*
Chlamys beringianus	*Chlamys behringiana*
Chlamys beringianus angustecostatus	*Chlamys behringiana*
Chlamys beringianus var strategus	*Chlamys behringiana*
Chlamys hindsii (Carpenter) *asiaticus*	*Chlamys sp.*
Chlamys wainwrightensis	*Chlamys albida*
LUCINIDA (Order)	
THYASIROIDEA (Superfamily)	
THYASIRIDAE (Family)	
Thyasiridae indet.	
Axinopsida sp.	
Axinopsida orbiculata	*Axinopsida orbiculata*
Axinopsida serricata	*Axinopsida serricata*
Thyasira flexuosa	*Thyasira flexuosa*
Thyasira gouldi	*Thyasira gouldii*
Thyasira gouldi (Philippi)	*Thyasira gouldii*
VENERIDA (Order)	
MACTROIDEA (Superfamily)	
MACTRIDAE (Family)	

Mactromeris polynyma	*Macromeris polynyma*
Spisula sp.	
Spisula alaskana	*Macromeris polynyma*
Spisula polynyma	*Macromeris polynyma*
Spisula voyi	*Spisula voyi*
UNGULINOIDEA (Superfamily)	
UNGULINIDAE (Family)	
Diplodonta aleutica	*Diplodonta aleutica*
Diplodonta orbella	*Zemysina orbella*
ANOMALODESMATA (Superorder)	
PANDOROIDEA (Superfamily)	
LYONSIIDAE (Family)	
Lyonsiidae indet.	
Lyonsia sp.	
Lyonsia arenosa	*Lyonsia arenosa*
Lyonsia norvegica	*Lyonsia norwegica*
Lyonsia norwegica	*Lyonsia norwegica*
PANDORIDAE (Family)	
Pandora glacialis	*Pandora glacialis*
THRACIOIDEA (Superfamily)	
PERIPLOMATIDAE (Family)	
Periploma alaskana	*Periploma aleuticum*
Periploma aleuticum	*Periploma aleuticum*
Periploma fragilis	*Periploma aleuticum*
THRACIIDAE (Family)	
Cyanthodonta dubiosa	*Cyanthodonta dubiosa*

Lampeia adamsi	*Lampeia adamsi*
Thracia sp.	
Thracia devexa	*Thracia devexa*
Thracia myopsis	*Thracia myopsis*
VENEROIDEA (Superfamily)	
VENERIDAE (Family)	
Veneridae indet.	
Gomphina (Liocyma) fluctuosa	*Liocyma fluctuosa*
Gomphina (Liocyma) viridis	*Liocyma fluctuosa*
Liocyma sp.	
Liocyma fluctuosa	*Liocyma fluctuosa*
Liocyma fluctuosum	*Liocyma fluctuosa*
Liocyma viridis	*Liocyma fluctuosa*
ADAPENDONTA (Order)	
HIATELLOIDEA (Superfamily)	
HIATELLIDAE (Family)	
Hiatellidae indet.	
Cyrtodaria sp.	
Cyrtodaria kurriana	*Cyrtodaria kurriana*
Hiatella arctica	*Hiatella arctica*
Mya priagus (Tilesius)	*Panomya priapus*
Panomya sp.	
Panomya ampla	*Panomya ampla*
Panomya arctica	*Panomya norvegica*
Panomya beringiana	*Panomya priapus*

Panomya norvegica	*Panomya norvegica*
SOLENOIDEA (Superfamily)	
PHARIDAE (Family)	
Siliqua sp.	
Siliqua alta	*Siliqua alta*
Siliqua media	*Siliqua sp.*
GALEOMMATIDA (Order)	
GALEOMMATOIDEA (Superfamily)	
LASAEIDAE (Family)	
Lasaeidae indet.	
Montacutinae (Subfamily)	
Mysella sp.	
Mysella aleutica	*Kurtiella tumida*
Mysella derjugini	*Kutiella derjugini*
Mysella gurjanoval gurjanval	*Mysella gurjanovae*
Mysella planata	*Mysella planata*
Mysella tumida	*Kurtiella tumida*
Neaeromya compressa	*Neaeromya compressa*
Pseudopythina compressa	*Neaeromya compressa*
PTERIOMORPHIA (Infraclass)	
MYTILIDA (Order)	
MYTILOIDEA (Superfamily)	
MYTILIDAE (Family)	
Mytilidae indet.	
Crenella columbiana	*Solamen columbianum*
Crenella decussata	*Crenella decussata*

Modiolus modiolus	*Modiolus modiolus*
Musculus sp.	
Musculus corrugatus	*Musculus glacialis*
Musculus discors	*Musculus discors*
Musculus discors var substriatus	*Musculus discors*
Musculus glacialis	*Musculus glacialis*
Musculus laevigatus	*Musculus discors*
Musculus niger	*Musculus niger*
Musculus nigra	*Musculus niger*
Mytilus edulis	*Mytilus edulis*
PROTOBRANCHIA (Subclass)	
NUCULANIDA (Order)	
NUCULANOIDEA (Superfamily)	
NUCULANIDAE (Family)	
Nuculanidae indet.	
Leda minuta	*Nuculana minuta*
Leda radiata	*Nuculana radiata*∗
Leda radiata var lamellosa	*Nuculana radiata*∗
Nuculana sp.	
Nuculana fossa	*Nuculana fossa*∗
Nuculana minuta	*Nuculana minuta*
Nuculana pernula	*Nuculana pernula*
Nuculana radiata	*Nuculana radiata*∗
YOLDIIDAE (Family)	
Yoldiidae indet.	
Portlandia aestuariorum	*Portlandia aestuariorum*

Portlandia arctica	*Portlandia arctica*
Portlandia arctica (siliqua) inflata	*Portlandia arctica*
Portlandia glacialis	*Portlandia glacialis*
Portlandia intermedia	*Yoldiella intermedia*
Yoldia sp.	
Yoldia (Yoldia) amygdalea	*Yoldia amygdalea*
Yoldia (Yoldia) amygdalea myaliformis	*Yoldia amygdalea*
Yoldia amygdalea	*Yoldia amygdalea*
Yoldia hyperborea	*Yoldia hyperborea*
Yoldia myalis	*Yoldia myalis*
Yoldia oleacina	*Yoldiella intermedia*
Yoldia scissurata	*Yoldia aeolica*
Yoldia seminuda	*Yoldia aeolica*
Yoldiella (Portlandia) lenticula	*Yoldiella lenticula*
Yoldiella fraterna	*Yoldiella nana*
NUCULIDA (Order)	
NCULOIDEA (Superfamily)	
NUCULIDAE (Family)	
Nuculidae indet.	
Ennucula tenuis cf.	*Ennucula tenuis*
Enucula tenuis	*Ennucula tenuis*
Leionucula bellotii (belotti)	*Ennucula tenuis*
Nucula belloti	*Ennucula tenuis*
Nucula inflata romboides	*Ennucula tenuis*
Nucula proxima	*Nucula proxima*
Nucula tenuis	*Ennucula tenuis*

Nucula tenuis expansa	*Ennucula tenuis*
Nucula tenuis inflata	*Ennucula tenuis*

APPENDIX J

FULL NATURAL HISTORY COLLECTION DATA

Appendix contains the full dataset for Chapter 3, available in the online supplement in the file: ***Appendix J_ARCTIC_NHC_Bivalve taxa_Meadows.zip***.

REFERENCES

[1] An act providing a civil government for Alaska. May 17, 1884., 1884. url: https://vilda.alaska.edu/digital/collection/cdmg21/id/2287/.

[2] *Harriman Alaska Expedition (1899)*. Smithsonian Institution, Washington, DC, USA, 1899. ISBN: 0096-8749. url: https://siarchives.si.edu/collections/auth_exp_fbr_eace0018.

[3] Benthic organisms data collected using sediment sampler casts from NOAA Ship OCEANOGRAPHER in the Chukchi Sea from 1986-09-06 to 1987-10-05 (NCEI Accession 8900299). Dataset NCEI Accession 8900299, University of Alaska, Institude of Marine Science (IMS/UAF), 2010. url: https://accession.nodc.noaa.gov/8900299.

[4] NODC Standard Format Intertidal Organisms and Habitats (F030) Data (1974-1980) (NCEI Accession 0014153). Technical report, US DOC/NOAA/NESDIS, 2010. url: https://accession.nodc.noaa.gov/0014153.

[5] NODC Standard Format Benthic Organisms (F132) Data (1957-1989) (NCEI Accession 0014198). Dataset NCEI Accession 0014198, US DOC/NOAA/NESDIS, 2011. url: https://accession.nodc.noaa.gov/0014198.

[6] Historical Sea Ice Atlas, University of Alaska, 2017.

[7] Oceanographic Data Sets for NMNH Invertebrate Collections: Albatross, 2017. Smithsonian National Museum of Natural History, Washington, D.C. url: https://web.archive.org/web/20171206192517/http://invertebrates.si.edu/albatross/albatross.cfm.

[8] 1784: First Russian Settlement in Alaska, 2020. Carnegie Corporation of New York. url: usrussiarelations.org.

[9] A. E. Aitken. Fossilization potential of Arctic fjord and continental shelf benthic macrofaunas. *Geological Society of London, Special Publications*, 53:155–176, 1990. doi:10.1144/gsl.sp.1990.053.01.09.

[10] P. Albano, Q. Hua, D. Kaufman, A. Tomašových, M. Zuschin, and K. Agiadi. Radiocarbon dating supports bivalve-fish age coupling along a bathymetric gradient in high-resolution paleoenvironmental studies. *Geology*, 48:589–593, 2020. doi:10.1130/G47210.1.

[11] E. T. Alexandersson. Marine maceration of skeletal carbonates in the Skagerrak, North Sea. *Sedimentology*, 26(6):845–852, 1979. doi:doi:10.1111/j.1365-3091.1979.tb00977.x.

[12] A. P. Allen, M. A. Kosnik, and D. S. Kaufman. Characterizing the dynamics of amino acid racemization using time-dependent reaction kinetics: A Bayesian approach to fitting age-calibration models. *Quaternary Geochronology*, 18:63–77, 2013. doi:10.1016/j.quageo.2013.06.003.

[13] R. C. Aller. Carbonate dissolution in nearshore terrigenous muds: The role of physical and biological reworking. *The Journal of Geology*, 90(1):79–95, 1982. doi:10.1086/628652.

[14] R. C. Aller. The Effects of Macrobenthos on Chemical Properties of Marine Sediment and Overlying Water. In P. L. McCall and M. J. S. Tevesz, editors, *Animal-Sediment Relations: The Biogenic Alteration of Sediments*, Topics in Geobiology, pages 53–102. Springer US, Boston, MA, 1982. doi: 10.1007/978-1-4757-1317-6_2.

[15] I. Almagro, P. Drzymała, K. Berent, C. I. Sainz-Díaz, M. G. Willinger, J. Bonarski, and A. G. Checa. New Crystallographic Relationships in Biogenic Aragonite: The Crossed-Lamellar Microstructures of Mollusks. *Crystal Growth & Design*, 16(4):2083–2093, 2016. doi:10.1021/acs.cgd.5b01775.

[16] D. L. Alverson, N. J. Wilimovsky, and F. Wilke. A preliminary report on marine investigations of the Chukchi Sea, August 1959. Report, Bureau of Commercial Fisheries, Seattle, Wash. Exploratory Fishing and Gear Research Base, Washington, DC, 1960. url: https://www.osti.gov/servlets/purl/4613231.

[17] W. G. Ambrose, P. E. Renaud, W. L. Locke, Finlo R. Cottier, J. Berge, M. L. Carroll, B. Levin, and S. Robert. Growth line deposition and variability in growth of two circumpolar bivalves (Serripes groenlandicus, and Clinocardium ciliatum). *Polar Biology*, 35(3):345–354, March 2012. url https://doi.org/10.1007/s00300-011-1080-4.

[18] R. P. Angliss, B. M. Allen, P. R. Wade, M. A. Perez, P. Clapham, L. W. Fritz, D. J. Rugh, K. E. W. Shelden, R. C. Hobbs, and R. G. Towell. Alaska marine mammal stock assessments, 2008. NOAA technical memorandum NMFS-AFSC 193, National Marine Fisheries Service (NMFS), Alaska Fisheries Science Center (U.S.), National Oceanic and Atmospheric Administration, 2009. url: https://www.fisheries.noaa.gov/resource/document/alaska-marine-mammal-stock-assessments-2008.

[19] A. Armstrong. *A personal narrative of the discovery of the northwest passage : with numerous incidents of travel and adventure during nearly five years' continuous service in the Arctic regions while in search of the expedition under Sir John Franklin*. Hurst and Blackett, London, United Kingdom, 1857. url: https://link.gale.com/apps/doc/CY0101138451/SABN?u=chic_rbwsid=SABNxid=2f375dca.

[20] M. Baker. *Geographic dictionary of Alaska*. Government Printing Office, Washington, 1902. url: https://www.biodiversitylibrary.org/item/98869.

[21] J. Baldwin and R. Powers. *Last Flag Down: The Epic Journey of the Last Confederate Warship*. Broadway Books, 2008. ISBN: 0-307-23656-0. url: https://books.google.com/books?id=mFzt2JOpvrICdq=Last+Flag+Down: +The+Epic+Journey+of+the+Last+Confederate+Warshiplr=.

[22] T. W. Barry. Observations on natural mortality and native use of eider ducks along the Beaufort Sea coast. *Canadian Field-Naturalist*, 82(2):140–144, 1968. url: https://www.biodiversitylibrary.org/item/89177page/152/mode/1up.

[23] J. Bart and S. L. Earnst. Breeding ecology of Spectacled Eiders Somateria. scheri in Northern Alaska. *Wildfowl*, 55(55):83–98, 2013.

[24] N. R. Bates, J. T. Mathis, and L.W. Cooper. Ocean acidification and biologically induced seasonality of carbonate mineral saturation states in the western Arctic Ocean. *Journal of Geophysical Research*, 114:C11007, 2009. doi:10.1029/2008jc004862.

[25] T. H. Bean. The Fishery resources and fishing grounds of Alaska. *The fisheries and Fishery industries of the United States*, v. 3:p. 81–116, 1884. url: https://www.biodiversitylibrary.org/item/115818page/9/mode/1up.

[26] F. W. Beechey. *Narrative of a voyage to the Pacific and Beering's strait, to co-operate with the polar expeditions: performed in His Majesty's ship Blossom, under the command of Captain F.W. Beechey ... in the years 1825, 26, 27, 28*, volume 1. H. Colburn and R. Bentley, London, 1831. url: https://www.biodiversitylibrary.org/item/28158.

[27] S. Belikov and A. Boltunov. Distribution and migration of polar bears, Pacific walruses and gray whales depending on ice conditions in the Russian Arctic. *Polar Biology*, 9, 1996. url: https://core.ac.uk/download/pdf/51484768.pdf.

[28] L. Black. *Russians in Alaska, 1732-1867*. University of Alaska Press, Fairbanks, Alaska, 2004. ISBN: 1889963046 (cloth : alk. paper) 1889963054 (pbk.).

[29] A. L. Blanchard. Variability of macrobenthic diversity and distributions in Alaskan sub-Arctic and Arctic marine systems with application to worldwide Arctic Systems. *Marine Biodiversity*, 45(4):781–795, 2014. doi:10.1007/s12526-014-0292-6.

[30] A. L. Blanchard, C. L. Parris, A. L. Knowlton, and N. R. Wade. Benthic ecology of the northeastern Chukchi Sea. Part I. Environmental characteristics and macrofaunal community structure, 2008–2010. *Continental Shelf Research*, 67:52–66, 2013. doi:10.1016/j.csr.2013.04.021.

[31] J. R. Bockstoce. *Whales, ice, and men: the history of whaling in the western Arctic*. University of Washington Press, 1986. ISBN: 0-295-96318-2 978-0-295-96318-1.

[32] J. R. Bockstoce and D. B. Botkin. The Harvest of Pacific Walruses by the Pelagic Whaling Industry, 1848 to 1914. *Arctic and Alpine Research*, 14(3):183–188, 1982. doi:10.2307/1551150.

[33] D. Borcard, F. Gillet, and P. Legendre. *Numerical ecology with R*. Springer Science & Business Media, 2011. doi:10.1007/978-1-4419-7976-6.

[34] E. W. Born, S. Rysgaard, G. Ehlmé, M. Sejr, M. Acquarone, and N. Levermann. Underwater observations of foraging free-living Atlantic walruses (Odobenus rosmarus rosmarus) and estimates of their food consumption. *Polar Biology*, 26(5):348–357, 2003. doi:10.1007/s00300-003-0486-z.

[35] A. Bradbury. *Length-weight models for intertidal clams in Puget Sound : (Bivalve Regions 1, 5, 6, 7, and 8)*. Washington, Dept. of Fish and Wildlife, Fish Program, Fish Management Division, Olympia, Washington, USA, 2005. url: http://catalog.hathitrust.org/api/volumes/oclc/63789526.html.

[36] S. A. Buturlin. The True Home of the Spectacled Eider. *The Condor*, 12(1):46–46, 1910. doi:10.1093/condor/12.1.46a.

[37] Tomoki C. and S. Sato. Invasion of *laguncula pulchella* (Gastropoda: Naticidae) and predator–prey interactions with bivalves on the Tona coast, Miyagi prefecture, northern Japan. *Biological Invasions*, 15(3):587–598, 2013. doi:10.1007/s10530-012-0310-1.

[38] S. Cai. *Paleoenvironmental interpretation of late glacial and post-glacial fossil marine molluscs, Eureka Sound, Canadian Arctic Archipelago*. Thesis, Masters of Science, University of Saskatchewan, 2006. doi:10388/etd-04212006-005035.

[39] M. Carroll, M. Kowalewski, M. Simões, and G. Goodfriend. Quantitative estimates of time-averaging in terebratulid brachiopod shell accumulations from a modern tropical shelf. *Paleobiology*, 29(3):381–402, 2003. doi:10.1666/0094-8373(2003)0292.0.CO;2.

[40] M. L. Carroll, Madelyn J. Mette, and W. G. Ambrose. Greenland cockles (Serripes groenlandicus Mohr 1786) from Bjørnøya (Bear Island), Svalbard record environmental change: Local and regional drivers of growth. *Estuarine, Coastal and Shelf Science*, 243:106892, September 2020. doi:10.1016/j.ecss.2020.106892.

[41] A. Chao, R. L. Chazdon, R. K. Colwell, and T.-J. Shen. A new statistical approach for assessing similarity of species composition with incidence and abundance data. *Ecology letters*, 8(2):148–159, 2005. doi:10.1111/j.1461-0248.2004.00707.x.

[42] A. G. Checa, F. J. Esteban-Delgado, and A. B. Rodriguez-Navarro. Crystallographic structure of the foliated calcite of bivalves. *J Struct Biol*, 157(2):393–402, 2007. doi:10.1016/j.jsb.2006.09.005.

[43] W. Cheng, E. Blanchard-Wrigglesworth, C. M. Bitz, C. Ladd, and P. J. Stabeno. NOAA's Arctic vision & strategy. *Geophysical Research Letters*, 43(22):11688–11696, 2011. doi:10.1016/j.ocemod.2016.02.009.

[44] L. Cherns and V. P. Wright. Quantifying the Impacts of Early Diagenetic Aragonite Dissolution on the Fossil Record. *Palaios*, 24(11):756–771, 2009. doi:10.2110/palo.2008.p08-134r.

[45] C. T. Clark, L. Horstmann, A. de Vernal, A. M. Jensen, and N. Misarti. Pacific walrus diet across 4000 years of changing sea ice conditions. *Quaternary Research*, pages 1–17, 2018. doi:10.1017/qua.2018.140.

[46] E. V. Coan, P. V. Scott, and F. R Bernard. *Bivalve seashells of western North America*. Santa Barbara Museum of Natural History Monographs; Studies in biodiversity. Santa Barbara Museum of Natural History, Santa Barbara, California, USA, 1 edition, 2000. ISBN: 978-0-936494-30-2.

[47] J. Cook. *A voyage to the Pacific Ocean : undertaken, by the command of His Majesty, for making discoveries in the northern hemisphere : performed under the direction of Captains Cook, Clerke, and Gore, in His Majesty's ships the Resolution and Discovery; in the years 1776, 1777, 1778, 1779, and 1780 : in three volumes*, volume v. 1. Printed by H. Hughs : G. Nicol and T. Cadell ..., London :, the second edition. edition, 1785. ur" https://www.biodiversitylibrary.org/item/276717.

[48] W. W. Cooke. *Distribution and migration of North American ducks, geese, and swans*, volume no.26 (1906). Govt. Print. Off., Washington, 1906. url: https://www.biodiversitylibrary.org/item/117248.

[49] L. W. Cooper, M. A. Janout, K. E. Frey, R. Pirtle-Levy, M. L. Guarinello, J. M. Grebmeier, and J. R. Lovvorn. The relationship between sea ice break-up, water mass variation, chlorophyll biomass, and sedimentation in the northern Bering Sea. *Deep Sea Research Part II: Topical Studies in Oceanography*, 65-70:141–162, June 2012. doi:10.1016/j.dsr2.2012.02.002.

[50] L. W. Cooper, M. G. Sexson, J. M. Grebmeier, R. Gradinger, C. W. Mordy, and J. R. Lovvorn. Linkages between sea-ice coverage, pelagic–benthic coupling, and the distribution of spectacled eiders: Observations in March 2008, 2009 and 2010, northern Bering Sea. *Deep Sea Research Part II: Topical Studies in Oceanography*, 94:31–43, 2013. doi:10.1016/j.dsr2.2013.03.009.

[51] L. W. Cooper, T. E. Whitledge, J. M. Grebmeier, and T. Weingartner. The nutrient, salinity, and stable oxygen isotope composition of Bering and Chukchi Seas waters in and near the Bering Strait. *Journal of Geophysical Research: Oceans*, 102(C6):12563–12573, 1997. doi:10.1029/97jc00015.

[52] L.W. Cooper and J. M. Grebmeier. Deposition patterns on the Chukchi shelf using radionuclide inventories in relation to surface sediment characteristics. *Deep Sea Research Part II: Topical Studies in Oceanography*, 152:48–66, 2018. doi:10.1016/j.dsr2.2018.01.009.

[53] R. A. Cooper, P. A. Maxwell, J. S. Crampton, A. G. Beu, C. M. Jones, and B. A. Marshall. Completeness of the fossil record: Estimating losses due to small body size. *Geology*, 34(4):241–244, 2006. doi:10.1130/G22206.1.

[54] M. J. Costello, P. Bouchet, G. Boxshall, K. Fauchald, D. Gordon, B. W. Hoeksema, G. C. B. Poore, R. W. M. van Soest, S. Stöhr, T. C. Walter, B. Vanhoorne, W. Decock, and W. Appeltans. Global Coordination and Standardisation in Marine Biodiversity through the World Register of Marine Species (WoRMS) and Related Databases. *PLOS ONE*, 8(1):e51629, January 2013. doi:10.1371/journal.pone.0051629.

[55] J. M. Creamean, J. N. Cross, R. Pickart, L. McRaven, P. Lin, and et al. Pacini, A. Ice nucleating particles carried from below a phytoplankton bloom to the Arctic atmosphere. *Geophysical Research Letters*, 46:8572–8581, 2019. doi:10.1029/2019GL083039.

[56] M. M. Cronin. An Almost Undiscovered Country. *Journalism History*, 42(1):24–32, 2016. doi:10.1080/00947679.2016.12059139.

[57] J. N. Cross, J. T. Mathis, N. R. Bates, and R. H. Byrne. Conservative and non-conservative variations of total alkalinity on the southeastern Bering Sea shelf. *Marine Chemistry*, 154:100–112, 2013. doi:10.1016/j.marchem.2013.05.012.

[58] J. N. Cross, J. T. Mathis, R. S. Pickart, and N. R. Bates. Formation and transport of corrosive water in the Pacific Arctic region. *Deep Sea Research Part II: Topical Studies in Oceanography*, 152:67–81, 2018. doi:10.1016/j.dsr2.2018.05.020.

[59] H. Cummins, E. N. Powell, and G. Staff. The size-frequency distribution in palaeoecology: effects of taphonomic processes during formation of molluscan death assemblages in Texas bays. *Palaeontology*, 29(3):495–518, 1986. url: https://www.palass.org/publications/palaeontology-journal/archive/29/3/article_pp495-518.

[60] E. S. Curtis, E. H. Harriman, and D. G. Inverarity. *Harriman Alaska Expedition, 1899*. Library of Congress, Washington DC, USA, 1899. url: https://www.wdl.org/en/item/15694/.

[61] W. H. Dall. *Collections sent to the Smithsonian Institution, Western Union Telegraph Expedition, 1865*, volume v1. Smithsonian Institution Archives, 1865. url: https://transcription.si.edu/project/7921.

[62] W. H. Dall. Western Union Telegraph Expedition, 1868.
url: http://edan.si.edu/transcription/pdf_files/7960.pdf, 1868.

[63] W. H. Dall. *Field notes, 1871*. Number SIA RU007073 in Smithsonian field book project : an initiative to improve access to field book content that documents natural history. Smithsonian Institution Archives, Washington, DC, USA, 1871. doi: 10.5962/bhl.title.88035.

[64] W. H. Dall. *Catalogue of shells from Bering Strait and the adjacent portions of the Arctic Ocean, with descriptions of three new species*. Smithsonian Institution Archives, Washington, D.C., 1874. ISBN: 0-665-14845-3. url: https://www.biodiversitylibrary.org/item/85625.

[65] W. H. Dall. *Field Notes, 1880*, volume 1. Smithsonian Institution Archives, Washington, DC, USA, 1880. url: https://transcription.si.edu/project/6980.

[66] W. H. Dall. Notes on Alaska and the vicinity of Bering Strait. *American Journal of Science*, 21:104–111, 1881. url: http://catalog.hathitrust.org/api/volumes/oclc/18541163.html.

[67] W. H. Dall. *Catalogue of the Marine Invertebrates collected by W. H. Dall in Alaska and other places in the Pacific Ocean, during the years 1866, 1867, 1871, 1872, 1873, 1874, and 1880. (A few Mollusks are not entered here)*. Smithsonian Institution, Washington, DC, 1890. url: https://siarchives.si.edu/collections/fbr_item_modsi9425.

[68] W. H. Dall. *Instructions for Collecting Mollusks, and Other Useful Hints for the Conchologist*. US Government Printing Office, Washington, DC, USA, 1892. url: https://catalog.lib.uchicago.edu/vufind/Record/4201963.

[69] W. H. Dall. Report on coal and lignite of Alaska. 17th Annual Report 1, US Geological Survey, Washington, DC, USA, 1896. url: https://catalog.hathitrust.org/Record/008899598.

[70] W. H. Dall. *Alaska and its resources*. Lee and Shepard, Boston, MA, 1 edition, 1897. url: https://catalog.hathitrust.org/Record/006691940.

[71] W. H. Dall. *Report of the Canadian Arctic Expedition 1913-18: Volume VIII: Mollusks, Echinoderms, Coelenterates, etc. Part A: Mollusks, Recent and Pleistocene, Southern Party, 1913-1916*, volume v.8:pt.A (1913-1920). F. A. Acland, Printer to the King, Ottawa, 1919. url: https://www.biodiversitylibrary.org/item/116075.

[72] W. H. Dall and H. M. Bannister. *List of the birds of Alaska, with biographical notes*. Chicago, IL, USA, 1869. doi: 10.5962/bhl.title.101944.

[73] W. H. Dall, Vitus Jonassen Bering, and P. Chaplin. *Early expeditions to the region of Bering Sea and Strait : from the reports and journals of Vitus Ivanovich Bering*. Government Printing Office, Washington, DC, USA, 1891. doi: 10.5962/bhl.title.53451.

[74] W. H. Dall, Asa Gray, J. Murdoch, P. H. Ray, C. V. Riley, C. A. Schott, and Corps United States. Army. Signal. *Report of the International Polar Expedition to Point Barrow, Alaska, in response to the resolution of the House of Representatives of December 11, 1884*. Government Printing Office, Washington, DC, USA, 1885.

[75] D. A. Dasher, T. Lomax, and I. Hartwell. Cruise ReportAlaska Monitoring and Assessment Program (AKMAP) Chukchi Sea 2012 Coastal Impact Assistance Program AssessmentAugust 5 – 15, 2012. Technical report, Alaska Department of Environmental Conservation, 2013. url: https://dec.alaska.gov/water/water-quality/monitoring/surveys/.

[76] D. A. Dasher, T. Lomax, B. Holladay, P. Rivera, H. Chenelot, N. R. Foster, M. K. Hoberg, R. Clark, J. Hartwell, I.and Quetsel, A. Stephens, and T. Morgan. Cruise ReportAlaska Monitoring and Assessment Program (AKMAP)Chukchi Sea 2011Coastal Impact Assistance Program AssessmentSeptember 04 –September 17, 2011. Technical report, Alaska Department of Environmental Conservation, 2011. url: https://dec.alaska.gov/water/water-quality/monitoring/surveys/.

[77] G. M. Dawson and R. G. McConnell. *Report on an exploration in the Yukon district, NWT, and adjacent northern portion of British Columbia, 1887*. Number 14884 in CIHM/ICMH microfiche series. SE Dawson, Montreal, Canada, 1898. doi: 10.5962/bhl.title.38379.

[78] G. W De Long. *Our lost explorers : the narrative of the Jeannette Arctic expedition as related by the survivors, and in the records and last journals of Lieutenant De Long*. American Publishing Company, Hartford, Connecticut, 1882. url: https://www.biodiversitylibrary.org/item/17075page/9/mode/1up.

[79] L.-A. Dehn, G. G. Sheffield, E. H. Follmann, L. K. Duffy, D. L. T., and T. M. O'Hara. Feeding ecology of phocid seals and some walrus in the Alaskan and Canadian Arctic as determined by stomach contents and stable isotope analysis. *Polar Biology*, 30(2):167–181, 2007. doi:10.1007/s00300-006-0171-0.

[80] B. Demuth. The Walrus and the Bureaucrat: Energy, Ecology, and Making the State in the Russian and American Arctic, 1870–1950. *The American Historical Review*, 124(2):483–510, 2019. doi:10.1093/ahr/rhz239.

[81] K Dunton, C. J Ashjian, R Campbell, L. W. Cooper, J. M. Grebmeier, B Konar, D Maidment, C. Ashjian, J. Trefry, T.J. Weingartner, and T. L Whiteaker. Ecosystem monitoring information collected in Hanna Shoal in the Chukchi Sea for the COMIDA CAB project from August 2012 to August 2013 (NCEI Accession 0123220). Dataset NCEI Accession 0123220, 2014. doi: 10.7289/v5gx48mn.

[82] K Dunton, B Konar, J Grebmeier, J. Trefry, R Cooper, L.and Harvey, and S Schonberg. Chemical and benthos data collected from CTD, bottle, and other instruments in the Chukchi Sea in 2009-2010 as part of the Chukchi Sea Offshore Monitoring in Drilling Area - Chemical and Benthos (COMIDA-CAB) project (NCEI Accession 0095566). Dataset NCEI Accession 0095566, 2012. doi: 10.7289/v5c8279z.

[83] C. R. Ely, C. P. Dau, and C. A. Babcock. Decline in a Population of Spectacled Eiders Nesting on the Yukon-Kuskokwim Delta, Alaska. *Northwestern Naturalist*, 75(3):81–87, 1994. doi:10.2307/3536829.

[84] S. R. Emerson, D. Archer, H. Charnock, J. Marmion Edmond, I. N. McCave, A. L. Rice, and T. R. S. Wilson. Calcium carbonate preservation in the ocean. *Philosophical Transactions of the Royal Society of London. Series A, Mathematical and Physical Sciences*, 331(1616):29–40, 1990. doi:10.1098/rsta.1990.0054.

[85] F. J. Esteban-Delgado, E. M. Harper, A. G. Checa, and A. B. Rodriguez-Navarro. Origin and expansion of foliated microstructure in Pterimorph bivalves. *The Biological Bulliten*, 214(2):153–165, 2008. doi:10.2307/25066672.

[86] V. Fabry, J. McClintock, J. Mathis, and Jacqueline Grebmeier. Ocean Acidification at High Latitudes: The Bellwether. *Oceanography*, 22:160–171, 2009. doi:10.5670/oceanog.2009.105.

[87] F. Fay and J. Burns. Maximal Feeding Depth of Walruses. *ARCTIC*, 41, 1988. doi:10.14430/arctic1724.

[88] F. H. Fay. Ecology and Biology of the Pacific Walrus, Odobenus rosmarus divergens Illiger. Technical Report 74, United States Department of the Interior, Fish and Wildlife Service, Washington, DC, USA, 1982. doi: 10.3996/nafa.74.0001.

[89] F. H. Fay, Y. A. Bukhtiyarov, S. W. Stoker, and L. M. Shultz. Foods of the Pacific walrus in winter and spring in the Bering Sea. NOAA technical memorandum NMFS 12, NOAA, Washington, DC, USA, 1984. url: https://repository.library.noaa.gov/view/noaa/5600/noaa_5600_DS1.pdfpage=87.

[90] F. H. Fay, L. L. Eberhardt, B. P. Kelly, J. J. Burns, and L. T. Quakenbush. Status of the pacific walrus population, 1950–1989. *Marine Mammal Science*, 13(4):537–565, 1997. doi:10.1111/j.1748-7692.1997.tb00083.x.

[91] F. H. Fay, B. P. Kelly, and J. L. Sease. Managing the exploitation of pacific walrus: A tragedy of delayed response and poor communication. *Marine Mammal Science*, 5(1):1–16, 1989. doi:10.1111/j.1748-7692.1989.tb00210.x.

[92] H. M. Feder, Nora R. Foster, S. C. Jewett, T. J. Weingartner, and Rae Baxter. Mollusks in the Northeastern Chukchi Sea. *Arctic*, 47(2):145–163, 1994.

[93] H. M. Feder, S. C. Jewett, and A. L. Blanchard. Southeastern Chukchi Sea (Alaska) macrobenthos. *Polar Biology*, 30(3):261–275, February 2007. doi:10.1007/s00300-006-0180-z.

[94] H. M. Feder, A. S. Naidu, S. C. Jewett, J. M. Hameedi, W. R. Johnson, and T. E. Whitledge. The northeastern Chukchi Sea: benthos-environmental interactions. *Marine Ecology Progress Series*, 111(1/2):171–190, 1994. url: https://www.jstor.org/stable/24847621.

[95] C. A. Ferguson. Nutrient pollution and the molluscan death record: Use of mollusc shells to diagnose environmental change. *Journal of Coastal Research*, 24(1A):250–259, 2008. doi:10.2112/06-0650.1.

[96] E. C. Fieller. Some Problems in Interval Estimation. *Journal of the Royal Statistical Society. Series B (Methodological)*, 16(2):175–185, 1954. url: https://www.jstor.org/stable/2984043.

[97] A. S. Fischbach, D. H. Monson, and C. V. Jay. Enumeration of Pacific walrus carcasses on beaches of the Chukchi Sea in Alaska following a mortality event, September 2009. Report 2009-1291, US Geological Survey, Washington, DC, USA, 2009. url: https://pubs.usgs.gov/of/2009/1291/pdf/ofr20091291.pdf.

[98] J. B. Fischer, A. R. Williams, and R. A. Stehn. Nest population size and potential production of geese and spectacled eiders on the Yukon-Kuskokwim Delta, Alaska, 1985-2016. Technical Report, US Fish and Wildlife Service, Migratory Bird Management, Anchorage, AK, 2017. url: https://www.fws.gov/r7/mbsp/mbm/waterfowl/surveys/pdf/201_YKD_Nest_Plot_Survey.pdf.

[99] K. W. Flessa. Well-traveled cockles: Shell transport during the Holocene transgression of the southern North Sea. *Geology*, 26(2):187–190, 1998. doi:10.1130/0091-7613(1998)026<0187:WTCSTD>2.3.CO;2.

[100] P. L. Flint, J. B. Grand, M. R. Petersen, and R. F. Rockwell. Effects of Lead Exposure, Environmental Conditions, and Metapopulation Processes on Population Dynamics of Spectacled Eiders. *North American Fauna*, pages 1–41, 2016. doi:10.3996/nafa.81.0001.

[101] P. L. Flint, M. R. Petersen, and J. Barry Grand. Exposure of Spectacled Eiders and other diving ducks to lead in western Alaska. *Canadian Journal of Zoology*, 75(3):439–443, 1997. doi:10.1139/z97-054.

[102] N. R. Foster. *Intertidal bivalves: a guide to the common marine bivalves of Alaska*. University of Alaska Press, Fairbanks, Alaska, USA, 1991. ISBN: 0-912006-49-8.

[103] A. Freiwald. Microbial maceration and carbonate dissolution on cold-temperate shelves. *Historical Biology*, 13(1):27–35, 1998. doi:10.1080/08912969809386570.

[104] K. E. Frey, G. W. K. Moore, L.W. Cooper, and J. M. Grebmeier. Divergent patterns of recent sea ice cover across the Bering, Chukchi, and Beaufort seas of the Pacific Arctic Region. *Progress in Oceanography*, 136:32–49, August 2015. doi:10.1016/j.pocean.2015.05.009.

[105] I. Gallmetzer, A. Haselmair, A. Tomašových, M. Stachowitsch, and M. Zuschin. Responses of molluscan communities to centuries of human impact in the northern Adriatic Sea. *PLOS ONE*, 12(7):e0180820, 2017. doi:10.1371/journal.pone.0180820.

[106] J. Garlich-Miller, J. G. MacCracken, J. Snyder, R. Meehan, M. Myers, J. M. Wilder, E. Lance, and A. Matz. Status review of the Pacific walrus (Odobenus rosmarus divergens). Technical report, U.S . Fish and Wildlife Service, Marine Mammals Management, Anchorage, AK, 2011. url: https://www.fishgame.state.ak.us/static/species/specialstatus/pdfs/walrus_2011_status_review.pdf.

[107] J. L. Garlich-Miller, L. T. Quakenbush, and J. F. Bromaghin. Trends in age structure andd productivity of pacific walruses harvested in the bering strait region of alaska, 1952-2002. *Marine Mammal Science*, 22(4):880–896, 2006. doi:10.1111/j.1748-7692.2006.00081.x.

[108] J.-P. Gattuso and L. Hansson. *Ocean Acidification*. OUP Oxford, September 2011. ISBN: 978-0-19-959109-1.

[109] E. Gilad, S. M. Kidwell, Y. Benayahu, and Y. Edelman-Furstenberg. Unrecognized loss of seagrass communities based on molluscan death assemblages: historic baseline shift in tropical Gulf of Aqaba, Red Sea. *Marine Ecology Progress Series*, 589:73–83, 2018. doi:10.3354/meps12492.

[110] C. P Glover and S. M Kidwell. Influence of organic matrix on the post-mortem destruction of molluscan shells. *The Journal of Geology*, 101(6):729–747, 1993. doi:10.1086/648271.

[111] C. L. Goethel, J. M. Grebmeier, and L.W. Cooper. Changes in abundance and biomass of the bivalve Macoma calcarea in the northern Bering Sea and the southeastern Chukchi Sea from 1998 to 2014, tracked through dynamic factor analysis models. *Deep Sea Research Part II: Topical Studies in Oceanography*, 162:127–136, April 2019. doi:10.1016/j.dsr2.2018.10.007.

[112] C. L. Goethel, J. M. Grebmeier, L.W. Cooper, and T.J. Miller. Implications of ocean acidification in the Pacific Arctic: Experimental responses of three Arctic bivalves to decreased pH and food availability. *Deep Sea Research Part II: Topical Studies in Oceanography*, 144:112–124, 2017. doi:10.1016/j.dsr2.2017.08.013.

[113] G. Goodfriend, J. Brigham-Grette, and G. Miller. Enhanced Age Resolution of the Marine Quaternary Record in the Arctic Using Aspartic Acid Racemization Dating of Bivalve Shells. *Quaternary Research*, 45(2):176–187, 1996. doi:10.1006/qres.1996.0018.

[114] C. S. Gorbics, J. L. Garlich-Miller, and S. L. Schliebe. Draft Alaska Marine Mammal Stock Assessments, 1998, Sea Otters, Polar Bear and Walrus. Technical report, US Fish and Wildlife Service, Alaska Region, Marine Mammals Management, Anchorage, AK, 1998. url: https://ecos.fws.gov/ServCat/DownloadFile/110010?Reference=69827.

[115] S. Gordillo and A. E. Aitken. Palaeoenvironmental interpretation of Late Quaternary marine molluscan assemblages, Canadian Arctic Archipelago. *Géographie physique et Quaternaire*, 54(3):301–315, 2000. doi:10.7202/005650ar.

[116] C. H. Graham, S. Ferrier, F. Huettman, C. Moritz, and A. T. Peterson. New developments in museum-based informatics and applications in biodiversity analysis. *Trends in Ecology & Evolution*, 19(9):497–503, September 2004. doi:10.1016/j.tree.2004.07.006.

[117] J. B. Grand, P. L. Flint, M. R. Petersen, and Christine L. Moran. Effect of Lead Poisoning on Spectacled Eider Survival Rates. *The Journal of Wildlife Management*, 62(3):1103–1109, 1998. doi:10.2307/3802564.

[118] J. M. Grebmeier. *The ecology of benthic carbon cycling in the northern Bering and Chukchi Seas*. Thesis, University of Alaska, Fairbanks, 1987. url: http://hdl.handle.net/11122/5222.

[119] J. M Grebmeier. Shifting patterns of life in the Pacific Arctic and sub-Arctic seas. *Annual Reviews in Marine Science*, 4:63–78, 2012. doi:10.1146/annurev-marine-120710-100926.

[120] J. M. Grebmeier, B. A. Bluhm, Lee W. Cooper, Stanislav G. Denisenko, Katrin Iken, x, M. dra, and Carlos Serratos. Time-Series benthic community composition and biomass and associated environmental characteristics in the Chukchi Sea during the RUSALCA 2004 - 2012 Program. *Oceanography*, 28(3):116–133, 2015. doi:10.5670/oceanog.2015.61.

[121] J. M. Grebmeier, B. A. Bluhm, L.W. Cooper, S. L. Danielson, K. R. Arrigo, A. L. Blanchard, J. T. Clarke, R. H. Day, K. E. Frey, R. R. Gradinger, M. Kędra, B. Konar, Kathy J. Kuletz, Sang H. L., J. R. Lovvorn, B. L. Norcross, and S. R. Okkonen. Ecosystem characteristics and processes facilitating persistent macrobenthic biomass hotspots and associated benthivory in the Pacific Arctic. *Progress in Oceanography*, 136:92–114, 2015. doi:10.1016/j.pocean.2015.05.006.

[122] J. M. Grebmeier and L. Cooper. PacMARS Surface Sediment Parameters (1970-2012). Technical report, Earth Observing Laboratory Data Archive, NCAR, UCAR, 2016. doi:10.5065/D6416V3G.

[123] J. M. Grebmeier and L. W. Cooper. The Saint Lawrence Island Polynya: A 25-year evaluation of an analogue for climate change in polar regions. In *Aquatic Microbial Ecology and Biogeochemistry: A Dual Perspective*, pages 171–183. Springer, Cham, 2016. doi:10.1007/978-3-319-30259-1_14.

[124] J. M. Grebmeier, L. W. Cooper, C. J Ashjian, B. A. Bluhm, R.B. Campbell, K. H. Dunton, J. Moore, S. R. Okkonen, G. Sheffield, J. Trefry, and S.Y. Pasternak. Pacific Marine Arctic Regional Synthesis (PacMARS) Final Report. Final Report, North Pacific Research Board, Washington, DC, USA, 2015.

[125] J. M. Grebmeier and L.W. Cooper. Benthic macroinfaunal samples collected from the Canadian Coast Guard Ship (CCGS) Sir Wilfrid Laurier, Northern Bering Sea to Chukchi Sea, 2014. Technical report, Arctic Data Center, 2018. doi: 10.18739/A2KK94B8Q.

[126] J. M. Grebmeier and L.W. Cooper. SWL13 Sediment parameters. Technical report, Arctic Data Center, 2018. doi:10.5065/D63X84PT.

[127] J. M. Grebmeier and L.W. Cooper. *SWL14 Sediment parameters*. Arctic Data Center, 2018. doi:10.5065/D6M043GJ.

[128] J. M. Grebmeier, L.W. Cooper, H. M. Feder, and B. I. Sirenko. Ecosystem dynamics of the Pacific-influenced Northern Bering and Chukchi Seas in the Amerasian Arctic. *Progress in Oceanography*, 71(2-4):331–361, 2006. doi:10.1016/j.pocean.2006.10.001.

[129] J. M Grebmeier and K. H Dunton. Benthic processes in the northern Bering/Chukchi seas: status and global change. Technical report, Marine Mammal Commision, Bethesda, MD, USA, 2000. url: https://www.mmc.gov/wp-content/uploads/seaicereport.pdfpage=82.

[130] J. M. Grebmeier, H. M. Feder, and C. P. McRoy. Pelagic-benthic coupling on the shelf of the northern Bering and Chukchi Seas. II. Benthic community structure. *Marine Ecology Progress Series*, 51:253–268, 1989. doi:10.3354/meps051253.

[131] J. M. Grebmeier, K. E. Frey, L.W. Cooper, and M. Kędra. Trends in Benthic Macrofaunal Populations, Seasonal Sea Ice Persistence, and Bottom Water Temperatures in the Bering Strait Region. *Oceanography*, 31(2):136–151, 2018. issn: 1042-8275. url: https://www.jstor.org/stable/26542660.

[132] J. M Grebmeier, C P. McRoy, and H. M Feder. Pelagic-benthic coupling on the shelf of the northern Bering and Chukchi Seas. I. Food supply source and benthic biomass. *Marine Ecology Progress Series*, 48:57–67, 1988. doi:10.3354/meps048057.

[133] J. M. Grebmeier, J. E. Overland, S. E. Moore, . Farley, Ed V, Eddy C. Carmack, L.W. Cooper, K. E. Frey, J. H. Helle, Fiona A. McLaughlin, and S. Lyn McNutt. A Major Ecosystem Shift in the Northern Bering Sea. *Science*, 311(5766):1461–1464, 2006. doi:10.1126/science.1121365.

[134] E. M. Harper. Are calcitic layers an effective adaptation against shell dissolution in the Bivalvia? *Journal of Zoology*, 251(2):179–186, 2000. doi:doi:10.1111/j.1469-7998.2000.tb00602.x.

[135] I. Hartwell, T. Lomax, D. A. Dasher, M. K. Hoberg, A. L. Blanchard, and S. Jewett. Characterization of Benthic Habitats and Contaminant Assessment i n Arctic Lagoons and Estuaries. Technical Report NOAA Technical Memorandum NOS NCCOS 253, National Oceanic and Atmospheric Administration, 2018. doi: 10.25923/a46e-tm48.

[136] M. A. Healy, S. B. McLenegan, and C. H. Townsend. *Report of the cruise of the Revenue Marine Steamer Corwin in the Arctic Ocean in the year 1885*. Government Printing Office, Washington, DC, USA, 1887. url: https://www.biodiversitylibrary.org/item/87301.

[137] M. A. Healy, S. B. McLenegan, and H. W. Yemans. *Report of the cruise of the Revenue Marine Steamer Corwin in the Arctic Ocean in the year 1884*. Government Printing Office, Washington, DC, USA, 1889. url: https://www.biodiversitylibrary.org/item/66306.

[138] E. Herder, B. Misiuk, E. Edinger, and A. Aitken. *Assessing spatial and temporal changes in benthic biodiversity over 59 years in Frosisher Bay*. Arctic Change 2017, Quebec City, Canada, 2017. url: http://www.arcticnetmeetings.ca/index.php?url=13217.

[139] E. Hill. The Historical Ecology of Walrus Exploitation in the North Pacific. In Todd J Braje and Torben C Rick, editors, *Human Impacts on Seals, Sea Lions, and Sea Otters: Integrating Archaeology and Ecology in the Northeast Pacific*, pages 41–64. University of California Press, California, USA, 2011. doi:10.1525/california/9780520267268.003.0003.

[140] J. I. Hodges and W. D. Eldridge. Aerial surveys of eiders and other waterbirds on the eastern Arctic coast of Russia. *Windfowl*, 52:127–142, 2001.

[141] B. W. Hoeksema, J. van der Land, S. E. T. van der Meij, L. P. van Ofwegen, B. T. Reijnen, R. W. M. van Soest, and N. J. de Voogd. Unforeseen importance of historical collections as baselines to determine biotic change of coral reefs: the Saba Bank case. *Marine Ecology*, 32(2):135–141, 2011. doi:10.1111/j.1439-0485.2011.00434.x.

[142] L. H. Hyman. Distribution and Ecology of the Marine Invertebrates of Point Barrow, Alaska. G. E. MacGinitie. *The Quarterly Review of Biology*, 32(4):381–381, 1957. doi:10.1086/402006.

[143] S. T. Jackson, J. L. Betancourt, R. K. Booth, and S. T. Gray. Ecology and the ratchet of events: Climate variability, niche dimensions, and species distributions. *Proceedings of the National Academy of Sciences*, 106(Supplement 2):19685, 2009. doi:10.1073/pnas.0901644106.

[144] C. V. Jay, J. M. Grebmeier, A. S. Fischbach, T. L. McDonald, L. W. Cooper, and F. Hornsby. Pacific Walrus (Odobenus rosmarus divergens) Resource Selection in the Northern Bering Sea. *PLOS ONE*, 9(4):e93035, 2014. doi:10.1371/journal.pone.0093035.

[145] C. V. Jay, B. G. M.t, and D. C. Douglas. Projected status of the Pacific walrus (Odobenus rosmarus divergens) in the twenty-first century. *Polar Biology*, 34(7):1065–1084, 2011. doi:10.1007/s00300-011-0967-4.

[146] S. Jewett, T. Lomax, B. Holladay, P. Rivera, H. Chenelot, N. R. Foster, M. K. Hoberg, R. Clark, A. Stephens, and T. Obritschkewtsch. Cruise Report AKMAP Chukchi Sea Ledyard Bay 2010Coastal Impact Assistance Program AssessmentAugust 21 –September 4, 2010R/V Norseman II. Technical report, Alaska Department of Environmental Conservation, 2010. url: https://dec.alaska.gov/water/water-quality/monitoring/surveys/.

[147] L.-Q. Jiang, R. A. Feely, B. R. Carter, D. J. Greeley, D. K. Gledhill, and K. M. Arzayus. Climatological distribution of aragonite saturation state in the global oceans. *Global Biogeochemical Cycles*, 29(10):1656–1673, 2015. doi:10.1002/2015GB005198.

[148] O. M. Johannessen, L. Bengtsson, M. W. Miles, S. I. Kuzmina, V. A. Semenov, G. V. Alekseev, A. P. Nagurnyi, V. F. Zakharov, L. P. Bobylev, L. H. Pettersson, K. Hasselmann, and H. P. Cattle. Arctic climate change: observed and modelled temperature and sea-ice variability. *Tellus A*, 56(4):328–341, 2004. doi:10.1111/j.1600-0870.2004.00060.x.

[149] K. G. Johnson, S. J. Brooks, P. B. Fenberg, A. G. Glover, K. E. J., A. M. Lister, E. Michel, M. Spencer, J. A. Todd, E. Valsami-Jones, J. R. Young, and J. R. Stewart. Climate Change and Biosphere Response: Unlocking the Collections Vault. *BioScience*, 61(2):147–153, February 2011. doi:10.1525/bio.2011.61.2.10.

[150] K. R. Johnson and C. H. Nelson. Side-Scan Sonar Assessment of Gray Whale Feeding in the Bering Sea. *Science*, 225(4667):1150, 1984. doi:10.1126/science.225.4667.1150.

[151] R. T. Jones. *Empire of Extinction: Russians and the North Pacific's Strange Beasts of the Sea, 1741-1867*. Oxford University Press, USA, 2014. doi:10.1093/acprof:oso/9780199343416.001.0001.

[152] R. A. Kastelein, N. M. Schooneman, and P. R. Wiepkema. Food consumption and body weight of captive Pacific walruses (Odobenus rosmarus divergens). *Aquatic Mammals*, 26(3):175–190, 2000. url: https://aquaticmammalsjournal.org/share/AquaticMammalsIssueArchives/2000/AquaticMammals_26-03/26-03_Kastelein.pdf.

[153] D. S. Kaufman. Temperature sensitivity of aspartic and glutamic acid racemization in the foraminifera *Pulleniatina*. *Quaternary Geochronology*, 1(3):188–207, 2006. doi:10.1016/j.quageo.2006.06.008.

[154] D. S. Kaufman, L. Polyak, R. Adler, J. E. T. Channell, and C. Xuan. Dating late Quaternary planktonic foraminifer Neogloboquadrina pachyderma from the Arctic Ocean using amino acid racemization. *Paleoceanography*, 23:PA3224, 2008. doi:10.1029/2008PA001618.

[155] M. Kędra, L.W. Cooper, M. Zhang, D. Biasatti, and J. M. Grebmeier. Benthic trophic sensitivity to on-going changes in Pacific Arctic seasonal sea ice cover–Insights from the nitrogen isotopic composition of amino acids. *Deep Sea Research Part II: Topical Studies in Oceanography*, 162:137–151, 2019. doi:10.1016/j.dsr2.2019.01.002.

[156] M. Kędra and B. Oleszczuki. *Pacific Arctic Benthic Species*, volume 2017. 2017. url: http://www.iopan.gda.pl/projects/DBO/.

[157] S. M Kidwell. Preservation of species abundance in marine death assemblages. *Science*, 294(5544):1091–1094, 2001. doi:10.1126/science.1064539.

[158] S. M. Kidwell. Mesh-size effects on the ecological fidelity of death assemblages: a meta-analysis of molluscan live–dead studies. *Geobios*, 35:107–119, 2002. doi:10.1016/S0016-6995(02)00052-9.

[159] S. M. Kidwell. Shell Composition Has No Net Impact on Large-Scale Evolutionary Patterns in Mollusks. *Science*, 307(5711):914, 2005. doi:10.1126/science.1106654.

[160] S. M. Kidwell. Discordance between living and death assemblages as evidence for anthropogenic ecological change. *Proceedings of the National Academy of Sciences*, 104(45):17701–17706, 2007. doi:10.1073 pnas.0707194104.

[161] S. M. Kidwell. Time-averaging and fidelity of modern death assemblages: building a taphonomic foundation for conservation palaeobiology. *Palaeontology*, 56(3):487–522, 2013. doi:10.1111/pala.12042.

[162] S. M Kidwell and D. W. J. Bosence. Taphonomy and time-averaging of marine shelly faunas. In PA Allison and DEG Briggs, editors, *Taphonomy: Releasing the data locked in the fossil record*, volume 9 of *Topics in Geobiology*, pages 115–209. Plenum Press, New York, USA, 1991. ISBN: 978-1-4899-5036-9 978-1-4899-5034-5.

[163] S. M. Kidwell, C.A. Meadows, and Y. Edelman-Furstenberg. Early Diagenetic Microstructural Alteration Relevant to Prolonged Residence of Bivalve Aragonite in the Mixed Layers of Tropical and Temperate Shelves. American Geophysical Union annual Meeting, Washington, DC, USA, 2018.

[164] S. M. Kidwell and A. Tomašových. Implications of Time-Averaged Death Assemblages for Ecology and Conservation Biology. *Annual Review of Ecology, Evolution, and Systematics*, 44(1):539–563, 2013. doi:10.1146/annurev-ecolsys-110512-135838.

[165] E. M. Kindle. The section at Cape Thompson, Alaska. *American Journal of Science*, 28(168):520–528, 1909. doi:10.2475/ajs.s4-28.168.520.

[166] E. M. Kindle. Observations on ice-borne sediments by the Canadian and other arctic expeditions. *American Journal of Science*, 7(40):251–286, 1924. doi:10.2475/ajs.s5-7.40.251.

[167] A. A. Kistchinski and V. E. Flint. On the biology of the spectacled eider. *Wildfowl*, 25(25):5–15, 1974.

[168] C. Wegner Koch, L.W. Cooper, C. Lalande, T. A. Brown, K. E. Frey, and J. M. Grebmeier. Seasonal and latitudinal variations in sea ice algae deposition in the Northern Bering and Chukchi Seas determined by algal biomarkers. *PLOS ONE*, 15(4):e0231178, April 2020. doi:10.1371/journal.pone.0231178.

[169] M. A. Kosnik, Q. Hua, and Wust R. A. Kaufman, D. S. Taphonomic bias and time-averaging in tropical molluscan deathassemblages: differential shell half-lives in Great Barrier Reef sediment. *Paleobiology*, 35(4):565–586, 2009. doi:10.1666/0094-8373-35.4.565.

[170] M. A. Kosnik and D. S. Kaufman. Identifying outliers and assessing the accuracy of amino acid racemization measurements for geochronology: II. Data screening. *Quaternary Geochronology*, 3(4):328–341, 2008. doi:10.1016/j.quageo.2008.04.001.

[171] M. Kowalewski, S. Casebolt, Q. Hua, K. E. Whitacre, D. S. Kaufman, and M. A. Kosnik. One fossil record, multiple time resolutions: Disparate time-averaging of echinoids and mollusks on a Holocene carbonate platform. *Geology*, 46(1):51–54, 2018. doi:10.1130/g39789.1.

[172] M. Kowalewski and A. P Hoffmeister. Sieves and fossils: Effects of mesh size on paleontological patterns. *Palaios*, 18(4-5):460–469, 2003. doi:10.1669/0883-1351(2003)018<0460:SAFEOM>2.0.CO;2.

[173] A. Krause. *Journey to the Tlingits by Aurel and Arthur Krause, 1881/82*. Haines Centennial Commission], Haines, Alaska, 1981. url: http://pi.lib.uchicago.edu/1001/cat/bib/523569.

[174] R. Krause, S. Barbour, M. Kowalewski, D. Kaufman, C. Romanek, M. Simões, and J. Wehmiller. Quantitative comparisons and models of time-averaging in bivalve and brachiopod shell accumulations. *Paleobiolgy*, 36(3):428–452, 2010. doi:10.1666/08072.1.

[175] L. Krishtalka and P. S. Humphrey. Can Natural History Museums Capture the Future? *BioScience*, 50(7):611–617, July 2000. doi:10.1641/0006-3568(2000)050[0611:CNHMCT]2.0.CO;2.

[176] I. Krupnik and G. C. Ray. Pacific walruses, indigenous hunters, and climate change: Bridging scientific and indigenous knowledge. *Deep Sea Research Part II: Topical Studies in Oceanography*, 54(23):2946–2957, 2007. doi:https://doi.org/10.1016/j.dsr2.2007.08.011.

[177] E. C. LaFond, R. S. Dietz, and D. W. Pritchard. Oceanographic measurements from the USS Nereus on a cruise to the Bering and Chukchi seas, 1947. NEL Report 91, U.S. Navy Electronics Laboratory, Research Division, San Diego, Calif., 1949. doi: 10.5962/bhl.title.46751.

[178] W. Larned, K. Bollinger, and R. Stehn. Late winter population and distribution of spectacled eiders (Somateria fischeri) in the Bering Sea 2009 & 2010. Project Report 820, US Department of Commerce, National Oceanic andAtmospheric Administration, as recommended by The North Pacific Research Board, Washington, DC, USA, 2012. url: https://www.fws.gov/r7/mbsp/mbm/waterfowl/surveys/pdf/spei_surveys_2009-10_report.pdf.

[179] C. R. Lawson, Y. Vindenes, L. Bailey, and M. van de Pol. Environmental variation and population responses to global change. *Ecol Lett*, 18(7):724–36, 2015. doi:10.1111/ele.12437.

[180] A. M. Lister. Natural history collections as sources of long-term datasets. *Trends in Ecology & Evolution*, 26(4):153–154, April 2011. doi:10.1016/j.tree.2010.12.009.

[181] J. R. Lovvorn, L.W. Cooper, L. Brooks, M, C. C. De Ruyck, J. K. Bump, and J. M. Grebmeier. Organic matter pathways to zooplankton and benthos under pack ice in late winter and open water in late summer in the north-central Bering Sea. *Marine Ecology Progress Series*, 291:135–150, April 2005. doi:10.3354/meps291135.

[182] J. R. Lovvorn, J. M. Grebmeier, L.W. Cooper, J. K. Bump, and Samantha E. Richman. Modeling marine protected areas for threatened eiders in a climatically changing Bering Sea. *Ecological Applications*, 19(6):1596–1613, 2009. doi:10.1890/08-1193.1.

[183] J. R. Lovvorn, C. A. North, J. M. Grebmeier, L. W. Cooper, and Jason M. Kolts. Sediment organic carbon integrates changing environmental conditions to predict benthic assemblages in

shallow Arctic seas. *Aquatic Conservation: Marine and Freshwater Ecosystems*, 28(4):861–871, 2018. doi:10.1002/aqc.2906.

[184] J. R. Lovvorn, C. A. North, Jason M. Kolts, J. M. Grebmeier, L.W. Cooper, and Xuehua Cui. Projecting the effects of climate-driven changes in organic matter supply on benthic food webs in the northern Bering Sea. *Marine Ecology Progress Series*, 548:11–30, April 2016. doi:10.3354/meps11651.

[185] J. R. Lovvorn, M. F. Raisbeck, L. W. Cooper, G. A. Cutter, M. W. Miller, M. L. Brooks, J. M. Grebmeier, A. C. Matz, and C. M. Schaefer. Wintering eiders acquire exceptional Se and Cd burdens in the Bering Sea: physiological and oceanographic factors. *Marine Ecology Progress Series*, 489:245–261, 2013. doi:10.3354/meps10439.

[186] J. R. Lovvorn, Samantha E. Richman, J. M. Grebmeier, and L.W. Cooper. Diet and body condition of spectacled eiders wintering in pack ice of the Bering Sea. *Polar Biology*, 26(4):259–267, 2003. doi:10.1007/s00300-003-0477-0.

[187] J. R. Lovvorn, J. J. Wilson, D. McKay, J. K. Bump, L.W. Cooper, and J. M. Grebmeier. Walruses Attack Spectacled Eiders Wintering in Pack Ice of the Bering Sea. *Arctic*, 63(1):53–56, 2010. url: http://www.jstor.org/stable/40513369.

[188] L. F. Lowry and F. H. Fay. Seal eating by walruses in the Bering and Chukchi Seas. *Polar Biology*, 3(1):11–18, 1984. doi:10.1007/BF00265562.

[189] L. F. Lowry, K. J. Frost, and J. J. Burns. Feeding of Bearded Seals in the Bering and Chukchi Seas and Trophic Interaction with Pacific Walruses. *Arctic*, 33(2):330–342, 1980. url: http://www.jstor.org/stable/40509032.

[190] J. L. Lozán, H. Grassl, and P. Hupfer. *Climate of the 21st Century: Changes and Risks : Scientific Facts*. Wissenschaftliche Auswertungen, 1998. ISBN: 978-3-00-002925-7.

[191] J. MacCracken, W. Beatty, J. Garlich-Miller, M. Kissling, and J. Snyder. Final species status assessment for the pacific walrus (*Odobenus rosmarus divergens*), May 2017 (Version 1.0). Technical report, U.S . Fish and Wildlife Service, Marine Mammals Management, Anchorage, AK, 2017. doi:10.13140/RG.2.2.29363.12325.

[192] J. G. MacCracken. Pacific Walrus and climate change: observations and predictions. *Ecology and Evolution*, 2(8):2072–2090, 2012. doi:10.1002/ece3.317.

[193] Nettie Macginitie. Marine Mollusca of Point Barrow, Alaska. *Proceedings of the United States National Museum.*, 109(3412):59–208, 1959. doi:10.5479/si.00963801.109-3412.59.

[194] B. Malkin. New records of Arachnida from Alaska. *The Pan-Pacific Entomologist*, 29:205–206, 1953. url: https://www.biodiversitylibrary.org/page/53425696page/235/mode/1up.

[195] J. M. Maniscalco, A. M. Springer, K. L. Counihan, T. Hollmen, H. M. Aderman, and M. Toyukak Sr. Contemporary diets of walruses in Bristol Bay, Alaska suggest temporal variability in benthic community structure. *PeerJ*, 8:e8735, 2020. doi:10.7717/peerj.8735.

[196] A. Mann and P. L. Ricker. Report on the diatoms of the Albatross voyages in the Pacific Ocean, 1888-1904. In *Systematic investigations in phanerogams, ferns, and diatoms*, Contributions from the United States National Herbarium, pages 221–442. US Government Printing Office, 1907. url: https://repository.si.edu/handle/10088/27168.

[197] R. Mann, D. M. Munroe, E. N. Powell, E. E. Hofmann, and J. M. Klinck. Bivalve Molluscs: Barometers of Climate Change in Arctic Marine Systems. In F. J. Mueter, D. M. S. Dickson, H. R. Huntington, J. R. Irvine, E. A. Logerwell, S. A. MacLean, L. T. Quakenbush, and C. Rosa, editors, *Responses of Arctic Marine Ecosystems to Climate Change*, pages 61–82. Alaska Sea Grant, University of Alaska Fairbanks, Fairbanks, Alaska, USA, 2013. doi:10.4027/ramecc.2013.04.

[198] C. R. Marshall, S. Finnegan, E. C. Clites, P. A. Holroyd, N. Bonuso, C. Cortez, E. Davis, G. P. Dietl, P. S. Druckenmiller, R. C. Eng, C. Garcia, K. Estes-Smargiassi, A. Hendy, K. A. Hollis, H. Little, E. A. Nesbitt, P. Roopnarine, L. Skibinski, J. Vendetti, and L. D. White. Quantifying the dark data in museum fossil collections as palaeontology undergoes a second digital revolution. *Royal Society: Biology Letters*, 14(9):20180431, September 2018. doi:10.1098/rsbl.2018.0431.

[199] J. T. Mathis. Seasonal observations of carbonate chemistry and ocean acidification in 2010. Technical report, ConocoPhillips Company, Shell Exploration & Production Company, and Statoil USA E & P, Inc, Anchorage, AK, 2011. url: https://pdfs.semanticscholar.org/c2e5/f295a3184e5960c1c9f9e0b2021ec827ed61.pdf.

[200] J. T. Mathis, J. N. Cross, and N. R. Bates. The role of ocean acidification in systemic carbonate mineral suppression in the Bering Sea. *Geophysical Research Letters*, 38:L19602, 2011. doi:10.1029/2011GL048884.

[201] J. T Mathis, J. N. Cross, W. Evans, and S. C Doney. Ocean acidification in the surface waters of the Pacific-Arctic boundary regions. *Oceanography*, 28(2):122–135, 2015. doi:10.5670/oceanog.2015.36.

[202] J. T Mathis, J. M Grebmeier, D. A Hansell, R. R Hopcroft, D. L Kirchman, Sang H L., S Bradley Moran, N. R Bates, S. VanLaningham, and J. N. Cross. Carbon biogeochemistry of the western Arctic: Primary production, carbon export and the controls on ocean acidification. In J. M. Grebmeier and W. Maslowski, editors, *The Pacific Arctic Region: Ecosystem Status and Trends in a Rapidly Changing Environment*, pages 223–268. Springer, Springer Netherlands, Dordrecht, Netherlands, 2014. doi: 10.1007/978-94-017-8863-2_9.

[203] J. T. Mathis and J. M. Questel. Assessing seasonal changes in carbonate parameters across small spatial gradients in the Northeastern Chukchi Sea. *Continental Shelf Research*, 67:42–51, 2013. doi:10.1016/j.csr.2013.04.041.

[204] P. A. McLaughlin. Survey of the benthic invertebrate fauna of the eastern Bering Sea. Special Scientific Report-Fisheries 401, US Department of the Interior, Fish and Wildlife Service, Washington, DC, USA, 1963. url: https://spo.nmfs.noaa.gov/content/survey-benthic-invertebrate-fauna-eastern-bering-sea.

[205] R. McNeely, A. S. Dyke, and J. R. Southon. Canadian Marine Reservoir Ages Preliminary Data Assessment. Technical Report Open File 5049, Natural Resources Canada, Geological Survey of Canada, 2006. doi:10.4095/221564.

[206] C. P. McRoy. Benthic taxonomy and benthic biomass data collected by the R/V Alpha Helix in support of the ISHTAR Project in the Bering and Chukchi Seas, 1984-1990 (NCEI Accession 0000085). Dataset NCEI Accession 0000085, University of Alaska, Institude of Marine Science (IMS/UAF), 2010. Last Modified: 2020-09-02.

[207] C.A Meadows. Estimating fossil biomass from skeletal mass in marine invertebrates. *Lethaia*, 52(3):323–334, 2019. doi:10.1111/let.12314.

[208] C.A Meadows, J. M. Grebmeier, and S. M. Kidwell. High-latitude benthic bivalve biomass and recent climate change: testing the power of live-dead discordance in the Pacific Arctic. *Deep Sea Research Part II: Topical Studies in Oceanography*, 162:152–163, 2019. doi:10.1016/j.dsr2.2019.04.005.

[209] C.A. Meadows, S. M. Kidwell, and D. S. Kaufman. The fate of cold-water carbonate: the scale of time averaging of molluscan aragonite on the productive Alaskan Arctic shelf. American Geophysical Union, Fall Meeting, San Francisco, CA, USA, 2019. url: https://agu.confex.com/agu/fm19/meetingapp.cgi/Paper/518712.

[210] T. E. Merrill. The status of Pacific Walrus (Odebenus rosmarus divergens) foraging habitat and diet around St. Lawrence Island. Master's thesis, University of Alaska, Fairbanks, Fairbanks, Alaska, USA, 2008. url: http://hdl.handle.net/11122/80.

[211] A. T. von Middendorf. *Reise in den aussersten Norden und Osten Sibiriens wahrend der Jahre 1843 und 1844 mit allerhochster Genehmigung auf Veranstaltung der Kaiserlichen Akademie der Wissenschaften zu St. Petersburg ausgefuhrt und in Verbindung mit vielen Gelehrten herausgegeben*. Buchdruckerei der Kaiserlichen Akademie der Wissenschaften, St. Petersburg, 1847. url: http:////catalog.hathitrust.org/Record/008886886.

[212] H. Middleton, C. De Nesselrode, and P. De Poletica. Convention Between the United States and Russia, 1825, 1825. url: http://www.explorenorth.com/library/history/blrusus1825.htm.

[213] G. H. Miller, D. S. Kaufman, and S. J. Clarke. AMINO ACID DATING. In S. A. Elias and Cary J. Mock, editors, *Encyclopedia of Quaternary Science (Second Edition)*, pages 37–48. Elsevier, Amsterdam, January 2013. doi:10.1016/B978-0-444-53643-3.00054-6.

[214] D. Mitchell. *Sold American: The Story of Alaska Natives and Their Land, 1867-1959 : the Army to Statehood*. Dartmouth College, 1997. ISBN: 0874517486.

[215] S. E. Moore and J. M. Grebmeier. The Distributed Biological Observatory: Linking Physics to Biology in the Pacific Arctic Region + Supplementary File (See Article Tools). *Arctic*, 71(5):1–7, 2018. doi:10.14430/arctic4606.

[216] A Mucci, B Sundby, M Gehlen, T Arakaki, S Zhong, and N Silverberg. The fate of carbon in continental shelf sediments of eastern Canada: a case study. *Deep Sea Research Part II: Topical Studies in Oceanography*, 47(3):733–760, April 2000. doi:10.1016/S0967-0645(99)00124-1.

[217] J. Muir. *The Cruise of the Corwin: Journal of the Arctic Expedition of 1881 in search of De Long and the Jeannette*. Houghton Mifflin, 1917. url: https://www.wdl.org/en/item/17365/.

[218] D. M. Munroe, E. N. Powell, R. Mann, J. M. Klinck, and E. E. Hofmann. Underestimation of primary productivity on continental shelves: evidence from maximum size of extant surfclam(Spisula solidissima)populations. *Fisheries Oceanography*, 22(3):220–233, 2013. doi:10.1111/fog.12016.

[219] M.D. Nascimento Ritter, F. Erthal, M. A. Kosnik, J. C. Coimbra, and D.C. Kaufman. Spatial variation in the temporal resolution of subtropical shallow-water molluscan death assemblages. *PALAIOS*, 32(9):572–583, 2017. doi:10.2110/palo.2017.003.

[220] C.-M. Naske. *Alaska: A history of the 49th state*. University of Oklahoma Press, 2 edition, 1987. ISBN: 0-8061-2573-X. url: https://books.google.com/books/about /Alaska_a_History_of_the_49th_State.html?id=TGADkAEACAAJ.

[221] C. H. Nelson, R. L. Philips, J. McRea, Jr, J. H. Barber, Jr, M. W. Mclaughlin, and J. L. Chin. Gray whale and Pacific walrus benthic feeding grounds and sea floor interaction in the Chukchi Sea. Technical Report for Minerals Management Service IA No. 14157, MMS 93-0042, US Department of the Interior, Minerals Management Service, Alaska Outer Continental Shelf Study. MMS 93-0042, Menlo Park, CA, USA, 1994. url: https://catalog.hathitrust.org/Record/008348879.

[222] E. W. Nelson, T. H. Bean, W. H. Edwards, H. W. Henshaw, and F. W. True. *Report upon natural history collections made in Alaska between the years 1877 and 1881*. Govt. Print. Off., Washington, 1887. url: https://www.biodiversitylibrary.org/item/114479.

[223] R. J. Nelson, C. J. Ashjian, B. A. Bluhm, K. E. Conlan, R. R. Gradinger, J. M. Grebmeier, V. J. Hill, R. R. Hopcroft, B. P. V. Hunt, H. M. Joo, D. L. Kirchman, K. N. Kosobokova, S. H. L., W. K. W. Li, C. Lovejoy, M. Poulin, E. Sherr, and K. V. Young. Biodiversity and Biogeography of the Lower Trophic Taxa of the Pacific Arctic Region: Sensitivities to Climate Change. In J. M. Grebmeier and W. Maslowski, editors, *The Pacific Arctic Region: Ecosystem Status and Trends in a Rapidly Changing Environment*, pages 269–336. Springer, Springer Netherlands, Dordrecht, Netherlands, 2014. doi: 10.1007/978-94-017-8863-2_10.

[224] J. K. Nielsen. Taphonomy in the light of intrinsic shell properties and life habits: marine bivalves from the Eemian of northern Russia. *Paläontologische Zeitschrift*, 78(1):53–72, 2004. doi:10.1007/BF03009130.

[225] H. C Nilsson and R. Rosenberg. Succession in marine benthic habitats and fauna in response to oxygen deficiency: analysed by sediment profile-imaging and by grab samples. *Marine ecology progress series*, 197:139–149, 2000. doi:10.3354/meps197139.

[226] A. E. Nordenskiöld. *The Voyage of the Vega Round Asia and Europe: With a Historical Review of Previous Journeys Along the North Coast of the Old World*. Cambridge University Press, 1885. doi: 10.1017/CBO9781139235938.

[227] K Oguri, N Harada, and O Tadai. Excess ^{210}Pb and ^{137}Cs concentrations, mass accumulation rates, and sedimentary processes on the Bering Sea continental shelf. *Deep-Sea Research II*, 61-64:193–204, 2012. doi:10.1016/j.dsr2.2011.03.007.

[228] J. Oksanen, R. Kindt, P. Legendre, B. O'Hara, M. H. H. Stevens, M. J. Oksanen, and M. Suggests. The vegan package. *Community ecology package*, 10:631–637, 2007. url: https://cran.r-project.org/web/packages/vegan/.

[229] J. Oliver, P. Slattery, E. F. O'Connor, and L Lowry. Walrus, Odobenus rosmarus, feeding in the Bering Sea: A benthic perspective. *Fishery Bulletin- National Oceanic and Atmospheric Administration*, 81:501–512, 1983. url: https://spo.nmfs.noaa.gov/content/walrus-odobenus-rosmarus-feeding-bering-sea-benthic-perspective.

[230] J.-F. Ouellet, C. Vanpé, and M. Guillemette. The body size-dependent diet composition of north american sea ducks in winter. *PloS one*, 8(6):e65667–e65667, 2013. doi:10.1371/journal.pone.0065667.

[231] S. Paige, W. T. Foran, and J. Gilluly. A reconnaissance of the Point Barrow region, Alaska. Technical Report 772, US Geological Survey, Washington, DC, USA, 1925. doi:10.3133/b772.

[232] J. M. Pearce, D. N. Esler, and A. G. Degtyarev. Nesting ecology of Spectacled Eiders Somateria fischeri on the Indigirka River Delta, Russia. *Wildfowl*, 49:110–123, 1998. url: http://pubs.er.usgs.gov/publication/70020228.

[233] T. Pennant. *Arctic zoology*. CIHM/ICMH Microfiche series = CIHM/ICMH collection de microfiches ;no. 40368. Printed by Henry Hughes, London, 1784. url: http://hdl.handle.net/2027/aeu.ark:/13960/t7br9m47f.

[234] M. R. Petersen, D. C. Douglas, and D. M. Mulcahy. Use of Implanted Satellite Transmitters to Locate Spectacled Eiders at-Sea. *The Condor*, 97(1):276–278, 1995. doi:10.2307/1369006.

[235] M. R. Petersen, W. W. Earned, and D. C. Douglas. At-Sea Distribution of Spectacled Eiders: A 120-Year-Old Mystery Resolved. *The Auk*, 116(4):1009–1020, 1999. doi:10.2307/4089681.

[236] M. R. Petersen, J. B. Grand, and C. P. Dau. *Spectacled Eider (Somateria fischeri), version 2.0*. In The Birds of North America, Cornell Lab of Ornithology, Ithica, NY, USA, 2000. doi:10.2173/bna.547.

[237] M. R. Petersen, J. F. Piatt, and K. A. Trust. Foods of Spectacled Eiders Somateria fischeri in the Bering Sea, Alaska. *Wildfowl*, 49:124–128, 1998. url: http://pubs.er.usgs.gov/publication/70020239.

[238] I. Petroff. *Report on the population, industries, and resources of Alaska*. US Government Printing Office, Washington, DC, USA, 1884. url: https://archive.org/details/reportonpopulati00petruoft.

[239] R. S Pickart and J. M Grebmeier. Distributed Biological Observatory – Northern Chukchi Integrated Study: Healy 1702 Cruise Report. Cruise Report, Woods Hole Oceanographic Institution, Woods Hole, Mass., USA, 2017. url: https://web.whoi.edu/healy-2017/.

[240] D. Piepenburg. Recent research on Arctic benthos: common notions need to be revised. *Polar Biology*, 28(10):733–755, October 2005. doi:10.1007/s00300-005-0013-5.

[241] D. J. Pilcher, D. M. Naiman, J. N. Cross, A. J. Hermann, S. A. Siedlecki, G. A. Gibson, and J. T. Mathis. Modeled Effect of Coastal Biogeochemical Processes, Climate Variability, and Ocean Acidification on Aragonite Saturation State in the Bering Sea. *Frontiers in Marine Science*, 5:508, 2019. doi:10.3389/fmars.2018.00508.

[242] R. Pirtle-Levy. *A Shelf-to-Basin Examination of Food Supply for Arctic Benthic Macrofauna and the Potential Biases of Sampling Methodology*. Thesis, 2006. url; https://trace.tennessee.edu/utk_gradthes/1764.

[243] P. Pischedda, J. C. Poggiale, P. Cuny, and F. Gilbert. Imaging Oxygen Distribution in Marine Sediments. The Importance of Bioturbation and Sediment Heterogeneity. *Acta Biotheor*, 56:123–135, 2008. doi:10.1007/s10441-008-9033-1.

[244] W. F. Ponder, G. A. Carter, P. Flemons, and R. R. Chapman. Evaluation of Museum Collection Data for Use in Biodiversity Assessment. *Conservation Biology*, 15(3):648–657, 2001. doi:10.1046/j.1523-1739.2001.015003648.x.

[245] E. N. Powell, K. M. Kuykendall, and P. Moreno. The death assemblage as a marker for habitat and an indicator of climate change: Georges Bank, surfclams and ocean quahogs. *Continental Shelf Research*, 142:14–31, 2017. doi:10.1016/j.csr.2017.05.008.

[246] E. N Powell and R. Mann. How well do we know the infaunal biomass of the continental shelf? *Continental Shelf Research*, 115:27–32, 2016. doi:10.1016/j.csr.2016.01.001.

[247] E. N. Powell and R. J. Stanton, Jr. Estimating biomass and energy flow of molluscs in palaeo-communities. *Paleontology*, 28(1):1–34, 1985. url: http://go.palass.org/4a9.

[248] G. H. Pyke and P. R. Ehrlich. Biological collections and ecological/environmental research: a review, some observations and a look to the future. *Biological Reviews*, 85(2):247–266, 2010. doi:10.1111/j.1469-185X.2009.00098.x.

[249] D. Qi, L. Q. Liqi Chen, B. S. Chen, Z. Y. Gao, W. L. Zhong, R. A. Feely, L. G. Anderson, H. Sun, J. F. Chen, M. Chen, L. Y. Zhan, Y. H. Zhang, and W. J. Cai. Increase in acidifying water in the western Arctic Ocean. *Nature Climate Change*, 7:195–199, 2017. doi:10.1038/nclimate3228.

[250] J. Rae and year = 1854 McClure, R. J. *The melancholy fate of Sir John Franklin and his party, as disclosed in Dr. Rae"s report; together with the despatches and letters of Captain M'Clure, and other officers employed in the Arctic expeditions*. J. Betts, London :. url: https://www.biodiversitylibrary.org/item/28262.

[251] C. J. Ramsey. Radiocarbon calibration and analysis of stratigraphy: the OxCal program. *Radiocarbon*, 37(2):425–430, 1995. url: https://c14.arch.ox.ac.uk/oxcal.html.

[252] G. C. Ray, J. McCormick-Ray, P. Berg, and H. E. Epstein. Pacific walrus: Benthic bioturbator of Beringia. *Journal of Experimental Marine Biology and Ecology*, 330(1):403–419, 2006. doi:https://doi.org/10.1016/j.jembe.2005.12.043.

[253] P. H. Ray, J. Murdoch, C. V. Riley, A. Gray, W. H. Dall, and C. A. Schott. *Report of the International Polar Expedition to Point Barrow, Alaska: In Response to the Resolution of the [US] House of Representatives of December 11, 1884*, volume 1. US Government Printing Office, Washington, DC, USA, 1885. url: https://www.biodiversitylibrary.org/bibliography/31919/summary.

[254] J. A. Reed, M. G. Sexson, M. M. Smith, J. A. Schmutz, and A. M. Ramey. Evidence for Haemosporidian Parasite Infections in Spectacled Eiders (Somateria fischeri) Sampled in Alaska, USA during the Breeding Season. *Journal of wildlife diseases*, 54(4):877–880, 2018. doi:10.7589/2018-01-012.

[255] J. C. Reed and Andreas G. Ronhovde. Arctic Laboratory. A History (1947-1966) of the Naval Arctic Research Laboratory at Point Barrow, Alaska. Technical report, Arctic Institute of North America, Arlington, VA, 1971. url: https://apps.dtic.mil/sti/citations/AD0733452.

[256] J.C. Reed. Exploration of Naval Petroleum Reserve No. 4 and adjacent areas, northern Alaska, 1944-53; Part 1, History of the exploration. Professional Paper 301, US Geological Survey, Washington, DC, USA, 1958. url: https://pubs.usgs.gov/pp/0301/report.pdf.

[257] P. J. Reimer, E. Bard, A. Bayliss, J. W. Beck, P. G. Blackwell, C. B. Ramsey, C. E. Buck, H. Cheng, R. L. Edwards, and M. Friedrich. IntCal13 and Marine13 radiocarbon age calibration curves 0–50,000 years cal BP. *Radiocarbon*, 55(4):1869–1887, 2013. doi:10.2458/azu_js_rc.55.16947.

[258] D. C. Rhoads. Rates of sediment reworking by Yoldia limatula in Buzzards Bay, Massachusetts, and Long Island Sound. *Journal of Sedimentary Research*, 33(3):723–727, September 1963. doi:10.1306/74D70F0B-2B21-11D7-8648000102C1865D.

[259] S.E. Richman and J.R. Lovvorn. Effects of clam species dominance on nutrient and energy acquisition by spectacled eiders in the Bering Sea. *Marine Ecology Progress Series*, 261:283–297, 2003. doi:10.3354/meps261283.

[260] C. Ringgold and J. Rodgers. *United States North Pacific Exploring Expedition under Commanders Ringgold and Rodgers, 1853-1856*. United States North Pacific Exploring Expedition. 1950. doi: 10.5962/bhl.title.147272.

[261] J. Ritter. Another New World, 2010. url: https://spoti.fi/2K1w9If.

[262] B. W. Robinson, L. H. Decicco, J. A. Johnson, and D. R. Ruthrauff. Unusual foraging observations associated with seabird die-offs in Alaska. *Marine Ornithology*, 46:149–153, 2018. url: https://pubs.er.usgs.gov/publication/70200230.

[263] A. Y. Roppel. Management of northern fur seals on the Pribilof Islands, Alaska, 1786-1981. NOAA Technical Report NMFS 4, National Oceanic and Atmospheric Administration, Washington, DC, USA, 1984. url: http://spo.nwr.noaa.gov/tr4.pdf, http://aquaticcommons.org/2818/.

[264] S. W Ross, M. C.T. Carlson, and Andrea M. Quattrini. The utility of museum records for documenting distributions of deep-sea corals off the southeastern United States:. *Marine Biology Research*, 8(2):101–114, 2012. doi:10.1080/17451000.2011.628680.

[265] V. Roy and J.-M. Gagnon. Natural history museum data on Canadian Arctic marine benthos. *Marine Biodiversity*, 48(3):1357–1367, September 2018. doi:10.1007/s12526-016-0610-2.

[266] I. C. Russell. Notes on the Surface Geology of Alaska. *GSA Bulletin*, 1(1):99–162, 1890. doi:10.1130/GSAB-1-99.

[267] S. T. Saalfeld, J. B. Fischer, R. A. Stehn, R. M. Platte, and S. C. Brown. Predicting Waterbird Nest Distributions on the Yukon–Kuskokwim Delta of Alaska. *The Journal of Wildlife Management*, 81(8):1468–1481, 2017. doi:10.2307/26608518.

[268] M. Sauer. *An Account of a Geographical and Astronomical Expedition to the Northern Parts of Russia*. Cambridge Library Collection - Polar Exploration. Cambridge University Press, Cambridge, 2013. doi:10.1017/CBO9781107338739.

[269] C. M. Scammon. *The marine mammals of the north-western coast of North America: described and illustrated; together with an account of the American whale-fishery*. JH Carmany, San Francisco, California, USA, 1874. doi: 10.5962/bhl.title.16244.

[270] M. Schmidt, H. Kreft, A. Thiombiano, and G. Zizka. Herbarium collections and field data-based plant diversity maps for Burkina Faso. *Diversity and Distributions*, 11(6):509–516, 2005. doi:10.1111/j.1366-9516.2005.00185.x.

[271] D. W. Scholl and C. L. Sainsbury. Marine geology and bathymetry of nearshore shelf of Chukchi Sea, Ogotoruk Creek area, northwest Alaska. Open File Report 60-123, US Geological Survey, Washington, DC, USA, 1960. doi:10.3133/ofr60123.

[272] S. V. Schonberg, J. T. Clarke, and K. H. Dunton. Distribution, abundance, biomass and diversity of benthic infauna in the Northeast Chukchi Sea, Alaska: Relation to environmental variables and marine mammals. *Deep Sea Research Part II: Topical Studies in Oceanography*, 102:144–163, April 2014. doi:10.1016/j.dsr2.2013.11.004.

[273] A. Seale. Notes on Alaskan Water Birds. *Proceedings of the Academy of Natural Sciences of Philadelphia.*, 50:126–140, 1898. url: https://www.biodiversitylibrary.org/part/84224.

[274] M. G. Sexson, M. R. Petersen, G. A. Breed, and A. N. Powell. Shifts in the distribution of molting Spectacled Eiders (Somateria fischeri) indicate ecosystem change in the Arctic. *The Condor*, 118(3):463–476, 2016. doi:10.1650/CONDOR-15-139.1.

[275] M.G. Sexson, M.R. Pearce, and J. M. Petersen. Spatiotemporal distribution and migratory patterns of Spectacled Eiders, Region, Alaska Outer Continental Shelf. Technical Report OCS Study BOEM 2014-665, USGS Alaska Science Center: U.S. Department of the Interior Bureau of Ocean Energy Management Alaska Outer Continental Shelf Region, Anchorage, AK, 2014. url: https://www.boem.gov/sites/default/files/uploadedFiles/BOEM /BOEM_Newsroom/Library/Publications/2014-665.pdf.

[276] G. Sheffield, F. Fay, H. Feder, and B. Kelly. Laboratory digestion of prey and interpretation of walrus stomach contents. *Marine Mammal Science*, 17:310–330, 2006. doi:10.1111/j.1748-7692.2001.tb01273.x.

[277] G. Sheffield and J. M. Grebmeier. Pacific walrus (Odobenus rosmarus divergens): Differential prey digestion and diet. *Marine Mammal Science*, 25(4):761–777, 2009. doi:10.1111/j.1748-7692.2009.00316.x.

[278] G. Sheffield and R. Stimmelmayr. A Transitioning Ecosystem: Food for Thought in the Northern Bering Sea/Bering Strait Region. In *AGUFM*, volume 2018, pages OS53B–01, Washington, DC, USA, 2018. American Geophysical Union. url: https://ui.adsabs.harvard.edu/abs/2018AGUFMOS53B..01S/abstract.

[279] M. B. Sherwood. George Davidson and the Acquisition of Alaska. *Pacific Historical Review*, 28(2):141–154, 1959. doi:10.2307/3636542.

[280] M. B. Sherwood. *Exploration of Alaska, 1865-1900*. Yale Western Americana series.7. Yale University Press, New Haven, 1965. url: http:////catalog.hathitrust.org/Record/001444361.

[281] B. I. Sirenko and S. y. Gagaev. Unusual abundance of macrobenthos and biological invasions in the Chukchi Sea. *Russian Journal of Marine Biology*, 33(6):355–364, 2007. doi:10.1134/s1063074007060016.

[282] J. G. Skellam. Random Dispersal in Theoretical Populations. *Biometrika*, 38(1/2):196, June 1951. doi:10.2307/2332328.

[283] A. M. Smith and C. S. Nelson. Effects of early sea-floor processes on the taphonomy of temperate shelf skeletal carbonate deposits. *Earth-Science Reviews*, 63(1-2):1–31, 2003. doi:10.1016/s0012-8252(02)00164-2.

[284] S. G. Speckman, V. I. Chernook, D. M. Burn, M. S. Udevitz, Anatoly A. Kochnev, A. Vasilev, C. V. Jay, A. Lisovsky, A. S. Fischbach, and R. Bradley Benter. Results and evaluation of a survey to estimate Pacific walrus population size, 20061. *Marine Mammal Science*, 27(3):514–553, 2011. doi:10.1111/j.1748-7692.2010.00419.x.

[285] A. M. Springer, J. A. Estes, G. B. van Vliet, T. M. Williams, D. F. Doak, E. M. Danner, K. A. Forney, and B. Pfister. Sequential megafaunal collapse in the North Pacific Ocean: An ongoing legacy of industrial whaling? *Proceedings of the National Academy of Sciences*, 100(21):12223, 2003. doi:10.1073/pnas.1635156100.

[286] P. J. Stabeno, S. W. Bell, N. A. Bond, D. G. Kimmel, C. W. Mordy, and M. E. Sullivan. Distributed Biological Observatory Region 1: Physics, chemistry and plankton in the northern Bering Sea. *Deep Sea Research Part II: Topical Studies in Oceanography*, Corrected Proof, 2018. doi:10.1016/j.dsr2.2018.11.006.

[287] G Staff, E. N Powell, R. J Stanton, and H. Cummins. Biomass: is it a useful tool in paleocommunity reconstruction? *Lethaia*, 18(3):209–232, 1985. doi:10.1111/j.1502-3931.1985.tb00700.x.

[288] G. M. Staff and E. N. Powell. Onshore–offshore trends in community structural attributes: death assemblages from the shallow continental shelf of Texas. *Continental Shelf Research*, 19(6):717–756, 1999. doi:10.1016/S0278-4343(98)00108-3.

[289] R. A. Stead and R. J. Thompson. The influence of an intermittent food supply on the feeding behaviour of Yoldia hyperborea (Bivalvia: Nuculanidae). *Journal of Experimental Marine Biology and Ecology*, 332(1):37–48, May 2006. doi:10.1016/j.jembe.2005.11.001.

[290] R. Stehn, C. Dau, B. Conant, and W. Butler. Decline of Spectacled Eiders Nesting in Western Alaska. *ARCTIC*, 46(3):246–277, 1993. doi:10.14430/arctic1352.

[291] W. Stimpson. *Journal of a cruise in the US ship, Vincennes, to the North Pacific Ocean, China Sea, Behring Strait, etc. by William Stimpson, 1853-1855*. Number SIA RU007253. Smithsonian Institution Archives, Washington, DC, USA, 1853. doi: 10.5962/bhl.title.146593.

[292] W. Stimpson and C. Ringgold. *Descriptions of some new marine invertebrata*. Academy of Natural Sciences, Philadelphia, PA USA, 1855. url: https://www.biodiversitylibrary.org/item/109315.

[293] S. W Stoker. *Benthic invertebrate macrofauna of the eastern continental shelf of the Bering and Chukchi Seas*. PhD Thesis, University of Alaska, Fairbanks, Alaska, USA, 1978. url: http://hdl.handle.net/11122/5290.

[294] T. R. Strobridge. *Alaska and the U.S. Revenue Cutter Service, 1867-1915*. Naval Institute Press, Annapolis, Md., 1999.

[295] E. Tammiksaar and I. Stone. Alexander von Middendorff and his expedition to Siberia (1842–1845). *Polar Record*, 43:193–216, 2007. doi:10.1017/S0032247407006407.

[296] J. Taylor and A. Kennedy, W.J. & Hall. The shell structure, mineralogy of the Bivalvia: Nuculacea-Trigonacea. *Bulletin of the British Museum (Natural History) Zoology*, 3:1–125, 1969.

[297] J. Taylor, W.J. Kennedy, and A. Hall. The shell structure and mineralogy of the Bivalvia. II. Lucinacea-Clavagellacea, conclusion. *Bulletin of the British Museum (Natural History) Zoology*, 22:255–294, 1973.

[298] C. J. F. ter Braak. Canonical Correspondence Analysis: A new eigenvector technique for multivariate direct gradient analysis. *Ecology*, 67(5):1167–1179, 1986. doi:doi:10.2307/1938672.

[299] C. J. F. ter Braak and P. F. M. Verdonschot. Canonical correspondence analysis and related multivariate methods in aquatic ecology. *Aquatic Sciences*, 57(3):255–289, 1995. doi:10.1007/bf00877430.

[300] J. Todd. NMITA Molluscan Life Habits databases, 2001. url: https://fossils.its.uiowa.edu/database/mollusc/mollusclifestyles.htm.

[301] A. Tomašových, I. Gallmetzer, A. Haselmair, D. K. Kaufman, D. Cassin, and M. Zuschin. Tracing the effects of eutrophication on molluscan communities in sediment cores: Outbreaks of an opportunistic species coincide with reduced bioturbation and high frequency of hypoxia in the Adriatic Sea. *Paleobiology*, 44(4):575–602, 2018. doi:10.1017/pab.2018.22.

[302] A. Tomašových, I. Gallmetzer, D.S. Haselmair, A. Kaufman, B. Mavrič, and M. Zuschin. A decline in molluscan carbonate production driven by the loss of vegetated habitats encoded in the Holocene sedimentary record of the Gulf of Trieste. *Sedimentology*, 66:781–807, 2019. doi:10.1111/sed.12516.

[303] A. Tomašových and S. M. Kidwell. Nineteenth-century collapse of a benthic marine ecosystem on the open continental shelf. *Proceedings in Biological Sciences*, 284(1856):20170328, 2017. doi:10.1098/rspb.2017.0328.

[304] A. Tomašových, S. M. Kidwell, C. R. A., and D. S. Kaufman. Millennial-Scale Age Offsets Within Fossil Assemblages: Result of Bioturbation Below the Taphonomic Active Zone and Out-of-Phase Production. *Paleoceanography and Paleoclimatology*, 34(6):954–977, 2019. doi:10.1029/2018PA003553.

[305] A. Tomašových, S. M. Kidwell, R. F. Barber, and D. S. Kaufman. Long-term accumulation of carbonate shells reflects a 100-fold drop in loss rate. *Geology*, 42(9):819–822, 2014. doi:10.1130/g35694.1.

[306] A. Tomašových, SM Kidwell, and RF Barber. Inferring skeletal production from time-averaged assemblages: skeletal loss pulls the timing of production pulses towards the modern period. *Paleobiology*, 42(1):54–76, 2016. doi:10.1017/pab.2015.30.

[307] M. S. Udevitz, R.L. Taylor, J. L. Garlich-Miller, L. T. Quakenbush, and J. A. Snyder. Potential population-level effects of increased haulout-related mortality of Pacific walrus calves. *Polar Biology*, 36(2):291–298, 2013. doi:10.1007/s00300-012-1259-3.

[308] J. W. Valentine, D. Jablonski, S. Kidwell, and Kaustuv Roy. Assessing the fidelity of the fossil record by using marine bivalves. *Proceedings of the National Academy of Sciences*, 103(17):6599–6604, 2006. doi:10.1073/pnas.0601264103.

[309] C. Van Hemert, S. K. Schoen, R. W. Litaker, M. M. Smith, M. L. Arimitsu, J. F. Piatt, W. C. Holland, D. R. Hardison, and J. M. Pearce. Algal toxins in Alaskan seabirds: Evaluating the role of saxitoxin and domoic acid in a large-scale die-off of Common Murres. *Harmful Algae*, 92:101730, 2020. doi:10.1016/j.hal.2019.101730.

[310] O. Vinn. Occurrence, formation and function of organic sheets in the mineral tube structures of Serpulidae (polychaeta, Annelida). *PLoS One*, 8(10):e75330, 2013. doi:10.1371/journal.pone.0075330.

[311] O. Von Kotzebue. *A Voyage of Discovery, Into the South Sea and Beering's Straits, for the Purpose of Exploring a North-East Passage: Undertaken in the Years 1815-1818, at the Expense of His Highness the Chancellor of the Empire, Count Romanzoff, in the Ship Rurick*, volume 3. Cambridge University Press, 2013. 1-108-05759-4.

[312] H. Waga, T. Hirawake, and M. Nakaoka. Influences of size structure and post-bloom supply of phytoplankton on body size variations in a common Pacific Arctic bivalve (Macoma calcarea). *Polar Science*, page 100554, July 2020. doi:10.1016/j.polar.2020.100554.

[313] J.E. Walsh, F. Fetterer, J. S. Stewart, and W. L. Chapman. A database for depicting Arctic sea ice variations back to 1850. *Geographical Review*, 107(1):89–107, January 2017. doi:10.1111/j.1931-0846.2016.12195.x.

[314] J.E. Walsh, R. L. Thoman, U. S. Bhatt, P. A. Bieniek, B. Brettschneider, M. Brubaker, S. Danielson, Rick Lader, F. Fetterer, and Kris Holderied. The high latitude marine heat wave of 2016 and its impacts on Alaska. *Bulletin of the American Meteorological Society*, 99(1):S39–S43, 2018. doi: 10.1175/BAMS-D-17-0105.1.

[315] G. R. Walther. Community and ecosystem responses to recent climate change. *Philos Trans R Soc Lond B Biol Sci*, 365(1549):2019–24, 2010. doi:10.1098/rstb.2010.0021.

[316] J. Weems, K. Iken, R. Gradinger, and M. Wooller. Carbon and nitrogen assimilation in the Bering Sea clams Nuculana radiata and Macoma moesta. *Journal of Experimental Marine Biology and Ecology*, 430-431:32–42, 2012. doi:10.1016/j.jembe.2012.06.015.

[317] C. Wegner, T.A. Brown, C. Lalande, J. M. Grebmeier, and L.W. Cooper. Utilization and Importance of Sea Ice Derived Organic Carbon to Benthic Communities of the Chukchi Sea: Evidence from Highly Branched Isoprenoid Biomarkers. AGU, February 2020.

[318] C. L. Wei, G. T. Rowe, E. Escobar-Briones, A. Boetius, T. Soltwedel, M. J. Caley, Y. Soliman, F. Huettmann, F. Qu, Z. Yu, C. R. Pitcher, R. L. Haedrich, M. K. Wicksten, M. A. Rex, J. G. Baguley, J. Sharma, R. Danovaro, I. R. MacDonald, C. C. Nunnally, J. W. Deming, P. Montagna, M. Levesque, J. M. Weslawski, M. Wlodarska-Kowalczuk, B. S. Ingole, B. J. Bett, D. S. Billett, A. Yool, B. A. Bluhm, K. Iken, and B. E. Narayanaswamy. Global patterns

and predictions of seafloor biomass using random forests. *PLoS One*, 5(12):e15323, 2010. doi:10.1371/journal.pone.0015323.

[319] W. Weil, A. Baddeley, I. Bárány, and R. Schneider. *Stochastic Geometry: Lectures given at the C.I.M.E. Summer School held in Martina Franca, Italy, September 13-18, 2004*. Springer, October 2006. ISBN 978-3-540-38175-4.

[320] S. Wisdom. Physical, chemical, biological, geophysical, and meteorological data collected in the Arctic Ocean and Chukchi Sea in support of the Chukchi Sea Environmental Studies Program (CSESP) from 2007 to 2014 (NCEI Accession 0124308). Dataset NCEI Accession 0124308, Alaska Ocean Observing System (AOOS), 2014.

[321] R.A. Woodgate. Increases in the Pacific inflow to the Arctic from 1990 to 2015, and insights into seasonal trends and driving mechanisms from year-round Bering Strait mooring data. *Progress in Oceanography*, 160:124–154, 2018. doi:10.1016/j.pocean.2017.12.007.

[322] W.P. Woodring. William Healey Dall, 1845-1927: A Biographical Memoir. In *National Academy of Sciences*, pages 92–113. Columbia University Press, New York, USA, 1958. url: http://www.nasonline.org/publications/biographical-memoirs/memoir-pdfs/dall-william.pdf.

[323] M Yamamoto-Kawai, T Mifune, T Kikuchi, and S Nishino. Seasonal variation of CaCO saturation state in bottom water of a biological hotspot in the Chukchi Sea, Arctic Ocean. *Biogeosciences*, 13:6155–6169, 2016. doi:10.5194/bg-13-6155-2016.

[324] Jordann K. Young, B. A. Black, J. T. Clarke, S. V. Schonberg, and K. H. Dunton. Abundance, biomass and caloric content of Chukchi Sea bivalves and association with Pacific walrus (Odobenus rosmarus divergens) relative density and distribution in the northeastern Chukchi Sea. *Deep Sea Research Part II: Topical Studies in Oceanography*, 144:125–141, October 2017. doi:10.1016/j.dsr2.2017.04.017.